SEDIMENTOLOGY AND PETROLEUM GEOCHEMISTRY OF

THE OULDBURRA FORMATION, EASTERN OFFICER BASIN,

AUSTRALIA

by

MOHAMMAD REZA KAMALI

(M.Sc. Geology, University of Mysore, India)

DECEMBER, 1995

A thesis submitted in fulfilment of the requirements for the award of the degree of

DOCTOR OF PHILOSOPHY

from

The National Centre for Petroleum Geology and Geophysics,

the University of Adelaide, South Australia

Dedicated to

Rozita, Roya and Amin

ABSTRACT

Deposition of the Early Cambrian Ouldburra Formation, a mixed siliciclastic/carbonate, marine carbonate and evaporite succession, occurred in the shallow marine setting of the Manya Trough. The observed variations between the facies are interpreted as both autocyclic and allocyclic in nature, largely controlled by sea level fluctuations.

Periodic exposure of the carbonates resulted in dolomitisation and secondary porosity development. Secondary porosity was generated within the siliciclastic-carbonate zone by carbonate matrix and grain dissolution, and also by dolomitisation.

The sedimentary facies and rock character suggest that sabkha and brine reflux models can be used to explain early dolomitisation within the Ouldburra Formation. Dolomite mainly occurs in two stages: (1) common anhedral dolomites formed early by replacement of pre-existing limestone and (2) saddle dolomite and coarse crystalline dolomite formed during the late stages of burial diagenesis and associated with hydrocarbon shows. The diagenetic path includes cementation, dolomitisation, dissolution, compaction, silicification, dedolomitisation, burial dolomitisation, sulphide mineralisation, pressure solution, fracturing and hydrocarbon migration. The dolomite reservoirs were ranked on the basis of their porosity distribution and texture into groups I to IV. Dolomites with rank I and II exhibit excellent to good reservoir characteristics respectively. Petrophysical logs, including gamma ray and density logs, helped to identify porous intervals.

Stable carbon and oxygen analyses, together with fluid inclusion microthermometry, suggest that the early dolomite with relatively heavy $\delta^{18}O$ but depleted $\delta^{13}C$ formed in a sabkha environment under relatively low temperatures, and the late replacement and saddle dolomites with depleted $\delta^{18}O$ suggest deposition under somewhat higher temperatures.

In the Manya Trough, the organic-rich carbonates were deposited under anoxic to suboxic conditions. They are mature to overmature and have Type III to IV kerogen. In the Tallaringa Trough, the carbonates were deposited under highly anoxic conditions. They are early mature to mature and have Type II kerogen. The occurrence of live oil, together with thucholites in proximity to the common lamalginite, are characteristic features associated

with these excellent quality, oil-prone source rocks. The recognition of *Gloeocapsomorpha prisca* in these source rocks is the first reported occurrence of this organism from the Early Cambrian.

Biomarker characteristics of the clay-free Tallaringa Trough limestones are unusual and are characterised by high abundances of hopanes and diasteranes relative to steranes. Other significant biomarkers are dinosterane and 24-isopropylcholestane, where the former is the first reported occurrence of this compound from an Early Palaeozoic rock. The latter confirms an earlier report of this compound from the Ouldburra Formation and strengthens its significance as an age-specific sponge marker.

TABLE OF CONTENTS

REPRINTS

KAMALI, M. R., LEMON, N. M. AND McKIRDY, D.M., 1993 - Ouldburra Formation as a potential source and reservoir for petroleum in the Manya Trough, eastern Officer Basin. In: ALEXANDER, E. M. AND GRAVESTOCK, D.I. (eds.), *Central Australian Basins Workshop, Alice Springs, Programme and Abstracts*, pp. 65–66.

KAMALI, M. R., LEMON, N. M., AND APAK, S. N., 1995 - Porosity generation and reservoir potential of the Ouldburra Formation in the Officer Basin. *The Journal of the Australian Petroleum Exploration Association*, 35(1), 106-120.

MICHAELSEN, B. H., KAMALI, M. R., AND McKIRDY, D. M., 1995 - Unexpected molecular fossils from Early Cambrian carbonates of the Officer Basin, South Australia. In: GRIMALT, J.O. AND DORRONSORO, D. (eds.), *Organic Geochemistry: Selected Papers from the 17th International Meeting on Organic Geochemistry*, Donostia-San Sebastian, Spain, pp. 218-221.

APPENDICES

Appendix I X-ray diffraction profiles (reservoir and source rocks)

Appendix II Petrographic descriptions of reservoir rocks

Appendix III Colour and black and white plates of thin sections and SEM micrographs

Appendix IV Porosity and permeability data

Appendix V Log profiles of selected porous intervals

Appendix VI Rock -Eval pyrolysis data

Appendix VII Organic petrographic descriptions of polished sections

Appendix VIII Colour and black and white plates of microfossils in organic-rich carbonates

Appendix IX Gas chromatograms of saturated hydrocarbons

Appendix X Pyrolysis-gas chromatograms of kerogen

Appendix XI Mass chromatograms of triaromatic hydrocarbons

Appendix XII Peak identities and Mass chromatograms (GC-MS; GC-MS-MS) of saturated hydrocarbons

LIST OF FIGURES

STATEMENT

This thesis contains no material which has been accepted for the award of any other degree or diploma in any university and that, to the best of the author's knowledge and belief, the thesis contains no material previously published or written by another person, except where due reference is made in the text of the thesis.

The author consents to the thesis being made available for photocopying and loan if accepted for the award of the degree.

Mohammad Reza Kamali

ACKNOWLEDGMENTS

CHAPTER 1

INTRODUCTION

1.1   General statement

A global increase in the consumption of petroleum products and a related decline in hydrocarbon reserves necessitate further research into the petroleum reserves of frontier areas, particularly those containing old strata.   Exploration for oil in Australia and worldwide has focused mainly on younger Phanerozoic basins, with only minor attention being given to Precambrian and Cambrian basins.   Nevertheless, potential hydrocarbon source rocks of Cambrian age have been reported from several Australian basins including Amadeus Basin (Jackson et al., 1984), Arrowie Basin (McKirdy, 1994), Georgina Basin (Cook, 1982), Officer Basin (McKirdy and Kantsler, 1980; McKirdy et al., 1984; Kamali et al., 1993), Siberia (Meyerhoff, 1980) and Oman (Al-Marjeby and Nash, 1986).

The petroleum potential of the Early Cambrian Ouldburra Formation in the Manya and Tallaringa Troughs of the eastern Officer Basin has not been investigated adequately. An integrated approach including detailed sedimentological and organic geochemical analyses, combined with the already defined stratigraphy and sedimentology of the Ouldburra Formation in the Manya Trough, is required to provide an insight into the reservoir potential of its carbonate and siliciclastic sequences and the hydrocarbon source potential of its organic-rich beds.

The Ouldburra Formation exhibits significant reservoir potential in the form of leached carbonate and dolomitised zones with high porosity and permeability (Dunster, 1987). Previous maturity studies indicated that its intraformational source beds have had different

I
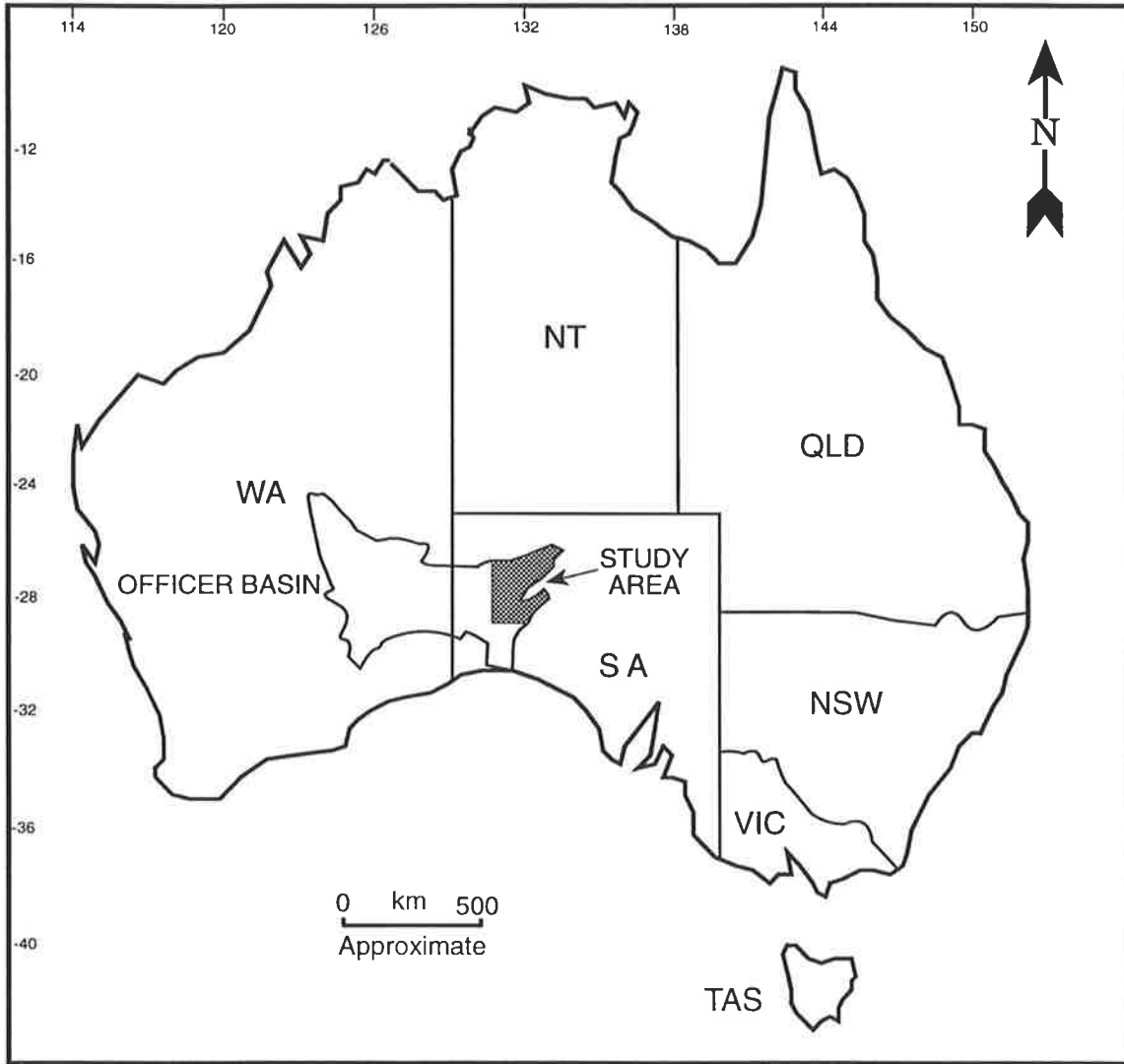
Figure 1.1 Locality map of the eastern Officer Basin, South Australia.

thermal histories, being overmature in the Manya Trough and immature to marginally mature in the Tallaringa Trough (McKirdy and Michaelsen, 1994). Recent palynological studies of microfossils such as acritarchs and coccoid cyanobacteria (W. Zang, pers. comm., 1995) confirm that organic-rich beds in the Tallaringa Trough have entered the early oil generation window, whereas their correlative beds in the Manya Trough are mature to overmature.

The search for hydrocarbons in the eastern Officer Basin began in the early 1960s. Sporadic exploration continued until 1979 when Byilkaoora 1, a stratigraphic well drilled by South Australian Department of Mines and Energy (SADME), intersected significant evaporite pseudomorphs and oil bleeds in the Early Cambrian Observatory Hill Formation. This encouraged exploration by Comalco, Amoco and CRA. Several other oil shows elsewhere in the Cambrian section were also reported from different mineral and stratigraphic drillholes (McKirdy and Kantsler, 1980). Despite these clear hydrocarbon indicators, the Officer Basin remains one of Australia's frontier onshore basins. To date, no wells have been targeted on plays in the Ouldburra Formation. Further exploration for hydrocarbons in the eastern Officer Basin calls for particular attention to detail and a careful assessment of the source, reservoir and seal potential of the candidate sequences.

1.2   Aims

The main objectives of this thesis were

- to understand the nature of the of Lower Cambrian sedimentary sequence which comprises the Ouldburra Formation;

- to determine the diagenetic history of the reservoir rocks and detail their porosity and permeability trends;

- to measure the organic carbon content and level of maturity of potential hydrocarbon source rocks within the sequence; and

- to ascertain the biomarker signatures of the organic-rich beds.

1.3   Location

The Ouldburra Formation is not known to crop out but is widespread in the subsurface throughout the area bordered by Lat. 27° 15' 00" S, 30° 47' 00" S and Long. 131° 55' 00" E, 134° 20' 00" E.

The study area is located at the northeastern part of Officer Basin in northwest SA (Fig. 1.1). The Manya Trough is accessed via Marla 1200 km north of Adelaide and 500 km south of Alice Springs, whereas the Tallaringa area, located 800 km northwest of Adelaide, is principally vacant land.   Access to the Marla-Manya area (Aboriginal land) was restricted in the past but a good deal of understanding and co-operation with Aboriginal people over recent years has enabled SADME to successfully acquire new seismic data.

1.4   Previous investigations

Previous sedimentological studies of the Ouldburra Formation were undertaken by Lydyard (1979) and by Youngs (1980) who worked on the carbonates intersected by drillholes in the Marla-Manya area.   The detailed sedimentology of the Ouldburra Formation was described by Dunster (1987).   The stratigraphy of this formation was revised by Brewer et al. (1987) and its sequence stratigraphy has recently been established by Gravestock and Hibburt (1991) and Moussavi-Harami and Gravestock (1995).

The source rock potential and preliminary biomarker geochemistry of the Ouldburra Formation have been examined by McKirdy and co-workers in various company reports that exist as Open File Envelopes in the Department of Mines and Energy, South Australia since 1976. Important aspects of this work together with new findings have been published in a series of key papers (e.g., McKirdy and Kantsler, 1980; McKirdy et al., 1984; Imbus and McKirdy, 1993, McKirdy et al., 1995).   Weste et al. (1984)

attempted to quantify the total organic carbon (TOC) content of stromatolitic algal bindstones from the Ouldburra Formation.

It is noteworthy that the term of "Ouldburra Formation" for the Early Cambrian marine carbonates has only been in use since 1987. According to recent geological work in the eastern Officer Basin, the Early Cambrian marine carbonates that were previously referred to as Observatory Hill Beds (White and Young, 1980) and subsequently as Wintinna Formation (Weste et al., 1984) are stratigraphically older than the nonmarine carbonates (Observatory Hill Formation) and are now assigned to the Ouldburra Formation (Brewer et al., 1987).

Recent advances in our knowledge of the eastern Officer Basin include the first application of sequence stratigraphy to the Early Cambrian section (Gravestock and Hibburt, 1991); insights of the siliciclastic reservoirs (Sansome and Gravestock, 1993); seismic data acquisition together with tectonics of the Officer Basin (Hoskins, 1993); and a detailed study of Neoproterozoic and Early Palaeozoic acritarchs (Zang and McKirdy, 1993).

1.5   Techniques used in Part I

The techniques used in the sedimentological analyses associated with this study are summarised in a flow chart (Fig. 1.2) and are described below.

1.5.1   X-ray diffraction analysis

X-ray diffraction analysis (XRD) was used for bulk mineral and clay mineral identification. Samples were gently crushed by mortar and pestle to reduce the mean particle diameter to ca 5-10mm, and then transferred onto a glass slide using acetone. After drying, samples
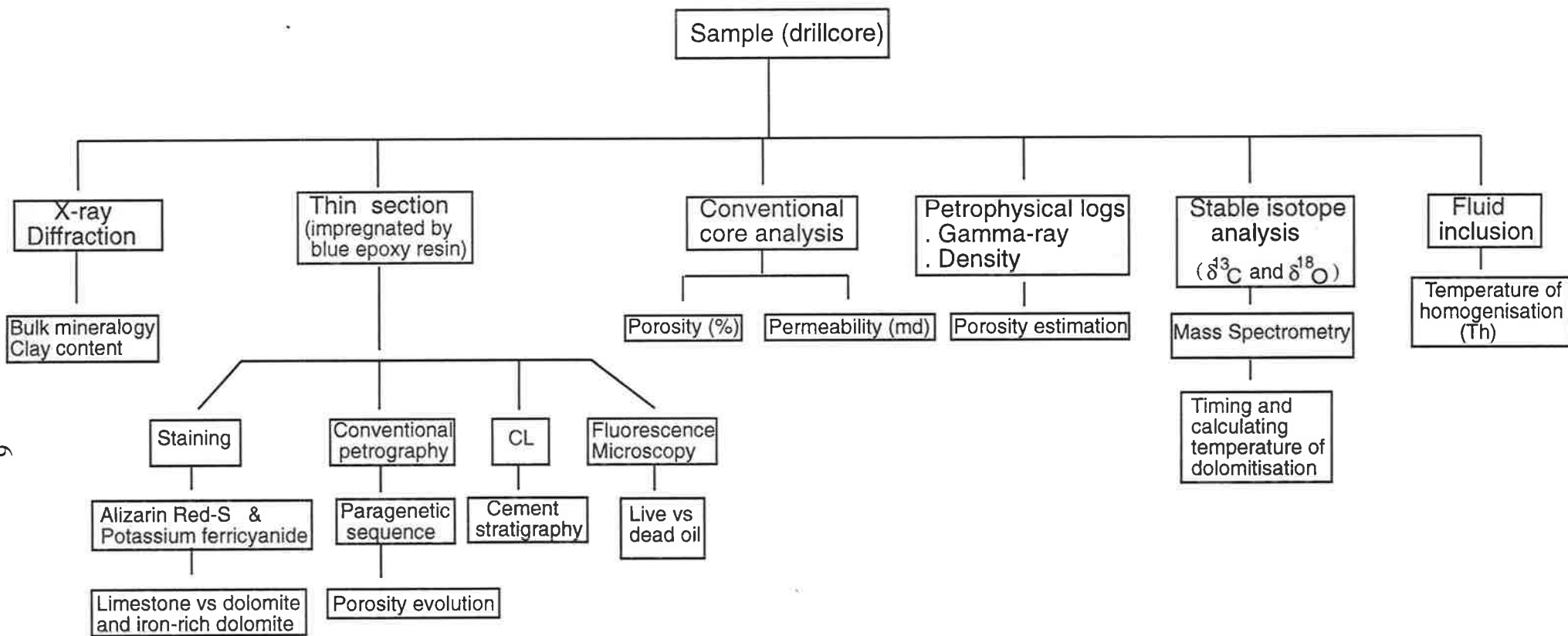
Figure 1.2 Flow diagram showing the sedimentological techniques used in this study.

were analysed with a Philips™ PW 1050 X-ray diffractometer/monochromator fitted with a cobalt tube operating at 50 kV and 30 mA.

1.5.2   Transmitted light microscopy

Forty-two thin sections were prepared in the laboratories of the Department of Geology and Geophysics, the University of Adelaide. In addition, a total of 146 thin sections were also made available by the South Australian Department of Mines and Energy (SADME). Some of these samples were impregnated with blue dye (Araldite glue) before grinding in order to assist determination of the, amount and type of porosity. Petrographic study of the thin sections was performed at the National Centre for Petroleum Geology and Geophysics using an OLYMPUS™ BH-2 transmitted light microscope equipped with ultra violet light and camera.

1.5.3   Staining

In addition to thin sections previously stained by SADME, 12 more were prepared for this study using Alizarin red S and potassium ferricyanide mixture following the procedure outlined by Dickson (1966). Alizarin red S differentiates calcite from dolomite while potassium ferricyanide distinguishes ferroan from non-ferroan calcite and/or dolomite.

1.5.4   Cathodoluminescence (CL) microscopy

Cathodoluminescence microscopy was used to evaluate the cement stratigraphy following the work of Meyers (1974) and Machel et al. (1991).

Luminescence is the emission of light from a solid when it is excited by some form of energy. The colour and intensity of the resulting luminescence is commonly controlled by

the balance of activator and quencher centres. For example, Mn^{2+} is the main activator causing luminescence in calcite, whereas Fe^{2+} is the main quencher in the same mineral. For this study, 12 highly polished thin sections were examined using a TECHNOSYN 98200 MK 11) Luminoscope. Operating conditions for cathodoluminescence microscopy and photomicroscopy (Kodak Ektapress 1600 ASA film) were 12 to 18 kV for beam energy and between 150 and 200 microamps for beam current.

1.5.5 Scanning electron microscopy (SEM)

Fourteen selected samples were examined under scanning electron microscope (Philips 505) in order to elucidate their texture, microporosity, leaching and associated diagenetic minerals. These samples were obtained from cores and coincide with thin section locations. These samples were cut into cubes (approximately 9 x 9 x 9 mm), attached to aluminium stubs using "Araldite" and then double coated with carbon and gold / palladium in an evaporative coating unit.

1.5.6 Stable isotope analysis

Powdered samples from fifteen selected carbonate rocks were carefully removed using a modified dental drill. Approximately 10 to 15 mg of untreated powder were reacted with 100 % phosphoric acid for 17 hours at $50^\circ C$ for dolomite and $25^\circ C$ for calcite. The evolved CO_2 was then collected via a gas extraction system and sealed in glass tubes. The equipment used for the stable isotope analyses was a MICROMASS^{TM} VG 602E Stable Isotope Ratio Mass Spectrometer. The reference gas, against which all samples were measured, was collected from calcite which had been reacted at $25^\circ C$. Analysis of a dolomite standard (ANU-P3) was also conducted for comparison. Results are reported in conventional per mil (‰) notation relative to the PDB standard. No corrections for acid

fractionation were made for dolomite. Precision, based on selected replicate analysis, is better than ±0.2 ‰ for both ^{18}O and ^{13}C values.

1.5.7   Fluid inclusion microtherrmometry

Fluid inclusion microthermometry was performed on selected samples to evaluate formation temperatures and salinities of inclusions in the individual diagenetic phases. Selected samples were prepared as doubly polished plates 200 mm thickness. The samples were prepared under low temperature (<50°C) conditions to avoid possible stretching or decrepitation. Primary fluid inclusions were of most interest as these inclusions record the pore fluids at the time when a particular cement was precipitated.

Fluid inclusions were analysed using a USGS-type gas flow heating and freezing system. Precision in measuring both last melt and temperature of homogenisation is between ±0.2-0.3°C.

1.6   Techniques used in Part II

The techniques used in organic geochemical analysis are summarised in a flow chart (Fig. 1.3) and are described as follows:

1.6.1   TOC analysis and Rock-Eval pyrolysis

A total of 73 samples were screened for total organic carbon (TOC) analysis and Rock-Eval pyrolysis (cf. Peters, 1986). In addition, TOC data were available on another 68 samples previously analysed by Comalco. Rock-Eval pyrolysis of a 100 mg portion of powdered rock was undertaken in a Girdel IFP-Fina Mark 2 instrument (operating mode, Cycle 10 at Amdel Petroleum Services, Adelaide. Rock-Eval pyrolysis data are given in Appendix VI.
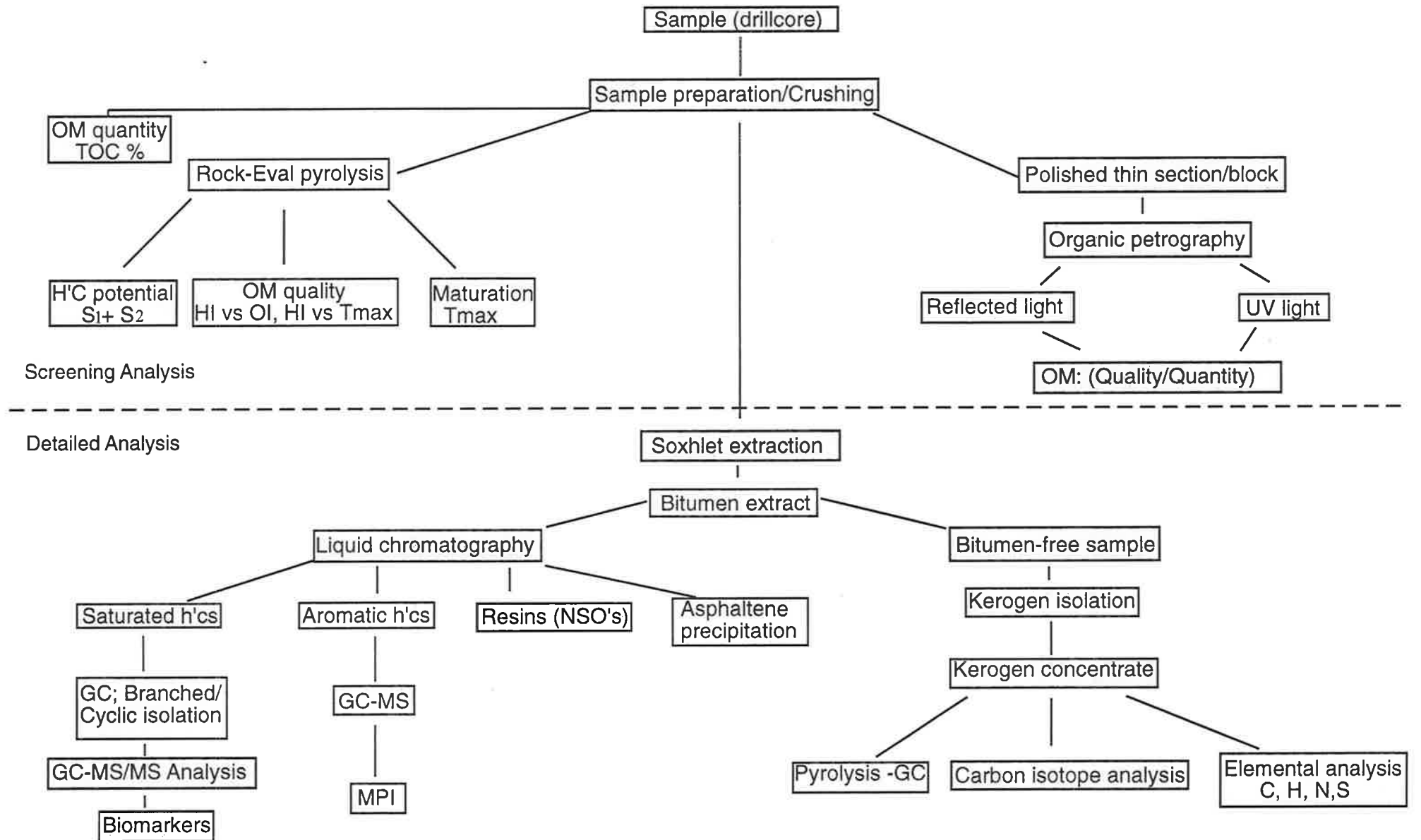
Figure 1.3 Flow diagram of techniques used in organic geochemical analyses.

1.6.2 Soxhlet extraction, and liquid column chromatography

Only 20 selected samples (15 from the Manya Trough and 5 from the Tallaringa Trough) were subjected to soxhlet extraction and liquid column chromatography. The core samples were scraped and brushed clean to remove surficial contamination. After crushing in a Siebtechnik mill, the powdered rock was extracted in Soxhlet apparatus using an azeotropic solvent mixture (CH_2Cl_2 : CH_3OH, 93 : 7) for 72 hours. Activated copper turnings were used to remove elemental sulphur. Rotary evaporation removed the excess solvent, and the weight of extracted bitumen was recorded. The bitumen was fractionated by liquid column chromatography on activated silica and alumina into saturated hydrocarbons, aromatic hydrocarbons and polar compounds (resins and asphaltenes). Solvents used to elute saturates, aromatics and resins were petroleum ether (80 ml), petroleum ether : dichloromethane (50 : 50, 80 ml) and dichloromethane : methanol (35 : 65, 80 ml), respectively. The fractions were then dried, weighed for reporting in ppm.

1.6.3 Organic petrography

Sub-specimens of the core samples were cut perpendicular to bedding, mounted in resin and polished for petrographic analysis. Duplicate polished thin sections were also prepared for more detailed observation. The polished sections were then studied under a Leitz Ortholux II Pol microscope equipped for both white light and UV-blue light observation and photography. Fluorescence-mode observation utilised a 3 mm BG3 excitation filter (UV light) with a 510 nm suppression filter.

Reflectance measurements on thucholites were carried out at Amdel Petroleum Services, Adelaide using a Leitz MPV1.1 microphotometer fitted to a Leitz Ortholux microscope and calibrated against synthetic standards (YAG = 0.920 % and Spinel = 0.420 %).

Measurements were made in oil immersion (n = 1.518) with incident monochromatic light (wavelength = 546 nm) at a temperature of 23°C.

1.6.4 Kerogen isolation, elemental analysis and pyrolysis gas chromatography (Py-GC)

Soxhlet-extracted powdered samples (n = 5) were submitted to Amdel Petroleum Services, Adelaide, for isolation, elemental analysis (C, H, N, S) and Py-GC analysis of their kerogen fraction.

The bitumen-free samples were acid-macerated using 1:1 conc. HCl and 50 % HF, washed in distilled water, briefly centrifuged and the kerogen float decanted. The isolated kerogen was then subjected to re-extraction with dichloromethane to remove any residual bitumen present. A portion of this kerogen (1-2 mg) was then pyrolysed in the injector of a Perkin-Elmer Sigma 2 gas chromatograph equipped with a BP-1 column (25 m x 0.3 mm i.d., 0.25 μm film thickness) using a CDS 190 extended pyroprobe at 700°C. Nitrogen was used as the gas carrier. The GC oven was held isothermal at 0°C for 1 minute and then heated to 300°C at 8° min^{-1} and held until all peaks eluted. Methylstyrene was used as an internal standard. Data acquisition and processing of chromatographic information was performed using computer-based processing software.

1.6.5 GC , GC-MC and GC-MS-MS analyses

A Varian 3400 gas chromatograph was used to analyse the saturated (total alkane) fraction. The instrument was fitted with a 25 m x 0.22 mm i.d fused silica column (BP-1, 0.25 μm film thickness; SGE Australia). Samples in n-hexane were injected using a split/splitless injector operating in split mode. Hydrogen was used as the carrier gas (linear velocity of 30 cm s^{-1}) with injector and detector (FID) temperatures of 300°C. The oven temperature

was held at 60°C for 5 minutes then programmed from 60 to 300°C at 4°C min^{-1}. Interpretation of the GC traces was aided by Mac Lab software using a personal computer connected to the gas chromatograph.

The GC-MS analyses were undertaken for 8 selected samples using a Varian 3400 gas chromatograh interfaced with a Finnigan TQS 70 mass spectrometer. The gas chromatograph was fitted with a 60 m x 0.25 i.d fused silica column (DB-1, 0.25 μm film thickness; J&W Scientific). Helium was used as the carrier gas at an inlet pressure of approximately 100 kPa. Samples in n-hexane were injected using a split/splitless injector (split mode : valve setting = 0.2 min, temperature = 280°C). The program of the oven was as follows: 50°C for 2 min, 50°C to 120°C at 8°C min^{-1}, 120°C to 300°C at 4°C min^{-1} and then held at 300°C for 35 min. The samples were analysed in full scan mode from 47 to 500 amu at a scan rate of 0.5 s scan^{-1}. Other MS operating parameters included an ionisation voltage of 70 eV, a filament current of μA and a typical photomultiplier voltage of 1400 V.

GC-MS-MS facility was employed to analyse three selected samples on the same instrument (CAD, parent ion mode; cf. Peters and Moldowan, 1993). Helium was used as the mobile phase at an inlet pressure of approximately 24 psi. Total alkane samples in *n*-hexane were injected on-column. The injector was programmed 60°C for 6 seconds then ramped to 300°C at 180°C min^{-1} and held at 300°C for 5 min. The program of the oven was as follows: 50°C to 120°C at 8°C min^{-1}, 120°C to 300°C at 4°C min and then held at 300°C for **35** min. MS operating conditions included an ionisation voltage of 70 eV, a filament current of 200 μA and a photomultiplier voltage of 1900. Argon was used as the collision gas (-20 eV) to induce disassociation in the second quadrupole (Q2). Most tandem MS methodologies discussed in the biogeochemical literature (cf. Peters and

Moldowan, 1993) describe an MS-MS technique whereby the parent quadrupole (Q1) scans (typically m/z 300-500) for possible precursor molecules, and the daughter quadrupole (Q3) selectively monitors the fragmented ions produced by collision-induced decomposition (CID). The Q3 was used in scan mode from m/z 350-450. However, to provide analyses with enhanced sensitivity, the equipment was operated with Q1 and Q3 in selective-ion mode to monitor the following decomposition reactions:

m/z (Q1)		m/z (Q3)	Target compounds
370.4	$\rightarrow$	191.2	C_{27} hopanes (e.g. Ts. Tm)
384.2	$\rightarrow$	191.2	C_{28} hopanes (e.g. 28, 30-BNH)
398.4	$\rightarrow$	191.2	C_{29} hopanes (e.g. C_{29} Ts)
412.4	$\rightarrow$	191.2	C_{30} hopanes (e.g. C_{30} Ts, C_{30})
440.4, 454.4, 468.4, 482.4	$\rightarrow$	191.2	C_{31}-C_{35} homohopanes

Aromatic hydrocarbons fractions in CH_2Cl_2 were analysed using similar conditions to those described above, except that the fractions were injected on-column and the photomultiplier voltage was 1100 V. The injector was held at 50°C for 10 seconds then ramped to 300°C at 180°C min^{-1}, and held for 5 minutes. A 30 m x 0.25 μm film thickness (DB-5; J&W Scientific) fused silica column was used (H2 ca 10 psi) and the mass spectrometer was programmed (MID mode) to monitor m/z 178 (phenanthrene) and m/z 192 (methylphenanthrenes).

CHAPTER 2

CAMBRIAN GEOLOGY OF THE EASTERN OFFICER BASIN

2.1 Introduction

The Officer Basin extends across the southern part of the continent from the Yilgarn Block in Western Australia to the Gawler Craton in South Australia (Fig. 2.1). The basin is an arcuate depression 500 km long, containing mainly flat to gently dipping Neoproterozoic (Adelaidean) and early Palaeozoic sediments (Pitt et al., 1980). In the South Australian sector, the two major depocentres, the Birksgate Sub-basin and Munyarai Trough, contain up to 5 km of marine and fluvio-lacustrine sediments. Major northeast-trending faults, thrust-wrench fault complexes and basement ridges separate the Munyarai Trough from the Gawler Craton to the southeast (Pitt et al., 1980). The intervening Manya, Wintinna and Tallaringa Troughs contain mainly Early Cambrian sediments (Fig. 2.2) which were laid down typically as shallow marine, subtidal wackestone, intertidal cyanobacterial boundstone and archaeocyathan bioherms (Dunster, 1987; Gravestock and Hibburt, 1991). Sabkha evaporites, alkaline playa lake sediments and redbed aeolian dunes interfinger with these marine sediments and attest to a warm, dry, coastal setting. The shallow marine Early Cambrian carbonates, mixed carbonate-siliciclastics and evaporites of the Ouldburra Formation are thick in the Manya Trough but thinner in the Tallaringa Trough. These troughs are separated by the parallel Nawa Ridge which was a palaeohigh accentuated by the Alice Springs Orogeny (SADME-94A-D).
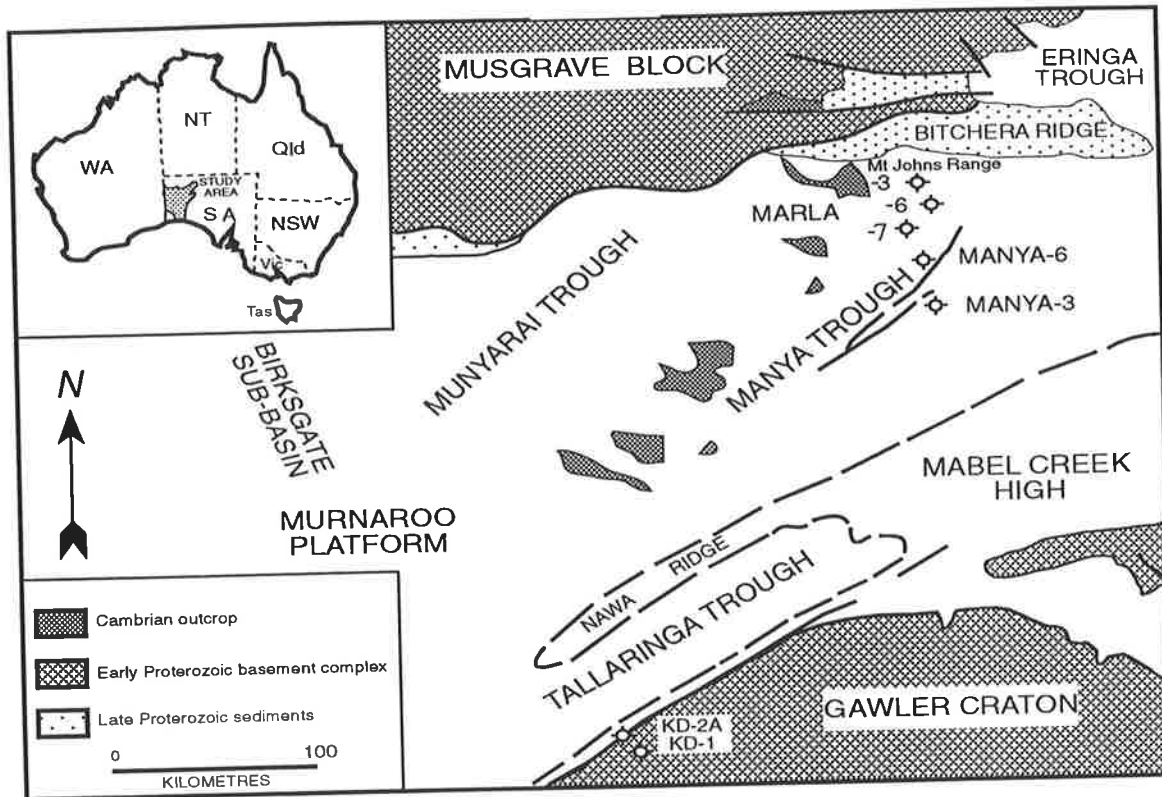
Figure 2.1 Location of the study area and principal geological features in the eastern Officer Basin, South Australia (modified from MESA, 1994).
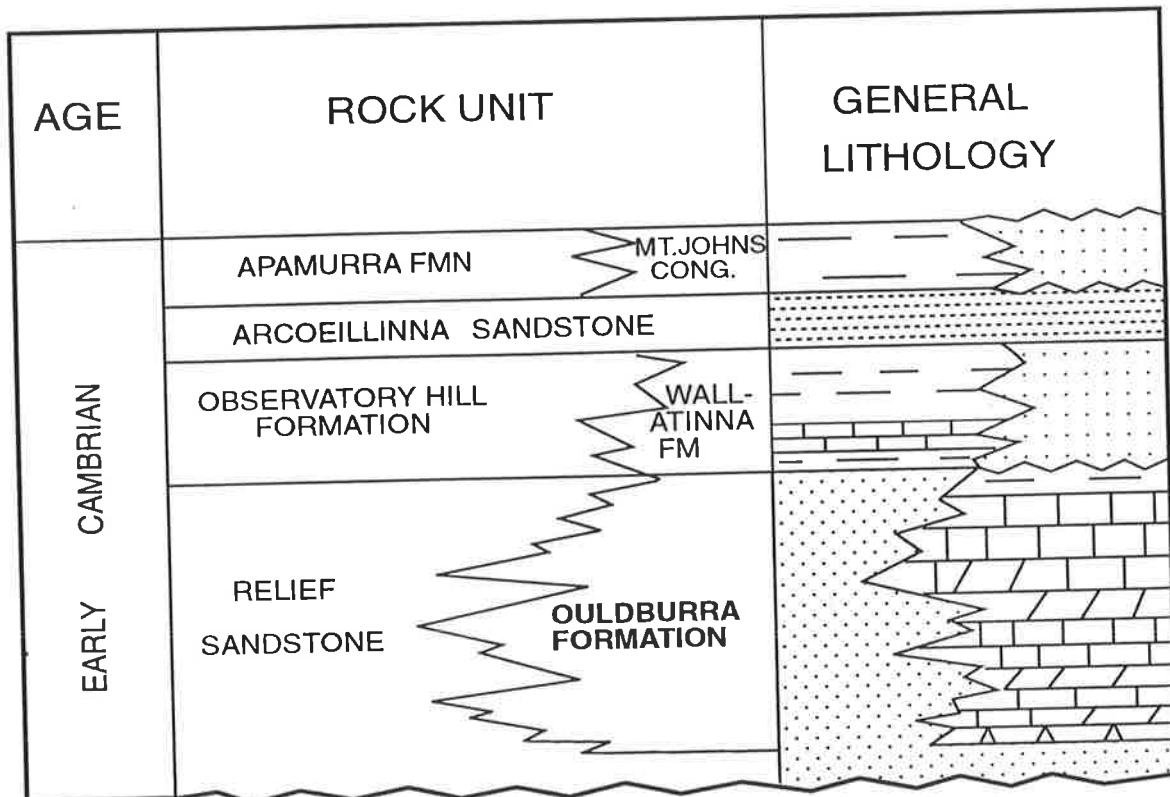
Figure 2.2 The Early Cambrian stratigraphy of the eastern Officer Basin (modified from MESA, 1994).

16

2.2   Stratigraphy

The Cambrian lithostratigraphy of the northeastern Officer Basin has been defined by Benbow (1982) and revised by Brewer et al. (1987). The Early Cambrian marine carbonates (Ouldburra Formation) had been previously correlated with Observatory Hill Beds (Pitt et al., 1980) but were subsequently assigned to the Ouldburra Formation (Brewer et al., 1987). The Ouldburra Formation is thickest in the Manya Trough and relatively thin in the Tallaringa Trough. It conformably overlies the Relief Sandstone and passes upwards into the gypsiferous redbeds of the lower portion of the Observatory Hill Formation, which in turn shows a lateral intertonguing relationship with the Wallantinna Formation in the Mount Johns Range (Benbow, 1982).

The type section of the Ouldburra Formation in Manya-6 comprises 1114 m of mixed carbonates and siliciclastics, marine calcareous and dolomitic carbonates, and evaporites, including halite and anhydrite (Brewer et al., 1987) in which Gravestock and Hibburt (1991) recognised three depositional sequences (C1.1 - C1.3). The first sequence starts with a lowstand tract which was deposited in isolated salinas on a shallow marine to emergent sandy mudflat fringed by marginal coastal sands and partly aeolian dunes (Relief Sandstone). These initial deposits pass upwards into transgressive shallow marine carbonates including archaeocyathan and cyanobacterial bioherms. Withdrawal of the sea and subaerial exposure is marked by a carbonate breccia at the top of the sequence. A second transgressive-regressive cycle resulted in deposition of a thick sequence of subtidal wackestone overlain by sabkha evaporites and redbeds (C1.2). The upper Ouldburra Formation is a regressive sequence of shallow marine to exposed carbonate mudstones and red anhydritic siltstones. The most recent stratigraphic overview (Fig. 2.3), incorporating sequences and sea level curves, is that given by Moussavi-Harami and Gravestock (1995).

AGE	AGE Ma	ROCK UNIT	GENERAL LITHOLOGY	SEA LEVEL (T / R)	STRATIGRAPHIC SEQUENCES	TECTONIC EVENTS
EARLY CRETACEOUS	95 / 114 / 130	BULLDOG SHALE		MFS or HST	J-K.2	
	130	CADNA-OWIE SANDSTONE		HST		J-K
	140	ALGEBUCKINA SANDSTONE		TST	J-K.1	
LATE JURASSIC	140			LST		
EARLY to MIDDLE JURASSIC	152 / 205					CONTINENTAL UPLIFT
TRIASSIC	250					
LATE PERMIAN	250 / 260	WAITOONA BEDS MT TOONDINA FORMATION				
EARLY PERMIAN	270 / 280 / 290	STUART RANGE FORMATION		HST / TST	P	
		BOORTHANNA FORMATION				ALICE SPRINGS OROGENY
CARBONIFEROUS	355					
LATE DEVONIAN	360 / 375	UNNAMED		?HST / ?TST	D	
EARLY & MIDDLE DEVONIAN	410					RODINGAN EVENT
SILURIAN	438					
MIDDLE & LATE ORDOVICIAN	472					
EARLY ORDOVICIAN		BLUE HILLS SANDSTONE (MINTABIE / CARTU BEDS)		HST		
	481	INDULKANA SHALE		MFS	O	
	484 / 487	MT CHANDLER SANDSTONE		TST		
	490	BYILKAOORA FMN		LST		
LATE CAMBRIAN	498	KULYONG				DELAMERIAN OROGENY
MIDDLE CAMBRIAN	505					
	508	TRAINOR HILL SANDSTONE		HST		
		APAMURRA FMN MT JOHNS CONGL.		TST	C2.2	
	510	ARCOEILLINNA SANDSTONE		LST		C2
	512			HST / TST		
		OBSERVATORY HILL FMN WALL-ATINNA FMN		LST	C2.1	
EARLY CAMBRIAN	516 / 518	CADNEY PARK FORMATION				
	525			HST	C1.3	
				TST / LST		
	530	RELIEF SANDSTONE OULDBURRA FORMATION		MFS or HST	C1.2	C1
	535			TST / LST	C1.1	
	540			TST / LST		PETERMANN RANGES OROGENY
EDIACARIAN	560	MENA MUDSTONE		HST / TST	E.4	
	570	MUNTA LIMESTONE		HST / TST	E.3	
	575	WILARI DOLOMITE & LEEMURRA MUDSTONE RODDA BEDS		IVF & TST		E
	585	KARLAYA LIMESTONE		HST / TST	E.2	
	590	DEY-DEY MUDSTONE		HST / MFS / TST	E.1	
	600	MURNAROO FORMATION		LST		
MARINOAN	615	MERAMANGYE FORMATION		HST / MFS / TST	M	
	640	TARLINA SANDSTONE		LST		
STURTIAN	650 / 700	CHAMBERS BLUFF				GLACIO-GENIC UPLIFT
	720 / 760					
	780	CADLAREENA				
WILLOURAN	800	ALINYA FORMATION		HST / TST	W	
	820	PINDYIN SANDSTONE		LS		

MESA 94-1530

Figure 2.3 Generalised stratigraphic column, sequences and sea level curve of the eastern Officer Basin (Moussavi-Harami and Gravestock, 1995).

18

2.3 Tectonics

Early workers have invoked late Proterozoic aulacogen development as the precursor to Palaeozoic infracratonic development (Doutch and Nicholas, 1978; Milanovsky, 1981; Veevers et al., 1982). Accordingly, subsidence in the eastern Officer Basin began in the Late Proterozoic and was accompanied by deposition of a thick sequence of a Adelaidean sediments. This was terminated about 600 Ma by the Petermann Ranges Orogeny which folded and faulted the Adelaidean sediments in the northeastern margin of the basin.

A second sequence of events began in the Mid-Cambrian (Veevers et al., 1982) and culminated in the ? Devonian to Early Carboniferous Alice Springs Orogeny. The latest orogenic phase was proposed to be a series of major northeast-southwest trending thrust faults that appear to have been reactivated from Precambrian extensional faults.

However, some recent workers consider the Officer Basin to be an intra-cratonic basin, which was part of the larger Centralian Superbasin (Walter et al., 1994). The latter formed in response to Late Proterozoic basin-wide subsidence with local tectonism (Gravestock and Sansome, 1994), including extensive thrust faulting in the eastern Officer Basin (Gravestock and Lindsay, 1994).

The Petermann Ranges Orogeny lasted from 600 Ma to 540 Ma. This major event involved uplift and reverse faulting, and the formation of stacked thrust sheets (Hoskins and Lemon, 1995) which caused local structural inversion prior to Cambrian deposition (Gravestock and Lindsay, 1994; Gravestock and Sansome, 1994).

A second episode of tectonism related to further thrusting and reactivation of previous structure during middle to late Cambrian.

Later, during the Alice Springs Orogeny, tectonism was limited to the reactivation of existing structures. There was minimal thrust sheet formation at this stage because the

major structures were emplaced during the Petermann Ranges and Delamerian Orogenies (Hoskins and Lemon, 1995).

A cross-section (Fig. 2.4) shows the major structural elements, including thrust faulting, in the Marla area.
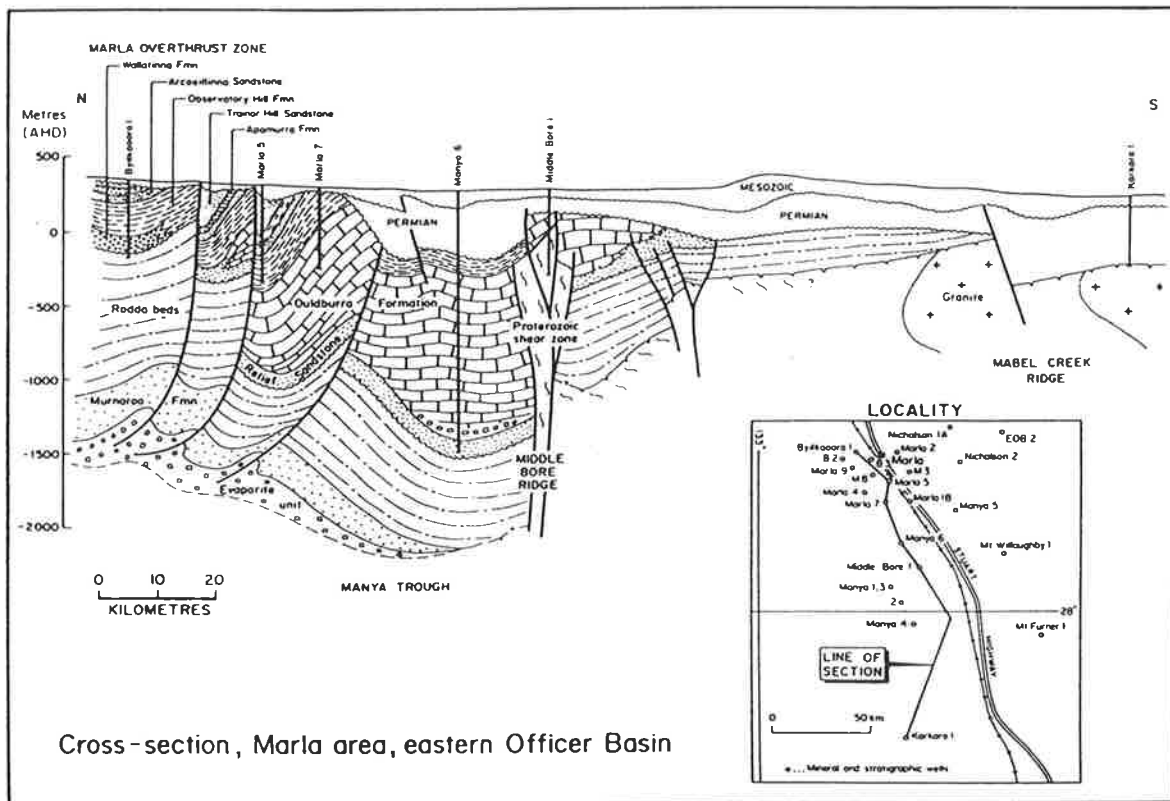
Figure 2.4 Schematic section across the Marla area, Officer Basin (modified from MESA).

2.4   Depositional model-Ouldburra Formation

In the Marla-Manya area, deposition of the Early Cambrian Ouldburra Formation began in small, isolated, halite salinas on sand flats overlying and intertonguing with the marginal marine and partly aeolian Relief Sandstone. Subsequent sporadically emergent conditions

20

resulted in deposition of mixed carbonate and siliciclastic mud flat facies. This stage was followed by widespread deposition of shallow marine carbonates during a marine transgression. Thin carbonate units formed during sea level highstands. Archaeocyathan and algal bioherms, stromatolitic and thrombolitic algal mounds, and thin ooid shoals were developed offshore (Dunster, 1987). Periodic exposure resulted in dolomitisation of these early limestone deposits. Repeated lowering of sea level is evident from supratidal features such as plate breccia, mud cracks and evaporites. Final regression of the epeiric sea, possibly during the late Early Cambrian, is marked by subaerial exposure, culminating in pervasive dolomitisation and secondary porosity generation. A generalised model of the Early Cambrian marine carbonate deposition in the Marla-Manya area is given in Figure 2.5. A palaeolatitude of approximately 5-15°N is inferred for the Ouldburra Formation, based on the Early Cambrian palaeogeographical reconstructions of Cook (1982) and Shergold et al. (1985).

Organic-rich carbonate beds are thin but probably widespread and formed as part of transgressive and highstand systems tracts. Corresponding source rock facies are carbonate mudstone, dolomitic limestone, stromatolitic algal bindstone, microstylolitic limestone and silty dolomitic mudstone which were deposited under anoxic to suboxic conditions.

Primary productivity and early diagenetic processes including bioturbation, partial oxidation and bacterial degradation at the sediment-water interface greatly influenced the quantity and quality of organic matter preserved in these beds.
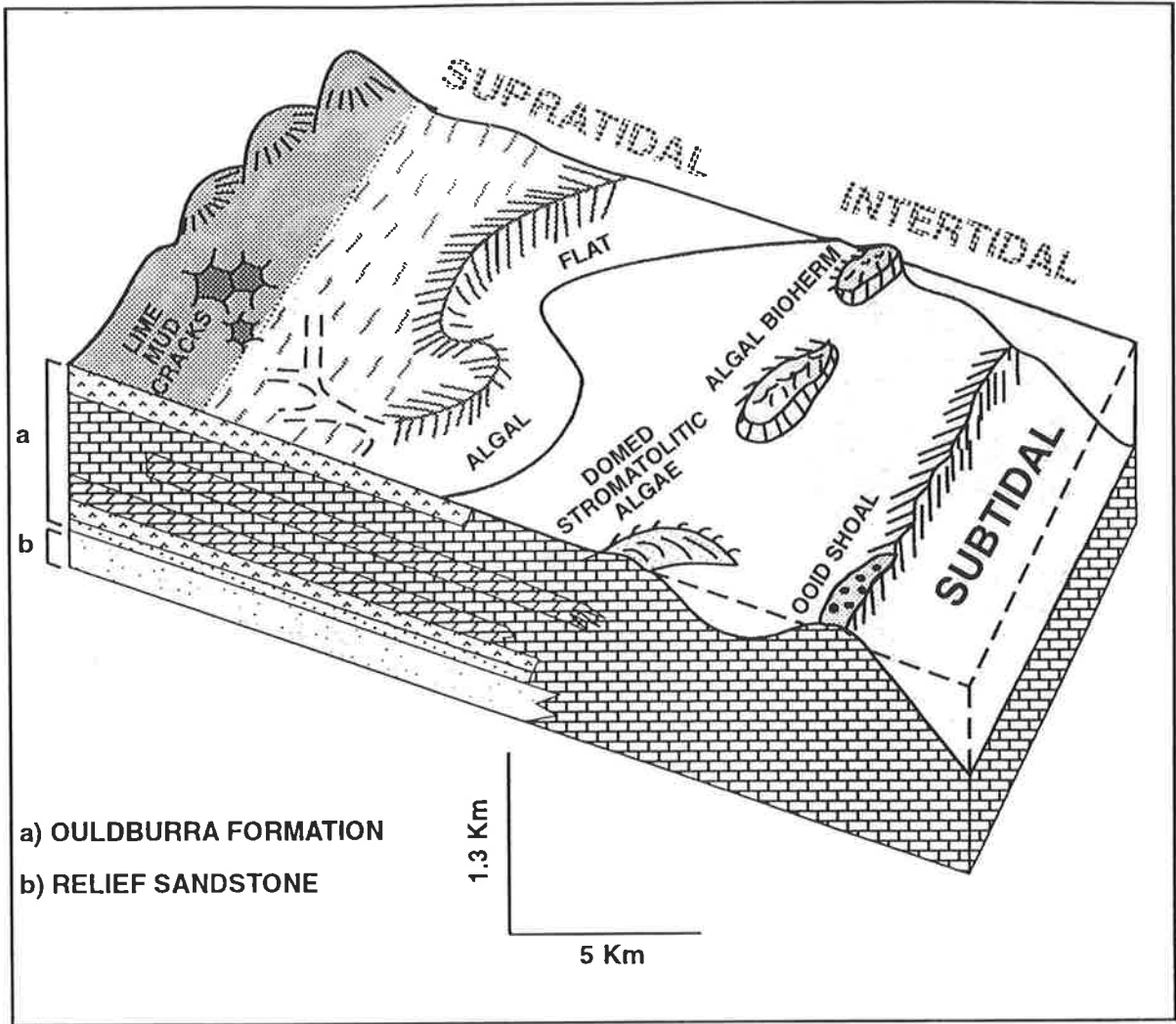
Figure 2.5 Depositional model of the Ouldburra Formation during the Early Cambrian.

CHAPTER 3

DIAGENESIS I - RESERVOIR CHARACTERISATION

3.1   Introduction

Carbonate rocks and sandstones are the two common kinds of reservoir rocks. Most these reservoirs have undergone complex diagenetic processes during and/or after burial. Understanding of these diagenetic changes is essential to exploration for, and optimum development of, hydrocarbon reservoirs in carbonate and sandstone rocks. Carbonate and sandstone diagenesis, although discussed at length in literature, is briefly reviewed here.

Carbonate rocks may be characterised by high initial porosities linked to high-energy environments of deposition. Initial carbonate porosity can sometimes reach 40 to 70 % in modern carbonate sediments (Warren, 1992). This original porosity is usually reduced by early diagenetic cementation, compaction, pressure solution and late-stage cementation. In some reservoirs, initial porosity is preserved or enhanced by dissolution involving both the original particles and any cement, resulting in so-called secondary porosity.

Nevertheless, the occurrence and formation of porosity in carbonate rocks is more variable than in sandstones, because of complex diagenetic processes commonly involved in carbonate rocks which are more susceptible to dissolution.

As a comparison, primary porosity in sandstone is a direct function of texture, fabric, size, sorting, and shape. Thus, porosity is mainly controlled by depositional processes. In the case of carbonates, size and sorting are often controlled by biological rather than the physical parameters associated with transport and deposition. Porosity is superimposed by post-depositional processes such as cementation, compaction, dissolution, neomorphism,

dolomitisation and so on. Furthermore, clastic diagenesis usually involves addition of material to the pore spaces whereas carbonates, being essentially soluble materials, are greatly affected by dissolution and re-precipitation (Lemon, 1992).

Most cementation in carbonates occurs at shallow depths in one of the major diagenetic environments: the vadose, meteoric phreatic zone, mixing zone, and marine phreatic zone (Longman, 1980; Harris et al., 1985). However, the impact of burial diagenesis, particularly in ancient carbonate hydrocarbon reservoirs, may play a major role. Although the understanding of burial diagenesis is very limited, many workers have invoked mechanical compaction, chemical compaction (pressure solution), and deep subsurface brines as porosity reducing agents. The nature of the rocks is also important in responding to chemical compaction prior to burial. This is best illustrated in the study of Halley and Schmoker (1982), in which they derived their Florida data from those rocks that had 75 % or more dolomite and those that had 75 % or more limestone. The shallow limestones have greater porosity than shallow dolomites. However, limestones compact more readily with depth, such that at depths greater than 5700 feet, the dolomite rocks are more porous than the limestone-rich rocks. This is not surprising given that dolomite is a much stronger mineral than calcite both physically and chemically, and will retain its porosity and permeability to greater depth of burial despite chemical and mechanical compaction. In addition, crystals have regularities of size and shape not commonly encountered in limestones (Wardlaw, 1979). These features in general, partly explain why dolomites are more favourable reservoirs than limestones.

Permeability, being a function of pore interconnection, is often very low in carbonate when compared to sandstone reservoirs, but it is often enhanced by fracturing, which is more prevalent and important in carbonates than sandstone reservoirs. As further analysis and discussion of these aspects are beyond the scope of this study, the interested readers are

referred to Choquette and James (1990), Scoffin (1987), Land (1983), Gregg and Sibley (1984), Friedman (1965), Tucker and Wright (1990) and Tucker (1993).

The Ouldburra Formation in the eastern Officer Basin is 1114 m thick in the type section and contains leached carbonate and dolomite zones with significantly higher rates of porosity and permeability. These carbonates together with mixed siliciclastic-carbonate intervals, occur in a series of repeated cycles. The individual limestone and dolomite beds are from 1 to 10 m thick and are widespread (Dunster, 1987). The collective thickness of the dolomitised beds in the type section is 212 m or almost 18 per cent of the total thickness of the formation (Fig. 3.1).
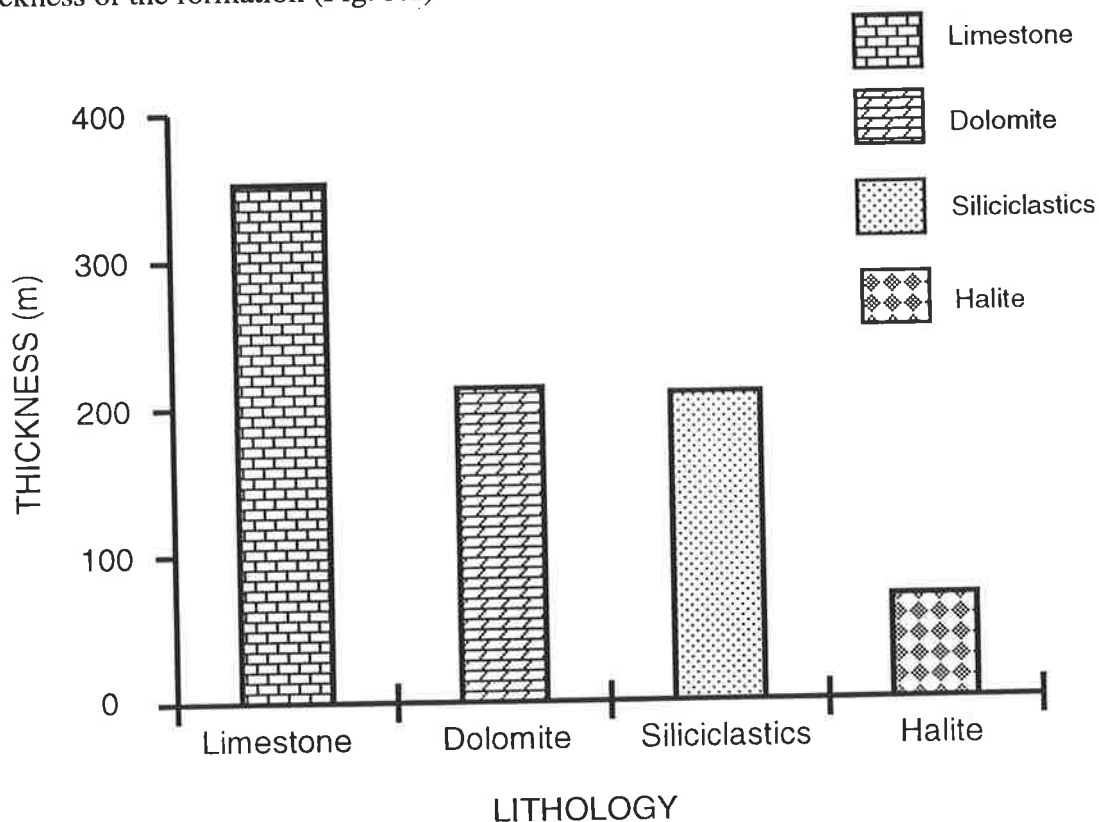
Figure 3.1   Distribution of the main lithologies in type section Manya-6, Ouldburra Formation.

Identification and distribution of dolomite and associated tight mudstone facies are significant from the hydrocarbon reservoir point of view because, in many instances,

25

DOLOMITE   TEXTURES

Syngenetic
(Primary Dolomite)

Replacement Dolomite

Dolomite Cement

Polymodal
Planar-s

Planar(e/s)

Nonplanar
(polymodal)

C.C.D.   P.S.D.   S.D.

Unimodal   Polymodal

Planar(e/s) Planar-e Nonplanar

(nonmimic allochem)   (mimic allochem)   (nonmimic allochem)   (mimic allochem)   Polymodal   Polymodal   Polymodal
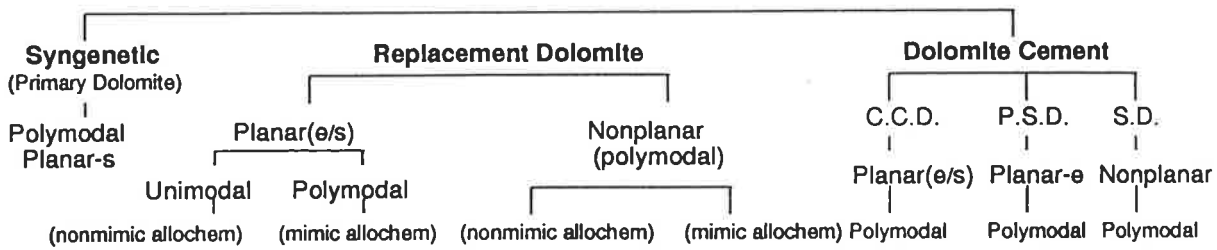
C.C.D. = Coarse crystalline dolomite, P.S.D. = pressure solution dolomite , S.D. = saddle dolomite.

Figure 3.2 Textural classification of dolomite in the Ouldburra Formation (simplified from Sibley and Gregg, 1987).

Study of several dolomitised intervals in Maya-6 indicates that coarse crystalline dolomite (<1 mm) is commonly the non-planar polymodal form and less frequently exhibits planar-s or-e texture. While very coarse crystalline dolomite (<4 mm) exclusively displays a non-planar polymodal texture. Replacement dolomite including fine (<0.062 mm) and medium (<0.25 mm) with nonplanar polymodal texture occurs more frequently than the same but with planar-e and -s texture (Fig. 3.3).
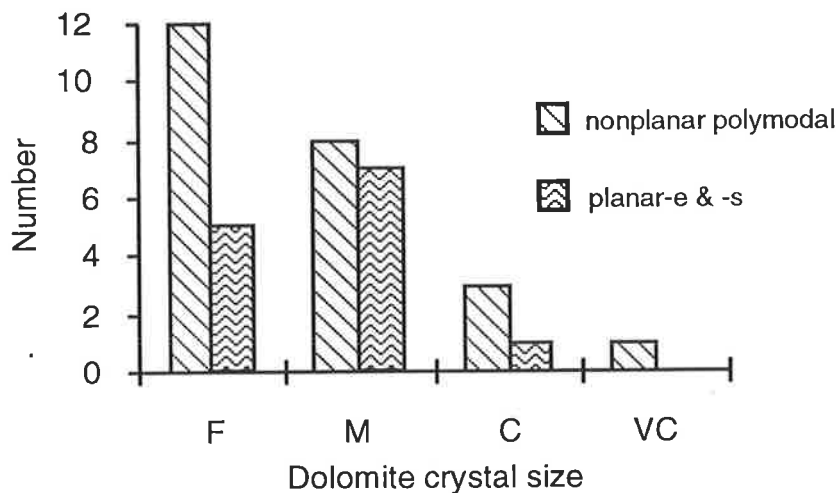
Figure 3.3 Dolomite crystal size distribution in Manya-6.

In a strict sense, planar dolomite crystals have straight boundaries and exhibit straight extinction whereas nonplanar dolomite crystals have curved, lobate, serrated, indistinct, or otherwise irregular boundaries, and they commonly show undulatory extinction. Planar textures are further subdivided as euhedral (planar-e) or subhedral (planar-s) types. Saddle dolomite is classified as nonplanar dolomite.

At low saturation and/or low temperature, crystal growth occurs by nucleation at active sites, producing facetted crystals and planar interfaces. At a higher saturation, referred to as the critical saturation, or above a given temperature, referred to as the critical roughening temperature (50°- 100°C), growth occurs by the random addition of atoms to the crystal surfaces, thereby resulting in nonplanar forms (Sibley and Gregg, 1987).

3.4   Dolomite types

Two genetic types of dolomite, (excluding later diagenetic cement) namely syngenetic (or primary) dolomite and replacement dolomite, are recognised.

Primary dolomite occurs as thin dolostone beds and is the result of penecontemporaneous dolomitisation (Friedman and Sanders, 1967). The presence of lithoclasts of dolostone in lithofacies with an unaltered matrix may be taken as evidence supporting a primary origin. Texturally, syngenetic dolomite crystals are polymodal, planar-s and microcrystalline to very finely crystalline, 15 μm to 70 μm in diameter. This material was precipitated as mud. Primary dolomite is associated with anhydrite and rip-up clasts. Recrystallised anhydrite laths grow displacively within the mud (Plate 3.1a). Dolomitic mudstone of this type is characteristic of an evaporative sabkha environment and more specifically, of an evaporative mudflat environment (J.K Warren, pers. comm., 1993).

Anhydrite occurs both in finely crystalline and elongate forms up to 100 μm in diameter and constitutes almost 5 per cent of the total rock. Much of the anhydrite occurs in distorted laminae. Clastic grains associated with the syngenetic dolomite are mainly quartz with common potash feldspar. Very fine to coarse quartz grains are subangular to rounded and poorly sorted. The clastic grains generally float in carbonate matrix and rarely show point or tangential contacts.

Replacement dolomite is volumetrically the most widespread type observed in the Ouldburra Formation. In fact, recrystallised dolostone is one of the most conspicuous elements of the upper part of the formation. Finely crystalline, non-planar (polymodal) dolomite is the dominant crystal fabric and is believed to have formed at supersaturation, probably at low temperatures. In some stratigraphic intervals, dolomitisation is so pervasive that the fabric of the original limestone is almost obscured (Plate 3.2c). Mimic replacement requires abundant dolomite nuclei unless the allochem being replaced is a single crystal (Sibley and Gregg, 1987). This type of dolostone fabric commonly has low reservoir potential unless associated with neomorphism of early dolomite.

On the other hand, replacement dolostone with mainly planar/polymodal texture, displays varying crystal sizes depending on the original texture of the carbonate rock. The size range is from 50 μm to 100 μm, corresponding to planar-s (sucrosic) and euhedral/subhedral textures respectively. Planar/polymodal dolomite may show mimic or nonmimic replacement. The mimically-replacing dolomite is the most widespread. Retention of the original fabric and allochem ghosts (mimic ooids) recognised in finely crystalline dolomite is related to preferential dolomitisation of a fine grained precursor where nucleation sites favour fabric preservation. Unimodal size distribution generally

indicates a single nucleation event on a unimodal substrate (Sibley and Gregg, 1987). However, in many instances, relict patches of precursor limestone are still retained, indicating incomplete or partial dolomitisation.

In transmitted light, many dolomite crystals (nonplanar, replaced allochems) have a mottled appearance and commonly exhibit straight extinction. Dolomite with these characteristic features was earlier classified as hypidiotopic to chiefly xenotopic (Friedman, 1965; Gregg and Sibley, 1984).

3.5   Dolomite cement

Three genetic types of dolomite cement were identified in the carbonate sequences of the Ouldburra Formation, namely saddle or baroque dolomite, coarse crystalline dolomite, and pressure solution dolomite.

Coarse-crystalline dolomite cement occurs in voids, cavities, in intra-rhomb pore spaces and in fractures (Plate 3.1b). The crystal size is in the range 0.4 mm to 1 mm. The most outstanding feature of coarse-crystalline dolomite cement is that the crystal size increases towards the centre of cavities, much in the way of drusy calcite spar, and it typically exhibits undulose extinction under crossed nicols. Under CL, the coarse-crystalline dolomite typically shows zoning. Alternate orange and dark bands suggest changes in the chemical composition of the depositing fluids. The orange bands may indicate calcium-rich water and dark bands are suggestive of iron-rich fluids (Plate 3.1c). Ferroan dolomite is confirmed by XRD analysis (Appendix I). The occurrence of ferroan dolomite cement is thought to be related to higher temperatures, where crystals grow into cavities and are affected by impurities such as clay and organic matter (Tucker and Wright, 1990). This

30

type of mid to late, coarse crystalline dolomite cement has to be differentiated from limpid dolomite cement (Folk and Land, 1975; Gao et al., 1990), which is clean, rhombohedral and often occurs as void-filling and cross-cutting late cement. Unlike cavity-filling cement, the limpid dolomite cement shows straight extinction.

Pressure solution dolomite is another late cement commonly associated with solution seams and stylolites. It is a planar-e, polymodal, fine to medium crystalline dolomite with straight extinction which was probably precipitated from migrating hydrocarbon-bearing fluids when stylolites were active fluid conduits.

Saddle or baroque dolomite is considered here as nonplanar cement and is common in the Ouldburra Formation. Baroque dolomite is associated with the middle to late stages of burial diagenesis and generally fills the centres of vugs and cavities. The size range of the individual crystals is often between 1 and 4 mm ; crystals are white, and crystal faces are curved, with accompanying sweeping extinction under crossed nicols (Plate 3.1b). The white colour is caused by an abundance of two-phase aqueous fluid inclusions (Allen and Wiggins, 1993). Saddle dolomite is thought to form within the oil window, at temperatures of 60 to 150°C (Radke and Mathis, 1980). This is consistent with the thermal maturity of intraformational source rocks as measured by organic geochemical methods (refer Chapter 7, section 7.8).

The oil-window temperature range of crystallisation of saddle dolomite, the intimate association with migrated hydrocarbons and the presence of abundant two-phase aqueous fluid inclusions, reasonably allows the suggestion that saddle dolomite in the Ouldburra Formation was precipitated by fluids associated with hydrocarbon migration.

31

Determination of homogenisation temperatures of fluid inclusions in saddle dolomite holds much promise for future studies.

3.6   Porosity evolution

A number of factors are involved in porosity development in Ouldburra Formation carbonates. The type of porosity and its extent was mainly controlled by diagenesis. While primary porosity seems to have been low, significant secondary porosity occurs as vugs, intercrystalline pores, grain and matrix dissolution fabrics and rare moldic porosity in carbonate and mixed carbonate-siliciclastic sequences. In the latter, secondary porosity formed at relatively late stages of diagenesis.

Original shelf carbonates that have not been subjected to dolomitisation show little remaining primary porosity. The original voids and vugs are either completely or partially filled by dolomite and silica (chalcedony) cements. The dolomite cements are coarsely crystalline and saddle types related to late stages of burial diagenesis.

The most porous units are widespread, thin dolostone beds 1 to 4m thick, with a thicker leached porous dolomite bed in the upper portion of the Ouldburra Formation in Manya-6.

In addition to intercrystalline porosity, the mixed dolomite-sandstone units show further enhancement of secondary porosity by carbonate matrix, anhydrite and feldspar dissolution. The latter pores formed during the later stages of diagenesis. Consequently, porosity values as high as 27 per cent have been measured from thin mixed dolomite-sandstone units (Fig. 3.4).

3.7   Dolomite reservoirs

The potential dolomite reservoirs identified in this study are ranked on the basis of their porosity distribution and texture into the following groups:-

Rank-I (excellent)

Rank-II (good)

Rank-III (fair to poor)

Rank- IV (very poor)

3.7.1   Rank-I (excellent)

The measured porosities in this rank are in the range of 20 to 27 per cent with corresponding values of permeability from 1400 to 1600 md.   Leached, vuggy and intercrystalline porosities associated with dolomite intervals are conspicuous features of the Ouldburra Formation carbonates and occur at several stratigraphic intervals in most studied wells. Periods of aerial exposure resulted in secondary porosity development (Fig. 3.4). In Manya-6, leached dolomite (Plate 3.3a) is nearly 14 m thick, corresponding to a highstand systems tract which immediately overlies a transgressive tract (Gravestock and Hibburt, 1991). Similar dolomite reservoir units, widespread mainly in the upper portion of the Ouldburra Formation, occur in other wells (Manya-3, Marla-3, Marla-6 and Marla-7), but their thickness varies between 1 and 4 metres. Petrographically, dolomite crystals display planar-s, polymodal textures with sizes in the range of 50 μm to 250 μm (Plate 1d). In most samples, the dolomite crystals are associated with bitumen residue. Gamma ray and density log characters of these potential reservoir units are consistent with petrographical observation and core analysis (Fig. 3.4).
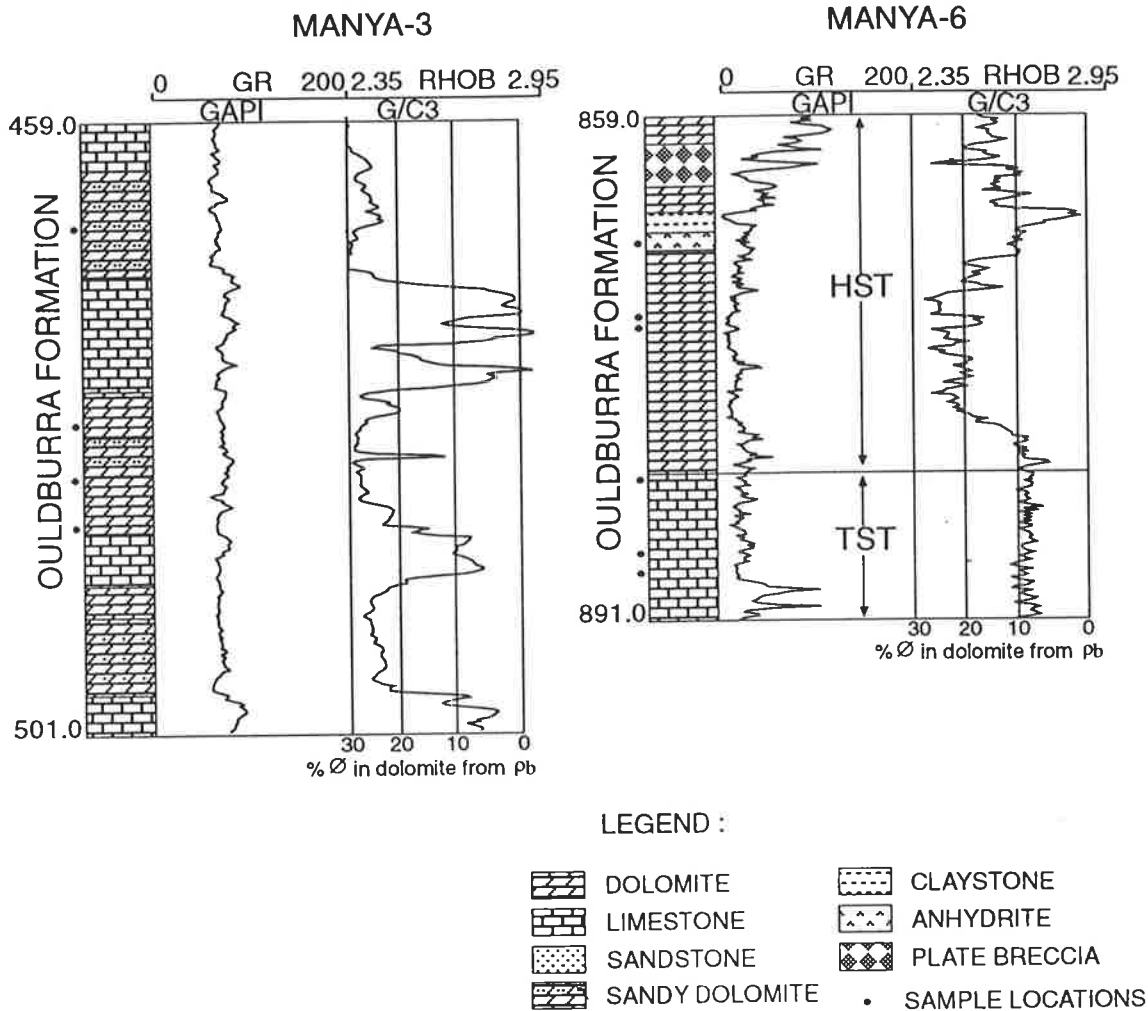
Figure 3.4 Porosity distribution pattern, Ouldburra Formation. Higher porosity occurs mainly in dolomite and mixed carbonate siliciclastics corresponding to highstand systems tracts, whereas the transgressive facies limestones are relatively tight.

The dolomite reservoir unit from Marla-3 (Plate 3.1e) shows uncommon moldic porosity with core porosity of 21 per cent and permeability of 23 md. Although moldic porosity is generally considered to give ineffective permeability due to poor interconnection, grain fracture and cement dissolution have facilitated interconnectivity to some extent in this case. Dolomite crystals occur as both planar-e, cement-replacing, and nonplanar, allochem-replacing dolomite with crystal sizes 90 μm and 15 μm in diameter respectively. Mimic calcite cement is still present and indicates fresh water vadose (meniscus cement)

34

and fresh water or marine phreatic environments (blocky and drusy spar). The original sediment was intraclastic-ooid packstone or wackestone limestone.

Sucrosic (sugary) dolomite with typical intercrystalline porosity is the best potential reservoir unit recognised in this study from Marla-6 (Plates 3.1f and 3.3b). The sugary dolomite displays planar-e and unimodal textures with crystal sizes in the range of 15 μm to 40 μm. It is often associated with hydrocarbon staining. Porosity is generally greater than 25 per cent and effective permeability is high.

3.7.2 Rank-II (good)

The measured and estimated porosities and permeabilities of this reservoir type are in the range 10 to 15 per cent and greater than 300 md respectively. Vuggy and intercrystalline secondary porosity is formed mainly by diagenetic processes. Potential exists for intercrystalline micro-porosity, which is difficult to see using a conventional petrographic microscope. SEM conducted on selected samples revealed further details such as crystal shape, packing, leaching at crystal edges and the presence of intercrystalline microporosity (Plate 3.4). Dolomite crystals occur as planar-s or a mixture of planar-e and nonplanar polymodal textures (Plate 3.2a). Dolomite reservoirs with a mixture of planar-e and nonplanar polymodal textures occur more frequently and are commonly associated with vuggy porosity. Crystal sizes are in the range of 30 μm (nonplanar) to 100 μm (planar-e) with straight compromise boundaries and many crystal-face junctions. This texture is interpreted to form at low supersaturation and/or low temperatures. Other characteristic features are the presence of relict limestone, a cloudy appearance and straight extinction. This evidence suggests that dolomitisation of an original grainstone resulted in two

different crystal textures; planar-e and nonplanar with different crystal sizes. Commonly, planar-e dolomite replaced the early cement while fossil allochems were replaced by nonplanar polymodal dolomite. Consequently, vuggy porosity is associated more with the cement. Two scenarios may explain this kind of relationship. Preferential dolomitisation of sparry calcite cement may result in relatively coarser planar dolomite crystals at cement sites. This is sometimes evident from mimic drusy calcite cement that coarsens towards the cavity centre. A second possible scenario is cavity-filling dolomite cement formed at later stages of diagenesis, indicating two different phases of dolomitisation. Under CL, the cavity-filling planar dolomite is typically zoned (Plate 3.1c).

3.7.3 Rank-III (fair to poor)

Estimated porosities of this group by visual petrographic observation range from 3 to 5 per cent, rarely 8 per cent, with low permeability. Dolomite crystals show planar-s to nonplanar polymodal textures, ranging in size from 30 μm to 250 μm. Mimic replacement and the occurrence of indistinct moldic porosity, together with intercrystalline porosity, are characteristic features. The replaced allochems have a dull, brownish colour that differentiates them from the relatively clean and coarser dolomite cement. The dull and dark appearance of replaced allochems may be explained by the presence of inclusions in the precursor rock. Different views have been proposed to explain the dull and cloudy appearance of the dolomite crystals, including the difference in chemical composition of early limestone, presence of inclusions and degree of supersaturation of dolomitising fluids. Although substantial moldic porosity is generated in places, it seems to be ineffective due to poor interconnectivity (Plate 3.2b). The molds correspond to leached grain nuclei that may have been inherited from an earlier diagenetic event prior to dolomitisation.

3.7.4 Rank-IV (very poor)

Estimated porosity, based on petrography, for this type of dolomite is commonly less than 3 per cent. The dolomite has a nonplanar, polymodal texture and crystal sizes in the range of 40 µm to 80 µm. Nonmimic replacement and ghost peloids are characteristic features, indicating a peloid wackestone precursor. Pervasive dolomitisation of early limestone was probably brought about by highly supersaturated fluids resulting in irregular, indistinct crystal boundaries (Plate 3.2c).

3.8   Hydrocarbon occurrences

Hydrocarbon traces occur in most of the drillholes studied, occurring both in dolostone and mixed carbonate-siliciclastic units. These are generally found as scattered bitumen residues. When associated with porosity, bitumen often fills a void or infills intra-rhomb spaces (Plate 3.2b). In some instances, a substantial amount of hydrocarbon residue is associated with solution seams (Plate 3.2d). Residues of this sort indicate that hydrocarbon migration took place after dolomitisation. The latter solution-seam-associated dolomite represents a synchronous relationship with the migrating hydrocarbon.

Live oil occurs in Marla-6, Manya-6, KD-1 and KD-2A and is thought to be indigenous. This is supported by Rock -Eval pyrolysis and detailed analysis of bitumen extracts of the stained samples (refer Chapter 7, section 7.5).

The hydrocarbons in the Early Cambrian Ouldburra Formation carbonates are found as indigenous material and bitumen residue (dead oil) left after migration. The indigenous material is associated with potential intraformational source rocks. However, the bitumen residues are generally found in association with porosity, fractures and stylolites, along migration paths. The implication is that hydrocarbons were generated and moved in the carbonate and mixed carbonate rocks of the Ouldburra Formation.

3.9   Paragenetic sequence

The paragenetic sequence and porosity evolution of these carbonates are summarised in Figure 3.5. The sequence is complex with a wide variety of diagenetic processes which include cementation, dolomitisation, dissolution, compaction, silicification, dedolomitisation, mineralisation, pressure solution, fracturing and hydrocarbon migration.

3.9.1   Cementation

Although in most cases the original fabric is obliterated due to intense diagenetic alteration, identification of early marine cement and mimic ooids, is still possible even after intensive silicification. Silica replacement is fabric selective (Fig. 3.6). The early calcite cements show meniscus, isopachous (bladed) and mammiliform (botryoidal) textures, indicating fresh water phreatic and marine phreatic environments. The occurrence of blocky equant calcite is another type of common early cement recognised in several samples, particularly in dolomitised sequences, where mimic features are still visible.

Anhydrite and gypsum are common evaporite minerals. Anhydrite is most widespread and replaces gypsum during burial diagenesis. Replacement by anhydrite, barite and celestite and remobilisation of anhydrite are significant diagenetic processes resulting from late burial diagenesis.

3.9.2 Dolomitisation

Dolomite can be explained by at least three types of dolomitisation models; the sabkha, brine reflux and evaporative pumping models (Dunster, 1987). However, the first two models appear to be more applicable. Dolomite commonly appears to have formed prior to compaction and often is fabric-preserving , and interbedded or associated with evaporites and evaporite-dissolution breccias. These features have been taken as evidence of brine reflux dolomitisation by many workers (Allan and Wiggins, 1993 ; Land, 1983).

The evaporative pumping model is a variant of the sabkha model, requiring evaporation to draw saline waters through the sedimentary pile. This is not favoured as the flux of water is thought insufficient to supply enough ions for complete dolomitisation (Morrow, 1988).

Saddle dolomite is thought to form both in mid and late stage diagenetic events, corresponding to sulphate mineral replacement and void filling. The latter saddle dolomite is closely related to hydrocarbon migration fluids.

3.9.3 Compaction

Compaction and overburden pressure also played important roles in late deep burial stages, leading to pressure solution and stylolite formation. Stylolites and solution seams are the most obvious features associated with burial diagenesis in the Ouldburra Formation carbonates. Most stylolites run parallel or slightly oblique to bedding (Plate 3.3c and d). In contrast to vertical stylolites that act as barriers to migrating fluids, the Ouldburra Formation stylolites facilitated lateral movement of migrating hydrocarbons. Recent studies (Leythaeuser et al., 1993) confirm the significance of stylolites in providing migration pathways in carbonate rocks.

		TIME →	
EARLY MARINE	1) Cementation . meniscus . isopachous . mammiliform 2) Minor allochem leaching		
HYPER-SALINE	1) Leaching 2) Dolomitization . Syngenetic . Replacement 3) Secondary Porosity (moldic, intercrystalline, vuggy) 4) Anhydrite cementation		
SHALLOW BURIAL	1) Compaction 2) Silicification 3) Dedolomitization		
DEEP BURIAL	1) Hydrocarbon migration 2) Burial dolomitization . Saddle Dolomite . Pressure solution 3) Mineralization . Pyrite . Sphalerite 4) Stylolitization 5) Fracturing 6) Dissolution		

☐ POROSITY

3.5   Paragenetic sequence and porosity evolution for the Early Cambrian Ouldburra Formation, eastern Officer Basin.

40
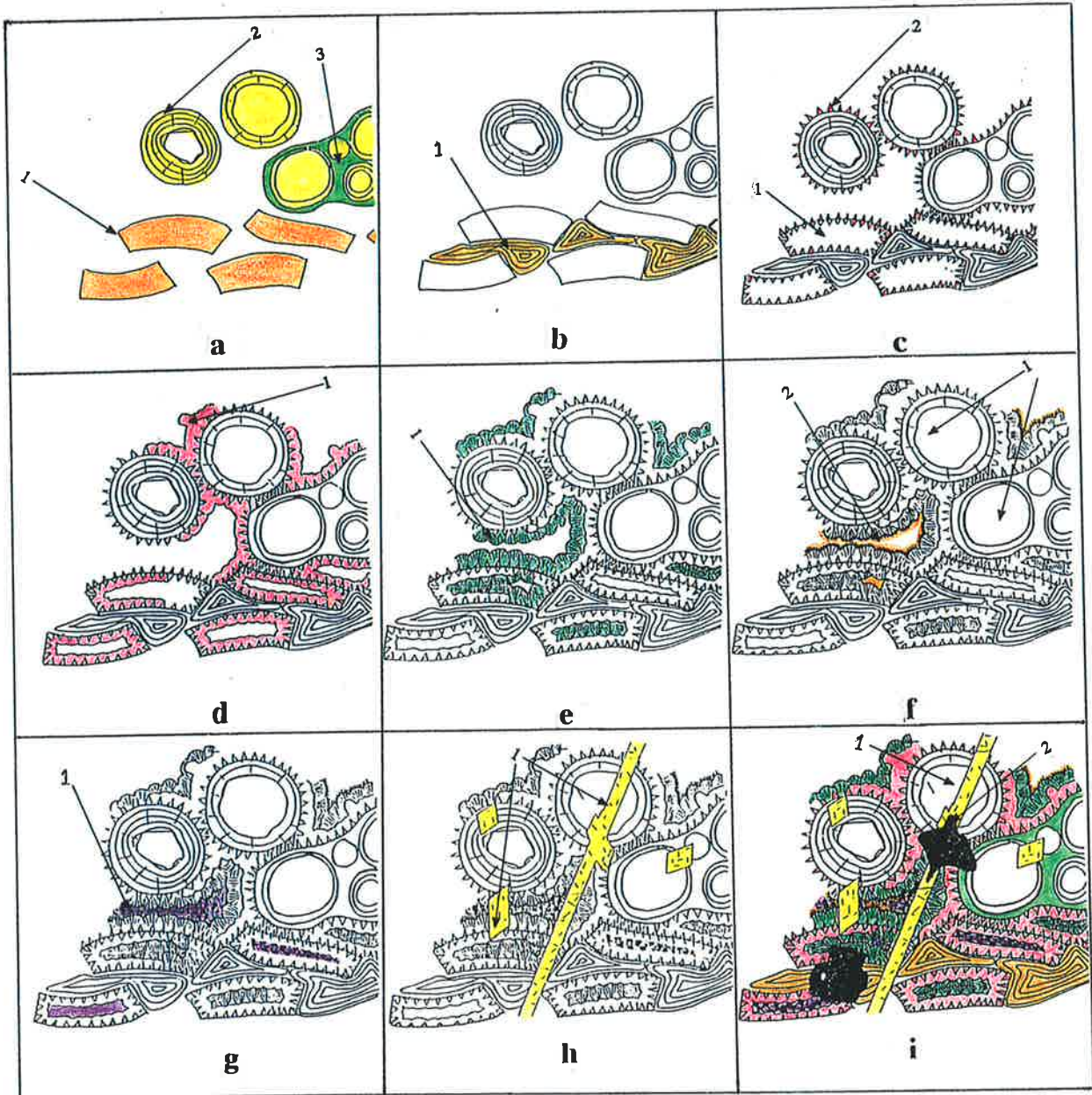
Figure was drawn by Nick Lemon.

Legend :

a (1) calcitic shell	c (2) isopachous cement	g (1) pore-fill chert
a (2) aragonitic ooid	d (1) botryoidal meniscus cement	h (1) cross-cutting dolomite
a (3) grapestone	e (1) mammiliform cement	i (1) dissolution
b (1) calcite cement	f (1) replacement by chert	i (2) sphalerite
c (1) moldic porosity	f (2) chert cement	

Figure 3.6 Diagenetic history of a partially silicified ooid grainstone (Marla-6, 679.33 m).

3.9.4 Silicification and mineralisation

Silicification was probably supplied by at least three different sources including hot hydrothermal fluids, sponge spicule dissolution and calcite cement replacement. The localised, hydrothermally-related silica is generally associated with deep burial diagenesis and is possibly synchronous with sphalerite mineralisation. Abnormally high temperatures, determined by calculated vitrinite reflectance (Ro = 1.68%), from a carbonate bed close to an intensively silicified unit, may support this view (refer Chapter 7, section 7.8).

Pyrite mineralisation is ubiquitous and is often associated with pressure solution textures. Sphalerite occurs relatively late in the sequence in association with silica and replaces early cements or fills fractures.

3.9.5 Dissolution

Grain and matrix dissolution during burial is a significant diagenetic process. Secondary porosity is created mainly by carbonate matrix dissolution with a limited contribution from feldspar grain fracturing and dissolution. Carbonate cement dramatically decreases with depth due to calcite dissolution, probably influenced by a combination of processes such as changes in the pH of the fluids within the basin or by decarboxylation. Acidic fluids produced by CO_2 generation from adjacent organic-rich carbonate layers, can readily dissolve calcite cement, leading to secondary porosity.

3.9.6 Fracturing

Subsurface fracturing in the Ouldburra Formation can be related to tectonic activity, solution collapse or the volume reduction created by pressure solution (Dunster, 1987). Fractures are associated with pressure solution and commonly run parallel or at a slight

angle to bedding (Plate 3.3c and d). In some cases, small fractures or veins are healed by late calcite cement.

3.10 Petrophysics

Gamma ray and density logs were used to assess the radioactivity and porosity distribution in the formation. Porosity was calculated from the density readout using the following equation :

$$\text{Porosity} \quad (\phi) \quad = \quad (\rho ma - \rho b) / (\rho ma - \rho f)$$

where $\rho ma =$ matrix density of dry rock (gm/cc)

$\rho b =$ bulk density recorded from the log

$\rho f =$ density of the fluid

Matrix density was determined by taking into account of mineralogy according to dolomite and sandstone percentages. This was aided by petrographic observation. A constant value of 1.1 gm/cc was used as density of fluid because the drilling fluid used was salt/polymer. In sandy dolomite lithologies, the density log is calibrated on the basis of sandstone and dolomite ratios (Schlumberger, 1979). The calculated porosity from density log is then correlated with plug porosity and that estimated by petrographical observation (Fig 3.7).

Fair to good visual-log correlation exists except for the samples where there is association of microporosity and/or vugs which are difficult to decipher by conventional microscopy. Good core-log correlation is achieved despite the limited number of samples.

43
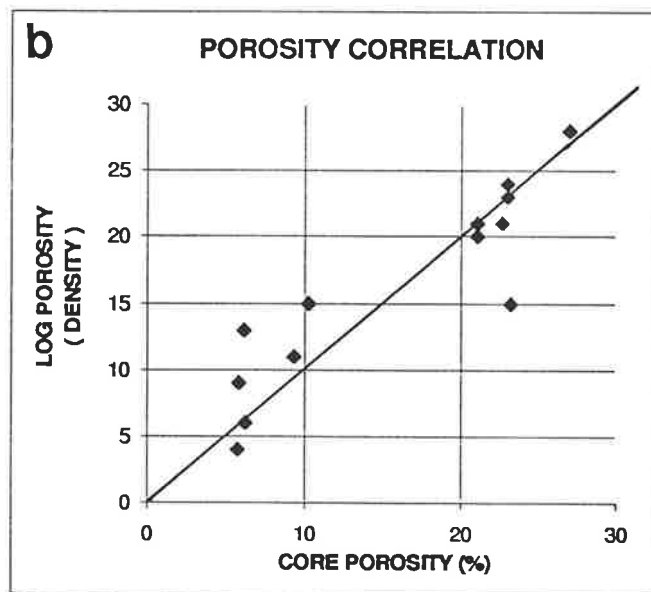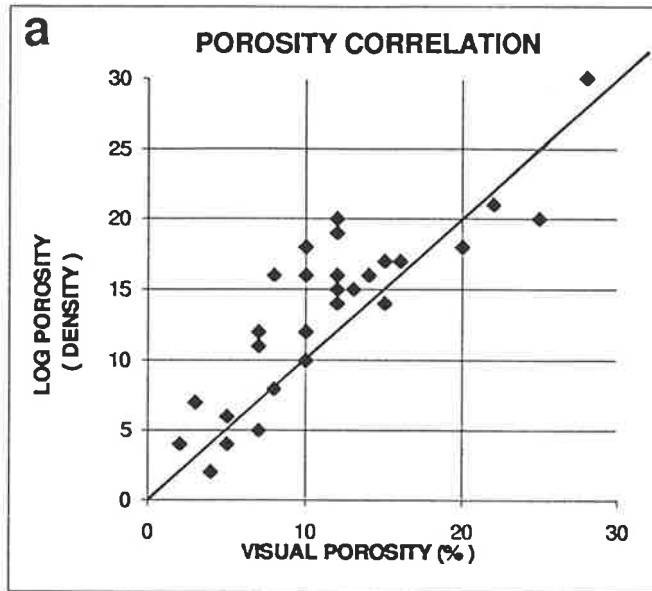
Figure 3.7 a) Visual porosity (thin section) vs log porosity (density) from dolomite and dolomitic sandstone reservoir units. b) Core porosity vs log porosity (density) from dolomite and dolomite sandstone reservoir units.

Porosity and permeability data from conventional core analysis together with porosity evaluation using petrogrphic microscopy and gamma ray and density logs are given in Appendices V and VI.

3.11   Summary

Relict textures of fossil fragments, peloids, ooids and intraclasts, preserved by mimic dolomite replacement and even silica replacement confirm the previous interpretation by Dunster (1987) that the Ouldburra Formation is a very shallow water to marine carbonate sequence interbedded with sandstones and mixed carbonate-siliciclastic beds. Periodic exposure during deposition has led to early dolomitisation and longer periods of subaerial exposure have resulted in pervasive dolomitisation and the development of secondary porosity.

The Ouldburra Formation has had a long and complex diagenetic history. Diagenesis commenced with early marine cements, vadose cement and possible marine phreatic cement. Dolomite replaced calcite, mimicking many of the depositional textures. There was some dissolution of carbonates throughout the formation and of feldspars in the mixed carbonate-siliciclastic units. Pressure solution on burial-created stylolites and was a possible cause of fracturing. There was late stage saddle dolomite cement and, in some cases, localised hydrothermal silicification and sulphide (sphalerite) mineralisation. The presence of evaporites, mainly anhydrite, at the top of shallowing-upwards cycles makes the sabkha and brine reflux models of dolomitisation the most applicable.

Hydrocarbon staining was observed in core and in thin section. This appears to be related to both maturation from kerogen within the sequence and from migrated oil.

The dolomite reservoirs have been described in textural terms and subdivided into Ranks I to IV, from very good, highly porous and permeable rock to very poor quality, tight reservoirs. Subdivision has been helped by reference to plug porosity and permeability measurements of core plugs and petrophysical analysis. The better reservoirs have sugary dolomite with intercrystalline porosity, some with leached vugs and minor moldic porosity linked by good intercrystalline porosity. Exposure early in the diagenetic history of these sequences is largely responsible for the good reservoir quality observed near the tops of shallowing-upwards cycles.

CHAPTER 4

DIAGENESIS II - STABLE ISOTOPE STUDY

4.1   Introduction:

Isotopes are atoms whose nuclei contain the same number of protons but a different number of neutrons.   Only stable, non-radioactive isotopes of oxygen, carbon and hydrogen are studied in dolomites and formation waters. The abundance of the key isotopes relevant to sedimentary studies is in nature is :

Oxygen $^{18}O = 0.2$ %, $^{16}O = 99.76$ %;

Carbon $^{13}C = 1.11$ %, $^{12}C = 98.89$ %   (adapted from Allan and Wiggins, 1993)

Hydrogen $^{2}H = 0.02$ %, $^{1}H = 99.98$ %

These isotopes are significant because they vary in natural substances as a function of processes such as photosynthesis, evaporation, precipitation, cementation and dolomitisation, and can therefore be used as tracers of these processes. The ratios of ^{18}O to ^{16}O in waters and rocks and of ^{13}C to ^{12}C in kerogen, oils and rocks are also of interest because they reveal diagenetic information (Allan and Wiggins, 1993).

Because the ratios between isotopes with such varied natural abundance produces unwieldy numbers, the δ ("delta") notation is used to express isotope proportions. $\delta^{18}O$, $\delta^{13}C$ are defined as :

$\delta^{18}O = [(^{18}O/^{16}O \text{ sample} - {}^{18}O/^{16}O \text{ standard}) / {}^{18}O/^{16}O \text{ standard}] * 1000$

$\delta^{13}C = [(^{13}C/^{12}C \text{ sample} - {}^{13}C/^{12}C \text{ standard}) / {}^{13}C/^{12}C \text{ standard}] * 1000$

The δ value is the relative, not the absolute, difference in these ratios between a sample and a standard. Differences are expressed in parts per thousand for $\delta^{18}O$ and $\delta^{13}C$, or "per mil", symbolised by "‰." If the $^{18}O/^{16}O$ ratio or $^{13}C/^{12}C$ is smaller in the sample than in the standard, then sample is depleted in ^{18}O or ^{13}C relative to the standard, and the δ value is a negative number. Conversely, if $^{18}O/^{16}O$ ratio is larger in the sample than in the standard, then the sample is enriched in ^{18}O relative to standard, and its δ value is a positive number. Substances which are depleted in the heavier isotope are referred to as "lighter" or just "depleted"; if they are enriched in the heavier isotopes, they are "heavier or enriched".

4.2 Results and discussion

For isotope analysis purposes, dolomites have been divided mainly into two groups, namely replacive dolomite and cement dolomite.

4.2.1 Replacive dolomite

Replacive dolomite is further subdivided into low-temperature fine crystalline dolomite and relatively high-temperature, coarse crystalline dolomite.

Early low-temperature dolomite that formed in sabkha and reflux marine environments, such as dolomite from drillholes Marla-3 (depth intervals, 557.60 m and 573.00 m) and Marla-6, 368.00 m), is interpreted as replacive. $\delta^{18}O$ values of these dolomite are close to -6.0 ‰ indicating relatively low temperature dolomitisation (Table 4.1). Vug-filling calcite associated with the sample (Marla-3, 573.00 m) showed more depletion in $\delta^{18}O$ (-12.82 ‰) and $\delta^{13}C$ (-4.64 ‰) values suggesting higher temperatures of precipitation of calcite cement

Table 4.1 Carbon and oxygen isotope data for the Ouldburra Formation dolomites, Early Cambrian, Officer Basin.

Well	Depth (m)	$\delta^{13}C$	$\delta^{18}O$	Description	Environment of dolomitisation
Manya-3	192.700	1.64	-9.45	coarse crystalline replacive dolomite (matrix)	shallow burial
Manya-3	357.86	-0.77	-11.10	coarse crystalline dolomite cement (vein-filling)	shallow to deep burial
Manya-3	385.00	-0.91	-15.21	**late deeper burial,** C.C.D. & saddle dolomite cement (vug-lining)	deeper burial
Manya-6	889.50	0.27	-18.63	**late deeper burial,** C.C.D. & saddle dolomite cement (vug-lining)	deeper burial
Manya-6	896.46	1.75	-9.48	**mid to late burial,** C.C.D. & saddle dolomite cement (vug-filling)	deep burial
Manya-6	956.83	1.86	-10.21	**mid to late burial,** C.C.D. & saddle dolomite cement (filling stromatactoid cavities)	shallow burial
Manya-6	1359.17	-1.53	-8.19	replacive dolomite (mixed dolomite/sandstone & evaporite)	shallow burial
Marla-3	557.60	-0.38	-5.91	replacive dolomite	sabkha, supratidal facies
Marla-3	573.00	-4.64	-12.82	**late** calcite and gypsum cements (vug-filling)	? shallow to deep burial
Marla-3	573.00	0.04	-6.00	replacive dolomite (matrix)	sabkha
Marla-6	368.00	-0.21	-6.06	replacive dolomite (sucrosic with bitumen traces)	sabkha
Marla-6	437.80	0.81	-7.67	replacive dolomite (matrix)	? sabkha or shallow burial
Marla-6	440.00	1.31	-8.35	replacive dolomite	shallow burial
Marla-6	440.00	-1.82	-9.65	**late** calcite & gypsum cements (vug-filling)	? shallow to deep burial
Marla-6	666.40	-0.72	-10.48	replacive dolomite & bitumen traces	? shallow to deep burial
ANU-P3		2.38	-0.06	PDB STANDARD	

N.B. C.C.D., coarse crystalline dolomite.

at later stages of burial diagenesis. The depletion in the $\delta^{13}C$ value of calcite cement may also indicate a minor hydrocarbon contribution as detected in the core plug.

Furthermore, low-temperature dolomite petrographically displays planar-e to planar-s fabric and straight extinction with crystal size that ranges between 15 μm to 40 μm. Some dolomite of this type is often associated with anhydrite and gypsum and lacks any evidence of alteration such as crystal ordering, exsolution, and solution precipitation. A supratidal type of environment may be inferred. Because the $\delta^{18}O$ signature of marine carbonate material was significantly lighter in the early Paleozoic (Cambrian through Devonian) than in the rest of the Phanerozoic (Allan and Wiggins, 1993), these three samples (Fig. 4.1a) are interpreted to be "least-altered" compared to other replacive dolomites.

Most replacive dolomites in the Ouldburra Formation have depleted $\delta^{18}O$ values i.e., more negative than -6.0 ‰, suggesting higher temperatures of formation but petrographic examination indicates that the initial low-temperature dolomite has been subjected to at least two phases of dolomitisation during early burial. Partial and complete recrystallisation of early dolomite is often evident. The $\delta^{18}O$ signature of such dolomites needs to be interpreted carefully (Gao, 1990, Gao and Land, 1991).

Petrographically, the recrystallised replacive dolomite has a larger crystal size with dark centres superimposed on early, relatively finely crystalline dolomite. This type of relationship is generally characteristic of dolomite with fair to good porosity. The recrystallisation at elevated temperatures during early burial must have changed the isotopic composition of the solid phase toward more depleted values (Land, 1983). Hence, replacive dolomite sediments of initially marine water origin, record surprisingly more depleted $\delta^{18}O$ values in the range of -7.67 ‰ to -10.48 ‰. This seems to be the most likely reason why some replacive dolomite in the Ouldburra Formation neither solely reflects the initial hypersaline signature, nor the

50
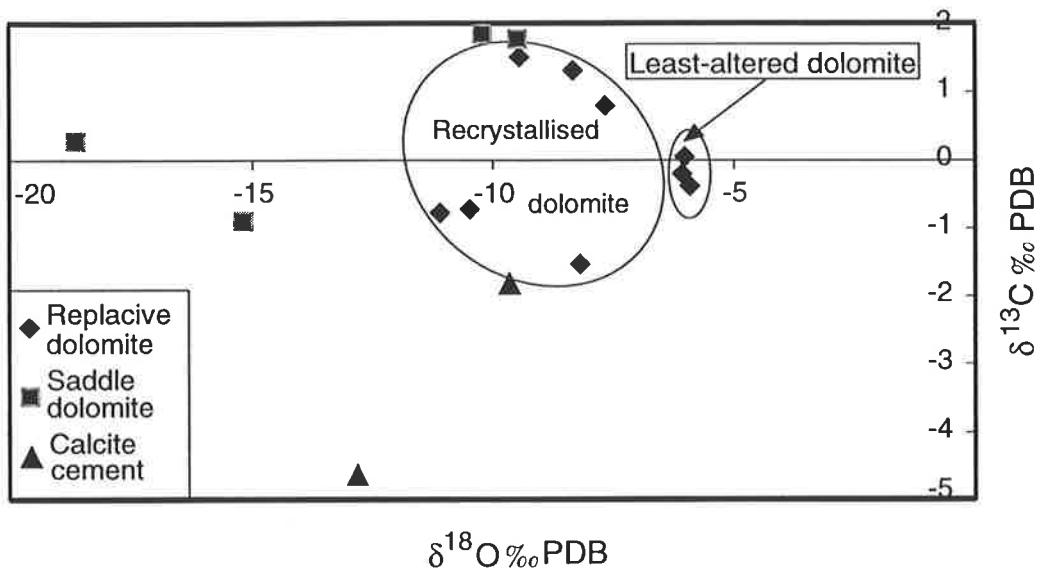
Figure 4.1 (a) Carbon and oxygen isotopic composition of dolomites from the
Ouldburra Formation, Officer Basin.
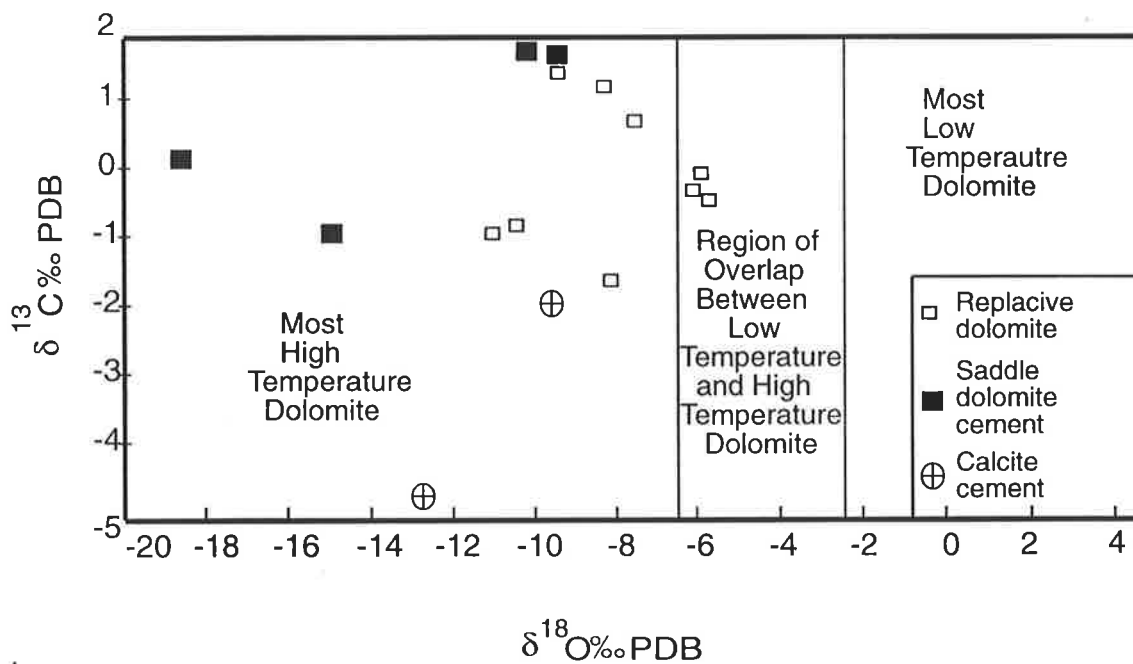
Figure 4.1 (b) Graphical summary of isotope data, showing regions of low,
high temperatures and region of overlap between the low and
high temperature dolomite (simplified from Allan and
Wiggins, 1993).

relatively vigorous reaction during acid treatment. The more depleted $\delta^{18}O$ value of this saddle dolomite when compared to other saddle dolomites is either caused by the co-existing calcite or by later burial dolomitising fluids. In such cases, determination of the homogenisation temperature of fluid inclusions in the saddle dolomite is recommended.

Figure 4.1a is a $\delta^{18}O$ vs $\delta^{13}C$ crossplot which compares the least-altered with the recrystallised dolomite, and indicates that most replacive dolomites could have formed at the surface or during shallow burial. The same carbon and oxygen isotope data shown in Figure 1a, is replotted on high temperature, low temperature dolomite plot (Fig. 4.1b). All but three values fall in the high temperature dolomite field. These three dolomites, from drillholes Marla-3 and -6 which have been assigned to the sabkha environment (Table 4.1), fall within the region of overlap between low temperature and high temperature dolomites.

Two saddle dolomites plot in the higher temperature field, consistent with their petrographic interpretation as mentioned before.

In addition to dolomite, late diagenetic calcite, filling fractures and vugs, was also subjected to carbon and oxygen analysis in order to assist petrographic interpretation.

Oxygen isotopic compositions ($\delta^{18}O$) of calcite cement are in the range of -9.65 ‰ to -12.82 ‰, more depleted in $\delta^{18}O$ values when compared to that of the host dolomite (Fig. 4.1a and b). Core and petrographic examinations of these samples clearly indicate that calcite cement postdates replacive dolomite.

Theoretically, the oxygen isotope values of dolomite that precipitated from seawater should be between 3 ‰ and 6 ‰ heavier than those of calcites precipitated in marine seawater (Fig. 4.2a). Natural examples, mostly from the Holocene with known reaction conditions, suggest 2 ‰ and 4 ‰ difference between a co-existing calcite and dolomite (Land, 1983).
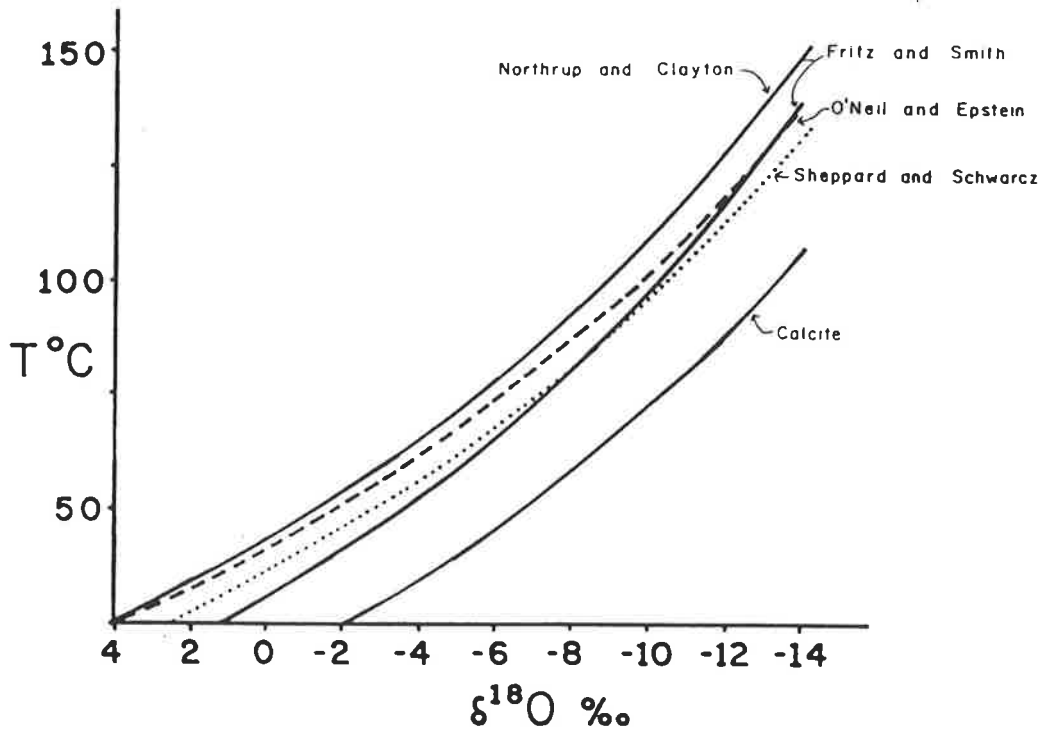
Figure 4.2 (a) Equations, by different investigators, that depict the relationship between isotopic compositions of dolomite, water and temperature. The equation for calcite is also plotted (O' Neil et al., 1969) that defines a Δ value (δ dolomite-δ calcite) which is between 3 and 6‰ (plus about 0.8 ‰ to allow for differences in phosphoric acid fractionation factors for the two minerals if reported on the PDB scale (after Land, 1983).
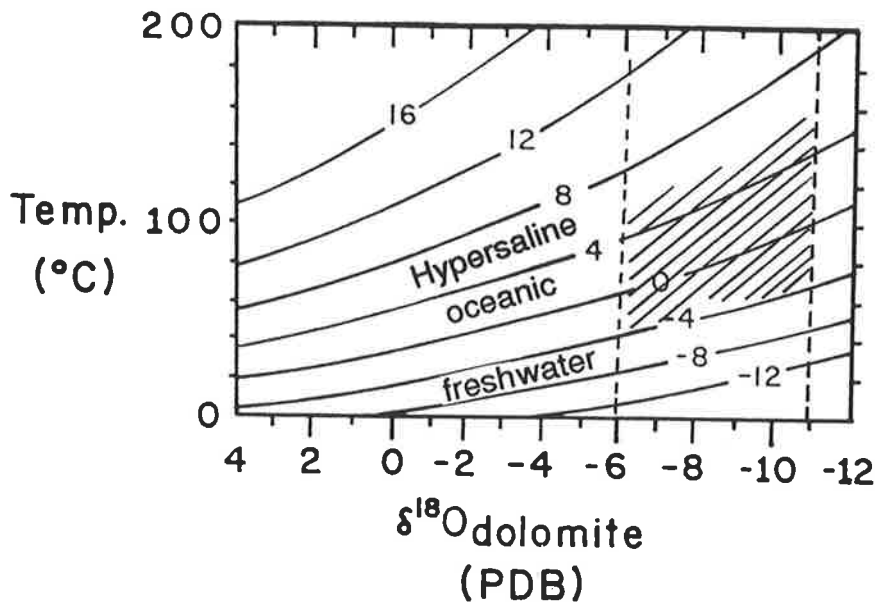
Figure 4.2 (b) Graphical representation of the oxygen isotopic equilibrium of dolomite and the water it precipitated from (SMOW scale) and temperature. The area between dotted represents the range of $\delta^{18}O$ values for the replacive dolomites from the Ouldburra Formation. The hachured region represents the possible range of fluid compositions (modified from Land, 1983).

Regardless of recrystallised dolomite, the oxygen isotopic signatures of the least-altered host dolomite and co-existing calcite is in agreement with the above view postulated by Land (1983). The sample from drillhole Marla-3, 573.0 m depth, clearly shows this kind of relationship (Table 4.1). In such instances, timing of calcite cementation solely on the basis of isotopic data has to be dealt with cautiously. Figure 4.2a illustrates the relationship.

4.2.3 Temperatures calculated from isotopes

Assuming that the least-altered dolomites formed from sea water depleted in $\delta^{18}O$ by as much (SMOW) as -3 ‰, with a relatively elevated temperature compared to present day, then the calculated temperature for all early replacive dolomite would be approximately 324° Kelvin or 52° Celsius.

Considering the $\delta^{18}O$ value of -5.9 ‰ (PDB) for the least-altered dolomite and corresponding $\delta^{18}O$ value of sea water as -3 ‰ (SMOW), the temperature at which dolomite crystallised can be calculated by using the following equations (Allan and Wiggins, 1993).

$\delta^{18}O$ (SMOW) = [(1.03086)] * $\delta^{18}O$ (PDB Scale) + 30.86   Eq.I

$\delta^{18}O_{dol} - \delta^{18}O_{water} = [3.20 * 10^6 \, T \, (°K)^{-2}] - 1.5$ Eq.II

First, the dolomite $\delta^{18}O$ value from PDB scale is converted to the SMOW scale using Eq.I :

$\delta^{18}O$ (SMOW) = [(1.03086 * (-5.91) + 30.86] = + 25.98

Using Eq.II, the temperature is then calculated :

$(25.98) - (-3) = [(3.2 * 10^6 * T(°K)^{-2}] - 1.5$

and rearranging :

$T(°K) = [(3.2 * 10^6) / (28.98 + 1.5)]^{1/2} = 324.2° \, K \text{ or } 51.7° \, C$

An alternative graphical method to obtain temperature from $\delta^{18}O$ is given in Figure 4.2b

4.3 Summary

Petrographic studies, together with carbon and oxygen analyses, suggest that at least three types of temperature-related dolomites are present.

Firstly, low-temperature dolomite referred as "least-altered" is assigned to sabkha and supratidal environments.

Secondly, replacive dolomite, which is volumetrically the most widespread, shows a range of light / depleted $\delta^{18}O$ values reflecting recrystallisation temperature rather than inheritance from an early low-temperature dolomite.

Thirdly, calcite cement formed during burial, postdates the early replacive dolomite and sometimes co-exists with late saddle dolomite.

Lastly, saddle dolomite cement is relatively more depleted in $\delta^{18}O$ values (<-10 ‰) suggesting it is a later cement phase with a higher temperature origin.

CHAPTER 5

DIAGENESIS III - FLUID INCLUSION MICROTHERMOMETRY

5.1   Introduction

The past decade has witnessed the significance of fluid inclusion studies in the understanding of the physical and chemical history of fluids in sedimentary basins. At present, fluid inclusion studies, together with detailed petrographic studies and geochemical methods provide an accurate interpretation of the diagenetic history of ancient rocks. As defined by Goldstein and Reynolds (1994), 'fluid inclusions are fluid-filled vacuoles sealed within minerals'. These inclusions may be considered to as time capsules storing information about ancient temperatures, pressures, and fluid compositions.

In this study, fluid inclusion work was performed in conjunction with detailed petrographic study and stable isotope analysis on carbonate cements (calcite and dolomite) from the Ouldburra Formation in order to understand composition and temperature of fluids within the paragenetic framework.

5.2   Results and discussion

Three representative samples with calcite and dolomite cements were selected from drillhole Manya-6 (depth interval 956.83–896.46 m). These contain isolated fluid inclusions characterised by an aqueous liquid and a small vapour bubble. Microthermometric measurements were focused on both calcite- and dolomite-hosted fluid inclusions (n = 35) which were mainly concentrated within the cores and crystal growth zones which suggest a primary and coeval origin. Cubic daughter crystals, identified as

halite, were observed in several inclusions hosted within dolomite, but none were observed within calcite. All the studied two-phase inclusions are liquid-dominated and have relatively consistent ratios of liquid to vapour.

5.2.1 Early calcite

The early calcite cement appears as void-filling crystals immediately overlain by saddle dolomite. The calcite contains large inclusions with the longest dimension (Fig. 5.1) up to 60 μm. Both all-liquid (one-phase) and liquid-vapour (two-phase) inclusions were recognised. The two-phase fluid inclusions homogenise at 41 to 50°C, indicating that the calcite cement formed within the temperature range 41– 50°C. The initial melting (Te) and final melting (Tm) temperatures for fluid inclusions hosted within the early calcite cement are from -52 to -50°C and -30 to -6°C (Table 5.1 and Fig. 5.3c) respectively, suggesting formation of the calcite from saline water with approximately 10 wt.% NaCl which is equivalent to a synthetic H_2O-NaCl model constructed by Goldstein and Reynolds (1994).

5.2.2 Late calcite

The late-calcite cement occurs as a void fill and is intimately associated with saddle dolomite and coarse crystalline dolomite. The fluid inclusions hosted within the late-stage calcite are relatively smaller in size (18.6 μm) than those in the early calcite and homogenise at higher temperatures (132–170°C). This suggests that late-calcite formed in a range between 130–170°C (Table 5.1). The initial (Te) and final (Tm) melting temperatures are recorded as -75 to -62°C and -32 to -30°C respectively, suggesting that fluids precipitating the late calcite cement were more saline in composition, probably

containing 25 wt. % NaCl corresponding to H_2O-NaCl-$CaCl_2$ system (Goldstein and Reynolds, 1994).

5.2.3 Early dolomite

Early dolomite cement appears as coarse crystalline crystals that commonly fills void spaces and contains inclusions that homogenise at intermediate temperatures (60 - 68°C). Unfortunately no Te and Tm measurements were made on inclusions hosted within the early dolomite cement because they decrepitated at the increased temperatures associated with the other fluid inclusion measurements. Only one three-phase fluid inclusion hosted within early calcite was noted which probably contains pure CO_2 (Shepherd, et al., 1985) that disappeared at -52°C, with Te and Tm recorded as -75°C and -30°C respectively. The temperature of homogenisation was 66°C.

5.2.4 Saddle dolomite

Saddle dolomite commonly occurs as coarse crystals (1 mm) and contains almost all types of fluid inclusions, including common all-liquid (one-phase), liquid-vapour and three-phase inclusions characterised by the presence of cubic halite daughter crystals (Fig. 5.2a). Most all-liquid inclusions in saddle dolomite are very small (<3 μm) and liquid-vapour inclusions are irregular in shape and range in diameter from 8 to 19 μm (longest dimension) . Halite-bearing inclusions have a bigger size range (15–19 μm) and almost always record a higher temperature compared to the surrounding smaller inclusions.

Table 5.1 Fluid inclusion results showing homogenisation (Th), eutectic (Te) and final melt (Tm) temperatures from the Ouldburra Formation carbonates Officer Basin.

Well	Depth/m	Mineral and inclusion type	Th (°C)	Te (°C)	Tm (°C)
Manya-6	889.50	**Early calcite**			
		primary, two-phase inclusion	41	-30	-6
		primary, two-phase inclusion	45	-51	-7
		primary, two-phase inclusion	49	-50	-6
Manya-6	896.46	primary, two-phase inclusion	50	-52	-27
		Late calcite			
		primary, two-phase inclusion	146	-72	-28
		primary, two-phase inclusion	170	-75	-30
Manya-6	956.83	primary, two-phase inclusion	132	-62	-32
		primary, two-phase inclusion	136	-	-
		primary, two-phase inclusion	140	-	-
		primary, two-phase inclusion	151	-	-
		primary, two-phase inclusion	160	-	-
		primary, two-phase inclusion	170	-75	-28
		Early dolomite			
Manya-6	896.46	primary, two-phase inclusion	60	-	-
		primary, two-phase inclusion	68	-	-
		primary, three-phase inclusion	66	-75	-30
		Saddle dolomite			
Manya-6	889.50	primary, two-phase inclusion	142	-60	-26
		primary, two-phase inclusion	159	-61	-27
Manya-6	896.46	primary, two-phase inclusion	124	-	-
		primary, two-phase inclusion	144	-	-
Manya-6	956.83	primary, two-phase inclusion	151	-65	-29
		primary, three-phase inclusion	160	-63	-30
		primary, two-phase inclusion	206	-65	-30
		primary, two-phase inclusion	222	-64	-27
		primary, two-phase inclusion	240	-65	-
		primary, three-phase inclusion	332	-65	-30

The sample from 956.83 m in Manya-6, with stromatactoid cavity-filling saddle dolomite and calcite cement, provided significant information regarding the temperature regimes experienced by the sedimentary basin. To the author's knowledge, this is the first attempt to evaluate the temperature regimes involved in the Early Cambrian carbonate sequences (Ouldburra Fm) by combining fluid inclusion, stable isotope and organic geochemical analyses. Fluid inclusions hosted in the aforementioned saddle dolomite homogenise at variable temperatures (124–332.2°C). Associated halite-bearing inclusions show higher homogenisation temperatures ranging from 160 to 332.2°C, and cubic halite daughter crystals disappear at temperature much lower than Th in all the examined three phase inclusions. Figure 5.2b-h illustrates the sequence of events occurring on heating. At 30°C, the larger three-phase inclusion characterised by the presence of a cubic halite crystal, and smaller two-phase inclusions located at the right are concentrated at crystal growth zones, reflecting a primary origin (Fig. 5.2b). On heating, the vapour bubble in the three-phase inclusion slightly contracts and halite crystal tends to loose its cubic shape (Fig. 5.2c) and the vapour bubble in the smaller inclusions starts moving to the centre. At 183°C, the halite daughter mineral becomes smaller but the vapour bubble does not show any significant changes, whereas the vapour bubble in the smaller inclusions has just homogenised (Fig. 5.2d). On excess heating, at 207°C, the daughter halite mineral has almost totally dissolved and the vapour bubble changes in size (Fig. 5.2e). The temperature of halite disappearance defines the bulk density of the fluid inclusion. On further heating (297 to 312°C), the vapour bubble is quite small and rounded in shape (Fig. 5.2f and g). At 332.2°C (temperature of homogenisation) the vapour bubble disappears (Fig. 5.2h). The homogenisation temperature in this particular sample was measured three times and precision was ± 0.1°C. Recorded Te and Tm for the three-phase inclusion are -65 and

-30°C indicating that fluid inclusion originated from saline waters containing about 27 wt % NaCl possibly brought from dissolution of halite layers at the bottom of the formation. An H_2O-NaCl-$CaCl_2$ model composition with approximately 27 wt. % NaCl may be applied (Goldstein and Reynolds, 1994). Homogenisation and final melt temperatures of the early dolomite and saddle dolomite fluid inclusions are graphically represented in Figure 5.3b and c.

The extremely high temperatures of homogenisation recorded in this case are meaningless in terms of temperature of cement formation but merely reflect the trapping of fluids from a heterogeneous system. Goldstein and Reynolds (1994), on the basis of extensive research on fluid inclusions, vehemently argue that the occurrence of such anomalously high temperature inclusions is related to partial re-equilibration and stretching of previously formed inclusions at elevated temperatures due to invasion of hot burial fluids. The thermal re-equilibration is facilitated by leakage and refilling of primary cavities with later fluids with elevated temperatures. Nevertheless, mechanisms which significantly cause Th to exceed the temperature of cement formation, such as internal generation of methane due to hydrocarbon cracking, are not ruled out. On the other hand, the irregular shape and large size of the inclusion, and the less resistant nature of the hosting mineral, would suggest re-equilibration of the fluid inclusion. Furthermore, the same dolomite crystal records at least four different temperatures of homogenisation (163, 206, 226 and 332.2°C), indicating some fluid inclusions have re-equilibrated significantly beyond their entrapment temperatures. Significantly smaller inclusions (<5 μm) are unaffected or least re-equilibrated. However, the presence of these inclusions recording different temperatures (Th) in close proximity in the same growth zone (identified only in transmitted light), may

also suggest fluid entrapment at different times, perhaps millions of years apart. In instances like this, luminescence techniques may provide valuable information as to the origin of these inclusions (Goldstein and Reynolds, 1994).

Although re-equilibration commonly causes changes to inclusions which leave them unrepresentative of original entrapment conditions, they still preserve a later record of burial temperatures and fluid compositions which might be gleaned from the inclusions (Goldstein and Reynolds, 1994).

It appears that less than 10 % of the fluid inclusions hosted within the saddle dolomite with Th in the range of 151–161°C record faithful conditions of dolomite precipitation. As already mentioned, this Th corresponds to small (<5 μm) inclusions with spherical shapes that survived re-equilibration at elevated temperatures.

The fluid inclusion data is entirely consistent with petrographic observation and accurately defines the timing of the diagenetic phases as discussed in previous chapter.

The question whether or not the unusual higher temperatures detected by the fluid inclusion study are related to invasion of hot hydrothermal fluids operating locally or on a large scale is a point which warrants further investigation. However, organic geochemical maturity parameters (VRcalc derived from methylphenanthrene index analysis) provided new data for thermal history analysis. The VRcalc is on the basis of six samples from four drillholes (Manya-6, Marla-3, 6 and 7) located in the northeastern Officer Basin which show a variable range (1.00–1.68 %; refer Chapter 7, section 7.8).

It is unlikely that the basin has experienced higher temperatures on a large scale otherwise all the organic matter would reflect these elevated temperatures.

a

b

c

d
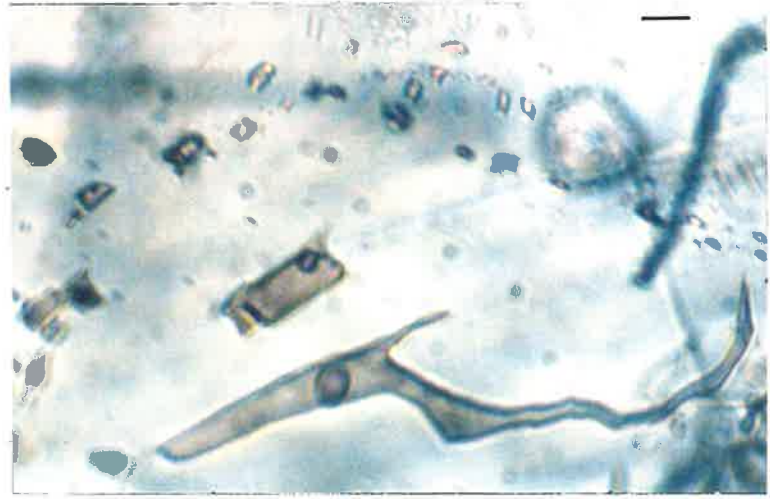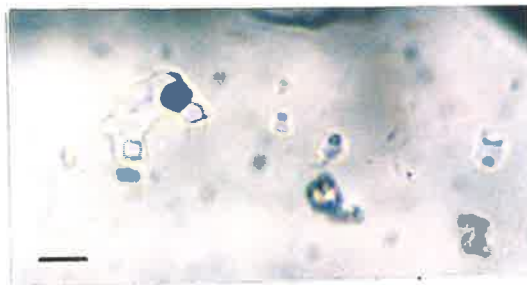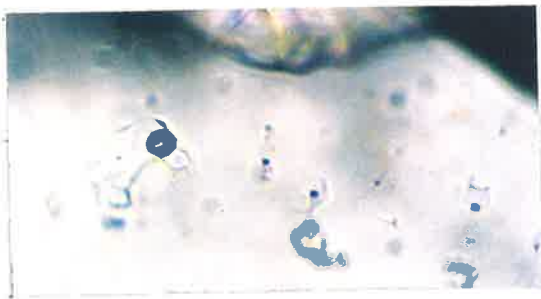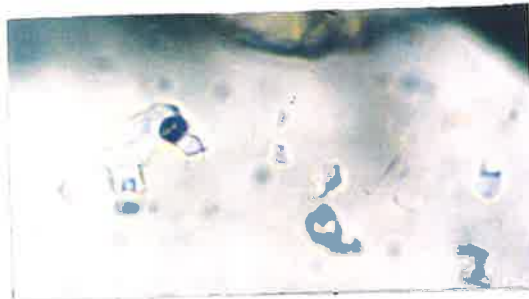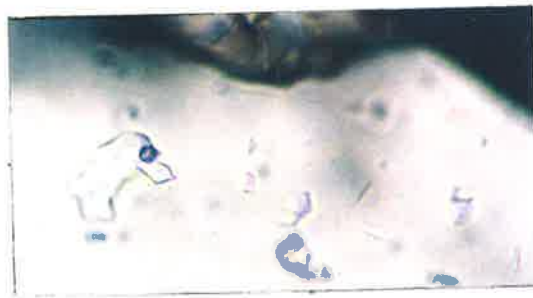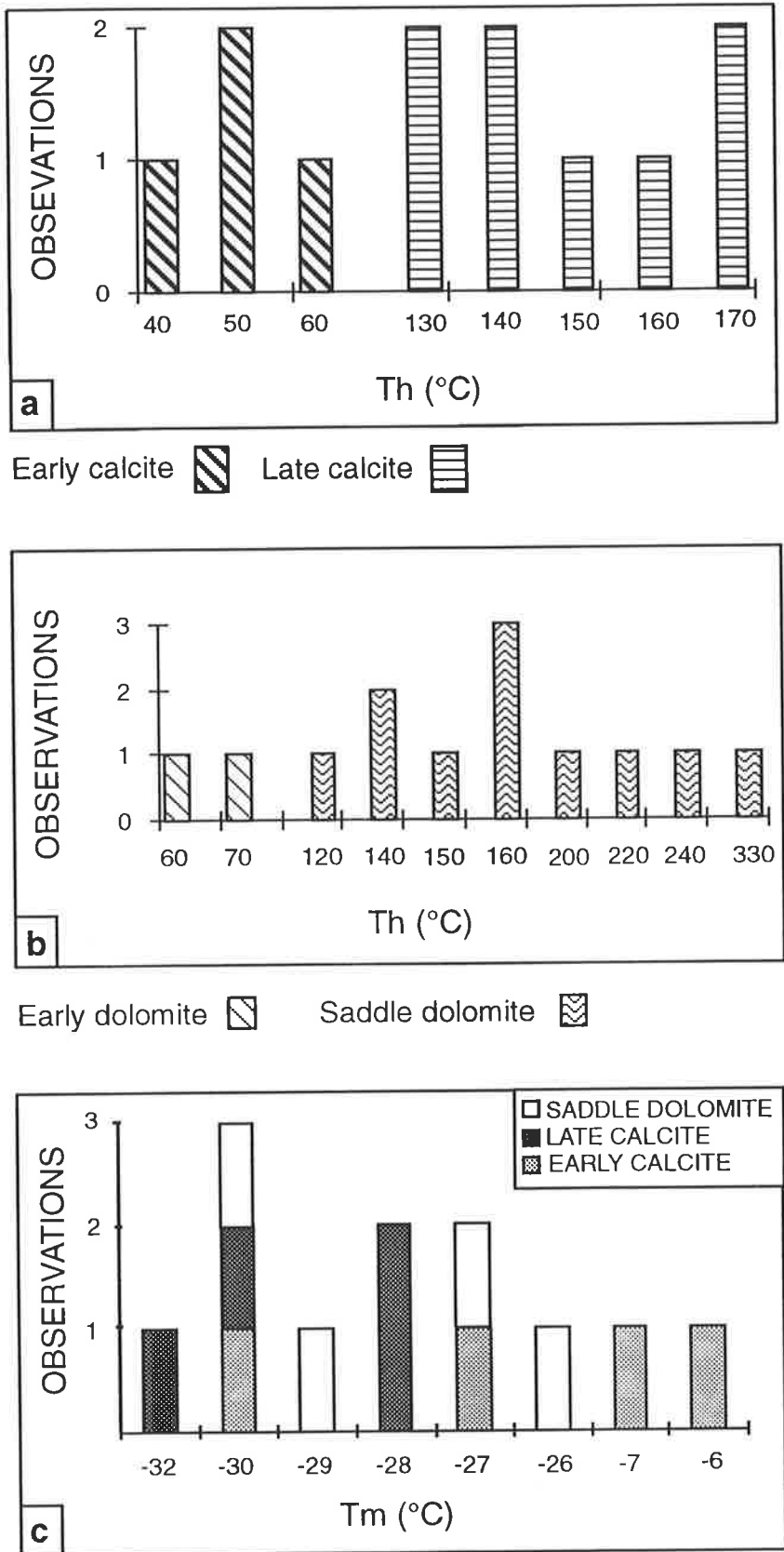
Fgure 5.3 (a) Homogenisation temperatures (Th) of early and late calcites, (b) early and saddle dolomites. (c) Final melting temperatures (Tm) for saddle dolomite , early and late calcites.

66

CHAPTER 6

OULDBURRA FORMATION SANDSTONE AND MIXED

SILICICLASTIC / CARBONATE ROCKS

6.1   Introduction

Accurate prediction of porosity and permeability in reservoir targets prior to drilling is one of the important tasks facing the petroleum geologist (Horbury and Robinson, 1993). Understanding diagenesis, porosity and permeability trends will not only provide significant information regarding reservoir quality of undrilled basins but also is useful for maximising production and recovery in producing fields.

It is the diagenetic effect on porosity and permeability that has the greatest economic influence in terms of petroleum geology. It has long been recognised that these two factors are greatly reduced and may be even totally destroyed in the early stages of burial diagenesis. More recent work has shown that this can be greatly altered at greater burial depths by dissolution to produce secondary porosity (Lemon, 1992).

Siliciclastic beds occur sporadically as thin beds at the upper part of the Ouldburra Formation type section (Manya-6) but they are dominant in the basal part of this formation, ranging in thickness from 5–23 metres.

Identification and study of intra-Ouldburra sandstones and mixed siliciclastic/carbonates is significant because, in favourable circumstances, hydrocarbons generated from a basinal/outer shelf organic-rich mudstone sequence could be reservoired in shelf sandstones (Galloway and Hobday, 1983). The shelf mudstone carbonate may function as

a reservoir or seal as well as source rock, depending on the sequence of diagenetic events. Much of the current research has been focused on diagenesis and particularly on porosity generation in sandstone and mixed siliciclastic beds.

Petrographic study together with XRD analysis of intra-Ouldburra sandstones and mixed siliciclastic/carbonate units was performed in parallel to conventional core analysis. Detailed petrographic description and XRD files of selected core samples from five drillholes (Manya-3, 6 and Marla-3, 6 and 7) are given in Appendices I and II. Measured porosity and permeability values from the conventional core analysis are represented in Table 6.1.

Table 6.1 Conventional core analysis data.

Well	Depth (m)	Porosity %	Permeability (md)	Formation	Sequences	Lithology
Manya-3	187.00	9.00	0.80	Ouldburra	C1.3	Sandstone
Manya-3	198.40	3.00	0.78	"	C1.3	Silty sandstone
Manya-3	199.60	16.00	0.47	"	C1.3	Sandstone
Manya-3	294.10					
Manya-3	333.30	14.60	38.20	"	C1.3	Sandstone
Manya-3	414.20	23.2	0.76	"	C1.3	Silty carbonate
Manya-3	468.00	21.00	596.00	"	C1.2	Sandstone
Manya-3	468.85	23.00	372.00	"	C1.2	Sandstone
Manya-6	906.60	10.20	8.80	"	C1.1	Sandstone
Manya-6	1471.00	6.10	0.08	"	C1.1	Sandstone
Manya-6	1687.20	1.20	0.46	"	C1.1	Sandstone

Summary of Table 6.1:

Porosity Range   : 1.2-23.0 %

Average Porosity   : 12.73 %

Permeability Range   : 0.08-596 md

Average Permeability : 101.83 md

6.2 Discussion

Study of these siliciclastics is significant because certain units have good reservoir potential. Although primary porosity is low ~6 %, porosity has increased with depth during burial diagenesis by processes such as leaching and dissolution of carbonate matrix and evaporite minerals and by feldspar grain dissolution and fracturing.

The distribution of sandstone and mixed siliciclastic/carbonate units with high porosity corresponds to thin, but probably widespread beds in the upper part of the Ouldburra Formation. These siliciclastic beds contain variable proportions of dolomite and commonly occur interbedded with dolomite having good to excellent reservoir characteristics as previously discussed in Chapter 3.

Identification of the porous units was also aided by using a combination of gamma ray and density logs as shown in Figure 6.1 and Appendix V. Increased gamma ray values, reflected in dolomite and dolomitic sandstones, is attributable to organic content and traces of clay minerals in carbonate-rich beds and the presence of potash feldspar and mica in sandstone beds. The density log is consistent with petrographic observations and appears to faithfully estimate porosity, particularly in leached dolomitic zones.

6.3 Diagenetic history

Diagenesis commenced with marine carbonate and anhydrite cements. Subsequent leaching and partial dolomitisation of early limestone was followed by compaction, late cements (quartz and feldspar overgrowths, dolomite and anhydrite), dissolution and hydrocarbon migration. A brief description of each of these diagenetic processes is given below:

6.3.1 Cementation and compaction

Common micritic calcite and dolomite cement with subordinate amounts of anhydrite formed during early digenesis. Only small amounts of quartz and feldspar overgrowths (2-4 %) were observed at the bottom of the type section (Manya-6) and elsewhere these overgrowths occur in sandstone beds with little or no carbonate cement. However, the rocks have undergone compaction during burial diagenesis, giving rise to tangential and concavo-convex contacts noticed at basal part of Manya-6. The effect of compaction is more prominent where carbonate matrix and cement were already dissolved (Plate 6.1d). On the other hand, rocks with intact cements were least affected by compaction.

Deep burial and overburden pressure resulted in pressure solution. The so formed microstylolites and dissolution seams are parallel or sometimes oblique to the bedding. These dissolution seams are often associated with organic matter and/or bitumen discussed in Chapter 3.

6.3.2 Hydrocarbon shows

Oil stains were noticed in several thin sections from different wells, particularly in the deeper part of the Manya-6, where migrated hydrocarbon was noticed as a bitumen residue infilling the intergranular pore spaces. The non-fluorescing character of this residue/dead oil under ultra violet light distinguishes it from live oil (Plate 6.1g and h).

6.3.3 Secondary porosity

As suggested by Schmidt and McDonald (1979), the generation of secondary porosity requires a fluid to leach away unstable components and is created particularly by CO_2 generation from organic-rich sediments prior to liquid hydrocarbon generation. This view is a more likely process in the case of the Ouldburra Formation as sandstones are often

MARLA-7

Figure 6.1 Distribution of porous sandstone and mixed siliciclastic/ carbonate units in Marla-7, Ouldburra Formation, Officer Basin. Total thickness of beds with porosity about 10 % is approximately 4 m. .
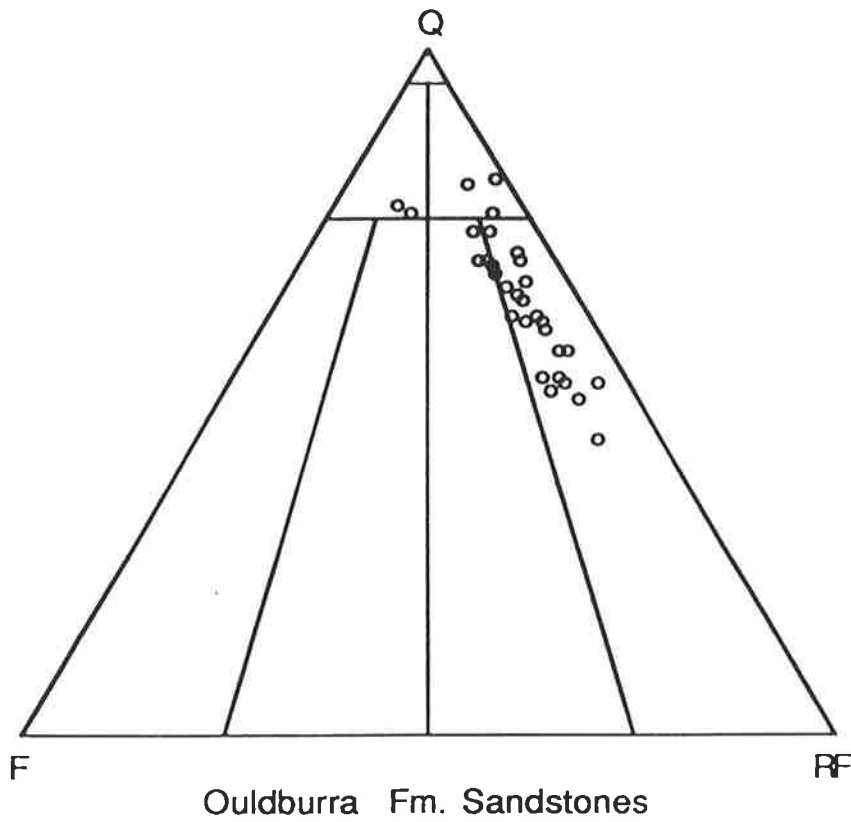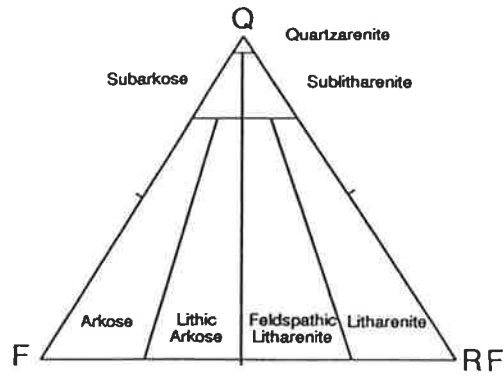
Figure 6.2 Sandstone ternary diagram showing compositions of the intraformational sandstones, Ouldburra Formation (after Folk, 1974).

interbedded with organic-rich carbonates. Alternatively, some calcite might have dissolved by meteoric water during subaerial exposure. Periodic subaerial exposure has been documented by Dunster (1987) and Gravestock and Hibburt (1991).

Petrographically, following the Folk's classification of sandstones (1974), the majority of the Ouldburra sandstones are classified as litharenite with few exceptions which are plotted as sublitharenite and subarkose (Fig. 6.2). Anhydrite and dolomite are important components of these Lower Cambrian sandstones.

The sandstone (sublitharenite) unit encountered in the basal part of the Ouldburra Formation, conformably overlies the Relief Sandstone and is consequently rich in quartz and contains minor amounts of calcite cement which has been partially dissolved, supposedly by the decarboxylation processes. This kind of relationship is commonly noticed where the rock has been stained with migrating hydrocarbons. Very limited hydrocarbon shows (less than 1 %) occur in residual primary porosity which is associated with grains which do not exhibit overgrowths (Plate 6.1g and h). The honeycombed nature of the few feldspar grains is strong evidence for post-depositional leaching as they would rapidly disintegrate during sediment transport. In some instances, particularly in the lower part of the formation, in addition to the leaching calcite and feldspar grains, the leaching of volcanic and mudrock clasts gave rise to porosity up to 20 % (Plate 6.1e and f; Manya-6, 1471.00 m). Although leaching of unstable grains (calcite and feldspar) and grain-fracturing (feldspar) led to the generation of secondary porosity, insignificant amounts of quartz and feldspar overgrowths have partially occluded intergranular pore spaces. The sandstone bed encountered in the middle part of the Ouldburra Formation contains soft grains such as mudrock clasts and anhydrite which were deformed and squeezed between rigid grains by compaction (Plate 6.1a and b). Therefore, most of the primary porosity was

destroyed and only insignificant amounts of porosity exists, related to mechanical fracturing of feldspar and subsequent anhydrite dissolution.

Sandstone sequences encountered in the upper part of the Ouldburra Formation often contain abundant lithic clasts which reduce their framework stability. The importance of sandstone framework stability to porosity and permeability has been discussed by Nagtegaal (1978), who showed that quartz fragments are the most stable. However, quartz-rich (>75 %) sandstone (sublitharenite and subarkose) has the potential to preserve high porosity and permeability during burial diagenesis and has also been influenced by dissolution of calcite cement.

It is notable that the siliciclastics have minimal or no detrital clay except for minor amounts in the more basinal areas.

6.4   Depositional environments

It is suggested that cyclic changes in sea-level was a shelf wide phenomenon during deposition of the Ouldburra Formation. It is reflected by the vertical stacking of the various facies within the formation.

Silts and sands were transported across the shelf and to the shelf margin during sea-level lowstand and outer-shelf clastics were reworked during subsequent rises in sea-level. Siliciclastics were likely to have been reworked by longshore and storm processes, an explanation of the absence of fines (clays).

Repeated and interbedded carbonate and siliciclastic deposition may be related to relative fluctuations in sea-level, sediment-input fluctuations, and/or syndepositional salt movement. These processes were involved during deposition of the sediments in the basal part of the Ouldburra Formation whereas in the upper section, alternation of carbonate and

siliciclastic beds suggests that deposition took place in a ephemeral mud-flat environment. The mud-flat hypothesis is also supported by the frequent occurrence of gypsum and anhydrite nodules growing displacively between clastic grains (J.K. Warren, pers. comm., 1993). This in turn suggests that evaporitic mud-flat environments existed from time to time. Thin and fine-grained silty beds, characterised by a relatively high evaporite mineral content, formed in this environment and have a good seal potential.

In summary, rocks were cemented prior to compaction and substantial amounts of secondary porosity has been generated during burial mainly due to matrix and anhydrite dissolution and to lesser extent by feldspar dissolution and fracturing. However, reservoir quality and hydrocarbon presence and type are strongly influenced by the depositional settings, proximity to carbonate interbeds and complex diagenetic history.

CHAPTER 7

SOURCE ROCK CHARACTERISATION

7.1   Introduction

The organic matter in hydrocarbon-producing source rocks of Cambrian age was derived solely from marine phytoplankton (including cyanobacteria), bacteria and to some extent benthonic algae and zooplankton (McKirdy, 1971; McKirdy et al., 1984; Tissot and Welte, 1978). Land plants are absent from the pre-Devonian geological record, and since then an increasing amount of primary production has been contributed by terrestrial vegetation. Organic-rich Cambrian carbonates were deposited in shallow marine or lacustrine settings, and the preservation of organic matter (OM) implies the existence of reducing conditions at, or above, the sediment-water interface. Because Cambrian source rocks and related crude oils have a restricted precursor biota, their biological markers provide clear geochemical clues to their origin (McKirdy et al., 1984).

In his classic paper, Palacas (1984) outlined the unique characteristics of carbonate source rocks and carbonate-derived oils from the world's giant petroleum fields. High yields of extractable organic matter rich in resins and asphaltenes, expelled early, appears to be common in carbonate source rocks under thermally immature to marginally mature conditions. In general, oils derived from such source rocks are characterised by: (1) high sulphur contents (>1%), (2) low API gravities (<30°), (4) low GOR ratios, (5) a prominent branched-cyclic hump in the triterpane-sterane region of the alkane chromatogram, (6) predominance of even-carbon-numbered n-alkanes (C_{22}-C_{30}), (7) Pr/Ph<1 and Ph>n-C_{18},

(8) pentacyclics>steranes, and (9) a high C_{23} tricyclic component in the tricyclic-tetracyclic terpane distribution.

Organic-rich, fine-grained carbonate rocks are widespread in both time and space and are the probable source of at least 30-40 % or more of the world's petroleum reserves (Jones, 1984). Effective carbonate source rocks have been identified in some of the world's largest petroleum fields in the Middle East, Mexico, and western Canada. For example, Aptian argillaceous limestone of the Kazhdumi Formation in southwest Iran has a TOC that varies from 3 to 11% and HI ranging from 200-450 (Bordenave and Burwood, 1990). Likewise, Callovian Oxfordian and Jurassic carbonate rocks in Saudi Arabia are the major source of oil (Palacas, 1984). The kerogen in these prolific oil-prone source rocks is most commonly Type II.

Many workers (e.g. Hunt, 1979; Tissot and Welte, 1984) suggest that carbonate source rocks contain at least 0.3 wt % TOC. This view is largely based on Gehman's (1962) pioneering work on about 1400 ancient rocks (carbonates and shales) from many parts of the world. Tissot and Welte (1984) emphasised that TOC = 0.3 % is a minimum value which should not necessarily be regarded as a positive indication of a petroleum source rock.

7.2   Distribution of organic matter

A total of 141 drillcore samples of the Ouldburra Formation, mostly fine-grained carbonate rocks, from 6 drillholes (Manya-3, Manya-6. Marla-3, Marla-6, Marla-7, KD-1 and KD-2A) were subjected to routine TOC analysis to determine their organic richness.

7.2.1 *Manya Trough*

In the Manya Trough, the type section of the Ouldburra Formation at Manya-6 provided valuable information regarding the occurrence, distribution and deposition of organic matter in various shallow marine environments. This information is based chiefly on 93 samples subjected to organic geochemical analysis, aided by a diagenetic study of the same formation which is discussed in Kamali et al. (1995).

The marine Ouldburra Formation in the Manya-6 type section comprises 1114 m of mixed carbonates and siliciclastics, calcareous and dolomitic carbonates, and evaporites including halite and anhydrite (Brewer et al., 1987) in which Gravestock and Hibburt (1991) recognised three depositional sequences discussed previously in Section 2.2. These sequences (C1.1-C1.3) and their system tracts are shown in Figure 7.1.

A detailed TOC profile of the formation (Fig. 7.1) reveals that subtidal, sabkha and halite-associated carbonates are for the most part equally lean (mean TOC = 0.25–0.30 %). The richest potential source beds are thin, but probably widespread, and occur sporadically in both sabkha and highstand shallow marine facies. The distribution and preservation of organic matter is controlled by a combination of factors such as primary productivity, bioturbation, oxidation, and bacterial degradation during deposition and late diagenesis.

As shown in the TOC profile (Fig. 7.1) five major cycles of organic preservation are recognised. These cycles are separated from each other by exposure surfaces and sabkha overprints such as plate breccia and desiccational features as described below:

Cycle 1

This cycle occurs at 1500–1214 m depth and coincides with the lowstand system tract of sequence C1.1 defined by Gravestock and Hibburt (1991). Cycle 1 is characterised by low

Figure 7.1   Organic matter distribution pattern, drillhole Manya-6, the Ouldburra Formation.
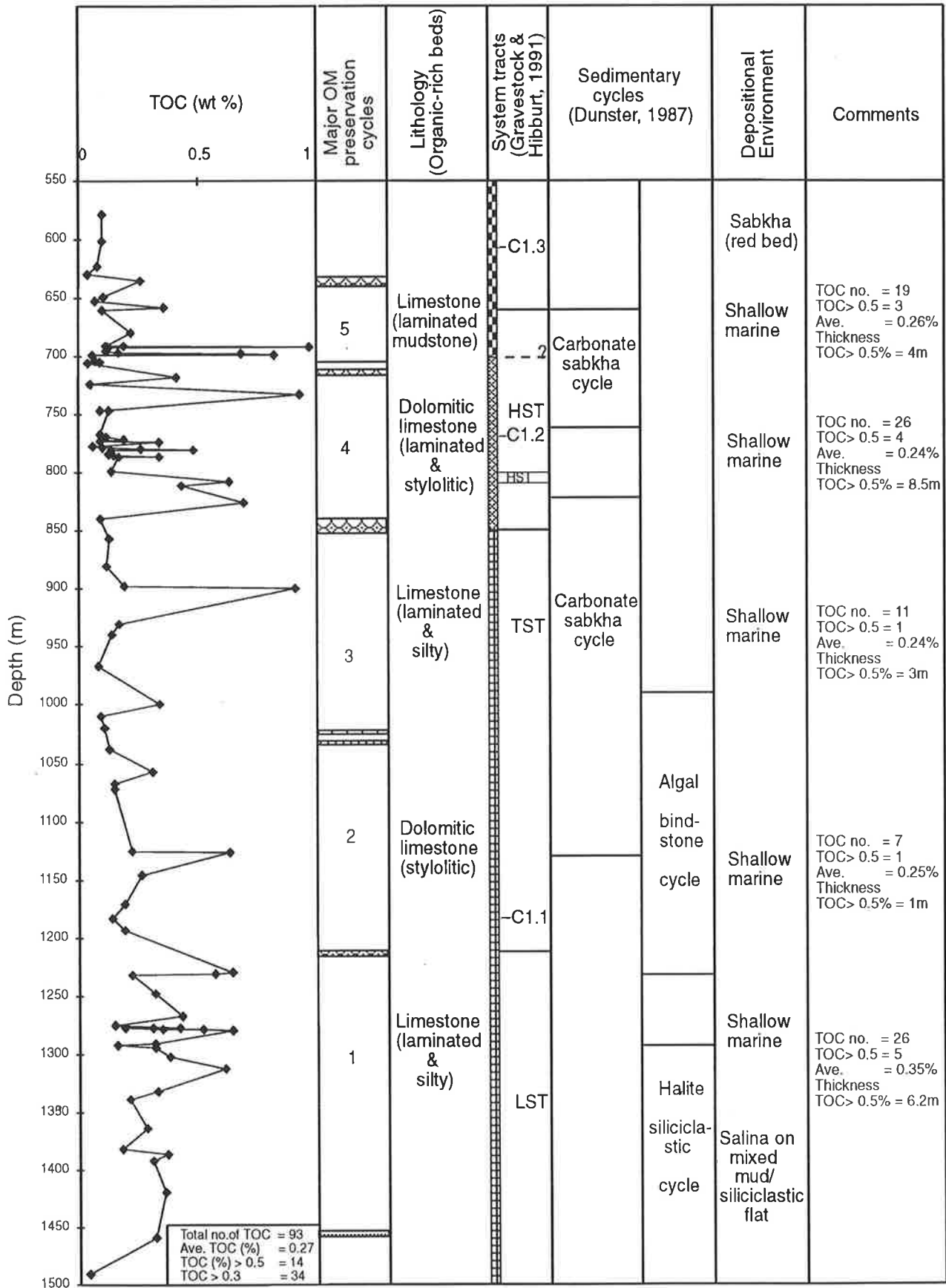
LST, lowstand system tract; TST, transgressive system tract; HST, highstand system tract.

▨▨▨▨, Sabkha overprint (plate breccia, desiccation).

79

TOC values (mostly in the range 0.15–0.38 %), but includes 3 narrow richer intervals as follows:

Interval (a) : This interval occurs at 1313–1312.70 m depth and is a laminated, silty, dolomitic mudstone with TOC reaching as high as 0.61 %. Dark organic-rich layers exhibit a microlaminated texture of probable algal origin (Plate 7.1a). This narrow interval passes upward into halite-bearing sediments suggesting a change from carbonate platform to a hypersaline environment. Halite pseudomorphs, as well as acicular anhydrite crystals, occur on bedding surfaces of some organic-rich layers. These features indicate the episodic development of isolated salinas at the bottom of the type section. Thus, a close relationship between anoxia and high salinity can be assumed. This led to the deposition of organic-rich beds.

Interval (b) : This interval covers the depth 1280–1279 m and is characterised by dark laminated limestone, with minor amounts of silt. TOC content varies from 0.52–0.64 %.

Interval (c) : This narrow interval spans the depth interval 1231.50–1229.50 m and lithologically is a dark limestone with abundant halite crystal and minor anhydrite. TOC is in the range 0.57–0.64 %.

Cycle 2

This cycle is encountered at 1212–1035 m depth and consists of limestone and/or dolomitic limestone, commonly stylolitic. Stromatolitic algal bindstone associated with minor anhydrite and rare dolomite suggests deposition in a shallow marine or, more specifically, intertidal zone (Flugel, 1982). The background TOC values are from 0.13–0.26 % and the maximum TOC recorded in this suite of carbonate rocks is 0.63 %. Sponge

spicules and trilobite fragments occur between 1073 and 1056 m depth. The calcitic sponge spicules are most common in a micritic limestone (Plate 7.1b and c). Both monoaxon and multiaxon spicules have been identified. The spicules were probably siliceous in origin, and subsequently became calcitised. Their abundance in this cycle may suggest maximum flooding surfaces (D. Gravestock, pers. comm., 1993). Therefore, shallow marine to sporadically flooding conditions existed. The microstylolites, often stained with kerogen and rarely bitumen, generally run parallel to bedding. These features are ascribed to a stage of advanced oil generation (Plate 7.1d and e). Cycle 2 of OM preservation corresponds to the algal bindstone cycle described by Dunster (1987).

Cycle 3

This cycle of OM preservation refers to the depth interval 1035–851 m and comprises thinly bedded and laminated limestone and/or dolomitic limestone often associated with thin silty layers. It corresponds to the transgressive system tract of sequence C1.1 (Gravestock and Hibburt, 1991) and a carbonate sabkha cycle defined by Dunster (1987). Little organic matter is preserved in this cycle (TOC mostly ≤ 0.3 %), possibly due to oxygenation of the seafloor. The resulting bioturbation of the sediment is illustrated by the presence of burrows in thin sections. An exception is the sample at depth interval 899.8 m (TOC = 0.91 %) where periodic sea-level highstands together with reducing conditions led to somewhat better organic matter preservation. Abundant fossil fragments were noticed at 889.50 m depth (Plate 7.1f). The presence of fossil fragments, ooids, coated grains and peloids suggests an agitated shallow marine environment. Lowering of sea level from time to time is marked by an input of siliciclastics.

This cycle also contains thin, dolomitised carbonates which are potential reservoirs (Kamali et al., 1995). These dolostones have been leached by meteoritic fresh water on

subaerial exposure. Hence, dolostones with excellent reservoir qualities are intimately associated with organic-poor beds.

Cycle 4

This cycle occurs at 840–710 m depth and is generally composed of laminated limestone (carbonate mudstone) with dolomite and anhydrite. Other striking features of this cycle are the presence of microstylolites and dissolution seams. This cycle contains three thin organic-rich carbonate beds with TOC values exceeding 0.5 % (maximum recorded TOC value = 0.93 %). This kind of rhythmic development of organic-rich layers suggests periodic anoxic to suboxic conditions during deposition.

Cycle 5

This cycle spans the depth interval 703 to 635 m and is composed of limestone (microlaminated mudstone) analogous to that in organic cycle 4. Periodic sea-level highstands led to better organic matter preservation with TOC values as high as 0.97 % and individual organic-rich beds up to 2 m thick were deposited which immediately pass upwards into organic-lean dolomites, thin siliciclastics and anhydrite beds corresponding to supratidal facies. In rare circumstances the presence of the coarse-grained siliciclastic beds may reflect episodic events like floods and storms. This suite of rocks has been described as a carbonate sabkha cycle by Dunster (1987).

To summarise, Ouldburra carbonates from Manya-3 (n = 15), Marla-3 (n = 11), Marla-6 (n = 8), and Marla-7 (n = 9) have TOC contents mostly <0.5 %. Notable exceptions occur at 619.60 m (0.79 % TOC) and 626.25 m (0.66 % TOC); 416.0 m (1.34 % TOC) and 671.25 m (1.13 % TOC) in Marla-6; and 392.85 m (0.53 % TOC) in Marla-7.

7.2.2 Tallaringa Trough

A limited number of samples collected from drillholes KD-1 (n = 2) and KD-2A (n = 3) were subjected to TOC analysis.

In the Tallaringa Trough, approximately 300 km southwest of the Manya Trough, deposition of the Ouldburra Formation took place in a range of restricted lagoonal and intertidal shallow marine environments marginal to the stable Gawler Craton. These carbonates contain pellets, stromatolites and evaporite minerals (gypsum and anhydrite). The thickness of individual organic-rich beds varies considerably but rarely exceeds 2 m. Potential source beds are laminated limestones, commonly silty and pyritic. These source beds emit a strong petroliferous odour during crushing and grinding. Like the carbonates from the Manya Trough, carbonate rocks from the Tallaringa Trough show variable TOC values (0.2–1.2 %) (Table 7.1b). The organic-rich beds (TOC = 1.2 %, Pr/Ph = 0.7) and organic-poor beds (TOC = 0.2 %, Pr/Ph = 1.4) correspond to anoxic and suboxic conditions, respectively (Table 7.5b).

In summary, in the northeastern Officer Basin (Manya Trough), the organic-rich layers within the Lower Cambrian Ouldburra Formation show many similarities. Their deposition took place mainly in two types of environments: shallow subtidal and sabkha. The richest source beds are thin, but may extend for kilometres. Organic-rich mudstone (TOC = 0.3—1.3 %) was deposited in an environment (highstand of sea-level) where circulation of the water column was sluggish and dissolved oxygen concentrations were low, resulting in the preservation of OM. Organic-poor carbonate (TOC = <0.3 %) was deposited in an environment (lowstand of sea-level) where water circulation was strong, dissolved oxygen concentration was high and burrowing organisms thoroughly reworked the sediment, resulting in the degradation of OM (HI generally <100: see Section 7.3).

At later stages of their burial these source rocks underwent compaction resulting in the formation of stylolites and dissolution seams that run parallel or oblique to bedding and, in places, increase TOC content locally. The organic matter distribution pattern (Fig. 7.1) is in agreement with other geological information (sedimentology and sequence stratigraphy) and therefore can serve as a model for prediction of OM distribution in similar geological settings.

In the Tallaringa Trough, the Ouldburra carbonates were deposited in restricted lagoonal and intertidal shallow marine environments and have TOC contents that range from 0.2 to 1.2 %. Unlike their counterparts from the Manya Trough, carbonates from the Tallaringa Trough contain organic matter less altered by oxidation, bacterial degradation and compaction. Periodic anoxic conditions existed as inferred from Pr/Ph ratios less than one (see Section 7.8) and with relatively high HI values (372–510: Fig. 7.4). The organic matter is predominantly autochthonous and of marine origin.

In general, better source rocks are developed within the Tallaringa Trough than in the Manya Trough.

7.3   Rock-Eval data

Rock-Eval pyrolysis conducted on carbonate samples from the Manya Trough (Table 7.1a; Appendix VI) showed that they have low hydrogen indices (HI<100) suggesting the presence of poor quality Type III or IV kerogen or, in some cases, overmature OM (e.g. Manya-6, 698.60 m). Given the low TOC contents of these carbonates, the mineral matrix effect (Katz, 1983; Espitali'e et al., 1985) may also contribute to their low measured hydrogen indices.

The mineral matrix effect is most likely to be a problem in those carbonates where clay

minerals (kaolinite, illite and chlorite) occur, albeit in trace amounts (see e.g. Fig. 7.2

which reveals the presence of clays in the sample from Marla-7, 392.85 m). The

corresponding TOC value is 0.53 % and VRcalc is 1.22 %. The anomalously low Tmax

value (403°C) of this sample is an artefact of the small, ill-defined S_2 peak, due to a

combination of advanced maturity and the mineral matrix effect.

Table 7.1a Rock-Eval data on samples selected for liquid chromatographic and gas
chromatographic analysis, Ouldburra Formation (Manya Trough).

Well	Depth m	TOC %	T_{max}	S1	S2	S3	S1+S2	PI	S2/S3	PC	HI	OI
Manya-6	691.75	0.97	[307]	0.35	0.40	0.67	0.75	0.47	0.59	0.06	41	69
Manya-6	698.00	0.68	[438]	0.31	0.26	0.38	0.57	0.54	0.68	0.05	38	56
Manya-6	698.60	0.82	476	0.31	0.50	0.43	0.81	0.38	1.16	0.07	61	52
Manya-6	1279.15	0.52	[304]	0.09	0.06	0.69	0.15	0.60	0.09	0.01	12	133
Marla-3	619.60	0.79	438	0.20	0.63	0.22	0.83	0.24	0.26	0.06	79	27
Marla-3	626.25	0.66	[392]	0.03	0.02	0.41	0.05	0.75	0.04	0.00	3	62
Marla-6	416.00	1.34	422	0.22	1.22	0.41	1.44	0.15	2.97	0.12	91	30
Marla-6	671.25	1.13	[341]	0.14	0.13	0.18	0.27	0.54	0.72	0.02	11	15
Marla-7	392.85	0.53	[403]	0.11	0.32	0.25	0.43	0.26	1.28	0.03	60	47

Table 7.1b Rock-Eval data on samples selected for liquid chromatographic and gas
chromatographic analysis, Ouldburra Formation (Tallaringa Trough).

Well	Depth m	TOC %	T_{max}	S1	S2	S3	S1+S2	PI	S2/S3	PC	HI	OI
KD-1	263.35	1.18	427	0.59	4.59	5.37	5.18	0.11	0.85	0.43	388	455
KD-1	275.43	0.20	435	0.25	1.02	0.30	1.27	0.20	3.40	0.11	510	150
KD-2A	211.80	0.34	430	0.15	0.97	0.31	1.12	0.13	0.09	0.34	285	91
KD-2A	285.50	0.73	427	0.49	3.20	4.76	3.69	0.13	0.67	0.30	438	652
KD-2A	297.95	0.59	425	0.70	2.20	3.35	2.90	0.24	0.66	0.24	372	567

[ ] = Unreliable ; S2 peak small and ill-defined.
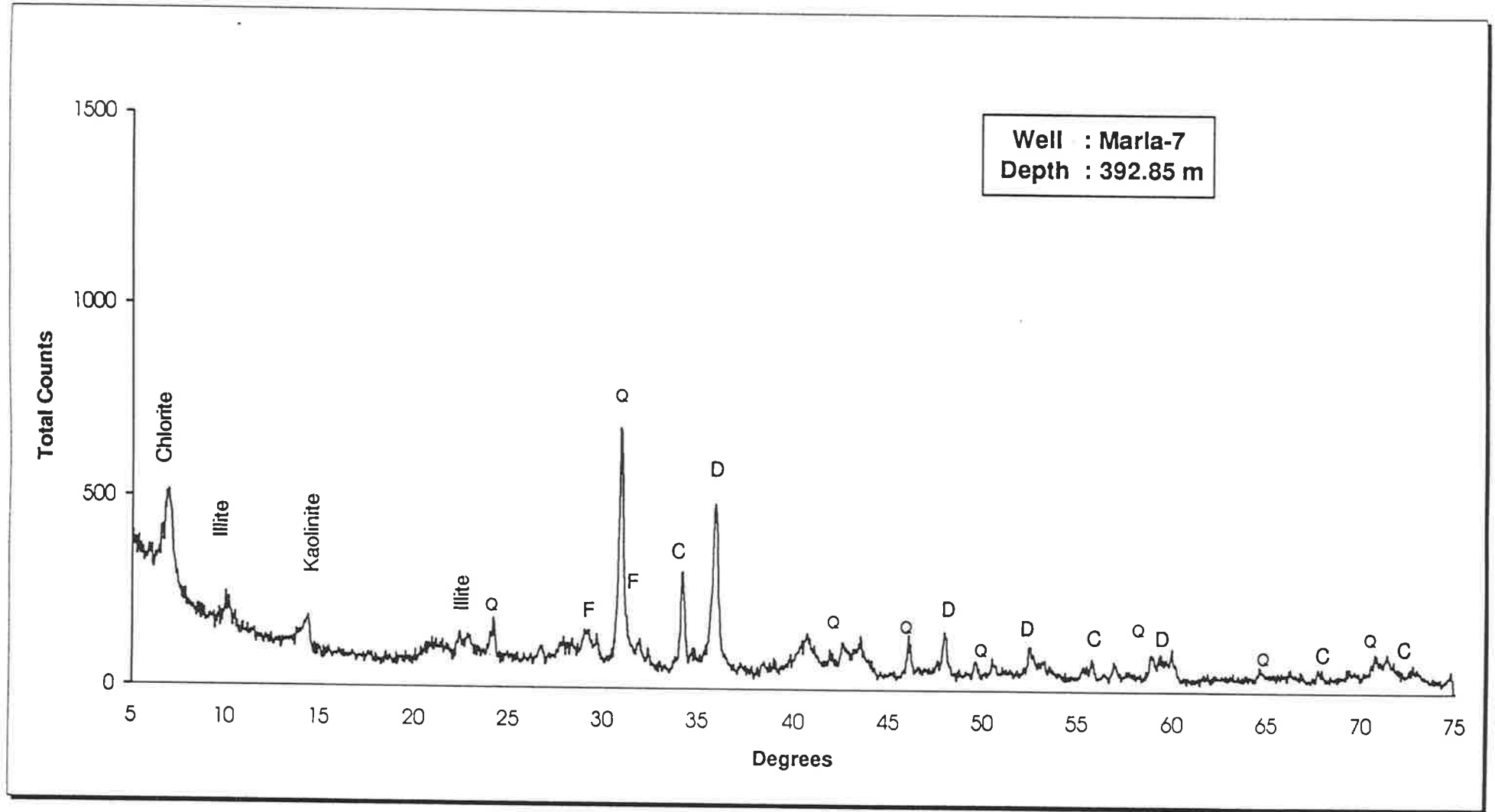
Figure 7.2 X-ray diffraction profile of a representative source bed from the Manya Trough.

One sample from drillhole Marla-6 (671.25 m) exhibited very high maturity (VRcalc = 1.7 %) which is consistent with petrographic evidence that hot hydrothermal fluids affected the adjacent source beds. The resulting S_2 value was too small to allow accurate measurement of Tmax. Therefore, Tmax is considered an unreliable maturity indicator in this case.

Oxygen indices are highly variable (OI = 11–312) and probably unreliable given that the host rock is carbonate (Peters, 1986). However, a plot of S_2 against TOC shows that selected organic-rich samples contain Type III kerogen (Fig. 7.3).
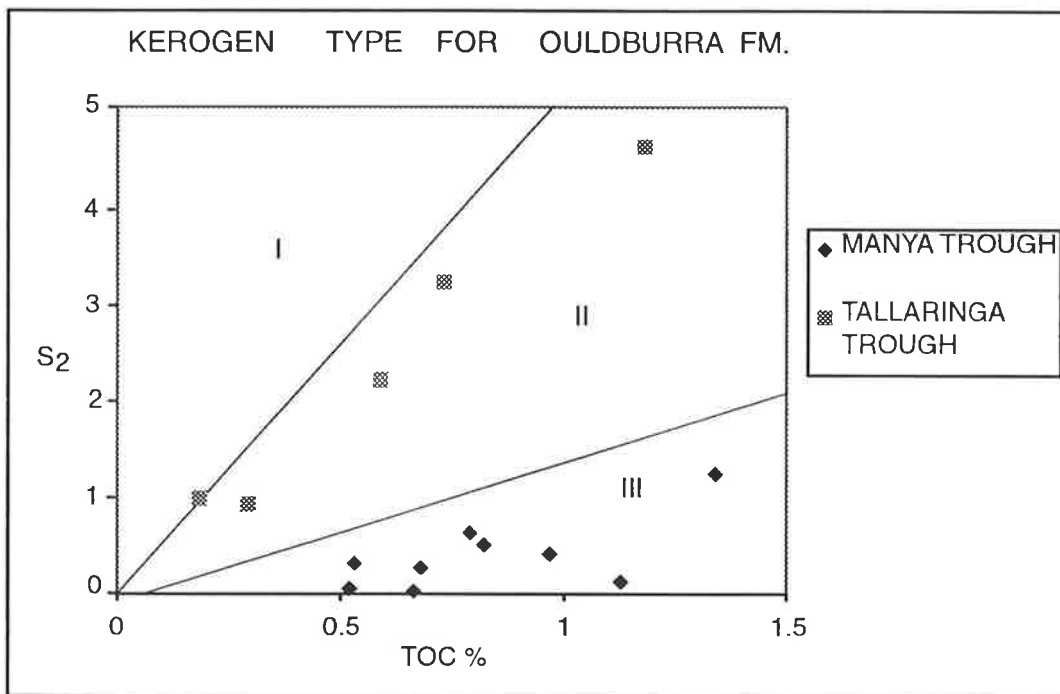
Figure 7.3 Kerogen Type in Ouldburra Formation as shown by the relationship between S_2 and TOC (after Langford and Blanc-Valleron, 1990).

In contrast, the organic-rich samples from the Tallaringa Trough have higher hydrogen indices (HI = 285–510), consistent with the presence of Type II kerogen (Figs. 7.3 and 7.
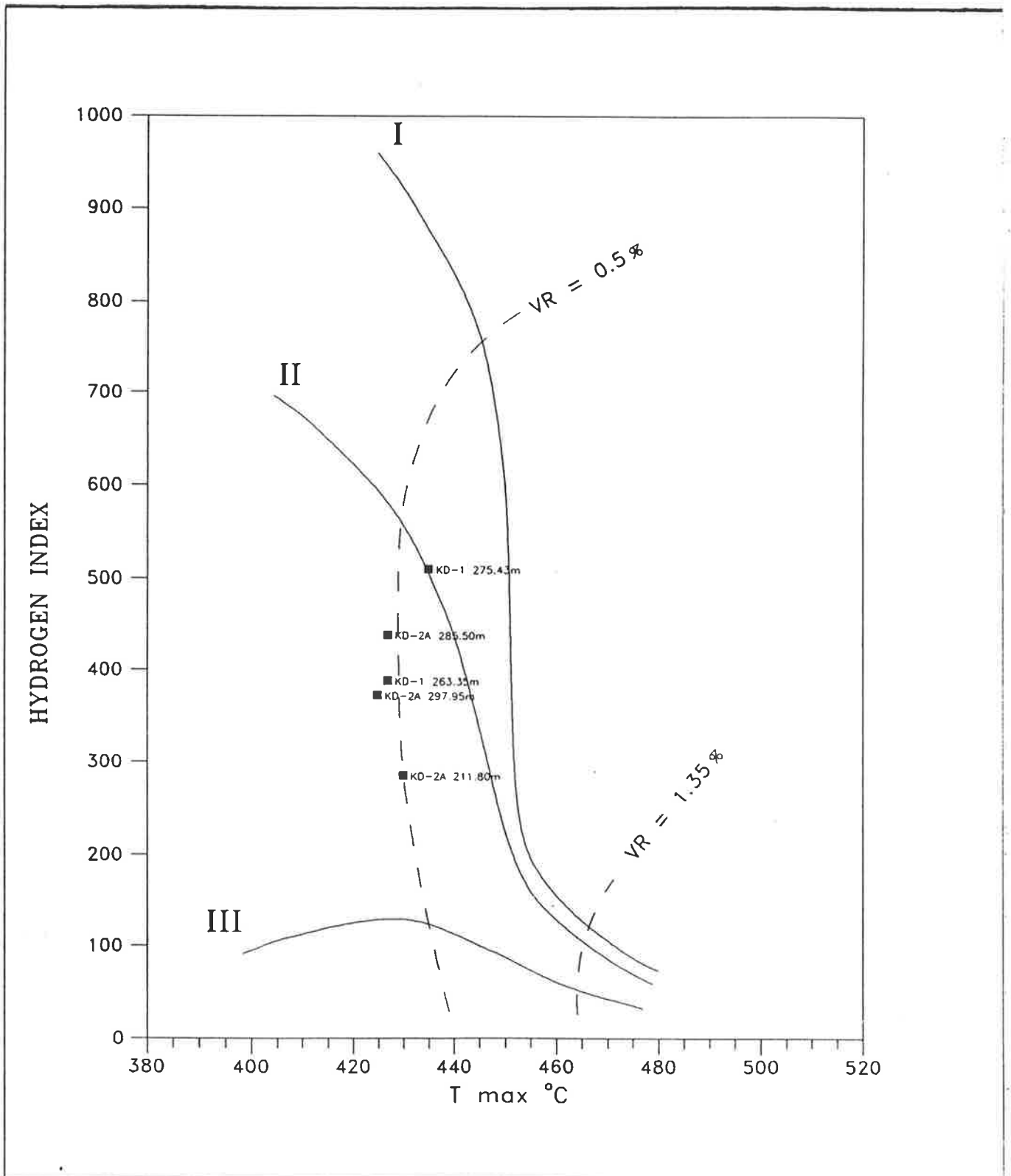
Figure 7.4 Hydrogen index vs T_{max} for samples from KD-1 and KD-2A (Tallaringa Trough).

Tmax, the primary index of maturity from Rock-Eval pyrolysis, does not provide a reasonable estimate of maturity in many Manya Trough source rocks (Table 7.1a and Appendix VI). This is evident from the small, ill-defined S_2 peaks in their Rock-Eval pyrograms which render Tmax unreliable as a maturity indicator for the OM. The small S_2 peaks noticed on Rock-Eval pyrograms may partly be due to a mineral matrix effect in those carbonates containing clay minerals. The presence of clay (kaolinite) in these source rocks is detected by X-ray diffraction analysis (Fig. 7.2 and Appendix I).

In contrast, the Tallaringa Trough source beds give more consistent Tmax values which are also in reasonable agreement with other maturity parameters (PI, MPI). The Tmax range is 425–435°C indicating marginally mature and the beginning of the oil-formation zone (Espitalie et al., 1985). Figure 7.4 is a plot of hydrogen index *vs* Tmax that graphically illustrates maturity and organic matter type. Comparison of the maturities indicated in Figure 7.4 with those derived from MPI measurement (VRcalc = 0.6–0.7 % : Table 7.6) suggests that Tmax is slightly suppressed in the richest samples. This may be due to the asphaltic nature of their EOM (D.M. McKirdy, pers. comm., 1995), causing them to behave like oil-stained source rocks (cf. Clementz, 1979).

7.4   Kerogen elemental data

The atomic H/C *vs* C/N plot as introduced by McKirdy (1995) in classifying South Australian Cambrian kerogens is another method of defining kerogen type in the carbonate source beds of the Ouldburra Formation (Fig. 7.5).

Kerogen elemental data (Table 7.2) indicate that samples from the Tallaringa Trough are richer in hydrogen than samples from the Manya Trough. Atomic H/C and C/N ratios are in the range of 0.57–0.70 and 76–84, respectively, for the Manya Trough samples; and the

corresponding values for the Tallaringa Trough samples are 1.25–1.27 and 45–50 (Table 7.2). A cross plot of these atomic ratios (Fig. 7.5) confirms that the kerogen is Type III/IV in the Manya Trough and Type II in the Tallaringa Trough.

Table 7.2 Kerogen elemental analysis, Ouldburra Formation.

| WELL | DEPTH | C | H | N | S | ASH | H/C | C/N |
	m	(%)	(%)	(%)	(%)	(%)	atomic	atomic
MANYA-6#	698.60	58.6	2.8	0.9	-	19.8	0.57	76
MARLA-6#	416.00	57.6	2.9	0.8	10.8	16.8	0.60	84
MARLA-7#	392.80	37.8	2.2	0.7	-	30.2	0.70	63
KD-1*	263.35	47.2	5.0	1.1	19.0	24.3	1.27	50
KD-2A*	285.50	62.2	6.5	1.6	10.8	12.1	1.25	45

= Manya Trough; * = Tallaringa Trough.

Samples from the Tallaringa Trough contain hydrogen-rich Type II kerogen which is a prolific oil source, whereas the hydrogen-poor Type III to Type IV kerogen in the Manya Trough source beds is gas-prone. This view is entirely consistent with the petrographic observations, as discussed in the next section. Bacterial degradation (sapropelisation) of a primary algal and/or cyanobacterial biota, and its probable oxidation at the sediment-water interface, may explain the trend to Type III kerogen composition in the Manya Trough source rocks. Source rocks with such characteristics have also been documented by other workers (e.g. McKirdy and Kantsler, 1984; Imbus and McKirdy, 1993) from the Early Cambrian Ouldburra Formation in the Officer Basin, and by Peat et al. (1978) for McMinn Formation of the Middle Proterozoic McArthur Basin. Moreover, intense bacterial degradation of the primary algal debris by anaerobic bacteria, including sulphate-reducers, would be reflected by an n-alkane profile which is either bimodal (maxima at n-C_{17} and n-C_{27}) or has a single maximum at n-C_{22} or n-C_{24} (McKirdy and Kantsler, 1984).
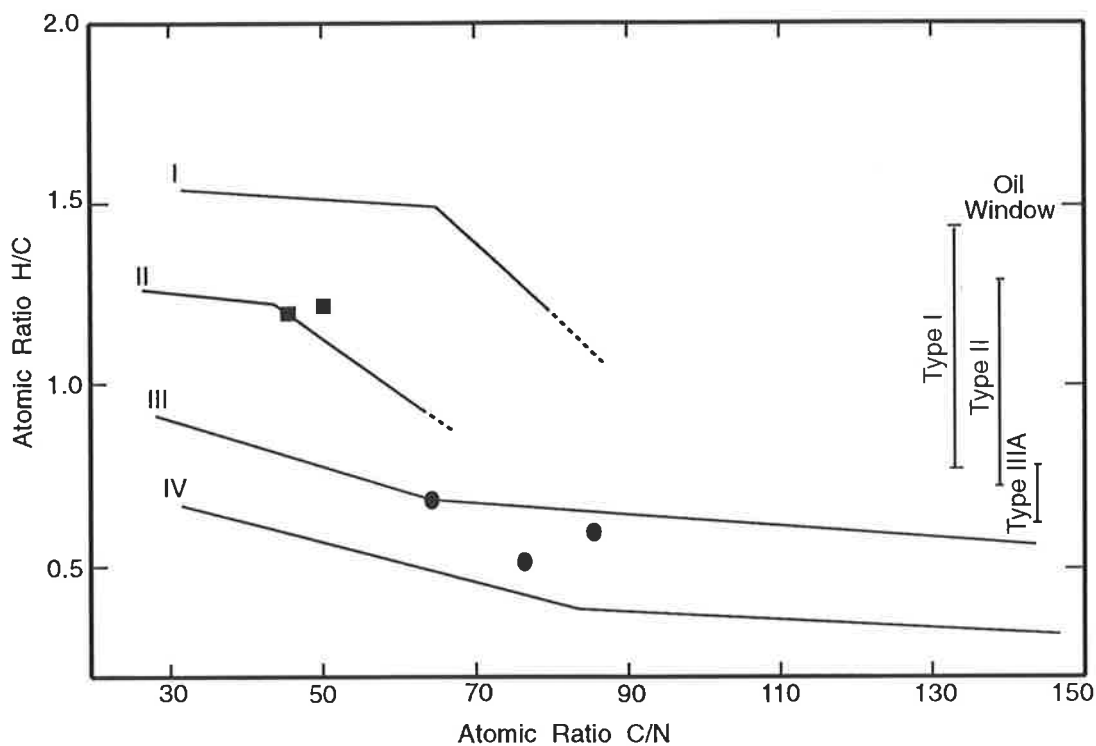
Figure 7.5 Kerogen types in the Ouldburra Formation (original plot devised by McKirdy, 1995).

In the Manya Trough sequence, differential preservation of a common algal and bacterial precursor, together with fluctuating suboxic and anoxic conditions and higher maturity levels would account for its different kerogen type. Sediment oxygenation is consistent with episodic clastic input by storms and floods, and with sediment reworking caused by burrowing organisms.

7.4.1 Sulphur content

The high-sulphur content (S = 10.8–19.0 %: Table 7.2) of kerogens from Tallaringa Trough source beds is attributable to their carbonate lithology. Clay-poor lime muds contain insufficient iron and other metals to scavenge all available sulphide, which instead becomes incorporated in the protokerogen (Tissot and Welte, 1984). This view is in agreement with the findings of Peters and Moldowan (1993, p.137) who stated that "many high sulphur kerogens and oils originated from clay-poor, marine rocks (carbonates and anhydrites) deposited under highly reducing to anoxic conditions".

High-sulphur kerogens generate liquid hydrocarbons earlier than other kerogens at lower levels of thermal exposure because a significant portion of the sulphur is presumed to be present as thermally labile sulphide and di-sulphide linkages (Waples, 1985; Powell, 1987 and references therein). Carbon-sulphur bonds break more easily than carbon-carbon bonds during catagenesis. According to Powell (1987, p. 35) "the sulphur-rich kerogens from hypersaline source facies initially break at weak sulphur linkages to provide large fragments leading to oils with high initial amounts of asphaltenes, resins and sulphur-rich aromatics with smaller amounts of saturated hydrocarbons. With increasing maturation the asphaltenes undergo maturation in much the same way as kerogen". Recent work by Baskin and Peters (1992) has shown that sulphur-rich kerogens from the Monterey Formation, California, release hydrocarbons at maturity levels significantly below the conventional oil generation threshold. Thus, source rock evaluation, including thermal history analysis, should take into account the sulphur content of kerogen in order to determine more precisely the onset of oil generation.

Another striking feature of the sulphur-rich kerogens from the Tallaringa Trough carbonates is that they contain the remains of the fossil alga (or cyanophyte) *Gloeocapsomorpha prisca*, albeit in low abundance (as discussed in Section 7.6).

Likewise, sulphur-rich Ordovician kerogen from the Decorah Formation (the Guttenberg oil rock) is reported by Douglas et al. (1991) to be composed predominantly of the remains of *G prisca* (Douglas et al., 1991). The question of how many other *G. prisca*-related kerogens were formed by incorporation of high levels of sulphur in a clay-free environment warrants further investigations. Meanwhile. the Ouldburra organic-rich carbonates in the Tallaringa Trough certainly exhibit many features characteristic of sulphur-rich, hypersaline source rocks. Early hydrocarbon expulsion is to be expected from these marginally mature source beds.

7.5 Pyrolysis-gas chromatography

Kerogen is that part of the organic matter in sedimentary rocks which is insoluble in common organic solvents, alkalis, and non-oxidising acids. The chemical composition of kerogen is complex due to its structural heterogeneity and high molecular weight, and is influenced by factors such as maceral composition, diagenetic modification and thermal evolution (Larter and Horsfield, 1993).

Pyrolysis-gas chromatography (Py-GC) is a technique which is widely used both to elucidate the structure of kerogens and to type them according to their chemical properties (Larter, 1984; Larter and Senftle, 1985; Horsfield, 1984). This method appears to accurately distinguish between oil-prone and gas-prone source rocks, both qualitatively and quantitatively (Dembicki et al., 1983). It also enables prediction of whether the primary oil product is paraffinic, paraffinic-naphthenic or aromatic-asphaltic (Powell, 1987). Furthermore, determining kerogen type by Py-GC can avoid the shortcomings of organic petrographic techniques, such as in distinguishing between hydrogen-poor and hydrogen-rich amorphous kerogen (Powell et al., 1982), and can overcome the problems associated with the Rock-Eval oxygen index (Katz, 1983). Larter and Horsfield (1993, p.272)

concluded that "the major identified pyrolysis products of kerogens are saturated and unsaturated normal, branched, and cyclic aliphatic hydrocarbons in the carbon number range C_1–C_{35}; alkylated one-to three-ring aromatic and naphtheno-aromatic hydrocarbons with side chains from C_1–C_{30+}; and alkylphenols with varying alkyl, methoxyl, and vinyl substituents". Immature to early mature kerogens are most readily discriminated from one another by the relative abundances of (1) selected aromatic and aliphatic compounds and (2) short-chain versus long-chain n-alkanes and n-alk-1-enes in the pyrolysate (Larter and Horsfield, 1993 and references therein).

To supplement kerogen elemental analyses, Py-GC was performed on five selected kerogen concentrates. These samples represent organic-rich carbonates from four different well locations, two in the Manya Trough and two in the Tallaringa Trough (Table 7.3). Kerogen isolation and pyrolysis-GC analyses were undertaken by Amdel Petroleum Services, as described in Chapter 1 (Section 1.6.5).

Calculations involved using C_5–C_8 (condensate) and C_{9+} (oil) normal alkane + alkene yields as a percentage of total pyrolysate; and C_1–C_4 (gas yield) and C_{5+} (liquid yield) values from the pyrolysis-GC and Rock-Eval data. It should be noted that the figures in both of these data sets reflect generative yields only and that expulsion efficiencies have not been taken into account.

Table 7.3 Pyrolysis gas chromatography data

Sample	Pyrolysis Yield (kg hydrocarbons /tonne)	Normal Alkanes + Alkenes				Gas Yield (kg hydrocarbons /tonne)	Liquid Yield (kg hydrocarbons /tonne)
		C_5-C_8 Yield (kg hydrocarbons /tonne)	C_{9+} Yield (kg hydrocarbons /tonne)	mg C_{9+} per g TOC	C_{9+} % of S2		
Manya-6, 698.60 m	0.50	<0.01	<0.01	0.49	0.97	0.02	0.48
Marla-6, 416.00 m	1.22	<0.01	<0.01	0.87	1.27	0.04	1.18
Marla-7, 392.80 m	0.32	<0.01	<0.01	0.33	1.45	0.02	0.30
KD-1, 263.35 m	4.59	0.13	0.28	23.53	8.77	0.75	3.85
KD-2A, 285.50 m	3.20	0.09	0.18	24.28	8.30	0.33	2.87

The yield of C_{9+} normal alkanes and alkenes per gram of TOC assesses the effective source quality of these intervals. Values of greater than 10 are indicative of good effective source rocks, whilst values of greater than 20 are indicative of excellent effective source rocks (Amdel Petroleum Services, pers. comm., 1995). This parameter indicates that the KD samples (Tallaringa Trough) have excellent effective source quality while the Manya and Marla samples (Manya Trough) have very poor effective source quality.

The proportion of C_{9+} normal alkanes and alkenes as a percentage of the total pyrolysate is also dependent on source quality. These values range from 0.97 to 8.77 % in the samples examined in this study. Values of greater than 8 % C_{9+} normal alkanes and alkenes as a percentage of the total pyrolysate are indicative of good source quality. Values of greater than 15 % C_{9+} normal alkanes and alkenes as a percentage of the total pyrolysate are indicative of excellent source quality (Amdel Petroleum Services, pers. comm., 1995). These values confirm that the organic matter in the Tallaringa samples has a significantly better effective source quality than the Manya and Marla samples.

Effective source richness for the generation of oil and condensate may be gauged from the yields of C_{9+} (oil) and C_5-C_8 (condensate) alkanes and alkenes (kg of hydrocarbons/tonne). Gas yields may be gauged from C_1-C_4 yields (kg of hydrocarbons/tonne). The following values may be used as guidelines in the assessment of effective source richness. It is unrealistic, however, to use these values as specific cut-off values (Amdel Petroleum Services, pers. comm., 1995):

Oil source richness (C_{9+} alkanes + alkenes)

. good > 0.5 kg hydrocarbons/tonne

. excellent > 1.0 kg hydrocarbons/tonne

Condensate source richness (C_5-C_8 alkanes + alkenes)

. good > 0.25 kg hydrocarbons/tonne

. excellent > 0.5 kg hydrocarbons/tonne

Gas source richness (C_1-C_4 yields)

. good > 3 kg hydrocarbons/tonne

. excellent > 6 kg hydrocarbons/tonne

The values of these ratios indicate that all of the samples appear to have poor effective source richness for the generation of gas, whereas the two Tallaringa Trough samples display excellent oil source richness. The Marla-6 (416 m) sample has excellent "condensate" source richness.

7.5.1 Kerogen molecular composition

Kerogen pyrolysates from Tallaringa Trough source beds are dominated by *n*-alkane / *n*-alkene doublets suggesting that these samples are rich in normal paraffins. The pyrograms also have prominent naphthene humps (Fig. 7.6 and Appendix X). These kerogens are also
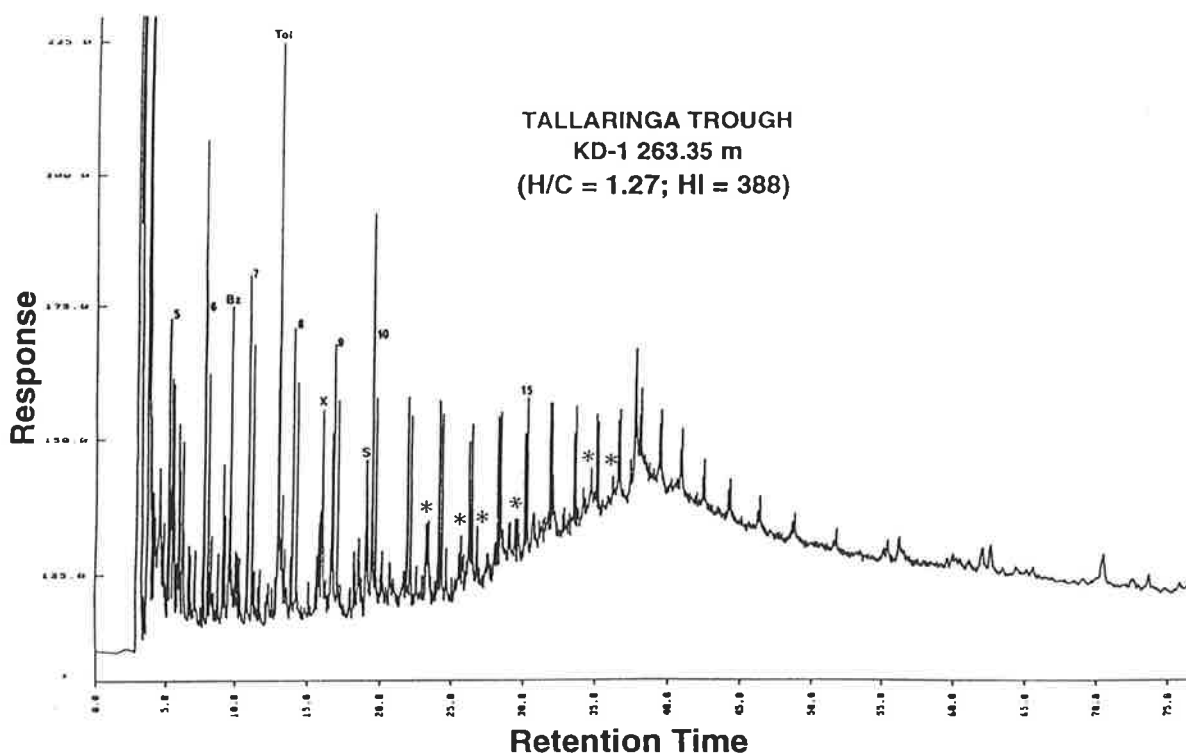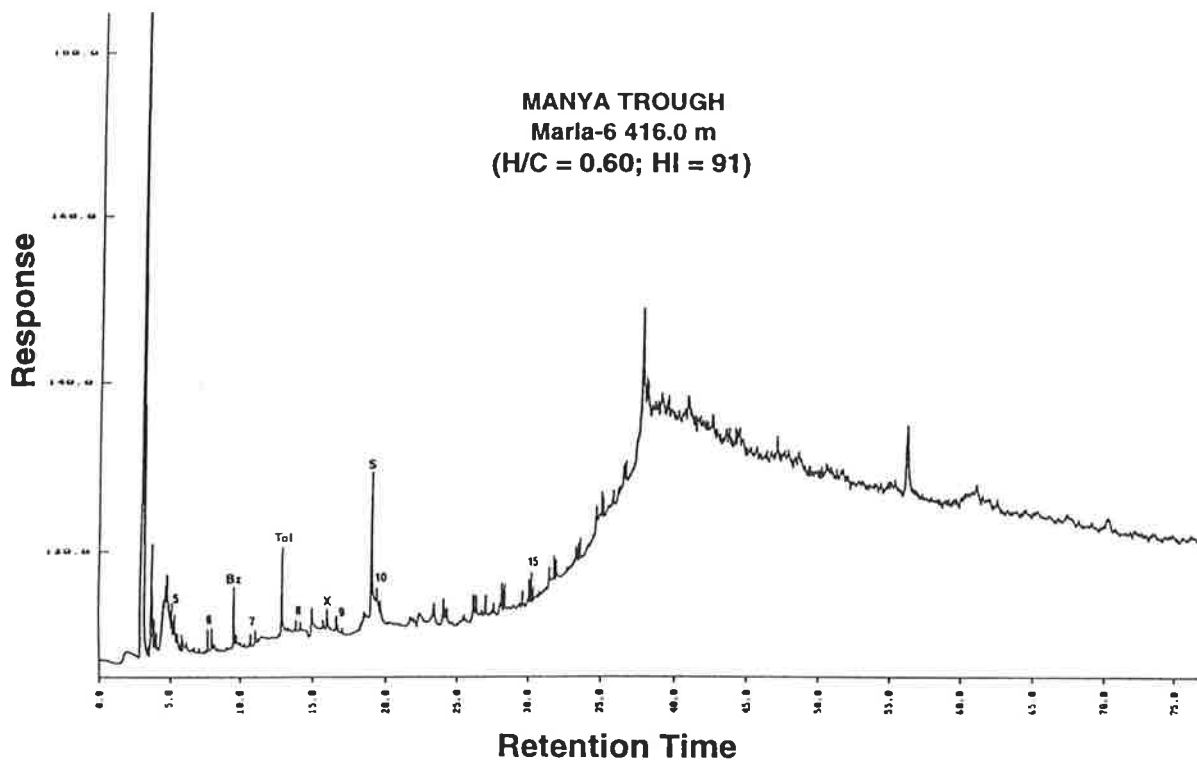
Figure 7.6 Gas chromatograms of kerogen pyrolysis products for Ouldburra Formation carbonates from Manya Trough (kerogen Type III) and Tallaringa Trough (kerogen Type II). Numbered peaks denote chain length of n-alk-1-ene and n-alkane doublets. Bz = Benzene. Tol = Toluene. X = Xylenes. S = Internal Standard. HI = Hydrogen index in mg/g org.C. H/C = Hydrogen/carbon atomic ratio. * = Acyclic isoprenoids.

97

characterised by a low proportion of normal alkanes longer than C22. Given that lamalginite is their dominant maceral (Section 7.6), the molecular composition of these kerogens, as indicated by the presence of n-alkane and n-alkene doublets eluting in C_5–C_{25} range, is very similar to that of a Type I paraffinic-naphthenic alginite (Fig. 7.7: Permian Tasmanite, Australia) analysed by Larter and Senftle (1985). However, kerogen elemental analysis (C, N, H) and Rock-Eval pyrolysis, have already suggested highly oil-prone, Type II kerogen for the Tallaringa Trough source beds.
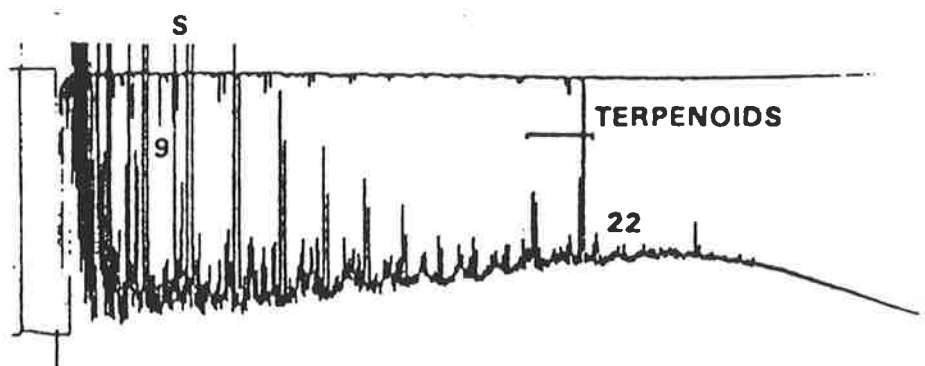
Figure 7.7   Kerogen Type I (Permian tasmanite, Australia) paraffinic-naphthenic with maturity level <0.8 % vitrinite reflectance equivalent (Larter and Senftle, 1985).

It is noteworthy that, the Py-GC traces of the Tallaringa Trough carbonates are somewhat dissimilar to those of the Ouldburra Formation carbonates (Wilkinson-1 and Wallira West-1) previously analysed by McKirdy et al. (1984). Kerogens from the Tallaringa Trough (KD-1 and KD-2A) limestones show a naphthene hump (between n-C_{12} and n-C_{32}), higher abundances of aromatics in the C_6–C_{10} region, and appreciable acyclic isoprenoids (Fig.7.6), features which are less pronounced in their correlatives from Wilkinson-1 and Wallira West-1. Hitherto, high concentrations of alkylbenzenes together with the acyclic isoprenoids have been taken by McKirdy et al. (1984) as evidence of an input from

archaebacteria in assessing the source characteristics of Type I kerogen in lacustrine carbonates (Byilkaoora-1) from the Observatory Hill Formation.

Kerogen pyrolysates from the Manya Trough source beds are characterised by very low amounts of paraffins and naphthenes (Fig. 7.6). Their major components are low molecular weight aromatic hydrocarbons (benzene, toluene). This is typical of poor quality, gas-prone kerogen. and advanced thermal maturity, as described in following sections.

7.6   Organic petrography

Ouldburra carbonates with a range of TOC contents were selected for petrographic analysis. For convenience and because of their different thermal maturities, these samples are divided into two groups according to locality: Manya Trough and Tallaringa Trough.

In the Manya Trough, organic matter is mainly micritinised bituminite which occurs as thin laminae or stylolitic films but is otherwise structureless. The bituminite is commonly associated with pyrite (Plate 7.2a). The micrinite granules occurring within the bituminite are oval or rounded and their size ranges from 2 μm to 5 μm. Under white reflected light these granules, together with pyrite crystals, are bright white. Bituminite is generally associated with a laminated carbonate matrix and appears dark brown in fluorescence mode. Such bituminite was probably derived from lamalginite through intense bacterial degradation at or near the sediment-water interface (B. L. Watson, pers. comm., 1994). The richest carbonate from drillhole Marla-6 (416.0 m depth; TOC = 1.4 %) is a fine grained dolostone. Small oval and round blebs of OM of varying size (1.5–11 μm), scattered in a fine micritic matrix, are yellow to orange under blue light excitation. Given the high maturity of this sample (VRcalc = 1.26 %) these oil blebs are almost certainly

generated *in situ* (Plate 7.2b). The presence of trace amounts of framboidal pyrite is attributable to bacterial sulphate reduction during early diagenesis.

No reflectance measurements were taken on any phytoclasts in the Manya Trough source rocks, but calculated vitrinite reflectance (VRcalc) values derived from methylphenanthrene index (MPI) measurements are in the range 0.91–1.68 % (Table 7.5).

Another striking feature of the Manya Trough source beds is the concentration of OM along microstylolites which are parallel or sub-parallel to the plane of bedding. This OM exhibits no fluorescence (Plate 7.1d and e). Microstylolites occur almost exclusively in carbonates and evaporites with different degrees of susceptibility to pressure solution (Warren, 1992). The insoluble material (including OM and clays) concentrated along the stylolitic contact appears to have been derived from the host rock.

In the Tallaringa Trough source beds, the DOM comprises several different types of liptinite. These include lamalginite, telalginite (possibly *Gloeocapsomorpha prisca*) and bacterial biomass, distinguishable because of the lower maturity of the host rock.

Lamalginite (A 2.6 from Australian Standard 285, 1986) is the predominant form of organic material observed in this suite of source rocks. It consists of fluorescent, filamentous and elongate OM aligned parallel to bedding (KD-1, 263.45 m : Plates 7.2d and 3d). The lamalginite commonly occurs as discontinuous grouped lamellae 40 μm to 200 μm in length and from 1.5 μm to 16 μm thick. Under white reflected light they appear grey and red brown, but fluoresce yellow to orange under blue light excitation. In organic-rich samples, the filaments locally form fine mat-like masses and OM appears to comprise up to 4 % (by volume) of the whole rock. Thus, much of the organic matter was autochthonous and probably deposited in a quiet lagoonal environment. This is confirmed by recent palynological studies which indicate that benthic cyanobacteria (blue green

algae), including filamentous and membrane-like forms (Plate 7.5), were the major organic precursor. These cyanophytes commonly are associated with sphaeromorph acritarchs and other coccoid cells (W. Zang, pers. comm., 1995).

In addition to lamalginite, discrete oval or disc-shaped algal bodies (telalginite) occur in organic-rich beds and exhibit strong yellow fluorescence. Preservation of the telalginite requires anoxic conditions and is accompanied by abundant lamalginite and framboidal pyrite (Plates 7.2d and 4d). Individual algal bodies are 18–30 μm long and 8–12 μm thick, usually with no recognisable internal structure.

Dominant lamalginite and primitive *G. prisca*-type telalginite is almost certainly responsible for the oil-prone character of these samples (HI = 388–510; kerogen H/C = 1.25–1.27; cf. Tables 7.1 and 7.2). Hitherto, the oldest reported occurrence of *G. prisca* was from a Middle Cambrian Shale (Mt. Cap Formation, Canadian Northwest Territories: Fowler, 1992). However, the Ouldburra sediments are unequivocally Early Cambrian in age. Biostratigraphically important fossils from the Manya Trough include Archaeocyatha (Dunster, 1987) and trilobites, notably (?) Redlichiidae (Jago and Youngs, 1980) and Wutingaspis (Dunster, 1987), thereby constraining the age to late Atdabanian/Early Botomian.

Attempts to elucidate the exact nature of *G. prisca* (i.e. whether prokaryote or eukaryote, benthonic or planktonic, photosynthetic or chemoauthotrophic) are discussed at length by various workers (e.g. Fowler and Douglas, 1984; Hoffmann et al., 1987; Fowler, 1992). However, Glaessner and Foster (1992) concluded that the most compelling microscopic and geochemical evidence points to *G. prisca* being a mat-forming cyanophyte.

Another striking feature of the DOM in the organic-rich source beds of the Tallaringa Trough is presence of the large (10–30 μm diameter) bitumen balls similar in appearance

to vitrinite (Plate 2f and 3a). Some of these balls have a zircon core (containing thorium and uranium) and hence are referred as "thucholite" (Gary et al., 1972). Its spherical shape, highly reflecting centre and lower reflecting rim differentiate the thucholite from a vitrinite maceral. Thucholite balls commonly display increasing fluorescence from the centre to the rim and occur where lamalginite and bitumen are in close proximity. This kind of relationship suggests that the thucholite is being formed by radiation-induced polymerisation of bitumen, released from the alginite during catagenesis. The source of the ionising radiation is the zircon at the core of the thucholite (Crick et al., 1988). Similar thucholites from the Ouldburra Formation in Wilkinson-1 are characterised by highly reflecting, non-fluorescent cores, surrounded by slightly fluorescing haloes of lower reflectance, suggesting that they are not strictly comparable with reservoir-type bitumens. Reflectance measurements from such bitumen balls are in the range of 0.5 to 1.1 % (McKirdy and Kantsler, 1980).

To summarise, the macerals recognised in the Ouldburra Formation appear to have been mainly derived from algal and/or cyanobacterial precursors, although a substantial bacterial input is inferred from the presence of bituminite. The OM occurs as poorly preserved lamalginite and bituminite in the Manya Trough source beds, and moderately to well preserved lamalginite, telalginite, bituminite and thucholite in the Tallaringa Trough source beds.

7.6.1   Thucholite reflectance

Only three samples from the Tallaringa Trough were used for reflectance measurements. A total of 19 thucholites of different sizes were measured. Regardless of size (small = 25 μm; medium = 25-35 μm; >35 μm), almost all thucholites show increasing reflectance towards the centre (Table 7.4). In other words, reflectance decreases from the centre

towards the edge. Large thucholites with either bigger (or several) zircon crystals at their core exhibit higher reflectances than do the thucholites which contain only one zircon.

The highest reflectance measurement recorded is Ro = 1.71 % from a large thucholite about 50 μm in diameter (in KD-2A, 297.95 m) which possesses three zircon crystals. Increase in reflectance with increasing depth is also noticed in medium and large thucholites, particularly the latter.

Calculated vitrinite reflectance (VRcalc) derived from MPI measurements (see Section 7.9) shows no relationship with the reflectance of coexisting thucholite. This is not surprising given the wide range of reflectance values within each sample and the strong influence exerted by the size of individual thucholites and the number of associated zircon crystals. Therefore, it is concluded that thucholites, exhibiting as they do highly variable reflectances, can not be effectively used in thermal maturity assessment. However, their presence does provide clear evidence for the generation and primary migration of hydrocarbons within the source rock.

Table 7.4 Thucholite reflectance data, Ouldburra Formation, Officer Basin.

Well	Depth (m)	Ro $_{max}$ (%)		
		Small	Medium	Large
KD-1	263.34	0.29-0.40	0.60-0.73	1.01
KD-2A	285.50	0.34-0.63	0.49-0.53	0.92
KD-2A	297.95	-	0.66-0.70	1.71

N.B. Measurements refer to thucholite centres, not edges. Size refer to diameter of thucholite (small = <25 μm; medium = 25-35 μm; large = >35 μm)

7.7　Extract yield and composition

The yields of C_{15+} soluble organic matter obtained for selected samples of the Ouldburra Formation, and its bulk composition as determined by liquid chromatography and gas chromatography, are summarised in Table 7.5. Extractable organic matter (EOM) yields from the Manya Trough samples are moderately low, both in the absolute terms (142–267 ppm whole rock) and as a proportion of the total organic matter (10–40 mg/g TOC) (Table 7.5a).

The hydrocarbon contents (saturates plus aromatics) of the EOM are highly variable, in the range of 19–77 %. Saturate to aromatic ratios also display considerable variation (0.26–3.8). The ternary diagram (Fig. 7.8) shows the relative proportions of the three separated fractions (saturated hydrocarbons, aromatic hydrocarbons and non-hydrocarbons i.e. asphaltenes and resins) in source rock samples from Manya-6, and Marla-3, 6 and 7. In this diagram, all the samples from the Tallaringa Trough fall in a region designated "hydrocarbons predominantly aromatics," but most samples from the Manya Trough plot in the region of "hydrocarbons predominantly saturates". The high proportion of saturates in the latter samples is attributed to higher levels of maturity.

Sample (Manya-6, 1279.15 m) shows an exceptionally large saturate fraction (61 %). The high proportion of hydrocarbons (84 % of EOM) in this sample, together with relatively high production index (PI = 0.60), appears to be due to staining by migrated hydrocarbons. Saturates from the other samples comprise only 9–38 % of the EOM; these samples are relatively rich in asphaltenes and resins. The low hydrocarbon yields of the Manya Trough source beds are entirely consistent with their poor original source quality which is confirmed by petrographic observation and maturity measurements.

Table 7.5a Liquid chromatographic and gas chromatographic data, Ouldburra Formation (Manya Trough, Officer Basin).

Well	Depth	TOC	EOM		SAT		ARO		NSO		ASPH		HCS		EOM%	SAT/	Pr/	Ph/	Pr/	CPI
	m	%	ppm	mg g⁻¹TOC	ppm	%	ppm	%	ppm	%	ppm	%	ppm	mg g⁻¹TOC		ARO	nC17	nC18	Ph	
Manya-6	691.75	0.97	142	15	54	38	22	15	56	39	10	7	76	56	53	2.5	0.4	0.3	1.2	1.0
Manya-6	698.00	0.68	150	22	49	33	25	17	51	34	25	16	74	53	50	1.9	0.26	0.3	1.0	1.2
Manya-6	698.60	0.82	195	24	24	12	91	46	48	25	32	16	115	35	58	0.26	0.5	0.4	1.0	nd
Manya-6	1279.15	0.52	210	40	128	61	33	16	44	21	5	2	161	134	77	3.8	0.28	0.25	0.9	0.9
Marla-3	619.60	0.79	267	35	83	31	36	14	116	43	32	12	119	88	45	2.2	0.2	0.2	1.0	1.0
Marla-3	626.25	0.66	182	28	16	9	19	10	105	58	42	23	35	19	19	0.9	0.5	0.4	0.9	1.3
Marla-6	416.00	1.34	241	18	65	27	38	16	114	47	24	10	103	68	43	1.7	0.4	0.3	1.6	1.0
Marla-6	671.25	1.13	108	10	41	38	21	19	6	6	40	37	62	43	57	2	0.7	0.4	2.6	0.8
Marla-7	392.85	0.53	151	28	17	11	24	16	51	34	59	39	41	22	27	0.7	0.5	0.3	1.7	0.9

Table 7.5b Liquid chromatographic and gas chromatographic data, Ouldburra Formation (Tallaringa Trough, Officer Basin).

Well	Depth	TOC	EOM		SAT		ARO		NSO		ASPH		HCS		EOM%	SAT/	Pr/	Ph/	Pr/	CPI
	m	%	ppm	mg g⁻¹TOC	ppm	%	ppm	%	ppm	%	ppm	%	ppm	mg g⁻¹TOC		ARO	nC17	nC18	Ph	
KD-1	263.35	1.18	1700	144	165	10	215	13	471	28	849	50	380	32	23	0.8	0.5	0.6	0.7	0.7
KD-1	275.43	0.20	655	328	73	11	148	23	406	62	28	4	221	110	34	0.5	0.15	0.13	1.4	0.8
KD-2A	211.80	0.34	582	172	48	8	49	17	353	60	132	15	97	28	25	0.9	0.7	0.6	1.2	1.4
KD-2A	285.50	0.73	2540	348	351	14	359	14	883	35	947	37	710	97	28	0.9	0.17	0.3	1.2	0.9
KD-2A	297.95	0.59	1082	183	121	11	181	17	377	35	403	37	302	51	28	0.7	0.2	0.2	1.2	1.4
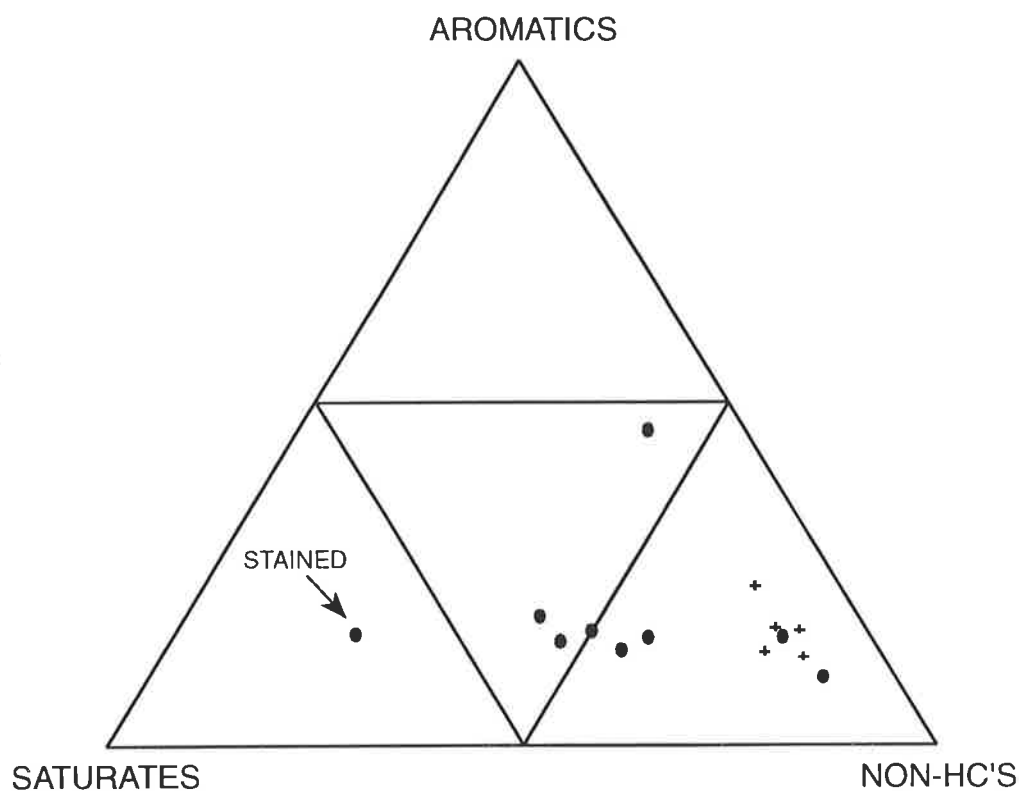
Figure 7.8   Distribution of saturates, aromatics and non-hydrocarbons in EOM of
Ouldburra carbonates, Manya and Tallaringa Troughs.

In contrast, samples from drillholes KD-1 and KD-2A in the Tallaringa Trough show high

EOM yields, both in absolute terms (582–2540 ppm, whole rock) and as a proportion of the

total organic carbon (144–348 mg/g TOC) (Table 7.5b).

Samples with yields of indigenous EOM in excess of 30 mg/g TOC are considered to have

source potential for liquid hydrocarbons (McKirdy, 1979). All but two of the analysed

samples, even those with TOC as low as 0.2 %, contain in excess of 50 mg of

hydrocarbons per gram of organic carbon, indicating good to excellent source potential

(Powell et al., 1989). The following classification of source quality can be used where the rock is in the main oil generation stage of catagenesis, although the boundaries between the classes are imprecise (Cooper and Ower, 1982) :

Hydrocarbon Yield mg per g TOC	Source Rock Quality
0–30	Gas source only
30–50	Wet gas source to fair oil source
50–100	Good oil source
100–200	*Prolific* oil source
Over 200	Migrated oil show or contamination

Samples rated as *prolific* oil sources (*viz.* KD-1, 263.35 m and KD-2A, 285.50 m and KD-2A, 297.95 m) have an intermediate asphaltene content (37–50 % of EOM, or 403–947 ppm of whole rock) suggesting early mobilisation of non-hydrocarbon substances. These asphaltenes, alternatively can be viewed as "lower molecular weight kerogens" which act, in addition to the solid kerogens, as major precursors of hydrocarbons. Their transformation into hydrocarbons presumably occurs under somewhat less intense thermal conditions (cf. Palacas, 1984). In fact, large amounts of early-generated asphaltenes are not unique to the Ouldburra source rocks but are common in other immature to marginally mature carbonate source beds, as documented by Palacas (1984).

Samples regarded as *intermediate* oil sources (KD-1, 275.43 m and KD- 2A, 211.80 m) have a low asphaltene content (4–15 %). The variation in the asphaltene content could be due to the disproportionation of asphaltenes into hydrocarbons and NSO compounds (resins) during initial hydrocarbon genesis (Palacas, 1984). Saturate/aromatic ratios are in the range of 0.5 to 0.9 indicating the lower saturate content of the total hydrocarbons.

Figure 7.8 shows the relative proportions of the three fractions of the EOM in the samples from the Manya and Tallaringa Troughs. A plot of TOC *vs* Hydrocarbons reveals that all

these samples fall in the region representing dolomite and limestone source rocks (Fig. 7.9).

The hydrocarbon-generative nature of these carbonate rocks is also evident from the petrographic character of their dispersed organic matter, as previously discussed. The primary algal biota are preserved as lamalginite and minor telalginite.
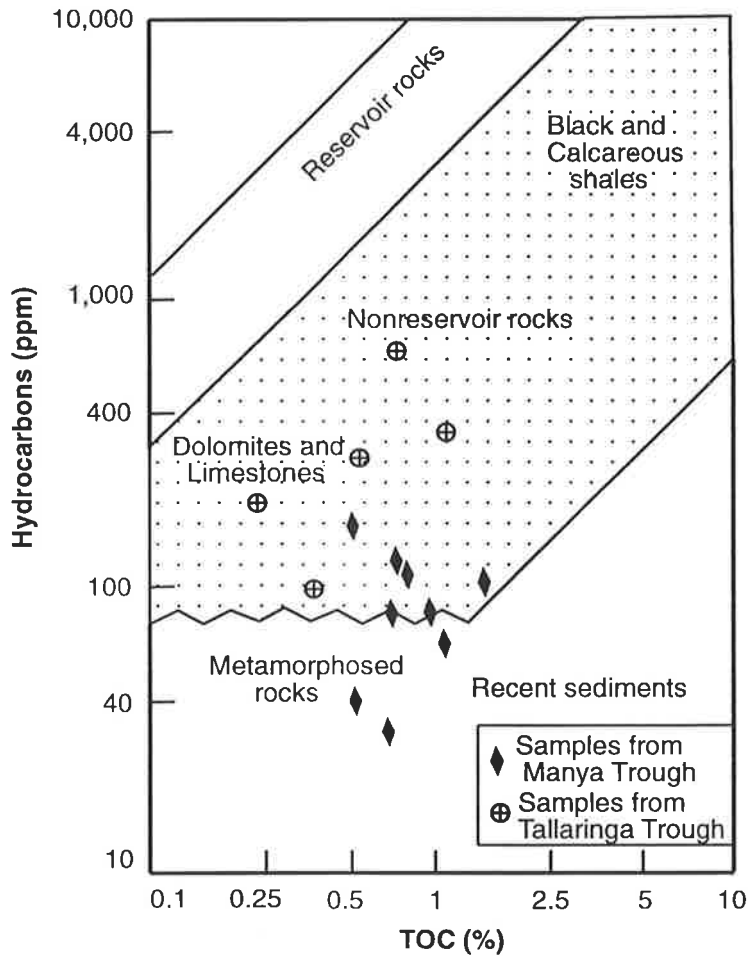
Figure 7.9 Total organic carbon (TOC) *vs* Hydrocarbons (C15+) plot. Hydrocarbon source rocks fall in shaded area above about 70 ppm hydrocarbons (simplified from Hunt, 1979).

It is worth noting that the most organic-rich sample (TOC = 1.4 %, HI = 91) from drillhole Marla-6, 416.0 m in the Manya Trough gave lower EOM and hydrocarbon yields (Table 5a

and b) compared to the most organic-poor sample (TOC = 0.2 %, HI = 510) from drillhole KD-2A, 275.85 m in the Tallaringa Trough. Organic geochemical data, together with petrographic observations, suggest that precursor algal biota in the former sample has been subjected to severe alteration, including bacterial degradation (sapropelisation), partial oxidation and advanced thermal maturation, resulting in a low quality source rock. Conversely, a lower organic input but better preservation, as noticed in the latter sample, gave a better potential source rock. Comparisons of this type, particularly in carbonate source rocks, suggest that source rock assessment based solely on the TOC content may lead to erroneous conclusions. Various geochemical parameters, including those derived from Rock-Eval pyrolysis, should be used to accurately define the source rock potential.

7.8   Gas chromatography of saturated hydrocarbons

The results of gas chromatography (GC) of the saturates fraction are summarised in Table 7.5. Selected saturates chromatograms are shown in Figures 7.10 to 7.14 and in Appendix IX.

Parameters used in the interpretation of the saturates chromatograms are :

- n-alkane distribution pattern (range, maximum, carbon preference index);

- ratio of the two acyclic isoprenoid alkanes, pristane and phytane (Pr/Ph);

- Pr/n-C$_{17}$ and Ph/n-C$_{18}$ ratios; and

- presence of branched (iso- and anteiso-) alkanes.

7.8.1   Manya Trough

A high concentration of C$_{14}$–C$_{22}$ n-alkanes with a maximum at n-C$_{17}$ suggests a primary algal and bacterial source for the OM. The saturates chromatograms of Marla-3 (619.60 m), Marla-6 (416.0 m) and Manya-6 (698.00 m) exhibit an algal/bacterial source affinity
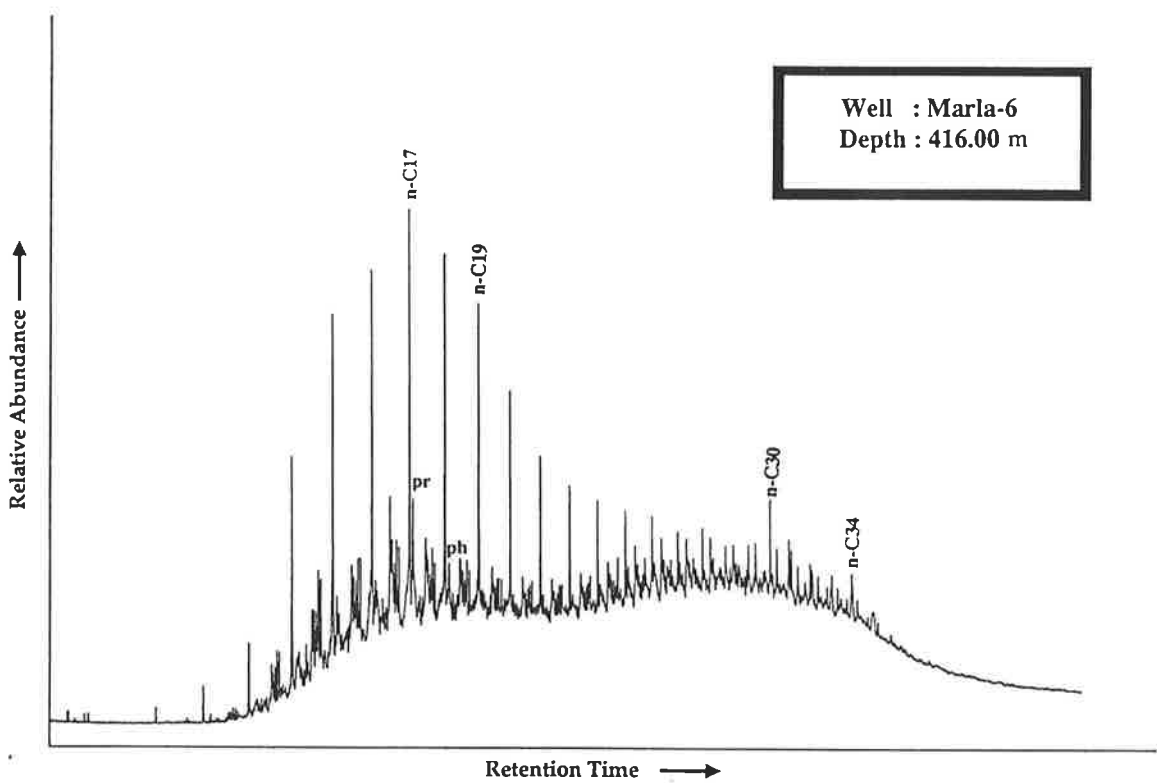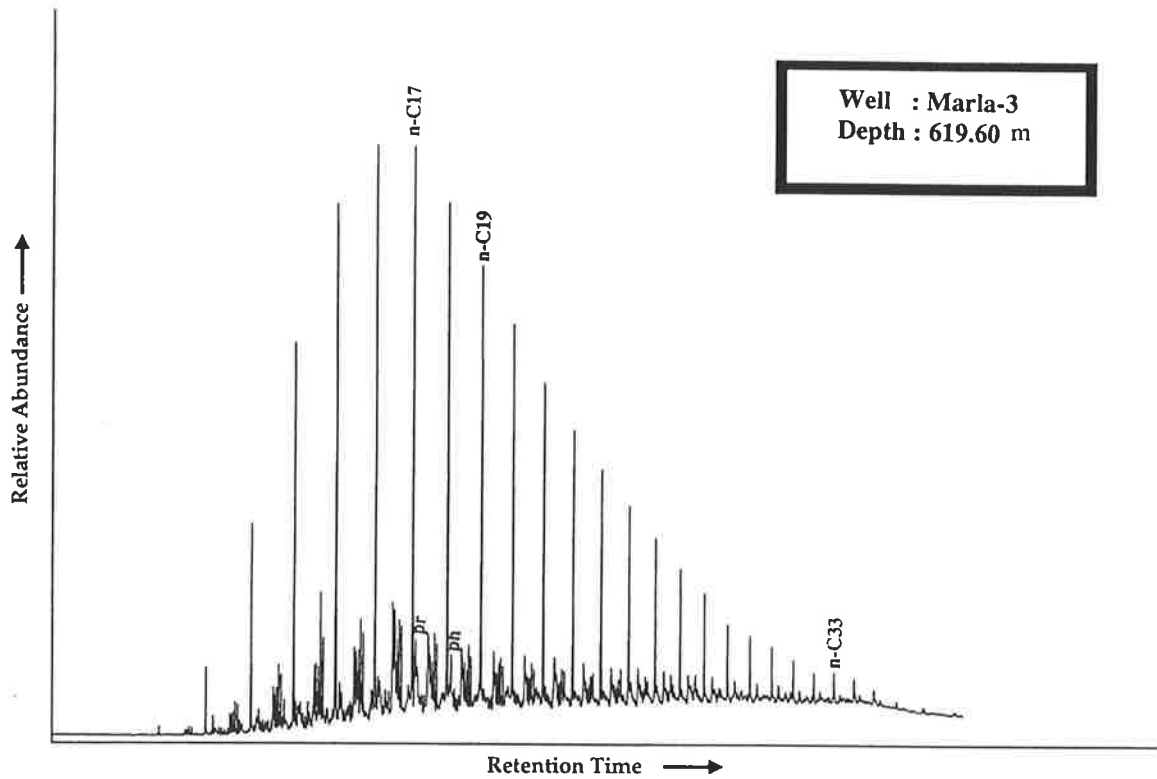
Figure 7.10 Gas chromatograms of alkanes from selected organic-rich samples of the Ouldburra Formation, Manya Trough.
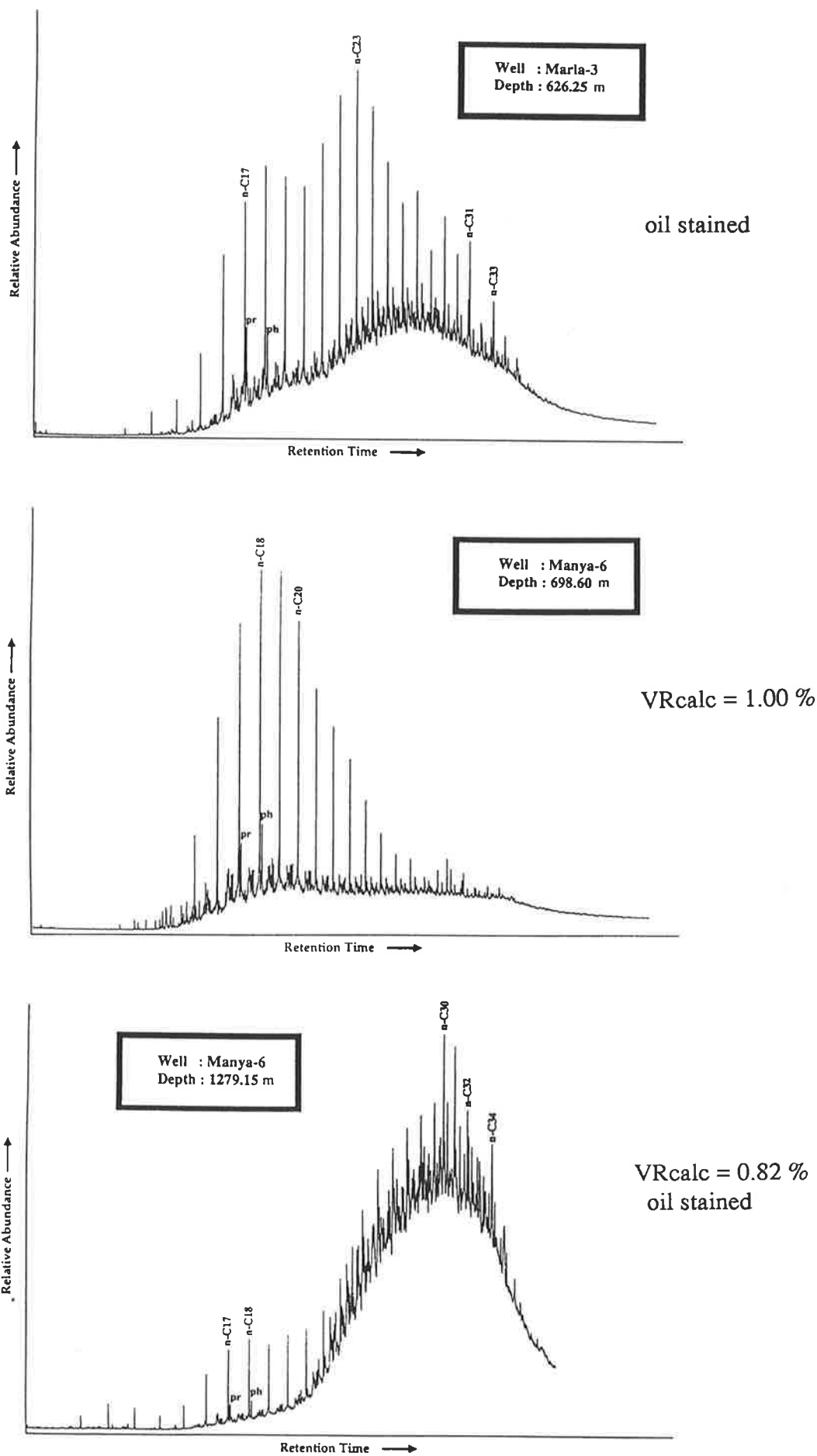
Figure 7.11 Gas chromatograms of alkanes from selected organic-rich samples of the Ouldburra Formation, Manya Trough, showing effect of staining.

111
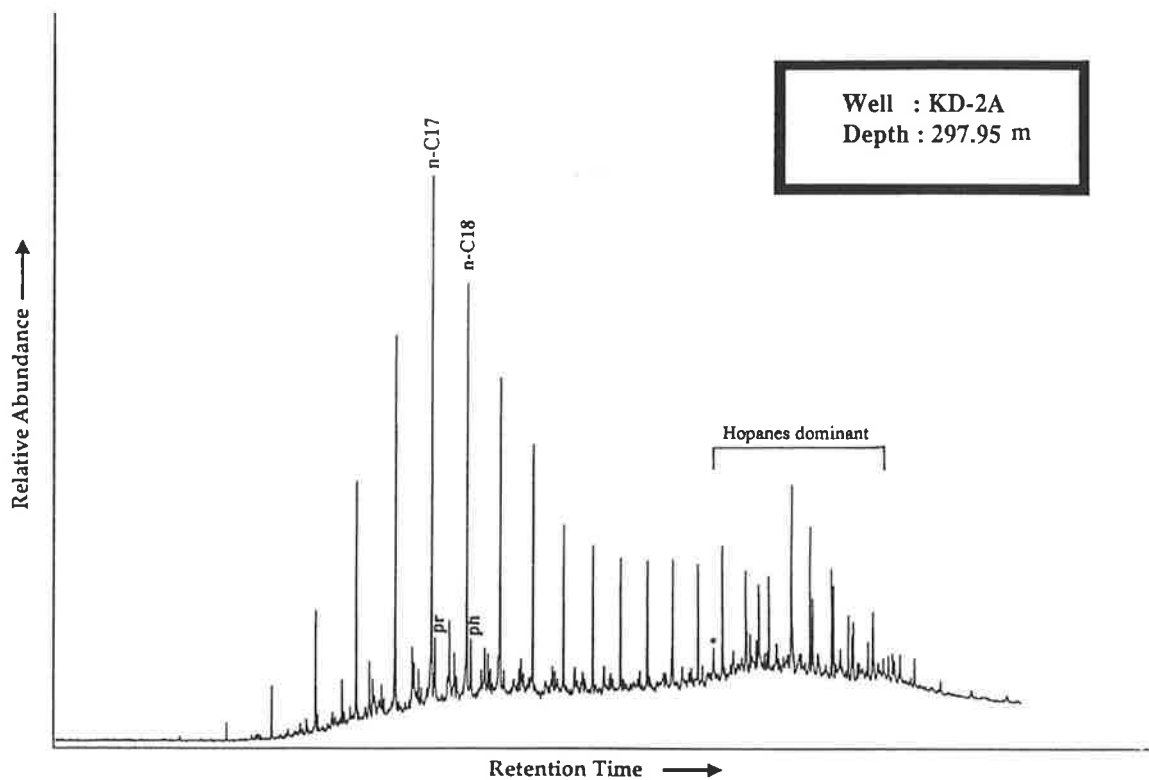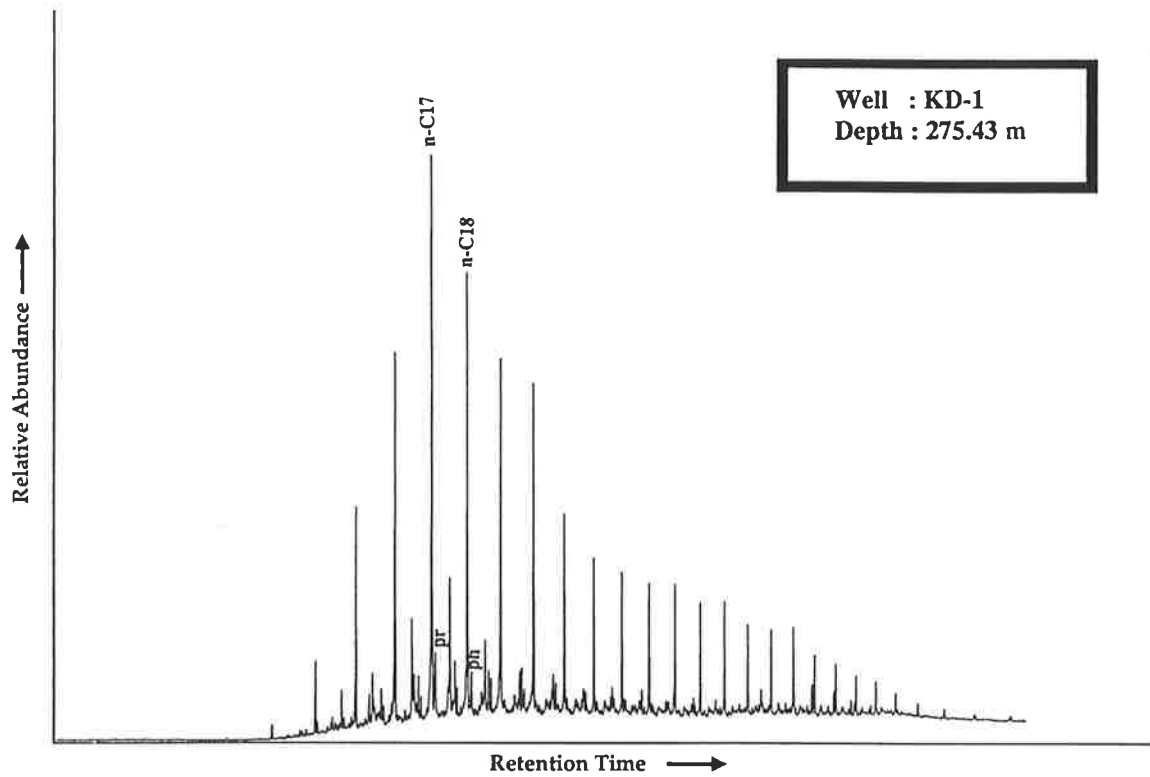
Figure 7.12 Gas chromatograms of alkanes characterised by dominant *n*-alkanes and low Pr/*n*-C$_{17}$ and Ph/*n*-C$_{18}$ ratios from selected organic-rich samples of the Ouldburra Formation, Tallaringa Trough. * is squalane.
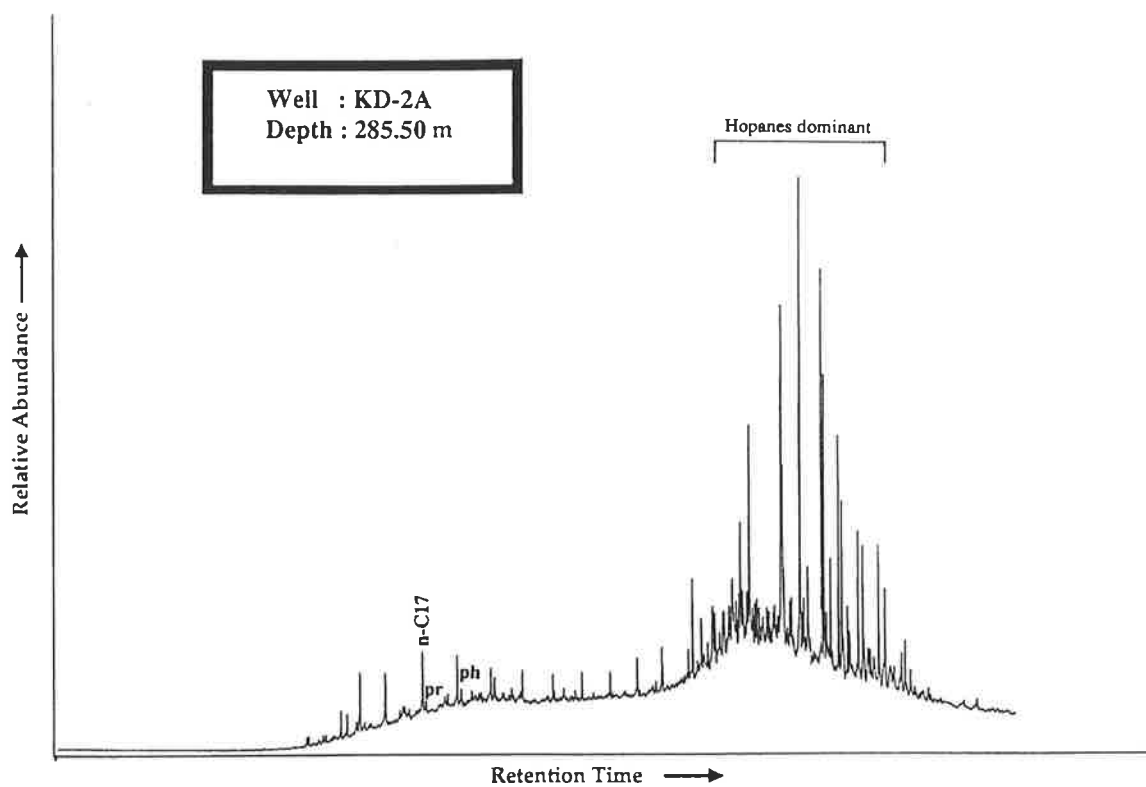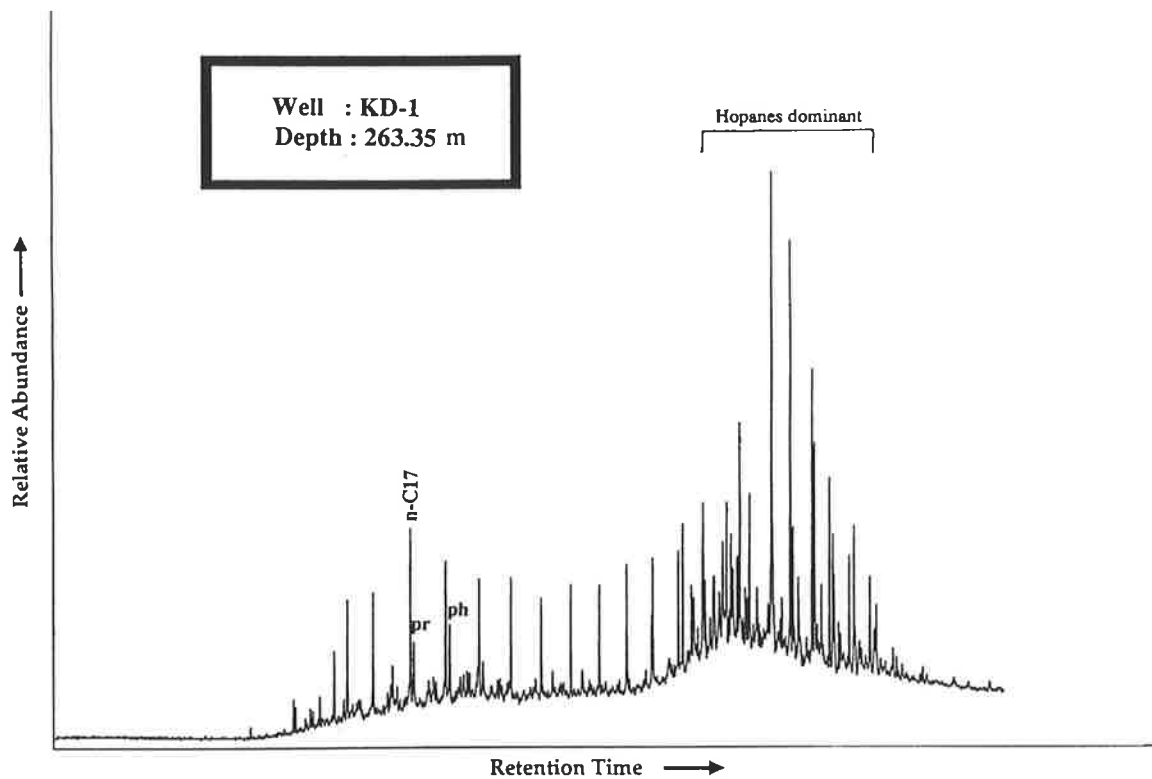
Figure 7.13 Gas chromatograms of alkanes characterised by dominant hopanes from selected organic-rich samples of the Ouldburra Formation, Tallaringa Trough.

Figure 7.14 Gas chromatogram of alkanes characterised by dominant n-alkanes with OEP in range $C_{21}-C_{35}$ and intermediate $Pr/n-C_{17}$ and $Ph/n-C_{18}$ ratios, form an organic-rich sample of the Ouldburra Formation, Tallaringa Trough. * is squalane.

Well : KD-2A
Depth : 211.80 m
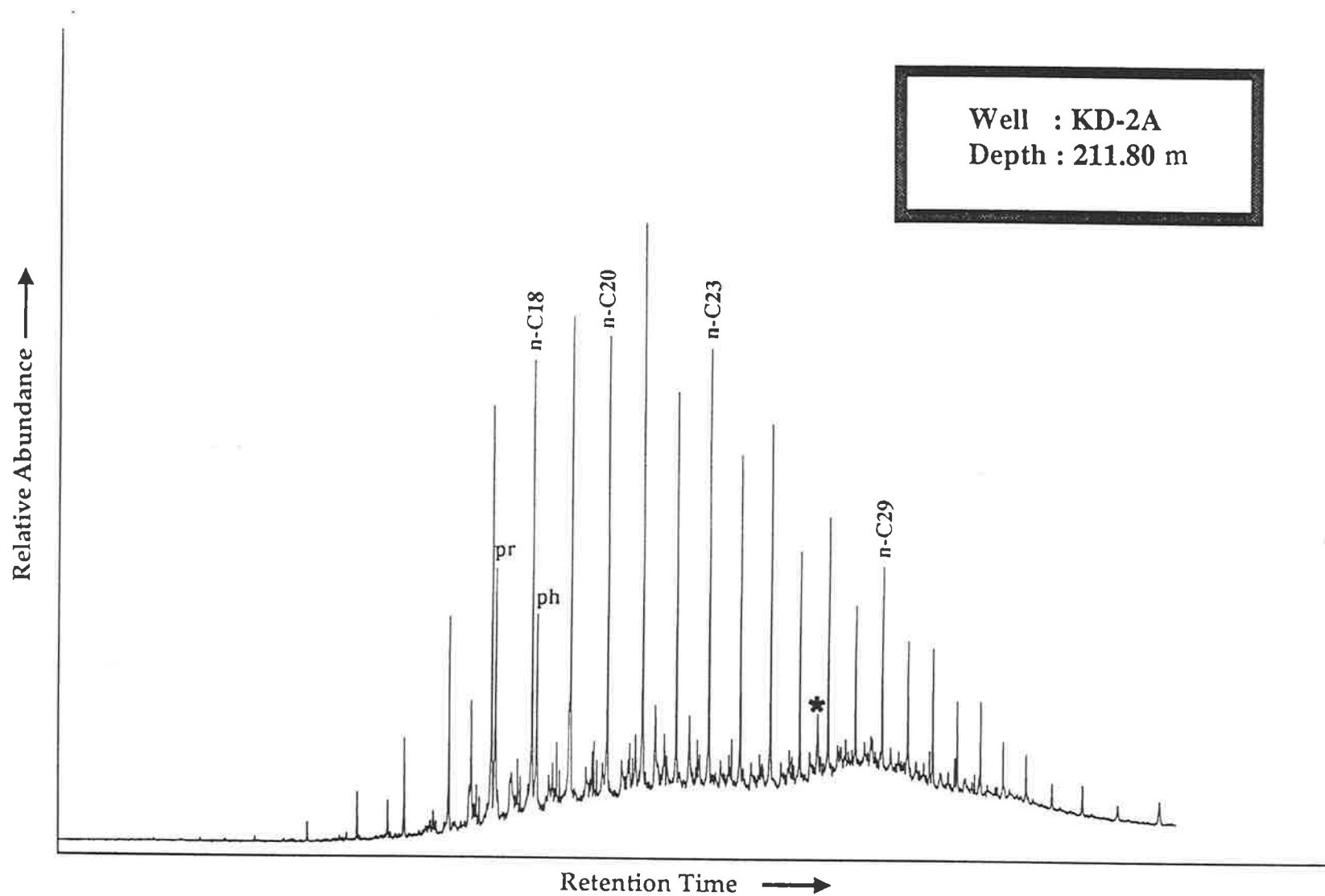
for the Manya Trough hydrocarbons (Figs. 7.10 and 7.11; Appendix IX). Smooth, unimodal, distribution of C_{15+} n-alkanes with a markedly lower concentration of n-alkanes in the C_{25}–C_{35} region and high relative concentrations of branched alkanes characterise the aforementioned samples. The bimodal distribution of n-alkanes, with maxima at C_{18} and C_{23}, in sample Marla-6, 626.25 m (Fig. 7.11), is somewhat uncommon in Manya Trough source rocks. This sample, together with that from Manya-6, 1279.15 m (Fig. 7.11), appears to be stained by migrating hydrocarbons (PI = 0.60 and 0.75, respectively: Table 7.1a). The latter sample showed anomalously low maturity (VRcalc = 0.82%) compared to the higher maturation levels exhibited by younger unit (Manya-6, 698.60 m) in the same well.

Pristane/phytane values of 0.9–1.6 indicate that anoxic to suboxic conditions existed during the deposition and early diagenesis of those carbonate muds (Table 7.5a). The pristane/n-C_{17} values for the aforementioned source rocks are in the range of 0.2–0.7, and the corresponding phytane/n-C_{18} values are in the range of 0.2–0.4, indicating reducing conditions during the deposition of algal / bacterial organic matter (Lijmbach, 1975: Fig. 7.15).

The relatively high saturate/aromatic values shown by most samples are consistent with their high levels of maturity.

7.8.2 Tallaringa Trough

Alkane chromatograms of the Tallaringa Trough carbonates (Figs. 7.12–7.14) are somewhat different from those of the Manya Trough sediments. High n-alkane concentrations noticed in the range of C_{14}–C_{20} with a maximum at n-C_{17} (Fig. 7.12, samples, KD-1, 275.43 m; ; KD-2A, 297.95 m), together with abundant branched alkanes,

again indicate algal and bacterial origins for the OM. However, strong hopane (C_{27}–C_{35}) concentrations are evident in some samples (*viz.* KD-2A, 211.80 m; KD-1, 263.35 m; KD-2A, 285.50 m) suggesting a major contribution from prokaryotic organisms, probably heterotrophic bacteria (Fig. 7.13).

A major difference is evident between the alkane patterns of the *prolific* (Fig. 7.13: KD-1, 263.35 m; KD-2A, 285.80 m) and *intermediate* (Fig 7.14: KD-2A, 211.80 m) oil sources. This may reflect a higher degree of bacterial reworking (i.e. sapropelisation) of the primary algal debris in the case of the prolific oil sources. Alternatively, it also could arise from the early generation of saturated hydrocarbons from the asphaltene fraction of the EOM, as suggested by McKirdy (1979) for similar carbonate source beds from the drillhole Wilkinson-1. The *n*-alkanes of some samples display a marked predominance of odd-carbon numbered homologues over the range C_{15}–C_{35} (e.g. samples: KD-1, 275.43 m; and KD-2A, 211.80 m: Figs 7.12 and 7.14). This is probably a sign of thermal immaturity, although an odd-carbon number preference in the C_{23+} *n*-alkanes is very unusual for sediments of Cambrian age. Such a feature generally is associated with OM derived from vascular plants and therefore is unexpected in pre-Devonian sedimentary rocks (McKirdy and Kantsler, 1980).

Uniformly low Pr/Ph values (0.7-1.4: Table 7.5a) indicate that anoxic to suboxic conditions prevailed during the deposition and early diagenesis of these carbonates. Pr/n-C_{17} and Ph/n-C_{18} values are in the range of 0.15 to 0.7 and 0.13 to 0.6, respectively, suggesting an algal and bacterial source and reducing conditions (Lijmbach, 1975: Fig. 7.15).

Saturate/aromatic values are uniformly low (0.5–0.9: Table 5) consistent with the lower maturity of the Ouldburra Formation where sampled in the Tallaringa Trough.
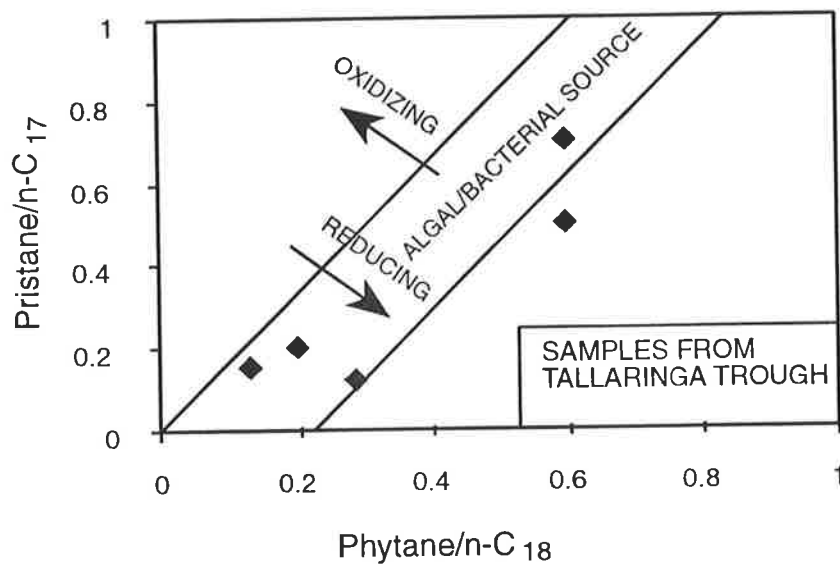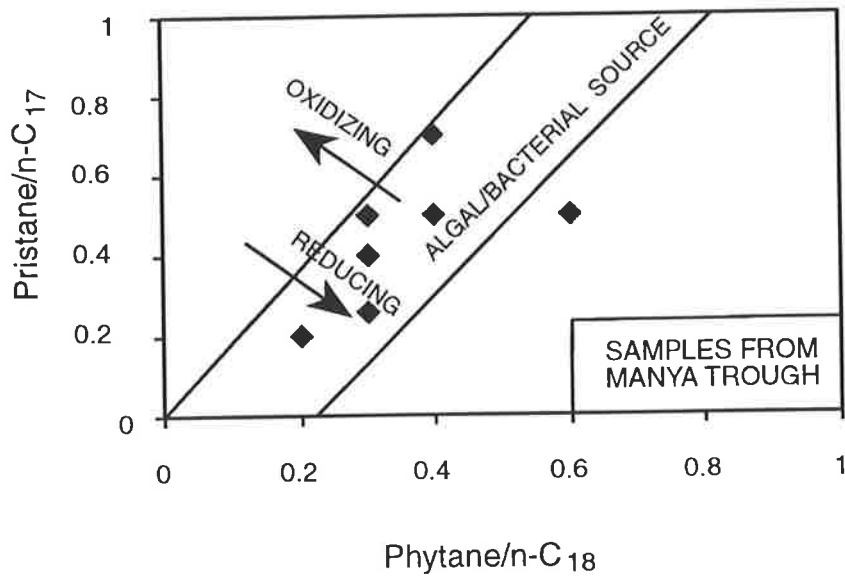
Figure 7.15 A simplified plot of pristane/n-C$_{17}$ vs Phytane/n-C$_{18}$ shown for hydrocarbons. (originally constructed by W.L. Orr, based on concepts first developed by Lijmbach, 1975).

7.9   Measurement of maturation level

Since the Ouldburra Formation sediments, like all pre-Devonian sediments, are devoid of vitrinite macerals on which maturity measurements can be made, triaromatic hydrocarbon distributions were used as alternative measures of maturity. These measurements include

the methylphenanthrene index (MPI), methylphenanthrene ratio (MPR) and calculated vitrinite reflectance (VRcalc) as proposed by Radke and Welte (1983), Radke et al. (1984), Radke (1987) and Boreham et al. (1988).

MPI, MPR and VRcalc are defined by the following equations:

$$(1) \quad MPI = \frac{1.5(2\text{-}MP + 3\text{-}MP)}{P + 1\text{-}MP + 9\text{-}MP}$$

$$(2) \quad MPR = \frac{2\text{-}MP}{1\text{-}MP}$$

(3)   VRcalc (a) =   0.6 MPI + 0.40 (for VR in the range 0.65–1.35 %; r = 0.96)

              =   -0.60 MPI + 2.30 (for VR>1.35 %)

(4)   VRcalc (a′) =   0.70 MPI + 0.22 (for VR in the range 0.5–1.7 %; r = 0.84)

(5)   VRcalc (b) =   0.99 log $_{10}$ MPR + 0.94 (for VR in the range 0.4–1.7 %; r = 0.84)

Where   P   =   Phenanthrene*

       1-MP   =   1-methylphenanthrene

       2-MP   =   2-methylphenanthrene

       3-MP   =   3-methylphenanthrene

       9-MP   =   9-methylphenanthrene

*Note a response factor of 0.69 was applied to the area of this peak in all GC-MS chromatograms (Appendix XI) when calculating MPI.

Equation (4), based on the analysis by Boreham et al. (1988) of a large number of coal and shale samples from the Australian continent, is an alternative to equation (3) developed by Radke and Welte (1983). However, the latter equation is likely to be more appropriate in the present study because the calibration was established using carbonate rocks.

Table 7.6 Aromatic maturity data, Ouldburra Formation Officer Basin.

Drillhole	Depth m	Formation	Sample type	MPI	MPR	VRcalc % (a)	VRcalc % (a´)	VRcalc % (b)
	Tallaringa	**Trough**						
KD-1	263.35	Ouldburra	extract	0.38	0.46	0.63	0.49	0.60
KD-2A	285.50	Ouldburra	extract	0.46	0.6	0.68		0.72
KD-2A	297.95	Ouldburra	extract	0.30	0.47	0.58		0.62
KD-2A	298.13*#	Ouldburra	extract	0.34	0.38	0.60	0.46	0.52
	Manya	**Trough**						
Marla-3	619.60	Ouldburra	extract	1.00	1.24	1.00	0.92	1.03
Marla-6	416.00	Ouldburra	extract	1.43	1.76	1.26	1.22	1.18
Marla-6	671.25	Ouldburra	extract	2.13	4.98	1.68	1.71	1.63
Marla-7	392.85	Ouldburra	extract	1.30	1.92	1.18	1.13	1.22
Manya-6	698.60	Ouldburra	extract	1.11	2.34	1.07	1.00	1.31
Manya-6	1279.15*	Ouldburra	extract	0.85	1.33	0.91	0.82	1.06

* = stained by oil   # = data from McKirdy (1986).

A total number of 9 aromatic fractions from the Manya Trough (n = 6) and Tallaringa Trough (n = 3) were subjected to MPI analysis. Calculated vitrinite reflectance (VRcalc) values derived from MPI and MPR are shown in Table 7.6 and representative mass fragmentograms are presented in Appendix XI.

In the Manya Trough, the Ouldburra Formation displays a higher degree of maturity (VRcalc = 1.00–1.68 % : late mature to overmature) and therefore is essentially gas-generative. One sample (Manya-6, 1279.15 m depth) has an anomalously low maturity (VRcalc = 0.91 %) with respect to the higher maturation level (VRcalc = 1.07 %) at 698.60 m depth in the same well, and is believed to be stained by migrated hydrocarbons (see previous discussion).

In drillholes KD-1 and KD-2A, located on the southern edge of the Tallaringa Trough, the Ouldburra Formation is early mature (VRcalc = 0.58–0.68 %) indicating that these oil-prone carbonate source beds are within the conventional oil window. The hydrocarbon generation model proposed by Powell and Snowdon (1983) is applicable to the aforementioned carbonate source rocks (Fig. 7.16).

The MPI measurements appear to provide the most accurate measure of maturation in these early mature carbonate source beds, which is also entirely consistent with the petrographic observations made under white reflected light and in fluorescence mode. Active expulsion of hydrocarbons from lamalginite is evident in organic-rich samples (KD-1, 263.43 m and KD-2A, 285.50 m). These hydrocarbons fill microfractures and veins in the carbonate matrix (Plates 7.3c and 4f).

The VRcalc values obtained from drillhole KD-2A (depth intervals, 285.50 m and 297.95 m) indicate that the deeper sample is significantly less mature than the shallower sample (Table 7.6). This type of internal inconsistency in the VRcalc values makes interpretation somewhat difficult. It may be due to a mineral or organic matrix effect which inhibited the catagenetic methylation of phenanthrene. Such problems are encountered when working with sediments containing non-humic matter (Type I or II kerogens) (Radke, 1987).
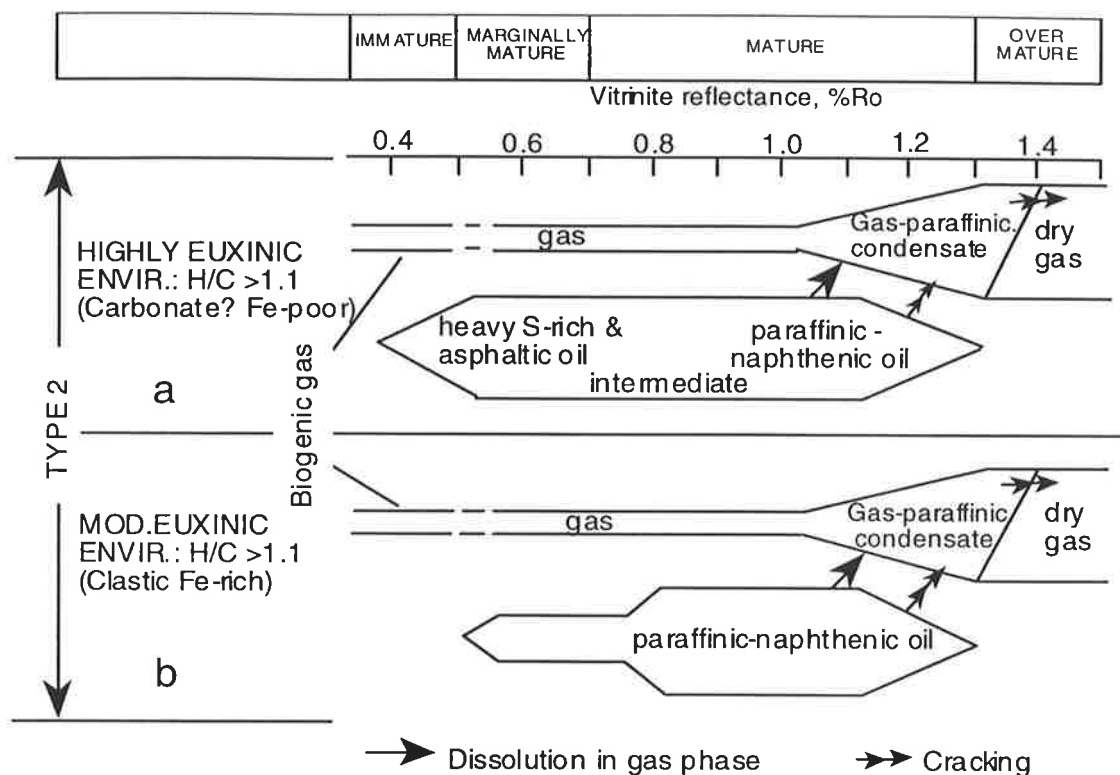
HYDROCARBON GENERATION MODE - MARINE ORGANIC MATTER

a) Algal dominated, input from photosynthetic bacteria, modification by addition of S from bacterial sulphate reduction - carbonate/evaporite mesosaline to hypersaline environment gives high S kerogens.

b) Algal dominated, varying input from terrestrial sources, some bacterial modification and addition biomass - environments are barred basins, epeiric seas, upwelling areas etc. - clastic sources (Fe-rich) give low S kerogens, carbonate sources give higher S kerogens.

Figure 7.16 Hydrocarbon generation model for kerogen Type II (after Powell and Snowdon, 1983).

7.10 Summary

In the Manya Trough, TOC content of the Ouldburra Formation varies between 0.2% and 1.4%, and the richest source beds are thin but widespread. These organic-rich beds were deposited in a range of shallow marine environments attributable to transgressive and

121

highstand systems tracts. Lithologically, they comprise laminated limestone, dolomitic limestone, and stylolitic limestone.

The pattern of organic matter distribution, discussed in conjunction with sequence stratigraphy and detailed sedimentology, can serve as a model for the prediction of source rock occurrence in similar geological settings.

Rock-Eval and elemental data indicate the presence of Type III to IV kerogen (HI <100) and calculated vitrinite reflectance is in the range 1.00–1.68 %.

Extractable organic matter yields are variable but low (142–267 ppm of the whole rock; 10-40 mg/g TOC). Saturates are the dominant hydrocarbon type in the EOM.

Hydrocarbon staining was recognised in two samples, and is also evident from their respective Rock-Eval data and gas chromatograms. The results of this study suggest that Ouldburra Formation source beds in the Manya Trough are late mature to overmature, and gas prone.

In the Tallaringa Trough, the organic-rich beds of the Ouldburra Formation are limestones and dolomitic limestones have variable TOC contents (0.2–1.2 %). The richest source beds are brown, thin ($\cong 2$ m) and emit a strong petroleum odour when scratched or freshly broken. These beds were deposited in a highly anoxic environment (probably a restricted lagoon). Petrographically, common lamalginite of cyanobacterial affinity, telalginite (*G. prisca*) and bacterial biomass constitute the bulk of the OM. The presence of indigenous oil in veins and fractures, together with thucholites in close proximity to abundant lamalginite, suggests that these source beds are within the oil-generating window.

The enigmatic fossil (?) alga *G. prisca* is reported for the first time from rocks of Early Cambrian age in this study.

Rock-Eval and elemental data indicate a Type II composition for the kerogen (HI = 285–510). Extractable bitumen yields are high (582–2540 ppm of the whole rock; 144–348 mg/g TOC). Aromatic hydrocarbons are more abundant than saturates in the bitumen. Calculated vitrinite reflectances derived from MPI are in the range 0.58–0.68 %. The results of this study suggest that the Ouldburra Formation in the Tallaringa Trough contains early mature to mature, good to excellent, oil-prone source beds.

CHAPTER 8

BIOMARKERS IN THE OULDBURRA FORMATION

8.1   Introduction

The last two decades have witnessed tremendous growth in the use of biomarkers as indicators of depositional environment, biological source input and thermal maturity for petroleum source rocks.

It has been known for a long time that different depositional environments are characterised by inputs of OM from particular groups of organisms. Abundant supplies of OM in a specific environment can produce a suite of diagnostic biomarkers (Peters and Moldowan, 1993). Imbus and McKirdy (1993) have recently outlined the common biological markers, with their probable precursor biota, occurring in Precambrian and early Palaeozoic sequences. For example, n-alkanes with dominant n-C_{15} and n-C_{17} indicate algal or cyanobacterial affinity whereas the presence of steranes (C_{26}–C_{30}) suggests a eukaryotic algal source. Hopanes (C_{27}–C_{35}) and methylhopanes (C_{28}–C_{36} 2-methyl) in sediments are derived from bacteria and methylotrophic bacteria, respectively. Therefore, the identification of high concentrations of these and other biomarkers in bitumens or oils will aid in recognition of the environmental conditions which existed during deposition of the source rock (Table 8.1).

Biomarkers may also provide useful data on the thermal maturity of rock extracts and oils (Table 8.2). These data, like the source-specific parameters listed in Table 8.1, may be used for oil-oil and oil-source correlations. However, some maturity-dependent

Table 8.1 Precambrian and Early Palaeozoic biological markers and their probable precursor biota and environments (modified from Imbus and McKirdy, 1993).

Biological marker	Precursor biota	Environment
n-Alkanes		
C_{12}–C_{20} with marked odd/even predominance	Bacteria, cyanobacteria	Lacustrine, marine
C_{17}	Cyanobacteria	Lacustrine, marine
C_{21}–C_{35}	Bacteria (e.g. sulphide reducers), eukaryotic algae, ?graptolites	Lacustrine, marine
Methylalkanes		
C_{12}–C_{20}, *iso* (2-Me) and *anteiso* (3-Me)	Bacteria	
C_{20}–C_{26}, mid-chain Me	?Bacteria	
Isoprenoid alkanes		
C_{15}–C_{20} regular	Photosynthetic algae	
C_{15}–C_{25} regular	Archaebacteria (methanogens, halophiles)	
C_{30}–C_{40} irregular including squalane	Archaebacteria (methanogens, halophiles)	Hypersaline
Pristane/phytane	Phototrophs, Archaebacteria	
<1 Anoxic		
1–2 Suboxic		
>2 Oxic		
Aryl isoprenoids		
C_{13}–C_{31} irregular	Green sulphur bacteria	Meta- to hypersaline
Alkylcyclohexanes		
C_{13}–C_{21} *n*-alkyl with odd/even predominance	Cyanobacteria, bacteria (including thermoacidophiles)	
C_{14}–C_{20} Me- *n*-alkyl with even/odd predominance	Cyanobacteria, bacteria (including thermoacidophiles)	
Tricyclic terpanes		
C_{19}–C_{33}	?Eukaryotic algae, bacteria	
Tetracyclic terpanes		
C_{24} dominant	?Bacteria	
Hopanes		
C_{27}–C_{30} dominant	Cyanobacteria, bacteria	
C_{31}–C_{35} dominant	Cyanobacteria, bacteria	
8,30-bisnorhopane	Cyanobacteria, bacteria	
C_{27}–C_{35} neohopanes	?Bacteria	
Methylhopanes		
C_{28}–C_{36} 2-methyl	Bacteria	Carbonate
Gammacerane	?Protozoa, Bacteria	Hypersaline
Steranes		
C_{26}–C_{30} desmethyl	Eukaryotic algae	
· C_{28} dominant	?Halophilic algae	Evaporitic
C_{30} 24-isopropylcholestane	Sponges	Marine
Methylsteranes		
C_{28}–C_{30} 2-3-, and 4-methyl	Eukaryotic algae	Marine, hypersaline
Dinosteranes	Dinoflagellates	Marine, hypersaline

biomarkers have a limited usage. For instance, the otherwise reliable C_{29}-sterane 20S/20R isomerisation ratio can only be effectively used below peak oil generation (Ro ~ 0.9 %) because, at this maturity level, the reactions it represents have reached equilibrium (Peters and Moldowan, 1993). Some biomarker maturity parameters which are useful at high levels of maturity (e.g. up to and above the equivalent of 1.0 % vitrinite reflectance) include absolute concentrations of steranes and hopanes, tricyclic/17α (H)-hopanes, diasteranes/steranes, and Ts/(Ts + Tm) (Van Graas, 1990). Moretanes, are unstable triterpanes which are commonly used as a maturity indicator for immature samples. Generally, the absolute concentrations of all biomarkers decrease with increasing maturity. Thus, in highly mature samples, biomarker concentrations may become too low for accurate quantification (Waples and Machihara, 1991).

Table 8.2 Approximate ranges of some biomarker thermal maturity parameters.

Biomarker	Thermal maturity domain	References
20S / (20R + 20S) C_{29} sterane	$0.25 \equiv 0.51 \pm 0.02$ % Ro $0.45 \pm 0.03 \equiv 0.65-0.79$ % Ro	Waples and Machihara, 1991
C_{29} 13β(H) 17α(H) 20R diasteranes / C_{29} 5α(H) steranes	-Source dependent; low in carbonate source rocks -Increases past peak oil generation -Increases via bacterially-mediated reactions	McKirdy et al., 1983; Rullkötter et al., 1985 Peters et al., 1990 Michaelsen et al., 1995
22S / (22S + 22R) $C_{31}-C_{32}$ homohopane	0.50-0.54 Barely entered oil generation 0.57-0.62 Reached or surpassed oil generation	Peters and Moldowan, 1993
17β(H) 21α(H)-moretane / 17α(H) 21β-hopane	~ 0.8-0.15 Immature oil <0.15 Mature source rocks	Mackenzie et al.,1980; Seifert and Moldowan, 1980
Ts / Ts + Tm	-Is source and facies dependent and decreases in an anoxic carbonate section -Increases above 0.9 % Ro	McKirdy et al., 1983, 1984; Peters and Moldowan, 1993 Van Graas, 1990

Table 8.3 Biomarker parameters of source, maturity and depositional environment in the

Ouldburra Formation.

Depth (m)	Lithology	Steranes		Terpanes			Acyclic Alkanes
		1	2	3	4	5	6
Manya Trough							
Manya -6 (698.60)	Dolostone	44: 23: 33	0.82	1.86	0.07	0.41	1.0
Manya-6 (1279.15)	Lam. limestone	43: 22: 35	0.86	1.91	0.07	0.31	0.9
Marla-3 (619.60)	Lam. dolostone	44: 23: 33	0.90	1.82	0.07	0.38	1.0
Marla-6 (416.0)	Dolostone	43: 21: 36	0.87	1.86	0.07	0.36	1.6
Marla-6 (671.25)	Lam. dolostone	46: 26: 28	1.30	1.74	0.04	0.35	2.6
Marla-7 (392.85)	Lam. dolostone	40: 27: 33	0.98	1.87	0.18	0.45	1.7
Tallaringa Trough							
KD-1 (263.35)	Lam. limestone	56: 30: 14	5.20	7.85	0.16	0.30	0.7
KD-2A (285.50)	Micritic limestone	56: 27: 17	1.55	6.30	0.21	0.27	1.2
KD-2A (297.95)	Micritic limestone	42: 37: 21	2.00	10.40	0.17	0.26	1.2

Key to biomarker parameters :

1 = C_{27}: C_{28}: C_{29} $5\alpha(H)$ $14\alpha(H)17\alpha(H)$ 20R steranes (m/z 217)

2 = C_{29} $13\beta(H)$ $17\alpha(H)$ 20R+20S diasteranes / C_{29} $5\alpha(H)$ steranes (m/z 217)

3 = C_{30} $17\alpha(H)$-hopane (m/z 191) / (C_{29} $\alpha\alpha\alpha$ (20S + 20R) regular steranes (m/z 217)

4 = C_{30} $17\beta(H)$ $21\alpha(H)$ moretane / $C_{30}17\alpha(H)21\beta(H)$ hopane (m/z 191)

5.= C_{27} $18\alpha(H)$-22,29,30-trisnorneohopane / C_{27} $18\alpha(H)$-22,29,30-trisnorneohopane + C_{27}

   $17\alpha(H)$-22,29, 30- trisnorhopane (Ts/Ts + Tm) (m/z 191)

6 = pristane / phytane

The Ouldburra Formation affords an ideal opportunity to examine Early Cambrian molecular fossils because its organic-rich carbonates are relatively unaffected by metamorphism (Moussavi-Harami and Gravestock, 1995). This view is also in agreement with the thermal maturity measurements (VRcalc = 1.00-1.68%) of these organic-rich carbonates in the Manya Trough previously reported by Kamali et al. (1993). Nine core samples from the Ouldburra Formation were selected for analysis: three laminated, micritic limestones from the Tallaringa Trough (KD-1, 2A), and five dolostones and one laminated limestone from the Manya Trough (Manya-6, Marla-3, 6 and 7). The operating conditions for GC, GC-MS and GC-MS-MS analyses are given in Chapter 1 (1.6.6). The biomarker parameters of source, maturity and depositional environment are summarised in Table 8.3.

8.2 Molecular indications of source biota and environment of deposition

Deposition of thin (1-2 m), organic-rich intervals in the Manya Trough took place in shallow marine environments as part of transgressive and highstand systems tracts (previously discussed in Chapter 7), whereas organic-rich limestones from the Tallaringa Trough were deposited in restricted subtidal to supratidal shallow marine environments characterised by a paucity of fauna and the presence of evaporite minerals (*viz.* anhydrite and gypsum with traces of dolomite) which suggest a warm and probably arid climate. The latter organic-rich beds commonly overlie oolitic-intraclastic limestone (grainstone) and pass upwards into marginal marine siltstone and continental red beds, indicating a change from intertidal to supratidal environment.

The major source biota are marine algae, cyanobacteria, heterotrophic bacteria (including sulphate reducers), and archaebacteria (e.g. halophiles and methanogens) (McKirdy et al., 1984). Petrographically, as discussed previously in Chapter 7, lipid-rich lamalginite occurs

as a major organic maceral with subsidiary amounts of telalginite, acritarchs (phytoplankton) and coccoid cells in the Tallaringa source beds. In the Manya source beds, lamalginite occurs in much lower concentrations and instead non-fluorescent bituminite appears as the dominant maceral.

GC-MS data from KD-1 (263.35 m; Fig. 8.1a and b) are typical of the intervals sampled in the Tallaringa Trough. The principal features of the m/z 191 mass fragmentogram for these anoxic sediments include a slight predominance of 17α-hopane (Fig. 8.1a: peak 8) over 17α-30-norhopane (Fig. 8.1a: peak 5). The rearranged hopanoid, 18α-30-norneohopane ($C_{29}Ts$: peak 6), and the compound previously identified as 18α-30-neohopane ($C_{30}Ts$: peak 9) by Michaelsen and McKirdy (1995), are clearly observed.

There is a conspicuous absence of 28,30-bisnorhopane, a biomarker commonly considered diagnostic of anoxic deposition. This feature is somewhat incongruous since the compound in question is present, albeit in low concentrations, in the Manya Trough sediments (Fig. 8.1c: peak 4; Michaelsen et al., 1995). The corresponding m/z 205 trace of the Tallaringa Trough carbonate demonstrates that its methylhopanes (Summons and Jahnke, 1992; Wang et al., 1993), derived from functionalised precursors in methylotrophic bacteria, are dominated by 2α(Me)-30-norhopane (Fig. 8.1b: peak 6) and 2α(Me)-hopane (peak 8). Other features include the 2α(Me) homologues of Ts, Tm and possibly $C_{29}Ts$ which are also present in high abundance.

Figure 8.2 illustrates the hopane (m/z 191) and sterane (m/z 217) distributions in two representative extracts from the Manya and Tallaringa Troughs. The mass chromatograms of other samples are given in Appendix XII. By comparison with the Manya extracts, the Tallaringa extracts exhibit higher hopane concentrations and appreciably higher
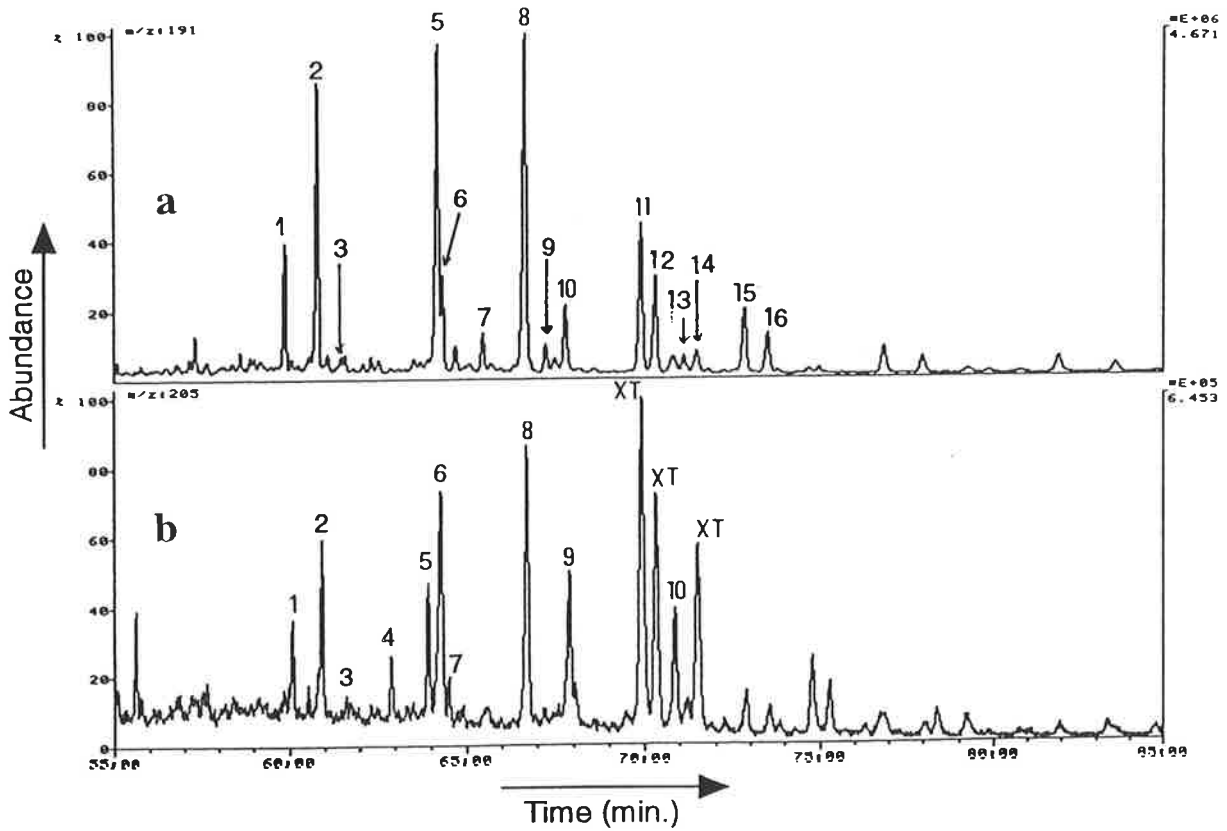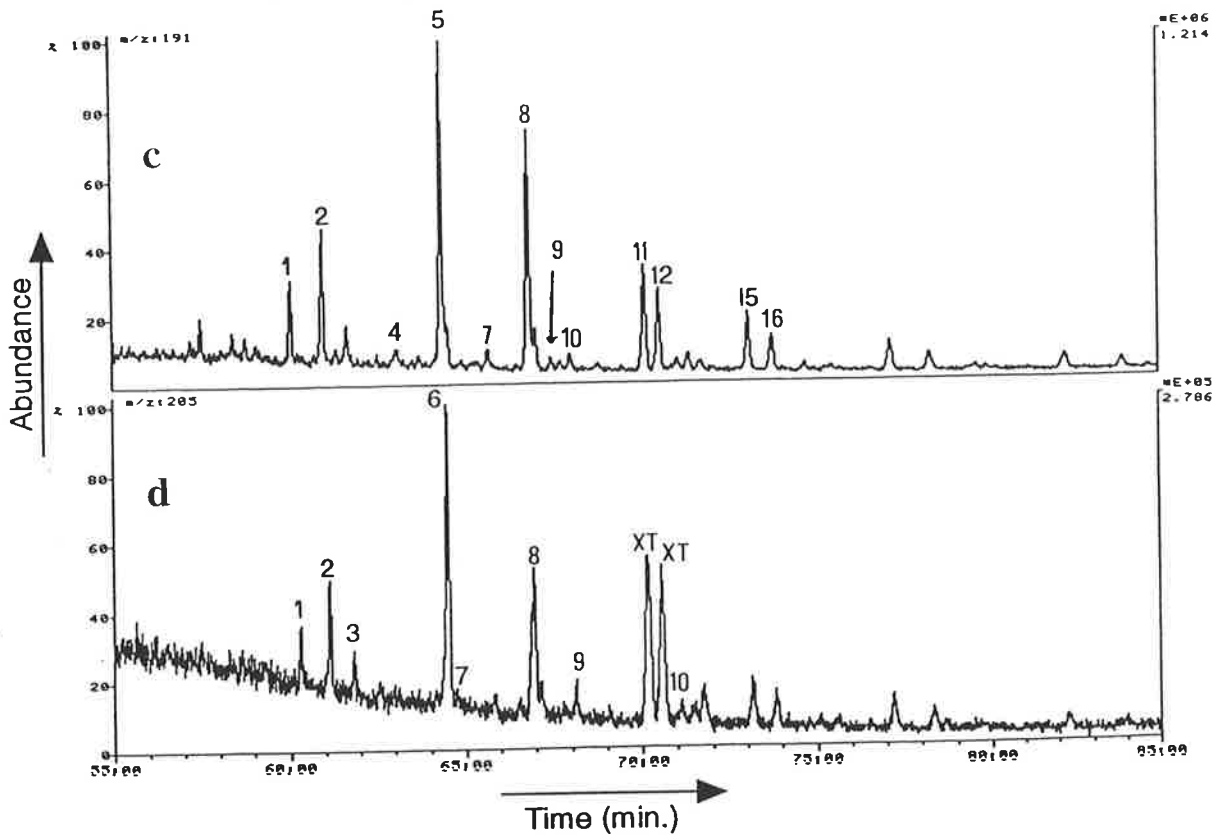
Figure 8.1 Mass chromatograms of terpanes (*m/z* 191 and *m/z* 205) in representative carbonates from the Tallaringa and Manya Troughs. Peak identities are given in Appendix XII.
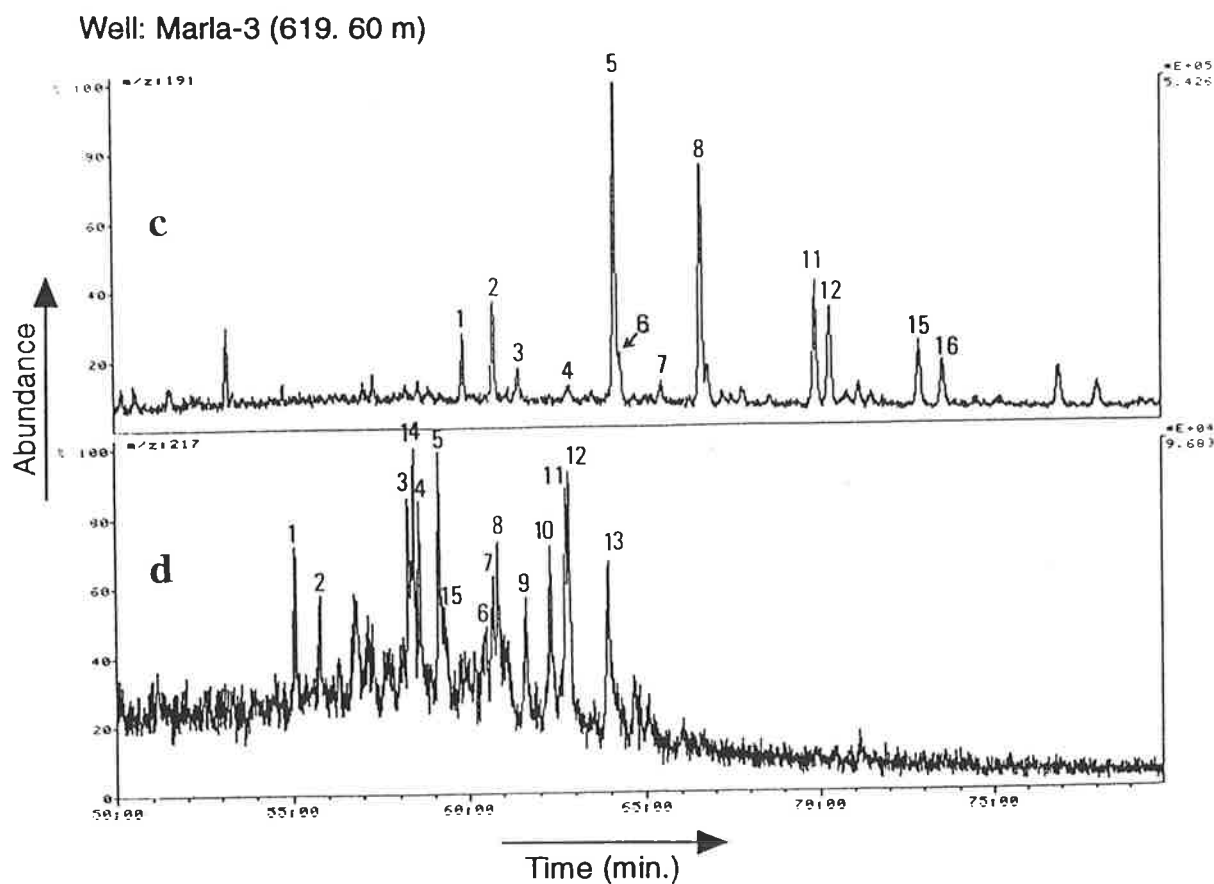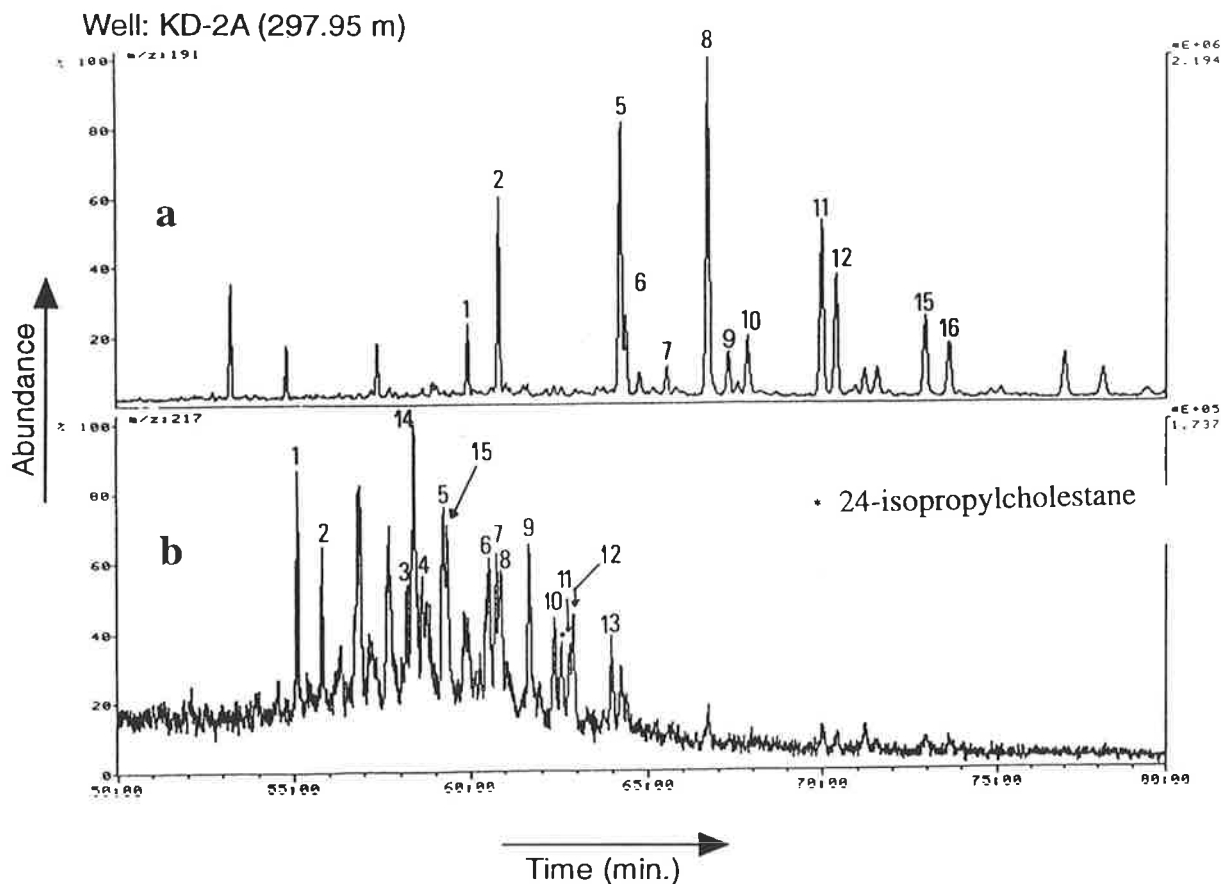
Figure 8.2 Mass chromatograms of terpanes (*m/z* 191) and steranes (*m/z* 217) in representative carbonates from the Tallaringa and Manya Troughs. Peak identities are given in Appendix XII.
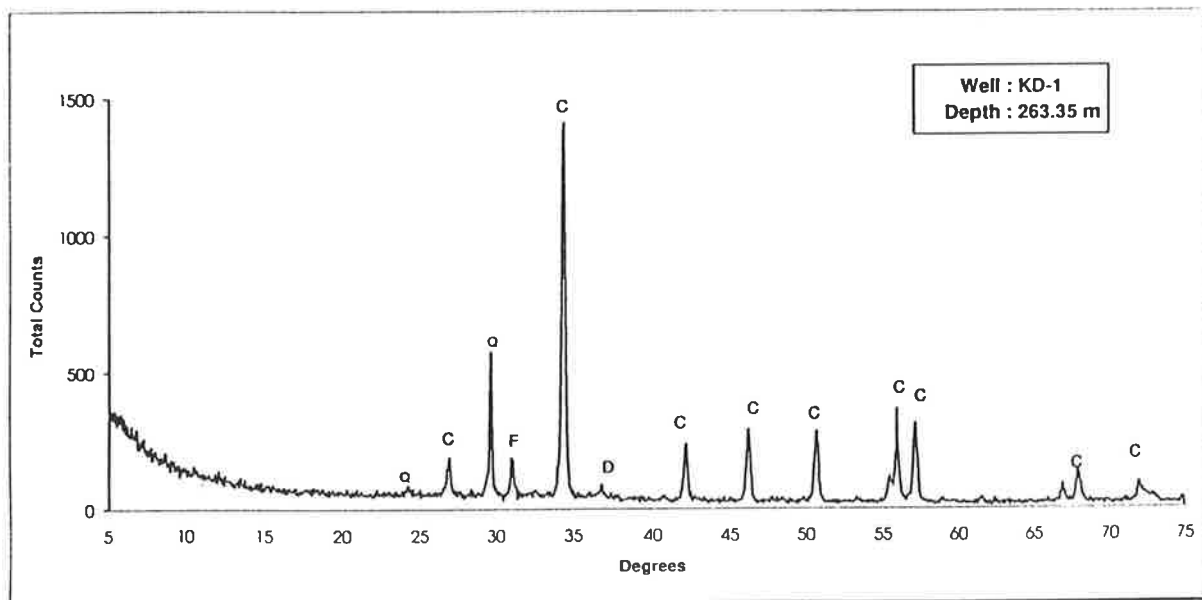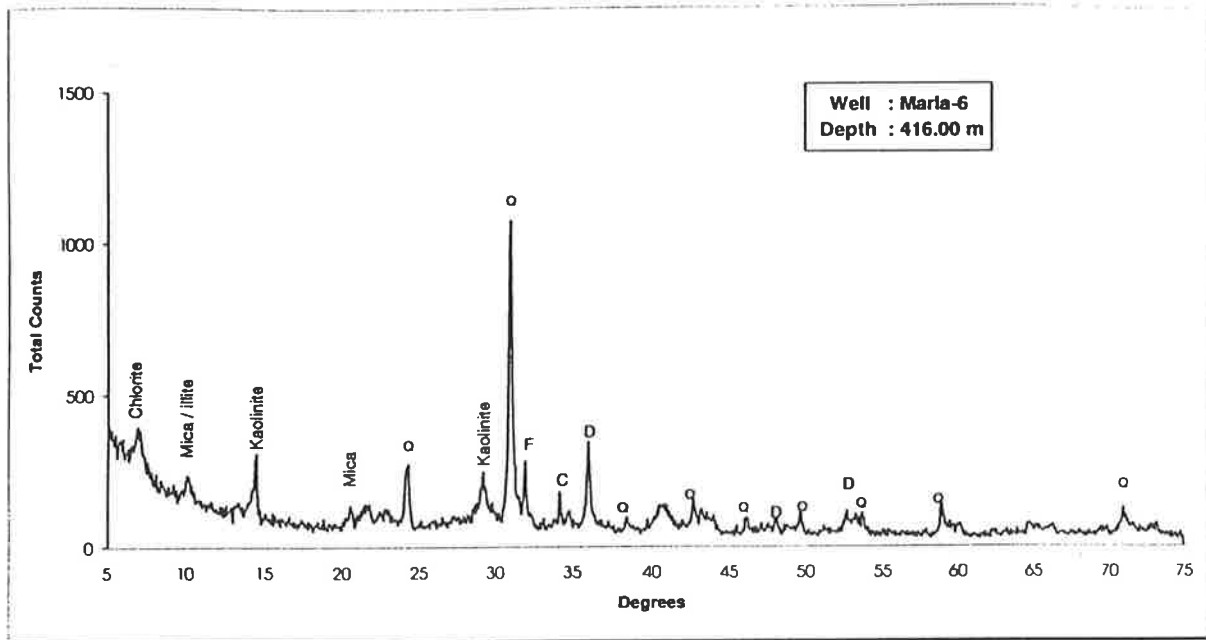
Figure 8.3 X-ray diffraction profiles of a laminated micritic limestone from the Tallaringa Trough (KD-1, 263.35 m) and a micritic dolostone from the Manya Trough (Marla-6, 416.00 m).
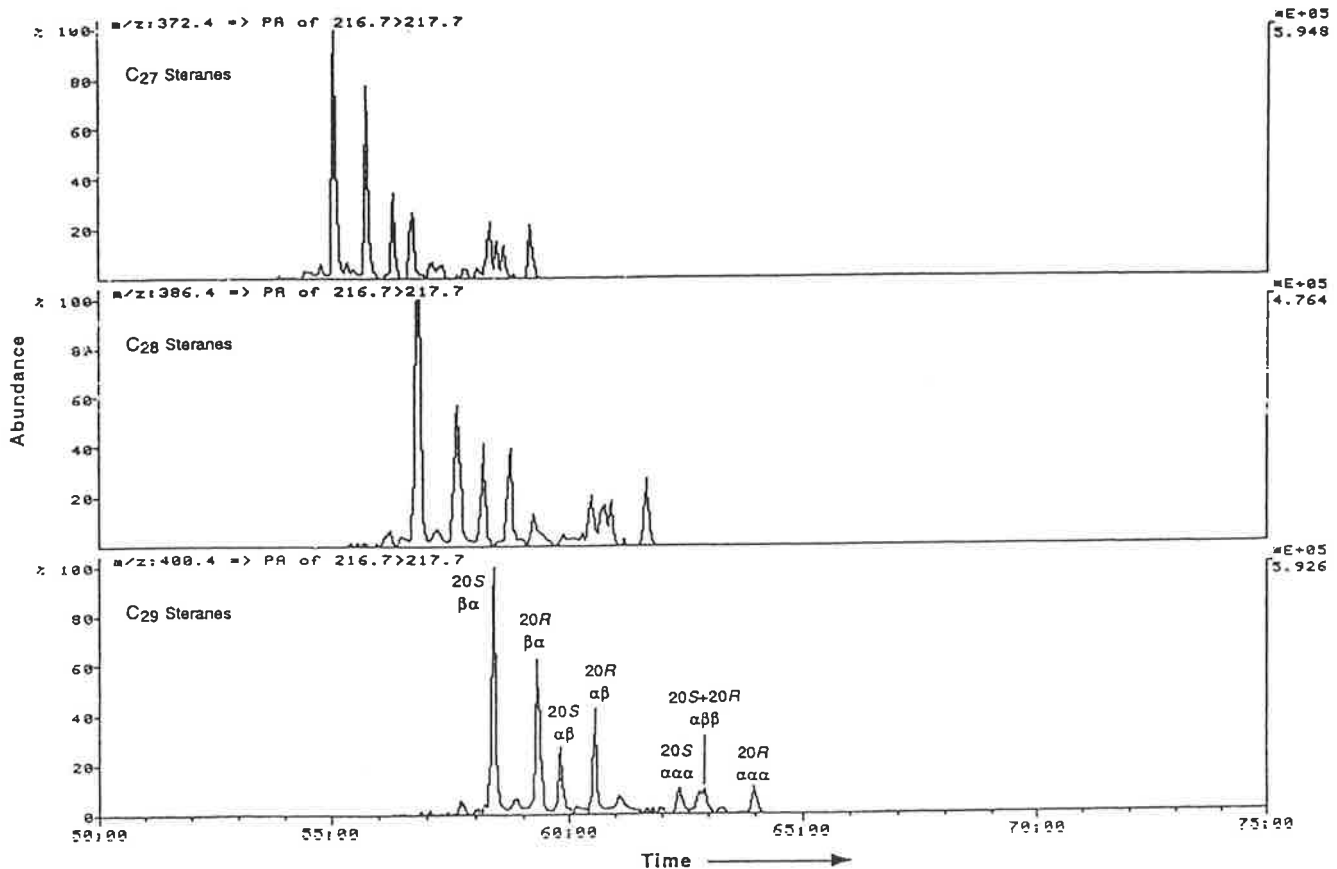
Figure 8.4: GC-MS-MS (CAD) m/z = 372, 386, 400$\rightarrow$217 transitions characteristic of C_{27}, C_{28} and C_{29} steranes in laminated limestone from KD-1, 263.35 m. Assignments refer to the C-20 stereochemistry (S or R) and $\beta\alpha$, $\alpha\beta$, $\alpha\alpha\alpha$ and $\alpha\beta\beta$ denote 13β (H), 17α (H)- and 13α (H), 17β (H)- diasteranes, and 5α (H), 14α (H), 17α (H)- and 5α (H), 14β (H), 17β (H)-steranes, respectively.

133

hopane/sterane ratios (6.3-10.4) and diasterane/sterane ratios (1.6–5.2), all suggesting greater bacterial reworking during early diagenesis.

Terpane distributions in the Manya Trough dolostones significantly differ from those in the Tallaringa Trough limestones. In particular, 17α-30-norhopane is dominant over 17α-hopane (Fig. 8.1c: peak 5 and 8) and all the rearranged hopanoids are less abundant relative to 17α-hopane. These dolostones contain kaolinite and illite (Fig. 8.3), although detrital clays comprise no more than 5 % of the total mineral matrix.

On the other hand, the Tallaringa Trough limestones are entirely devoid of surface active clay minerals (Fig. 8.3) which catalyse biomarker rearrangement reactions. Their greater abundance of rearranged hopanes (diahopanes and neohopanes) is therefore unexpected. Interestingly, these immature to marginally mature and clay-free limestones also have higher diasterane/sterane ratios (1.6–5.2) than do the mature to overmature Manya Trough dolostones (diasterane/sterane = 0.8–1.3). Further, examination of GC-MS-MS (CAD) data for the various $M^+ \rightarrow m/z$ 217 transitions reveals exceptionally high levels of diasteranes relative to steranes in the limestones (Fig. 8.4). Many workers (e.g. Hughes, 1984; Zumberge, 1984; Mello et al., 1988; Czochanska et al., 1988; Mattavelli and Novelli, 1990; Reidiger et al., 1990; Alajberg et al., 1990) have previously noted that diasteranes form most readily in the presence of acidic clay catalysts which play a significant role in transformation of steranes to diasteranes. Their initial presence can also be accounted for by high Eh (oxic conditions) during early diagenesis (Moldowan, et al., 1992). Thus, low concentrations of diasteranes relative to steranes in organic-rich carbonates were taken by McKirdy et al. (1983) to indicate very low Eh (anoxic conditions) during early diagenesis. Finally, it has been proposed that the more stable diasteranes become dominant with increasing maturity (Waples and Machihara, 1991). The scenario of high diasterane

concentrations in immature to marginally mature, clay-free Tallaringa carbonates deposited in an anoxic environment requires a different explanation.

The Tallaringa Trough limestones have cholestane-dominant regular sterane signatures (C_{27}> C_{28}> C_{29}), whereas the distribution of regular steranes in the Manya Trough dolostones is somewhat different (C_{27}> C_{29}< C_{28}). In the absence of land plants during the Early Cambrian, the substantial amounts of C_{29} steranes in the Manya Trough sediments may suggest a contribution from primitive green algae. Higher concentrations of C_{29} steranes in Carboniferous and younger sediments are generally attributed to terrestrial plants (e.g. Grantham, 1986; Rullkötter et al., 1986; Longman and Palmer, 1987; Fowler and Douglas, 1987). Their very uniform C_{27}-C_{29} sterane distributions (Table 8.1 and Fig. 8.5) indicate that the input of organic matter to all Manya source beds was alike, but different from that contributed to the Tallaringa source beds. Another factor influencing the relative abundance of C_{29} and C_{28} steranes may be their different resistances to oxidation. Marine-derived C_{29} steranes are more resistant to oxidation (Dahl et al., 1994). In the Manya samples, C_{28} steranes seem to have been reduced in concentration via oxidation-related processes, a feature which positively correlates with other geochemical parameters (e.g. Pr/Ph = 0.9–2.6) that indicate suboxic to oxic conditions prevailed during early diagenesis.

● = samples from Manya Trough   O = samples from Tallaringa Trough
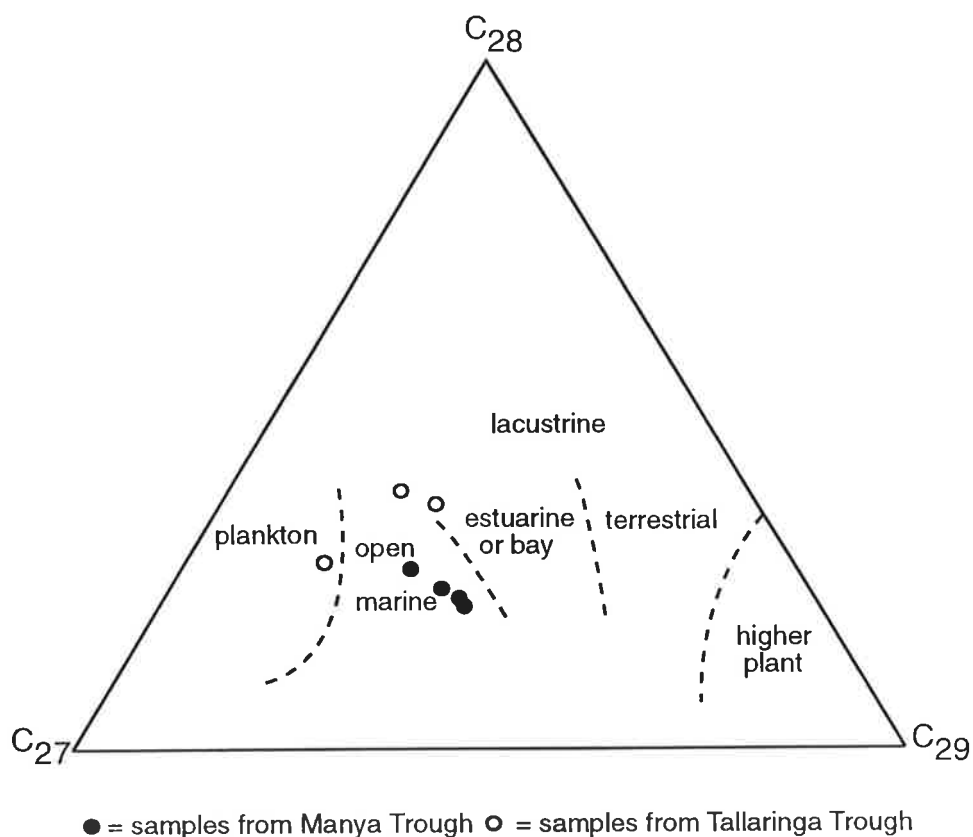
Figure 8.5 Ternary diagram showing the relative abundances of C_{27}, C_{28}, and C_{29} regular steranes in the saturate fractions of hydrocarbons determined by GC-MS (m/z 217). The proposed initial environments of deposition (adapted from Waples and Machihara, 1991) are shown by dotted lines.

The co-occurrence of rearranged steranes and rearranged (dia-and neo-) hopanes raises the possibility of a common mode of origin. The diagenetic formation of rearranged hopanes and diasteranes in these carbonates seems not to have involved clay-catalysed reactions of hopanoid and steroid precursors (cf. Peters and Moldowan, 1993). Given the prominent hopane signature in the alkanes of the Tallaringa limestones, their rearranged hopanes and steranes are expected to have formed via bacterially-mediated reactions (Michaelsen et al., 1995).

8.3   Unusual source-specific biomarkers

Another significant feature associated with Tallaringa Trough carbonates is the occurrence of significant amounts of an unusual compound which elutes between the $\alpha\alpha\alpha$ 20S and $\alpha\beta\beta$ 20R C_{29} regular steranes in the m/z 217 mass chromatogram (marked by asterisk in Fig. 8.2b and shown black in Fig. 8.6). This compound is probably 24-isopropylcholestane, a novel C_{30} steroid which occurs ubiquitously, albeit in trace quantities, in bitumens and oils derived from carbonates of Neoproterozoic and Cambrian age (R.E. Summons, pers. comm., 1995). McCaffrey et al. (1994) reported 24-isopropylcholestane in numerous Vendian and/or Early Cambrian-sourced samples from the Siberian platform, the Urals, Oman, India and Australia (including the Ouldburra Fm., Officer Basin). They proposed that a high ratio of 24-isopropylcholestane to 24-n-propylcholestane (≥ 1) is associated with Late Proterozoic (Vendian) and Early Cambrian oils and bitumens, while younger and older samples have a lower ratio (≤ 0.4). The i/n ≥ 1 signature in the Neoproterozoic and Cambrian appears to be related to the radiation of the Porifera (sponges), and particularly the early calcareous forms ($viz.$ the archaeocyathids and their Neoproterozoic ancestors : McCaffrey et al., 1994). It is noteworthy that (?) 24-isopropylcholestane is much less abundant in the Manya Trough carbonates and only appears to be prominent in the Tallaringa Trough limestones which were deposited in reducing, hypersaline environments. The age-specificity of the aforementioned compound makes it a powerful marker in oil-source and source-source correlations.

137
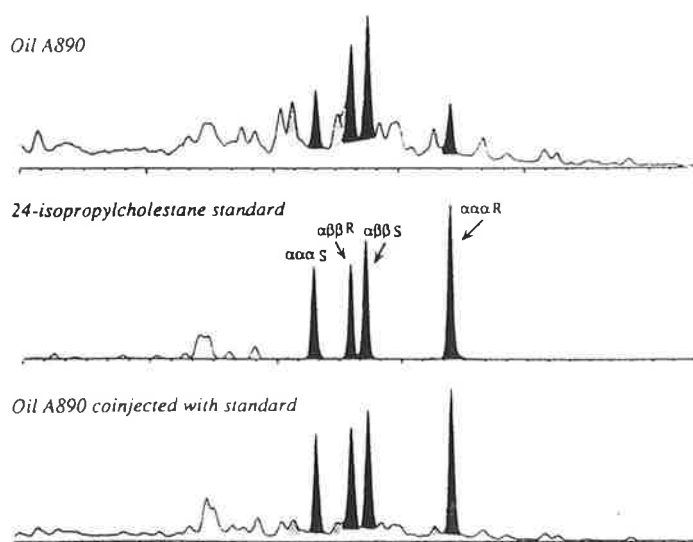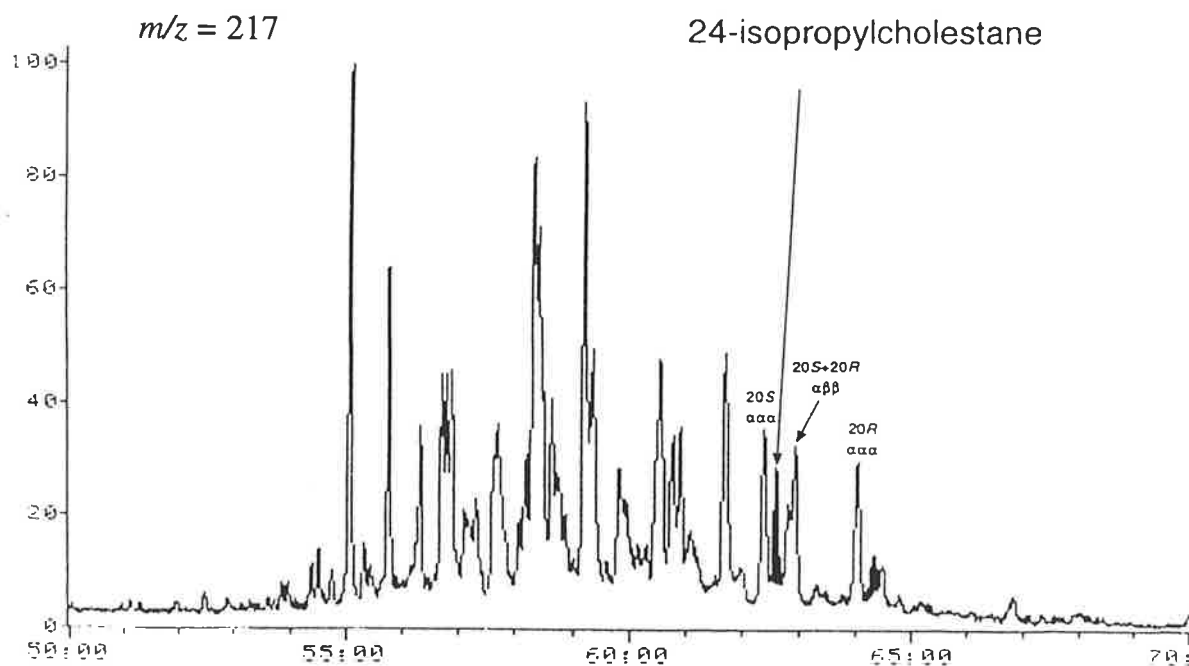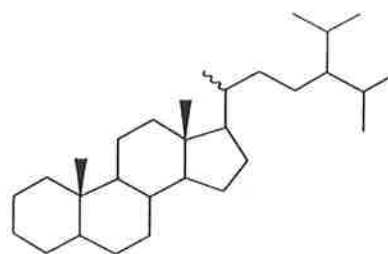
Figure 8.6 GC-MS-MS transition *m/z* 414→217 for a Vendian-reservoired East Siberian oil (oil A890) showing relative retention times of the isomers of 24-isopropylcholestane (black) and 24-ethylcholestane (stipple) (after McCaffrey et al., 1994).

Significantly, appreciable concentrations of the C_{30} irregular acyclic isoprenoid squalane (Fig. 8.7) were detected in two samples from the Tallaringa Trough (KD-2A, 211.80 m and KD-2A, 297.95 m: Appendix XII). This compound elutes just before n-C_{27} and is denoted by an asterisk in their respective alkane gas chromatograms (Appendix XII). However, the presence of squalane is more obvious in the m/z 183 mass chromatogram (Fig. 8.8a and b). The presence of squalane and the C_{21}-C_{25} regular extended isoprenoids in non-marine (Observatory Hill Fm., Byilkaoora-1) and marine (Ouldburra Fm., Wallira-West-1 and Wilkinson-1) Cambrian carbonate rocks from the Officer Basin was first reported by McKirdy et al. (1984) who took them as evidence of bacterial reworking by archaebacteria (e.g. halophiles and methanogens) during early diagenesis. In fact, recent studies consistent with this view (e.g. Volkman, 1988; ten Haven et al., 1988; Christiansen et al., 1993) have demonstrated that low Pr/Ph ratios, together with the presence of squalane, are common in hypersaline environments and both features may be attributed to an origin from halophilic bacteria. The latter organisms are a major alternative source of phytane.

From their evaluation of Precambrian and Phanerozoic biomarkers Summons et al. (1988) concluded that C_{21}-C_{30} acyclic isoprenoids, found in marine and non-marine hypersaline environments, are more likely to be derived from halophilic archaebacteria. Since methanogens are present in only low concentrations, and especially as they are terminal members of the anaerobic bacterial succession, high concentrations of their biomarkers in hypersaline environments are unexpected (Ward and Winfrey, 1985; Ward et al., 1987).

i-C_{30}
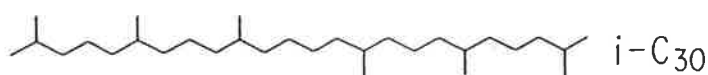
Figure 8.7 Structure of the irregular (tail- to -tail)acyclic isoprenoid alkane, squalane.

Dinosteranes and 4-methyl steranes are derived from dinoflagellates and other algae (Rubinstein et al., 1975; Robinson et al., 1984; Volkman et al., 1990). Various 4α(Me)-24-ethylcholestane isomers and the major dinosterane (4α,23R,24R-trimethylcholestane 20R) were detected in one Tallaringa Trough limestone sample analysed by GC-MS-MS (Fig. 8.9: KD-1, 263.35 m). This sample has a relatively high TOC content (1.2 %), and contains kerogen with a high H/C ratio (1.27) and a very high sulphur content (19% S). Because dinoflagellates are known to "bloom", the remarkable concentration of dinosterane in this sample is attributable to a high marine productivity. This is the first reported occurrence of dinosterane in a Cambrian rock (Michaelsen et al., 1995). However, Summons (1992) described dinosterane from Neoproterozoic sediments of the Bitter Springs (ca 850 Ma) and Pertatataka (ca 610 Ma) Formations in the Amadeus Basin. Zang and McKirdy (1993) also identified dinosterane in one sample from the Pertatataka correlative (Alinya Formation) in the Officer Basin. The latter contains unambiguous 4α(Me)-24-ethylcholestane. This molecular fossil and dinosterane have otherwise been detected only in rocks of Triassic age or younger (Summons, 1992). It is also noteworthy that Moldowan et al. (1995) have recently reported aromatised dinosteroids in Proterozoic and Ordovician (but not Cambrian) rocks.
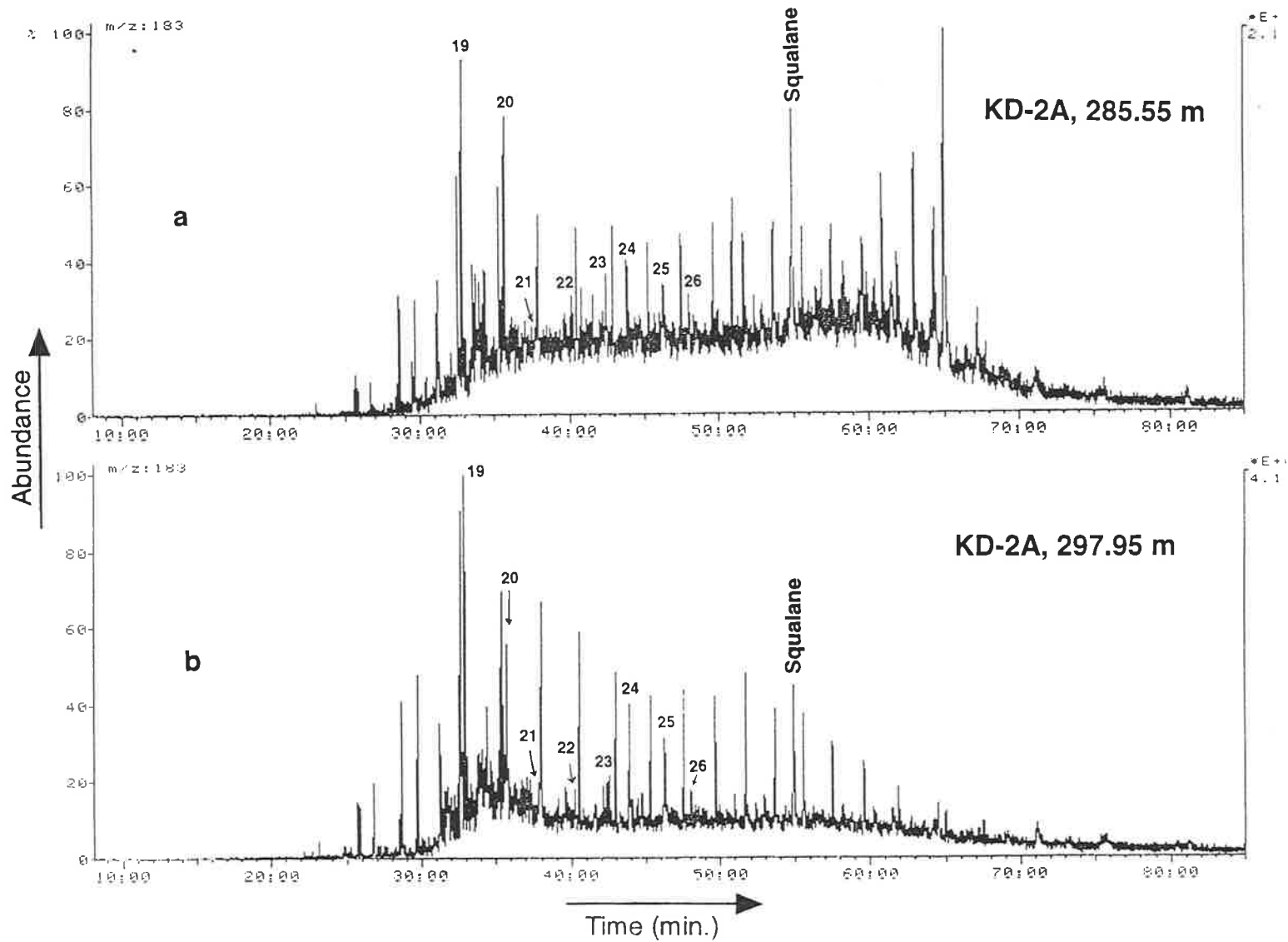
Figure 8.8 Mass chromatograms of acyclic isoprenoids (*m/z* 183) in two Tallaringa source rock extracts. Numbers refer to the carbon numbers of the regular (head- to -tail) isoprenoids. Squalane is a C_{30} irregular (tail- to -tail) isoprenoid.
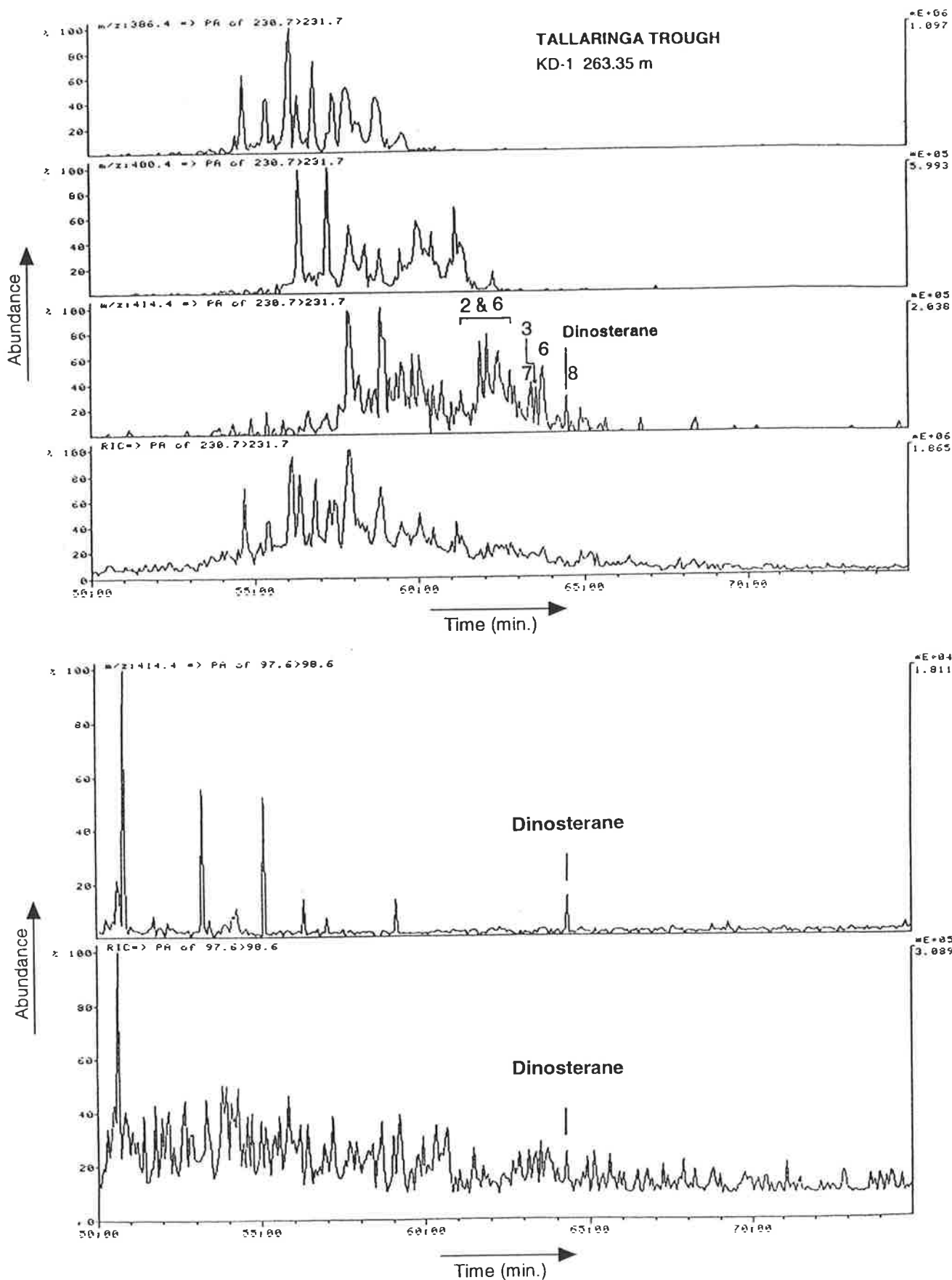
Figure 8.9   GC-MS-MS (CAD) m/z = 386, 400, 414→231 and 414→98 transitions characteristic of C_{28}; C_{29} and C_{30} 4α-Me steranes in laminated limestone from KD-1, 263.35 m. The latter transition is specific to dinosterane. Assignments of 4α- methyl-24 ethylcholestanes are by comparison of relative retation times with the literature (Peters and Moldowan, 1993; Summons et al., 1987). Peak identities are given in Appendix XII.

142

8.4 Oldest occurrence of *Gloeocapsomorpha prisca?*

Several colonies of the problematic *Gloeocapsomorpha prisca* Zalessky (1917) have been tentatively identified in two core samples (KD-1, 263.35 m; KD-2A 285.50 m) from the Tallaringa Trough. The petrographic characteristics of *G. prisca* are given in Chapter 7, Section 76.

Notwithstanding minor differences in their *n*-alkane distribution patterns, *G. prisca*-bearing Ouldburra carbonates share common geochemical features with previously reported cases from different basins. For example, *G. prisca*-rich kerogen from the Decorah Formation (Guttenberg oil rock: Douglas et al., 1991) is enriched in organic sulphur to much the same degree as that in the Ouldburra Formation (S = 11–19 %). Likewise, high hopane/sterane ratios, and unusually high diasterane concentrations in the absence of clays have been recorded in the Yeoman Formation kukersite (Ordovician, Saskatchewan; Fowler, 1992) and in Ordovician *G. prisca*-bearing carbonates from the Canning Basin (Ordovician, Western Australia: Hoffmann, 1987). Interestingly, the Yeoman kukersite, like the Tallaringa Trough sediments, also contains exceptionally high levels of C_{29}Ts and C_{30} and C_{30} Ts. This reinforces the possible formation of neohopanes without clay-induced acid catalysis and is in agreement with the findings previously mentioned. Elevated hopane / sterane ratios (6.3–10.4), and high concentrations of acyclic isoprenoids (Fig. 8.8), iso-alkanes and alkylcyclohexanes (Appendix XII) in *G. prisca*-bearing Tallaringa sediments are particular features supportive of a prokaryotic affinity (cf. Reed et al., 1986). Furthermore, the *G. prisca*-rich Ouldburra carbonates were deposited under a warm, arid climate in a low-latitude (0-15°N: Dunster, 1987) epicontinental sea during the Early Cambrian. Very similar palaeogeographical settings have been proposed by Foster et al. (1986) to account for the widespread sub-equatorial distribution of *G. prisca*-rich

sediments in Ordovician strata. The present study reveals that *G. prisca* first appeared during the Early Cambrian before becoming ubiquitous in the Ordovician.

The features outlined above suggest that anaerobic bacterial action upon lamalginite and *G. prisca*-related telalginite during early diagenesis has resulted in a suite of unexpected biomarkers. These same diagenetic processes resulted in the excellent source quality and oil-prone nature of the Tallaringa limestones.

8.5   Thermal maturity

The maturation-sensitive biomarker ratios of the Ouldburra Formation core samples (Table 8.1) are consistent with their level of maturity previously determined by MPI measurements and petrographic observations (Chapter 7). The Tallaringa sediments have higher moretane/hopane ratios (0.16–0.21) than do their counterparts from the Manya Trough (moretane/hopane = 0.04–0.07). The corresponding Ts/Ts + Tm ratios are in the range 0.26–0.30 and 0.31–0.41, respectively (Table 8.1).

Isomerisation at the C-22 position in the C_{31}-C_{35} 17α(H)-homohopanes (Fig. 8.1a) has been applied by Peters and Moldowan (1993) to indicate maturity up to the stage of oil generation. These authors stated that 22S/(22S + 22R) ratios in the range 0.52 to 0.54 would be expected in thermally immature source rocks, while ratios in the range 0.57 and 0.62 indicate that the main phase of oil generation has been reached or surpassed.

In the present study, C_{31} homohopane data were used to calculate the 22S/(22S + 22R) ratios. Two end members from the Manya Trough (Marla-6, 671.25 m) and the Tallaringa Trough (KD-1, 263.35 m) gave values of 0.52 and 0.61, respectively (Fig. 8.1a and c; Table 8.4). However, the sample with the higher 22S/(22S + 22R) ratio, a limestone deposited in highly reducing hypersaline environment (Pr/Ph = 0.7), is the less mature

144

(VRcalc = 0.6 %). The other sample (Marla-6, 671.25 m), a dolomite deposited in an oxic environment (Pr/Ph = 2.6), is thermally overmature (VRcalc = 1.7 %). This discrepancy in 22S/(22S + 22R) ratios exhibited by marginally mature and overmature end members may partly be controlled by their different lithofacies but is more likely to be due to unusual diagenetic pathways for hopanes in hypersaline environments (Peters and Moldowan, 1993).

Table 8.4 Conflicting maturity-related parameters (C_{31} homohopane, VRcalc) and redox indicator (Pr/Ph) from two different carbonate source beds.

WELL	LITHOLOGY	22S/(22S + 22R)	VRcalc (%)	Pr/Ph
Manya Trough				
Marla-6 671.25 m	lam. dolomite	0.52	1.7	2.6
Tallaringa Trough				
KD-1 263.35 m	lam. limestone	0.61	0.6	0.7

8.6   Summary

Clay-free micritic limestones of the Early Cambrian Ouldburra Formation, deposited under anoxic hypersaline conditions in the Tallaringa Trough, contain unexpectedly high concentrations of 17α-diahopanes (C_{29}-C_{30}), 18α-neohopanes (C_{29}-C_{30}), and 13β, 17α- and 13α, 17β-diasteranes (C_{27}-C_{29}) relative to coeval but slightly argillaceous carbonates that accumulated landward in a suboxic environment of the Manya Trough. The Tallaringa Trough samples also exhibit much higher hopane/sterane ratios (6.3–10.4) than do the Manya Trough sediments (hopane/sterane = 1.7–1.9). Co-occurrence of the rearranged

hopanes and diasteranes with various methylhopanes implies bacterial influence in the formation of the rearranged biomarkers.

Squalane, a strong indicator of hypersaline conditions, is prominent in limestones from the Tallaringa Trough. The recognition of 24-isopropylcholestane in the same samples confirms an earlier report of this compound in the Ouldburra Formation and strengthens its significance as an age-specific sponge marker. The identification of dinosterane (4α,23,24-trimethylcholestane) in marine sediments of Early Cambrian age significantly extends the stratigraphic range of this molecular fossil.

G. prisca -related telalginite is an important oil-prone maceral in the Ouldburra Formation from the Tallaringa Trough. The finding of this material in sediments not older than Botomian (middle Early Cambrian) age represents the earliest known occurrence of *G. prisca*.

CHAPTER 9

SUMMARY AND CONCLUSIONS

9.1   Dolomitisation

A significant portion of the Ouldburra Formation carbonates has undergone dolomitisation. Dolomitised beds in the type section attain a cumulative thickness of 212 m. Periodic exposure during deposition led to early dolomitisation. Longer subsequent periods of subaerial exposure have resulted in pervasive dolomitisation and the development of secondary porosity. Texturally, nonplanar, polymodal dolomite predominates over planar-e and -s types and in both cases, mimic replacement is more common than nonmimic replacement. Genetically, two relatively early types of dolomite (excluding later diagenetic cement) were recognised, syngenetic (primary) and replacement. The former occurs as thin dolostone beds associated with anhydrite and rip-up clasts. The latter type is quantitatively the most widespread, occurring over intervals 1 to 47 m thick.

Mid to late dolomite cements include coarse crystalline, saddle and pressure solution dolomites. The coarse crystalline and some pressure solution cements are enriched with iron, suggesting that crystal growth was influenced by impurities such as clay and OM at higher temperature. The occurrence of saddle dolomite is consistent with calculated vitrinite reflectance (VRcalc) data.

Bitumen residues are associated with intra-rhomb spaces, and in some cases, with localised hydrothermal silicification and sulphide mineralisation (sphalerite).

The presence of evaporites minerals, mainly anhydrite, at the top of shallowing-upwards cycles suggests the sabkha and brine-reflux models of dolomitisation the most applicable.

9.2   Porosity generation

A significant amount of secondary porosity has been generated in the form of vugs, intercrystalline pores, grain and matrix dissolution fabrics, and rare moldic porosity in carbonate and mixed carbonate-siliciclastic sequences.   Both intergranular and intragranular porosities which often host bitumen residue are evident in siliciclastic units.

The most porous units are thin (1 to 4 m) but probably widespread. However, a thicker dolomite bed (~14 m) occurs in the Manya-6 well. Porosity and permeability values as high as 27 % and 1600 md, respectively, have been recorded from both dolomite and mixed dolomite-sandstone units.

The potential dolomite reservoirs identified are ranked (I to IV) on the basis of their porosity distribution and texture. Dolomites with rank I and II exhibited excellent and good reservoir characteristics, respectively.

The distribution of porous intervals was discussed within a sequence stratigraphic framework. Higher porosity occurs in dolomite and mixed carbonate-siliciclastic units corresponding to highstand systems tracts, whereas the transgressive facies limestones are relatively tight. Early diagenetic exposure of these sequences is largely responsible for the good reservoir quality observed near the tops of shallowing-upwards cycles.

Petrophysical logs, including gamma ray and density logs, were used in conjunction with petrographic examination of thin sections to recognise porous intervals. Gamma ray response often shows somewhat higher values where stylolitic dolomites are associated with OM, clay and, to a lesser extent, potash feldspar. However, density logs seem to faithfully discriminate porous units from nonporous ones.

9.3   Hydrocarbon occurrence

Traces of OM, including both bitumen and residual kerogen, were recognised in several thin sections. This OM commonly infills intra-rhomb spaces or is associated with solution seams in dolomite and dolomitic limestones. In siliciclastic sediments, the bitumen occurs in intergranular and / or intragranular pores. Live oil was observed in fine-grained, organic-rich mudstone facies at Manya-6, Marla-6, KD-1, and KD-2A and is thought to be indigenous.

The occurrence of bitumen residues in reservoir units implies that hydrocarbons were generated from intraformational source beds to be migrated into the adjacent reservoir units.

9.4   Stable isotope and fluid inclusion analyses

Stable isotope and fluid inclusion analyses, performed on mid to late calcite and dolomite cements, provided information on the origin, timing, and temperature of the depositing fluids during early and mid to late diagenesis. Results of these analyses facilitated the identification of different dolomite types and their temperatures of formation.

Mid to late void-filling dolomite and calcites are clearly depleted in $\delta^{18}O$ and have a variable $\delta^{13}C$ values depending on whether or not they are associated with OM. Early dolomite has relatively heavy $\delta^{18}O$ but depleted $\delta^{13}C$ values suggestive of lower temperatures of precipitation.

Fluid inclusion microthermometry performed on diagenetic cements (calcite and dolomite) provided valuable information on formation temperatures and salinities for the individual diagenetic phases. Higher salinities are inferred for the three-phase inclusions within saddle dolomite which contain cubic halite crystals.

The highest temperature was recorded from late vug-filling calcite and co-existing saddle dolomite. The significance of the unusually high temperature of homogenisation (332°C) recorded from a three-phase saddle dolomite in Manya-6 well is still uncertain. It could either be due to decrepitation of early inclusions, or the local invasion of hot hydrothermal fluids in the Manya Trough. It appears that the latter is more likely the process because such hydrothermal invasion was also noticed at Marla-6.

9.5   Source rock potential

Some beds in the Manya Trough contain 0.3–1.4 % TOC, with the richest beds being thin but probably widespread. They were deposited in a range of shallow marine environments corresponding to transgressive and highstand systems tracts.

Rock-Eval and elemental data, coupled with detailed organic petrography, indicate kerogen Type III to IV. Extractable bitumen yields for these source beds are variable (142–267 ppm, 10–40 mg/g TOC) and extracted hydrocarbons are rich in the saturates (sat/arom >1). The dispersed OM is dominantly micritinised bituminite, occurring as thin laminae or stylolitic films but otherwise structureless. The richest source beds also contain lesser amounts of lamalginite which displays dark orange fluorescence under UV light. Calculated vitrinite reflectances (VRcalc) derived from MPI measurements are in the range 1.00–1.67 %, suggesting that these source rocks are mature to overmature.

Better quality source rocks were noticed in the Ouldburra Formation from the Tallaringa Trough where TOC ranges up to 1.2 %. The richest source beds are brown, thin (~2 m)

150

and emit a strong petroleum odour. These beds were deposited in highly anoxic environments and contain oil-prone Type II kerogen.

Interestingly, a sample with the least TOC (0.2 %) showed the highest hydrogen index (HI = 510).

EOM yields are high (582–2540 ppm, 144–348 mg/g TOC) as a proportion of the total OM. The bitumen extract is rich in resins and asphaltenes.

Calculated vitrinite reflectances (VRcalc) in the range 0.58–0.68 % suggest that these bituminous limestones are marginally mature for oil generation.

Lamalginite (comprising filamentous and mat-like cyanobacteria), telalginite (*G. prisca*), bacterial biomass and acritarchs, constitute the bulk of the organic matter. Associated indigenous live oil, together with thucholites, are characteristic features of these excellent quality source beds which confirm that these source beds have already entered the oil generating window.

The presence of *G. prisca* in the Ouldburra Formation is the first report of this organism from the Early Cambrian. It subsequently became ubiquitous during the Ordovician.

9.6 Biomarkers

Early mature to mature source beds in the Tallaringa Trough have biomarker signatures that appear to be unique from the view point of their age, depositional environment and source biota. Their characteristic biomarkers not only clearly discriminate them from their correlative carbonate source rocks located in Manya Trough, but also reveal much about the role and impact of early diagenetic processes in anoxic carbonates.

Clay-free micritic limestones from the Tallaringa Trough deposited under anoxic, hypersaline conditions as indicated by the dominance of phytane over pristane, and the

presence of squalane. These carbonates contain unexpectedly high concentrations of 17α-diahopanes (C_{29}-C_{30}), 18α-neohopanes (C_{29}-C_{30}), and 13β, 17α- 17β- diasteranes (C_{27}-C_{29}) relative to coeval but slightly argillaceous dolostones that were deposited in a suboxic environment. The Tallaringa Trough limestones also exhibited much higher hopane/sterane ratios (6–10) than did the Manya Trough dolostones (hopane/sterane <2). The presence of 24-isopropylcholestane in these Early Cambrian marine limestones further strengthens its stratigraphic significance as a sponge marker. The occurrence of dinosterane (4α, 23, 24- trimethylcholestane) in the same sediments significantly extends the stratigraphic range of this molecular fossil.

REFERENCES

AL-MARJEBY, A. AND NASH, D., 1986 - A summary of the geology and oil habitat of the eastern flank hydrocarbon province of South Oman. *Marine and Petroleum Geology*, 3, 306-315.

ALAJEBEG, A., BRITVIC, S. ŠVEL-CEROVECKI, CORNFORD, C., TODORIC, A., RAJKOVIC, J., BARIC, G., AND PUTNIKOVIC, A., 1990 - Geochemical studies of the oils and source rocks in the Pannonian Basin (Yugoslavia). *Organic Geochemistry*, 16, 339-352.

ALLAN, J.R., AND WIGGINS, W.D., 1993 - Dolomite reservoirs; Geochemical techniques for evaluating origin and distribution. *AAPG Continuing Course Note Series*, 36.

BALTZER, F., KENIG, F., BOICHARD, R., PLAZIAT, J.C., AND PURSER, B.H., 1994 - Organic matter distribution, water circulation and dolomitisation beneath the Abu Dhabi Sabkha (United Arab Emirates). In : PURSER, B., TUCKER, M., AND ZENGER, D. (eds.), *Dolomites*. Blackwell, Oxford, pp. 409-428.

BASKIN, D.K., AND PETERS, K.E., 1992 - Early Generation characteristics of a sulfur-rich Monterey kerogen, *The American Association of Petroleum Geologists Bulletin*, 7, 1-13.

BENBOW, M.C., 1982 - Stratigraphy of the Cambrian ? Early Ordovician, Mount Johns Range, NE Officer Basin, South Australia. *Transactions of the Royal Society of South Australia*, 106, 191-211.

BLATT, H., MIDDLETON, G., AND MURRAY, R., 1980 - *The Origin of Sedimentary Rocks*. Englewood Cliffs, Prentice Hall, 782 p.

BORDENAVE, M.L., AND BURWOOD, R., 1990 - Source rock distribution and maturation in the Zagros Orogenic Belt: Provenance of the Asmari and Bangestan Reservoir oil accumulations. *Organic Geochemistry*, 16, 369-387.

BOREHAM, C.J., CRICK, I.H. AND POWELL, T.G., 1988 - Alternative calibration of the methylphenanthrene index against vitrinite reflectance: application to maturity measurements on oils and sediments. *Organic Geochemistry*, 12, 289–294.

BRASIER, M.D., 1983 - *Microfossils*. George Allen & Unwin, London, pp. 9-18.

BRAY, E. E, AND EVANS, E. D., 1961 - Distribution of *n*-paraffins as a clue to recognition of source beds. *Geochimica et Cosmochimica Acta, 22*, 2–15.

BREWER, A.M., DUNSTER, J.N., GATEHOUSE, C.G., HENRY, R.L. AND WESTE, G., 1987 - A revision of the stratigraphy of the eastern Officer Basin. *Quarterly Geological Notes, Geological Survey of South Australia*, 102, 2-15.

CHOQUETTE, P.W. AND JAMES, N.P., 1990 - Limestones – The burial Diagenetic Environment. In: McIIREATH, I.A. AND MORROW, D.W. (eds.), *Diagenesis.* Geoscience Canada - Reprint Series 4, 75-111.

CHRISTIANSEN, F.G., PIASECKI, S., STEMMERIK, L., AND TELNAES, N., 1993 - Depositional environment and organic geochemistry of the Upper Permian Ravenefjeld Formation source rock in East Greenland, *The American Association of Petroleum Geologists Bulletin,* 77, 1519-1537.

CLEMENTZ, D.M., 179 - Effect of oil and bitumen saturation on source rock pyrolysis: *The American Association of Petroleum Geologists Bulletin,* 63, 608-626.

COOK, P.J., 1982 - The Cambrian palaeogeography of Australia and opportunities for petroleum exploration. *The Journal of the Australian Petroleum Exploration Association,* 22 (1), 42-64.

COOPER, B. S., AND OWER, J., 1982 - Elements of Geochemistry-*Robertson International Ltd.,* Ty'n Coed, London.

CRICK, I. H., BOREHAM, C. J., COOK, A. C., AND POWELL, T. G., 1988 - Petroleum Geology and Geochemistry of Middle Proterozoic McArthur Basin, Northern Australia In: Assessment of Source Rock Potential, *The American Association of Petroleum Geologists Bulletin,* 72, 1495–1514.

CZOCHANSKA, Z., GILBERT, T.D., PHILP, R.P., SHEPPARD, C.M., WESTON, R.J., WOOD, T.A., AND WOOLHOUSE, A.D., 1988 - Geochemical application of sterane and triterpane biomarkers to a description of oils from the Taranaki Basin in New Zealand. *Organic Geochemistry,* 12, 123-135.

DAHL, J.E.P., MOLDOWAN, J.M., TEERMAN, S.C., McCAFFREY, M.A., SUNDARARAMAN, P. AND STELTING, C.E., 1994 - Source rock quality determination from oil biomarkers I: A new geochemical technique, *The American Association of Petroleum Geologists Bulletin,* 78, 1507-1525.

DEER, W.A., HOWIE, R.A., AND ZUSSMAN, J., 1978 - An *Introduction to the Rock Forming Minerals.* Longman, pp. 456-459.

DEMBICKI, H., HORSFIELD, B., AND HO, T.T.Y., 1983 - Source rock evaluation by pyrolysis-gas chromatography. *The American Association of Petroleum Geologists Bulletin,* 67, 1094-1103.

DICKSON, J.A.D., 1966 - Carbonate identification and genesis as revealed by staining: *Journal of Sedimentary Petrology* 36, 491-505.

DOUGLAS, A.G., SINNINGHE DAMSTE', J.S., FOWLER, M.G., EGLINTON, T.I., AND DE LEEUW, J.W., 1991 - Unique distributions of hydrocarbons and sulfur compounds released by flash pyrolysis from the fossilised alga *Gloeocapsomorpha prisca,* a major constituent in one of four Ordovician kerogens. *Geochimica et Cosmochimica Acta,* 55, 275-291.

DOUTCH, H.F., AND NICHOLAS, E., 1978 - The Phanerozoic sedimentary basins of Australia and their tectonic implications. *Tectonophysics*, 48, 365-385.

DUNSTER, J. N., 1987 - Sedimentology of the Ouldburra Formation (Early Cambrian) northeastern Officer Basin. M.Sc. Thesis, University of Adelaide (unpublished).

ESPITALIE, J., DEROO, G. AND MARQUIS F., 1985 - Rock-Eval pyrolysis and its application. Preprints, Institut Francais du Petrole.

FLUGEL, E., 1982 - *Microfacies Analysis of Limestones*. Springer-Verlag, Berlin.

FOLK, R.L. AND LAND, L.S., 1975 - Mg/Ca and salinity; two controls over crystallisation of dolomite. *The American Association of Petroleum Geologists Bulletin*, 59, 60-68.

FOLK, R.L., 1974 - *Petrology of Sedimentary Rocks*: Hemphill Publishing Co., Austin, Texas, 182.

FOSTER, C.B., O'BRIEN, G.W., AND WATSON, S.T., 1986 - Hydrocarbon source potential of the Goldwyer Formation, Barbwire Terrace, Canning Basin, Western Australia. *The Journal of the Australian Petroleum Exploration Association*, 26 (1), 142-155.

FOWLER, M. G. AND DOUGLAS, A.G., 1984 - Distribution and structure of hydrocarbons in four organic-rich Ordovician rocks. *Organic Geochemistry*, 6, 105-114.

FOWLER, M. G. AND DOUGLAS, A.G., 1987 - Saturated hydrocarbon biomarkers in oils of Late Precambrian age from Eastern Siberia. *Organic Geochemistry*, 11, 201-213.

FOWLER, M. G., 1992 - The influence of *Gloeocapsomorpha prisca* on the organic geochemistry of oils and organic-rich rocks of late Ordovician age from Canada. In: SCHIDLOWSKI, M., GOLUBIC, S., KIMBERLEY, M.M., McKIRDY, D.M., AND TRUDINGER, P. A. (eds.), *Early Organic Evolution and Mineral and Energy Resources*, Springer-Verlag, Berlin, pp. 336–356.

FOWLER, M.G. AND DOUGLAS, A.G., 1984 - Distribution and structure of hydrocarbons in four organic-rich Ordovician rocks. *Organic Geochemistry*, 105-114.

FRIEDMAN, G.M., 1965 - Terminology of crystallisation textures and fabrics in sedimentary rocks. *Journal of Sedimentary Petrology*, 35, 643-655.

FRIEDMAN, G.M. AND SANDERS, J.E., 1967 - Origin and occurrence of dolostones in carbonate rocks : *Developments in Sedimentology 9A*. Amsterdam, Elsevier, pp. 267-348.

GALLOWAY, W.E., AND HOBDAY, D.K., 1983 - *Terrigenous Clastic Depositional Systems: Application to Petroleum, Coal, and Uranium Exploration*. New York, Springer-Verlag.

GAO, G., 1990 - Geochemical and isotopic constraints on the diagenetic history of a massive strata, Late Cambrian (Royer) dolomite, Lower Arbuckle Group, Slick Hills, southeastern Oklahoma, USA. *Geochimica et Cosmochimica Acta*, 54, 1979-1989.

GAO, G., AND LAND, L. S., 1991 - Early Ordovician Cool Creek Dolomite, Middle Arbuckle Group, Slick Hills, southeastern Oklahoma, USA: origin and modification. *Journal of Sedimentary Petrology,* 61, 161-173.

GAO, G., HOVORKA, S., AND POSEY, H., 1990 - Limpid dolomite in Permian San Anders halite rocks, Palo Duro Basin, Texas Panhandle; characteristics, possible origin, and implications for brine evolution. *Journal of Sedimentary Petrology,* 60, 118-124.

GARY, M., McAFEE, R. JR., AND WOLF, C. L., 1972 - *Glossary of Geology:* Alexandria, Virginia, American Geological Institute, 805 p.

GEHMAN, H.M., 1962 - Organic matter in limestones. *Geochimica et Cosmochimica Acta,* 26, 885-897.

GLAESSNER, M. F., AND FOSTER, C. B., 1992 - Paleontology and biogeochemical research: a powerful synergy. In: SCHIDLOWSKI, M., GOLUBIC, S., KIMBERLEY, M.M., McKIRDY, D.M., AND TRUDINGER, P. A. (eds.), *Early Organic Evolution and Mineral and Energy Resources,* Springer-Verlag, Berlin, pp. 194–202.

GOLDSTEIN, R.H., AND REYNOLDS, T.J., 1994 - *Systematics of Fluid Inclusions in Diagenetic Minerals.* SEPM Short Course 31.

GRANTHAM, P.J., 1986 - The occurrence of unusual C_{27} and C_{29} sterane predominances in two types of Oman crude oil. *Organic Geochemistry,* 9, 1-10.

GRAVESTOCK, D.I. AND HIBBURT, J.E., 1991 - Sequence stratigraphy of the eastern Officer and Arrowie Basins : a framework for Cambrian oil search. *The Journal of the Australian Petroleum Exploration Association,* 31 (1), 177-190.

GRAVESTOCK, D.I. AND LINDSAY, J.F., 1994 - Summary of 1993 seismic exploration in the Officer Basin, South Australia. *The Journal of the Petroleum Exploration Society of Australia,* 22, 65-67.

GRAVESTOCK, D.I. AND SANSOME, A., 1994 - Eastern Officer Basin, Geology and Hydrocarbon Potential. *Department of Mines and Energy, South Australia,* Open file envelope, 8591 (unpublished).

GREGG, J.M., AND SIBLEY, D.F., 1984 - Epigenetic dolomitisation and the origin of xenotopic dolomite texture. *Journal of Sedimentary Petrology,* 54 (3), 908-931.

GREGG, J.M., 1988 - Origins of dolomite in the offshore facies of the Bonneterre Formation (Cambrian), southeast Missouri. *Sedimentology and Geochemistry of Dolostones,* SEPM Special Publication *43,* 67-83.

HALLEY, R.B., AND SCHMOKER, J.W., 1982 - Carbonate porosity versus depth: A predictable relationship for South Florida. *The American Association of Petroleum Geologists Bulletin,* 66, 2561-2570.

HARRIS, D.C., AND MEYERS, W.J., 1987 - Regional dolomitisation of subtidal Shelf carbonates : Burlington and Keokuk Formation (Mississippian), Iowa and Illinois. In MARSHAL, J.D. (ed.), Diagenesis of sedimentary sequences, *Geological Society Special Publication 36*, 237-258.

HARRIS, P.M., KENDALL, C.G.St.C., AND LERCHE, I., 1985 - Carbonate cementation, a brief review. In SCHNEIDERMANN, N. AND HARRIS, P.M. (eds.), *Carbonate Cements*, SEPM Special Publication 36, 79-95.

HOFFMANN, C. F., FOSTER, C. B., POWELL, T. G. AND SUMMONS, R. E., 1987 - Hydrocarbon biomarkers from Ordovician sediments and the fossil alga *Gloeocapsomorpha prisca* Zalessky 1917. *Geochimica et Cosmochimica Acta, 51*, 2681–2697.

HORBURY, A.D., AND ROBINSON, A.G., 1993 - Diagenesis, basin development, and porosity prediction in exploration − An introduction. In: HORBURY, A.D. AND ROBINSON, A.G. (eds.), *Diagenesis and Basin Development*, AAPG Studies in Geology 36, Tulsa, Oklahoma, pp. 1-4.

HORSFIELD, B., 1984 - Pyrolysis studies and petroleum exploration. In: BROOKS, J., AND WELTE, D.H.(eds.), *Advances in Petroleum Geochemistry* I, Academic Press, pp. 247-292.

HOSKINS, D., AND LEMON, N, 1995 - Tectonic development of the Eastern Officer Basin, Central Australia. *Bulletin of the Australian Society of Exploration Geophysists* 26, 395-402.

HUGHES, W.B., 1984 - Use of thiophenic organosulfur compounds in characterizing crude oils derived from carbonate versus siliciclastic sources. In: PALACAS J.G. (ed.), *Geochemistry and Source Rock Potential of Carbonate Rocks*, AAPG Studies in Geology 18, Tulsa, Oklahoma, pp. 181-196.

HUNT, J. M., 1979 - *Petroleum Geochemistry and Geology*, W. H. Freeman and Company, San Francisco.

IMBUS, S. W. AND McKIRDY, D. M., 1993 - Organic geochemistry of Precambrian sedimentary rocks. In: ENGEL M. H. AND MACKO S.A. (eds.) *Organic Geochemistry*, Plenum Press, New York, pp. 657-683.

JACKSON, K.S., McKIRDY, D.M., AND DECKELMAN, J.A., 1984 - Hydrocarbon generation in the Amadeus Basin, central Australia. *The Journal of the Australian Petroleum Exploration Association*, 24 (1), 42-65.

JAGO, J. B. AND YOUNGS, B. C., 1980 - Early Cambrian trilobites from the Officer Basin, South Australia. *Transactions of the Royal Society of South Australia* 104, 197–199.

JONES, R.W., 1984 - Comparison of Carbonate and Shale Source Rocks. In: PALACAS, J.G. (ed.), *Petroleum Geochemistry and Source Rock Potential of Carbonate Rocks* AAPG Studies in Geology 18, AAPG, Tulsa, Oklahoma, pp. 163-180.

KAMALI, M. R., LEMON, N. M. AND McKIRDY, D.M., 1993 - Ouldburra Formation as a potential source and reservoir for petroleum in the Manya Trough, eastern Officer Basin. In: ALEXANDER, E. M. AND GRAVESTOCK, D.I. (eds.), *Central Australian Basins Workshop, Alice Springs, Programme and Abstracts*, pp. 65–66.

KAMALI, M. R., LEMON, N. M., AND APAK, S. N., 1995 - Porosity generation and reservoir potential of the Ouldburra Formation in the Officer Basin. *The Journal of the Australian Petroleum Exploration Association*, 35(1), 106-120.

KANTSLER, A.J., 1979 - Petrography of dispersed organic matter, Wilkinson-1. In: *South Australian Department of Mines and Energy Report Book* 79/88.

KATZ, B. J., AND ELROD, L. W., 1983 - Organic geochemistry of DSDP Site 467, offshore California, Middle Miocene to Lower Pliocene strata. *Geochimica et Cosmochimica Acta, 47*, 389-396.

KATZ, B. J., 1983 - Limitations of 'Rock-Eval' pyrolysis for typing organic matter. *Organic Geochemistry, 4*, 195–198.

LAND, L.S., 1983 - *Dolomitisation*. AAPG Education Course Note Series, 24.

LAND, L. S., 1983 - The application of stable isotopes to studies of the origin of dolomite and to problems of diagenesis of clastic sediments. In: ARTHUR, M.A., ANDERSON, T.F., KAPLAN, I.R., VEIZER, J., AND LAND, L.S. (eds.), *Stable Isotopes in Sedimentary Geology*, SEPM Short Course 10, Dallas.

LANGFORD, F. F. AND BLANC-VALLERON, M.,1990 - Interpreting Rock-Eval pyrolysis data using graphs of pyrolyzable hydrocarbons *vs* total organic carbon. *The American Association of Petroleum Geologists Bulletin, 74*, 799–804.

LARTER, S.R, AND SENFTLE, J., 1985 - Improved kerogen typing for petroleum source rock analysis. *Nature* 318, 277-280.

LARTER, S.R., 1984 - Application of analytical pyrolysis techniques to kerogen charaterisation and fossil fuel exploration/exploitation. In: VOORHEES, K. (ed.), *Analytical Pyrolysis Methods and Applications*, Butterworths, London, pp. 212-275.

LARTER, S.R., AND HORSFIELD, B., 1993 - Determination of structural components of kerogens by the use of analytical pyrolysis methods. In: ENGEL, M.E., AND MACKO, S.A. (eds.), *Organic Geochemistry*, Plenum Press, New York, pp. 271-287.

LEMON, N.M., 1992 - Sandstone reservoirs, the influence of diagenesis on reservoir quality. Course notes, NCPGG, The University of Adelaide.

LEYTHAEUSER, H., KROOSS, B., HILLEBRAND, T., AND PRIMO, R.D., 1993 - Hydrocarbon generation and expulsion in shale vs carbonate source rocks. *The American Association of Petroleum Geologists Bulletin, 77*, 1642.

LIJMBACH, G. W. M., 1975 - On the origin of petroleum. *Proceedings 9th World Petroleum Congress, 2*, Applied Science Publishers, London, pp. 357–369.

LONGMAN, M.W., AND PALMER, S.E., 1987 - Organic geochemistry of Mid-continent Middle and Late Ordovician oils. *The American Association of Petroleum Geologists Bulletin,* 71, 938-950.

LONGMAN, M.W., 1980 - Carbonate diagenetic textures from near-surface diagenetic environments. *The American Association of Petroleum Geologists Bulletin,* 64, 461-485.

LYDYARD, A.J., 1979 - A petrographic study of the sediments in seven Officer Basin stratigraphic wells. *South Australian Department of Mines and Energy Report* 79/55 (unpublished).

MACHEL, H.G., MASON, R.A., MARIANO, A.N., AND MUCCI, A., 1991 - Causes and emission of luminescence in calcite and dolomite. In: BARKER, C.E., AND KOPP, O.C. (eds.), *Luminescence Microscopy and Spectroscopy: Qualitative and Quantitative Applications.* SEPM Short Course 25, 9-25.

MCAKENZIE, A.S., PATIENCE, R.L., MAXWELL, J.R., VANDENBROUCKE, M., AND DURAND, B., 1980 - Molecular parameters of maturation in the Toarcian shales, Paris Basin, France-I. Changes in the configuration of acyclic isoprenoid alkanes, steranes, and triterpanes. *Geochimica et Cosmochimica Acta,* 44, 1700-1721.

MATTAVELLI, L. AND NOVELLI, L., 1990 - Geochemistry and habitat of oils in Italy, *The American Association of Petroleum Geologists Bulletin,* 74, 1623-1639.

MATTES, B.W., AND MOUTJOY, E.W., 1980 - Burial dolomitisation of the Upper Devonian Miette Buildup, Jasper National Park, Alberta. In: SENGER, D.N., DUNHAM, J.B. AND ETHINGTON, R.L. (eds.), *Concepts and Models of Dolomitisation.* SEPM Special Publication 28, 259-297.

McCAFFREY, M. A., MOLDOWAN, J.M., LIPTON, P.A., SUMMONS, R.E., PETERS, K.E., JEGANATHAN, A., AND WATT, D.S., 1994 - Paleoenvironmental implications of novel C_{30} steranes in Precambrian to Cenozoic age petroleum and bitumen. *Geochimica et Cosmochimica Acta,* 58, 529-532.

McKIRDY, D. M., ALDRIDGE, A. K., AND YPMA, P.J.M., 1983. A geochemical comparison of some crude oils from pre-Ordovician carbonate rocks. In: BJOROY, M. et al. (eds.), *Advances in Organic Geochemistry* 1981, Wiley, New York, pp. 99-107.

McKIRDY, D. M., KANTSLER, A.J., EMMETT, J. K., AND ALDRIDGE, A. K., 1984 - Hydrocarbon genesis and organic facies in Cambrian carbonates of the eastern Officer Basin, South Australia. In: PALACAS J.G. (ed.) *Petroleum geochemistry and Source Rock Potential of Carbonate Rocks,* AAPG Studies in Geology 18, Tulsa, Oklahoma, pp. 13-31.

McKIRDY, D. M., AND, MICHAELSEN, B. H., 1994 - Geochemical measurement of thermal maturity in Neoproterozoic and Cambrian sediments, eastern Officer Basin. *Report for Department of Mines and Energy South Australia.*

McKIRDY, D. M., MICHAELSEN, B .H. AND KAMALI, M. R., 1995. Officer Basin oil shows and source rocks: a geochemical window on the Larapintine petroleum system. *The Journal of the Petroleum Exploration Society of Australia* (in prep.).

McKIRDY, D.M. AND KANTSLER, A.J., 1980 - Oil geochemistry and potential source rocks of the Officer Basin, South Australia. *The Journal of the Australian Petroleum Exploration Association, 20 (1), 68–86.*

McKIRDY, D.M., 1971 - An organic geochemical study of Australian Cambrian and Precambrian sedimentary rocks. M.Sc. Thesis, The University of Adelaide.

McKIRDY, D.M., 1979 - Source Rock Analyses, Wilkinson-1 In: *South Australian Departments of Mines and Energy Report Book* No. 79/88.

McKIRDY, D.M., 1994 - Biomarker geochemistry of the Early Cambrian oil show in Wilkatana-1: implications for oil generation in the Arrowie and Stansbury Basins. *The Journal of the Petroleum Exploration Society of Australia, 22, 3-17.*

MELLO, M.R.N., TELNAES, N., GAGLIANONE, P.G., CHICARELLI, M.I., BRASSELL, S.C., AND MAXWELL, J.R., 1988 - Organic geochemical characterisation of depositional palaeoenvironments of source rocks and oils in Brazilian marginal basins. In: MATTAVELLI, L., AND NOVELLI, L. (eds.), *Advances in Organic Geochemistry* 1987, Oxford, Pergamon Press, pp. 31-45.

MEYERHOFF, A.A., 1980 - Geology and petroleum fields in Proterozoic and Lower Cambrian strata, Lena-Tunguska Petroleum Province, Eastern Siberia, USSR. In: HALBOUTY, M.T. (ed.), *Giant Fields of the Decade.* AAPG Memoir, 30, 225-252.

MEYERS, W.J., 1974 - Carbonate cement stratigraphy of the Lake Valley Formation (Mississippian) Scaramento Mountains, New Mexico. *Journal of Sedimentary Petrology,* 44, 837-861.

MICHAELSEN, B. H., KAMALI, M. R., AND McKIRDY, D. M., 1995 - Unexpected molecular fossils from Early Cambrian carbonates of the Officer Basin, South Australia. In: GRIMALT, J.O. AND DORRONSORO, D. (eds.), *Organic Geochemistry: Selected Papers from the 17th International Meeting on Organic Geochemistry,* Donostia-San Sebastian, Spain, pp. 218-221.

MICHAELSEN, B. H., AND McKIRDY, D. M., 1995 - A C_{30} 18α-neohopane and its application to basin analysis. In: GRIMALT, J.O. AND DORRONSORO, D. (eds.), *Organic Geochemistry: Selected Papers from the 17th International Meeting on Organic Geochemistry,* Donostia-San Sebastian, Spain, pp. 542-544.

MICHAELSEN, B. H., KAMALI, M. R., AND McKIRDY, D. M., 1995 - Rearranged hopanes: Products of clay catalysis or bacterially-mediated reactions. *Geochimica et Cosmochimica Acta,* in prep.

MILANOVSKY, E.E., 1981 - Aulacogens of ancient platforms: problems of their origin and tectonic development. *Tectonophysics, 73, 213-248.*

MINES AND ENERGY SOUTH AUSTRALIA, 1994 - OF-94A-D Officer Basin invitation for application (unpublished).

MOLDOWAN, J.M., SUDARARAMAN, P., SALVATORI, T., ALAJBEG, A., GJUKIC, B., LEE, C.Y., AND DEMAISON, G.J., 1992 - Source correlation and maturity assessment of selected oils and rocks from the Central Adriatic Basin (Italy and Yugoslavia). In: MOLDOWAN, J.M., ALBRECHT, P., AND PHILIP, R.P. (eds.), *Biological Markers in Sediments and Petroleum,* Prentice Hall, Englewood Cliffs, pp. 370-401.

MOLDOWAN, J.M., DAHL, F.J., SHETTY, R., WATT, D.S., JACOBSON, S.R., HUIZINGA, B.J., McCAFFREY, M.A., AND SUMMONS, R.E., 1995 - Correlation of biomarkers with geologic age. In: GRIMALT, J.O. AND DORRONSORO, D. (eds.), *Organic Geochemistry: Selected Papers from the 17th International Meeting on Organic Geochemistry*, Donostia-San Sebastian, Spain, pp. 418-420.

MORROW, D.W., 1988 - Dolomite - Part 2 : Dolomitisation models and ancient dolostones. In: McIlREATH, I.A., AND MORROW, D.W. (eds.), *Diagenesis*, Geoscience Canada, Reprint Series 4, 125-139.

MOUSSAVI-HARAMI, R. AND GRAVESTOCK, D., 1995 - Burial history of the eastern Officer Basin, South Australia. *The Journal of the Australian Petroleum Exploration Association,* 35 (1), 307-320.

NAGTEGAAL, P.J.C., 1978 - Sandstone-framework instability as a function of burial diagenesis. *Journal of the Geological Society of London*, 135, 101-105.

PALACAS, J.G., 1984 - Carbonate rocks as sources of petroleum: Geological and chemical characteristics and oil-source correlations. In: *Proceedings of the 11th World Petroleum Congress* 1983, London, 2, pp. 31-43.

PEAT, C. J., MUIR, M.D., PLUMB, K. A., McKIRDY, D. M., AND NORVICK, M. S., 1978 - Proterozoic microfossils from the Roper Group, Northern Territory. Bureau of Mineral Resources, *Journal of Australian Geology and Geophy*sics, 3, 1–17.

PETERS, K. E., 1986 - Guidelines for evaluating petroleum source rock using programmed pyrolysis. *The American Association of Petroleum Geologists Bulletin,* 70, 318–329.

PETERS, K.E., AND MOLDOWAN J.M., 1993 - *The Biomarker Guide: Interpreting Molecular Fossils in Petroleum and Ancient Sediments*. Prentice Hall, Engelwood Cliffs.

PETERS, K.E., AND MOLDOWAN J.M., AND SUDARARAMAN, P., 1990 - Effects of hydrous pyrolysis on biomarker thermal maturity parameters: Monterey Phosphatic and Siliceous Members. *Organic Geochemistry*, 15, 249-265.

PITT, G.M., BENBOW, M.C. AND YOUNGS, B.C., 1980 - A review of recent geological work in the Officer Basin, South Australia. *The Journal of the Australian Petroleum Exploration Association,* 20 (1), 209-220.

POWELL, T. G, BOREHAM, C.J., McKIRDY. D.M., MICHAELSEN, B.H., AND SUMMONS, R.E., 1989 - Petroleum geochemistry of Murta Member, Mooga Formation,

and associated oils, Eromanga Basin. *The Journal of the Australian Petroleum Exploration Association*, 29 (1), 114-129.

POWELL, T. G. AND SNOWDON, L. R., 1983 - A composite hydrocarbon generation model: implications for evaluation of basins for oil and gas: Erdol und Kohle-Ergas-Petrochemie, 36, 163–170.

POWELL, T. G., 1978. An assessment of the hydrocarbons source rock potential of the Canadian Arctic Islands. *Geological Survey Canada Paper*, 78-12.

POWELL, T. G., 1987 - Depositional controls on source rock character and crude oil composition. In: *Proceedings of the 12th World Petroleum Congress*, 2, 31-41.

POWELL, T. G., AND McKIRDY D. M., 1973. Relationship between ratio of pristane to phytane, crude oil composition and geological environment in Australia. *Nature (Physical Sciences)*, 243, 37–39.

POWELL, T. G., GREANEY, S., AND SNOWDON, L.R., 1982 - Limitations of use of organic petrographic techniques for identification of petroleum source rocks. *The American Association of Petroleum Geologists Bulletin*, 66, 430-435.

RADKE, B.M., AND MATHIS, R.L., 1980 - On the formation and occurrence of saddle dolomite. *Journal of Sedimentary Petrology* 50, 1149-1168.

RADKE, M. AND WELTE, D., 1983 - The methylphenanthrene index (MPI): a maturity parameter based on aromatic hydrocarbons. In: BJOROY, M. et al. (eds.), *Advances in Organic Geochemistry* 1981. Wiley, Chichester, pp. 504–512.

RADKE, M., 1987 - Organic geochemistry of aromatic hydrocarbons. In: BROOKS, J. AND WELTE, D. (eds.), *Advances in Petroleum Geochemistry*, 2, Academic Press, London, pp. 141–207.

RADKE, M., LEYTHAEUSER, D., AND TEICHMULLER, M., 1984 - Relationship between rank and composition of aromatic hydrocarbons for coals of different origins. *Organic Geochemistry*, 6, 423-430.

REED, J.D., ILLICH, H. A., AND HORSFIELD, B., 1986. Biochemical evolutionary significance of Ordovician oils and their sources. *Organic Geochemistry*, 10, 347-358.

REIDIGER, C.L., FOWLER, M.G., BROOKS, P.W., AND SNOWDON, L.R., 1990 - Triassic oils and potential Mesozoic source rocks, Peace River Arch area, Western Canada Basin. *Organic Geochemistry*, 16, 295-305.

ROBINSON, N., EGLINTON, G., BRASSEL S.C., AND CRANWELL, P.A., 1984 - Dinoflagellate origin for sedimentary 4α-methylsteroids and 5α(H)-stanols. *Nature*, 308, 439-442.

RUBINSTEIN, I., SIESKIND, O., AND ALBRECHT, P., 1975 - Rearranged steranes in a shale: Occurrence and simulated formation. *Journal of the Chemical Society, Perkin Transaction* I, 1833-1836.

RULLKÖTTER, J., MEYERS, P.A., SCHAEFER, R.G., AND DUNHAM, K.W., 1986 - Oil generation in the Michigan Basin: a biological marker and carbon isotope approach, In: LEYTHAEUSER, D., AND RULLKÖTTER, J. (eds.), *Advances in Organic Geochemistry* 1985, Pergamon, Oxford, pp. 359-376.

RULLKÖTTER, J., SPIRO, B., AND NISSENBAUM, A., 1985 - Biological marker characteristics of oils and asphalts from carbonate source rocks in a rapidly subsidising graben, Dead Sea, Israel. *Geochimica et Cosmochimica Acta*, 49, 1357-1370.
SCHLUMBERGER, 1979 - *Log Interpretation Charts*. Schlumberger Limited, Houston.

SANSOME, A., AND GRAVESTOCK, D., 1993 - Sandstone reservoirs in the eastern Officer Basin. In: ALEXANDER, E. M. AND GRAVESTOCK, D.I. (eds.), *Central Australian Basins Workshop, Alice Springs, Programme and Abstracts,* 66 p.

SCHMIDT, V., AND McDONALD, D.A., 1979. - *The Role of Seconday Porosity in the Course of Sandstone Diagenesis.* SEPM Special Publication, 26, 175-207.

SCOFFIN, T.P., 1987 - *An Introduction to Carbonate Sediments and Rocks.* Blackie, Glasgow, pp. 88-137.

SEIFERT, W.K., AND MOLDOWAN, J.M., 1981 - Palaeoreconstruction by biological markers. *Geochimica et Cosmochimica Acta,* 45, 738-794.

SHEPHERD, T.J., RANKIN, A.H., AND ALDERTON, D.H.M., 1985 - *A Practical Guide to Fluid Inclusion Studies.* Blackie, Glasgow, pp. 128-139.

SHERGOLD, J., JAGO, J., COOPER, R, AND LAURIE, J., 1985 - The Cambrian System in Australia, Antarctica and New Zealand. Correlation charts and explanatory notes. *International Union of Geological Science*, Publication No 19.

SIBLEY, D.F., AND GREGG, J.M., 1987 - Classification of dolomite rock textures. *Journal of Sedimentary Petrology,* 57, 967-975.

SUMMONS, R.E, BRASSELL, S.C., EGLINTON, G., EVANS, E.M HORODYSKI, R.J., ROBINSON, N., AND WARD, D.M., 1988 - Distinctive hydrocarbon biomarkers from fossiliferous sediment of the Late Proterozoic Walcott Member, Chuar Group, Grand Canyon, Arizona. *Geochimica et Cosmochimica Acta*, 52, 2625-2637.

SUMMONS, R.E., AND JEHNKE, L.L., 1992 - Hopenes and hopanes methylated in ring-A: Correlation of the hopanoids from extant methylotrophic bacteria with their fossil analogues. In: MOLDOWAN, J.M., ALBRECHT, P. AND PHILIP, R.P. (eds.), *Biological Markers in Sediments and Petroleum.* Prentice Hall, Englewood Cliffs, pp. 763-765.

SUMMONS, R.E., 1992 - Proterozoic biostratigraphy: abundance and composition of extractable organic matter. In: SCHOPF, J.W., AND KLEIN, C. (eds.), *The Proterozoic*

Biosphere: A Multidisciplinary Study. Cambridge University Press, Cambridge, pp. 101-115

TEN HAVEN, H.L., DE LEEUW, J.W., SINNINGHE DAMST'E, J.S., SCHENCK, P. A., PALMER, S.E., AND ZUMBERGE, J.E., 1988 - Application of biological markers in the recognition of palaeohypersaline environments. In: FLEET, A.J., KELTS, K., AND TALBOT, M.R. (eds.), *Lacustrine Petroleum Source Rocks.* Geological Society of London Special Publication, 40, pp. 123 - 130.

TISSOT, B. P. AND WELTE, D. H., 1978 - *Petroleum Formation and Occurrence.* First edition, Springer-Verlag, Berlin.

TISSOT, B. P. AND WELTE, D. H., 1984 - *Petroleum Formation and Occurrence.* Second edition, Springer-Verlag, Berlin.

TUCKER, M.E., AND WRIGHT, V.P., 1990 - *Carbonate Sedimentology.* Blackwells, Oxford, pp. 480-482.

TUCKER, M.E., 1993 - Carbonate diagenesis and sequence stratigraphy. In: WRIGHT, V.P. (ed.), *Sedimentology Review*, 1, 51-72.

VAN GRAAS, G.W., 1990 - Biomarker maturity parameters for high maturities: calibration of the working range up to the oil/condensate threshold. *Organic Geochemistry,* 16, 1025-1032.

VEEVERS, J.J., JONES, J.G., AND POWELL, C.Mc.A, 1982 - Tectonic framework of Australia's sedimentary basins. *The Journal of the Australian Petroleum Exploration Association,* 22 (1) , 283-300.

VOLKMAN, J.K, KEARNEY, P., AND JEFFREY, S.W., 1990 - A new source of 4-methyl and 5α(h)-stanols in sediments: prymnesiophyte microalgae of the genus Pavlova. *Organic Geochemistry*, 15, 489-498.

VOLKMAN, J.K., 1988 - Biological marker compounds as indicators of the depositional environments of petroleum source rocks. In: FLEET, A.J., KELTS, K., AND TALBOT, M.R. (eds.) *Lacustrine Petroleum Source Rocks.* Geological Society of London Special Publication, 40, pp. 103 - 122.

WALTER, M.R., AND GORTER, J.D., 1994 - The Neoproterozoic Centralian Superbasin. In: PURCELL, P.G., AND PURCELL, P.R. (eds.), Western Australia: *Proceedings of the Petroleum Exploration Society of Australia Symposium*, Perth, pp. 851-864.

WANG, H.D., PHILIP, R.P., AND ALAM, M., 1993 - Source rock and oil correlation using biomarker characteristics in the Anadarko Basin, Oklahoma, USA. In: OYGARD, K. (ed.), *The 16th International Meeting on Organic Geochemistry,* Stavanger, Falch Hurtigtrykk, Oslo, pp. 116-119.

WAPLES, D. W., 1985 - *Geochemistry in Petroleum Exploration.* D. REIDEL Publishing Company, Boston, pp. 170–180.

WAPLES, D. W., AND MACHIHARA, T., 1991 - *Biomarker for Geologists*. American Association of Petroleum Geologists, Methods in Exploration Series, No., 9.

WARD, D.M., AND WINFREY, M.R., 1985 - Interactions between methanogenic and sulfate-reducing bacteria in sediments. *Adv., Aq. Microbial.*,3, 141-179.

WARD, D.M., TAYNE, T.A., ANDERSON, K.L., AND BATESON, M.M., 1987 - Community structure, and interactions among community members in hot spring cyanobacterial mass. *Symp. Soc. Gen. Microbial.*, 71, 179-210.

WARDLAW, N.C., 1979 - Pore systems in carbonate rocks and their influence on reservoir performance. *AAPG Course Note Series* No. 11, E2-E3.

WARREN, J. K., 1992 - Carbonates General Concepts. NCPGG Course Notes, The University of Adelaide, 45–70.

WESTE, G., SUMMONS, R.E., McKIRDY, D.M., SOUTHGATE , P.N., HENRY, R.L., AND BREWER, A.M., 1984 - Cambrian palaeoenvironments and source rocks of the eastern Officer Basin. *Geological Society of Australia, Abstract Series* 12, 542-544.

WHITE,A.H., AND YOUNGS, B.C., 1980 - Cambrian alkali-playa lacustrine sequence in the northeastern Officer Basin, South Australia. *Journal of Sedimentary Petrology*, 50, pp. 1279-1286.

YOUNGS, B.C., 1980 - Lithologies and interpretations of the Observatory Hill Beds, Marla-1A and -1B. Report No. 10 of the Officer Basin Study Group. *Department of Mines and Energy South Australia Report* 80/79.

ZALESSKY, M.D., 1917 - On marine sapropelite of Silurian age formed by a blue-green alga. *Izv. Imp. Akad. Nauk.* IV Series, 3-18.

ZANG W. AND McKIRDY, D.M., 1993. Microfossils and molecular fossils from the Neoproterozoic Alinya Formation - a possible new source rock in the eastern Officer Basin. In: ALEXANDER, E. M. AND GRAVESTOCK, D.I. (eds.), *Central Australian Basins Workshop, Alice Springs, Programme and Abstracts*, pp. 62-63.

ZENGER, D. H., AND DUNHAM, J.B., 1988 - Dolomitisation of Siluro-Devonian limestones in a deep core (5,350M), southeastern New Mexico. *Sedimentology and Geochemistry of Dolostones.* SEPM Special Publication 43, 161-173.

ZUMBERGE, J.E., 1984 - Source rocks of the La Luna Formation (Upper Cretaceous) in the Middle Magdalena Valley, Colombia. In: PALACAS, J.G. (ed.), *Geochemistry and Source Rock Potential of Carbonate Rocks*, AAPG Studies in Geology 18, Tulsa, Oklahoma, pp. 127-133.

Kamali, M.R., Lemon, N.M. and McKirdy, D.M. (1993) Ouldbuna Formation as a potential source and reservoir for petroleum in the Manya Trough, eastern Officer Basin. In: *Central Australian Basins Workshop, Alice Springs, September 13-14, 1993: programme and abstracts, pp. 65-66, 1993*

Kamali, M.R., Lemon, N.M. and Apak, S.N. (1995) Porosity generation and reservoir potential of the Ouldburra Formation in the Officer Basin.
APPEA Journal, v. 35 (1), pp. 106-120, 1995

Michaelsen, B.H., Kamali, M.R., Lemon, N.M. and McKirdy, D.M. (1995) Unexpected molecular fossils from Early Cambrian marine carbonates, eastern Officer Basin. In: *Proceedings of the 17th International Meeting on Organic Geochemistry: Donostia-San Sebastian, Spain, 4-8 September, 1995, pp. 218-221, 1995*

APPENDIX I

X-RAY DIFFRACTION PROFILES

(RESERVOIR AND SOURCE ROCKS)

OULDBURRA FORMATION

OFFICER BASIN

X-RAY POWDER DIFFRACTION (XRD)

XRD is a basic tool in the mineralogical analysis of sediments particularly in the case of fine-grained sediments. Mineralogy, and to a lesser extent composition, are easily determined but percentages are only semiquantitative.

It is customary for bulk mineralogy of samples to be determined before detail petrographic description. Quantitative analyses were performed on twenty-two whole rock samples including carbonates and mixed carbonate/siliciclastics. XRD files (Appendix I) are labelled with mineral peaks using the following abbreviations for existing minerals:

Q = quartz, K = potash, Alb = albite, M = microcline, C = calcite, D = dolomite, A = anhydrite. The name of the other uncommon minerals are shown on their respective mineral peaks.

XRD analysis performed on carbonate and mixed carbonate/siliciclastic rocks indicates that calcite and dolomite comprise the major components in carbonate units but in siliciclastic units, quartz and feldspars predominate over carbonate minerals. Anhydrite, gypsum and halite constitute accessory minerals. A summary of the XRD results for carbonate/siliciclastic units is given in Table 1. The relative abundance in this table is based on the peak height (Fig. 1) seen in a sample and does not reflect the absolute abundance of each mineral. For example, in the case of mixed carbonate/siliciclastics, the response of carbonate minerals with respect to quartz is

much subdued so that equal peak heights suggest that carbonate actually dominates the sample. In addition , the peaks of certain minerals may overlap or interfere with those of others to make accurate determination difficult. For example, illite and muscovite are similar crystallographically and are therefore difficult to differentiate.
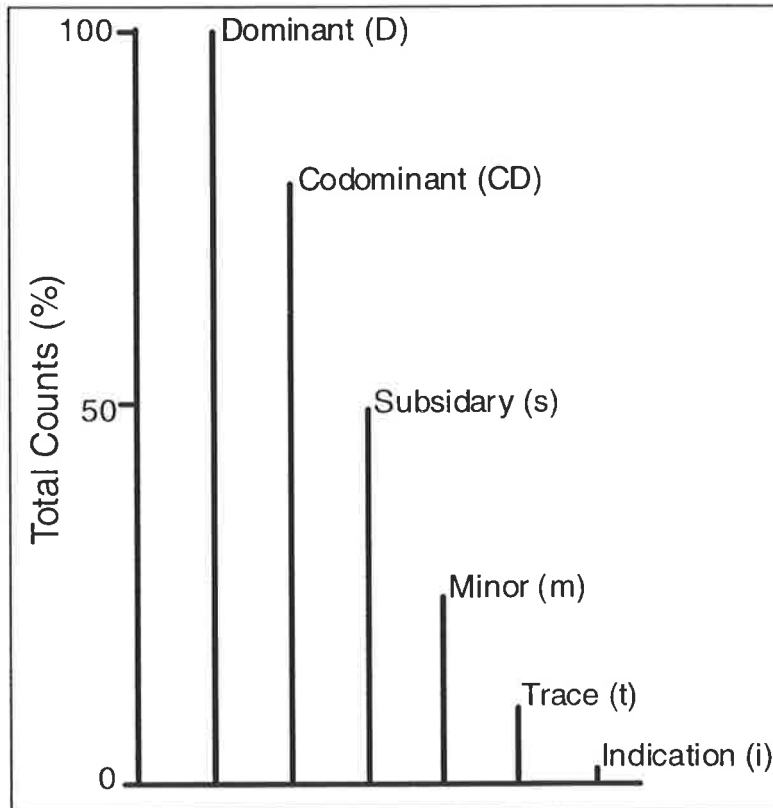
Figure 1 Relative proportion of minerals based on XRD peak height. Based on the relative peak height in a XRD trace, a mineral is assigned to one of the above codes using abbreviations outlined in Table 1.

Table **1** Summary of XRD results

Well	Depth (m)	Quartz	Albite	Orthoclase/ Microcline	Calcite	Dolomite	Biotite/ Muscovite	Clay	Anhydrite	Sphalerite
Manya-6	652.30	t	-	-	D	t	-	-	-	-
"	654.10	t	-	-	D	-	-	-	-	-
"	661.10	s	m	s	-	D	-	-	-	-
"	683.60	m	-	-	D	t	-	-	-	-
"	766.60	CD	CD	-	t	D	t	t	-	-
"	874.65	CD	-	t	t	D	t	t	-	-
"	906.75	D	-	t	i	CD	-	i	s	-
"	1009.50	CD	t	-	D	-	-	-	-	-
"	1020.05	CD	-	-	D	s	-	-	-	-
"	1039.90	CD	-	-	D	s	-	-	-	-
"	1072.10	CD	-	-	D	s	-	-	-	-
"	1145.70	CD	-	-	s	D	-	-	-	-
"	1165.85	D	CD	-	-	s	-	-	-	-
"	1178.75	m	-	-	D	m	-	-	-	-
"	1180.90	D	m	s	-	CD	-	i	-	-
"	1230.60	s	CD	t	D	m	-	-	-	-
Marla-3	519.70	m	t	-	-	D	-	-	-	-
"	532.25	t	-	-	-	D	-	-	-	-
Marla-6	446.80	CD	-	t	-	D (ferroan)	-	-	-	-
"	602.80	m	-	i	i	D	-	-	-	-
"	697.33	D	-	i	t	m	-	i	-	CD

D = dominant, CD = codominant, s = subsidary, m = minor, t = trace, i = indication

MANYA-6 (652.30 m)
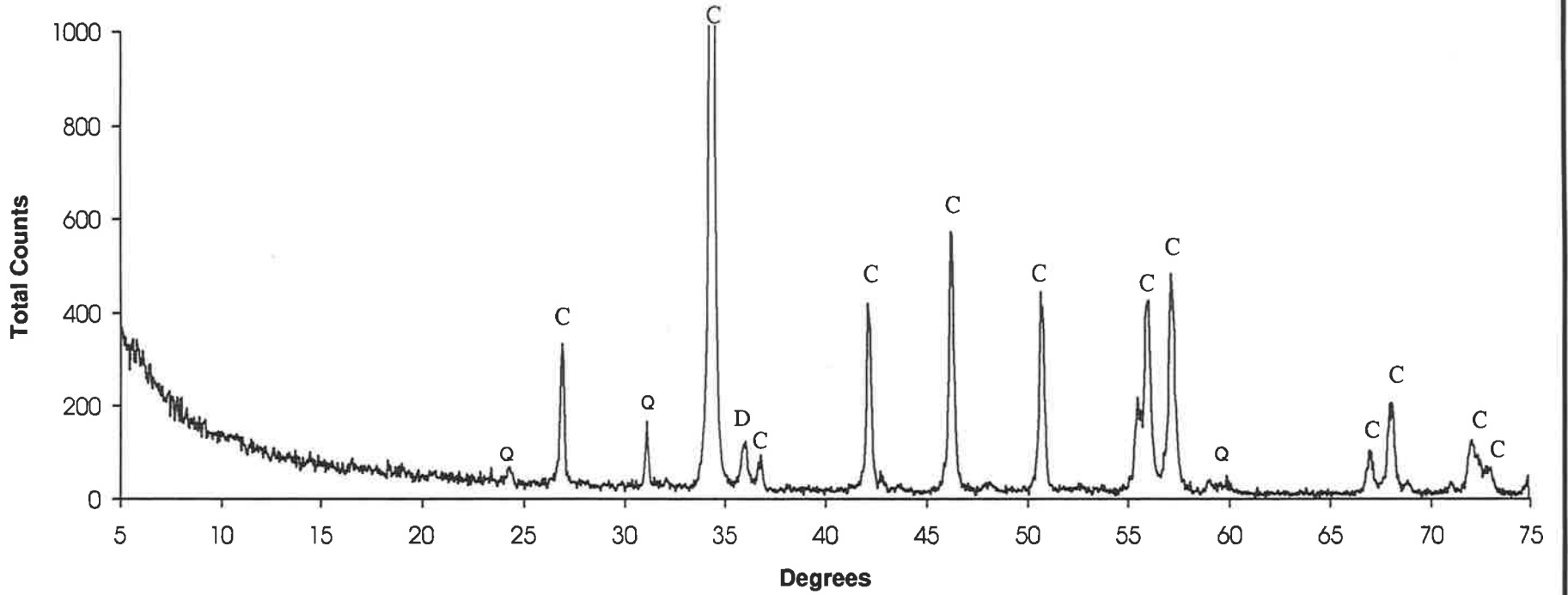
MANYA-6 (654.10 m)
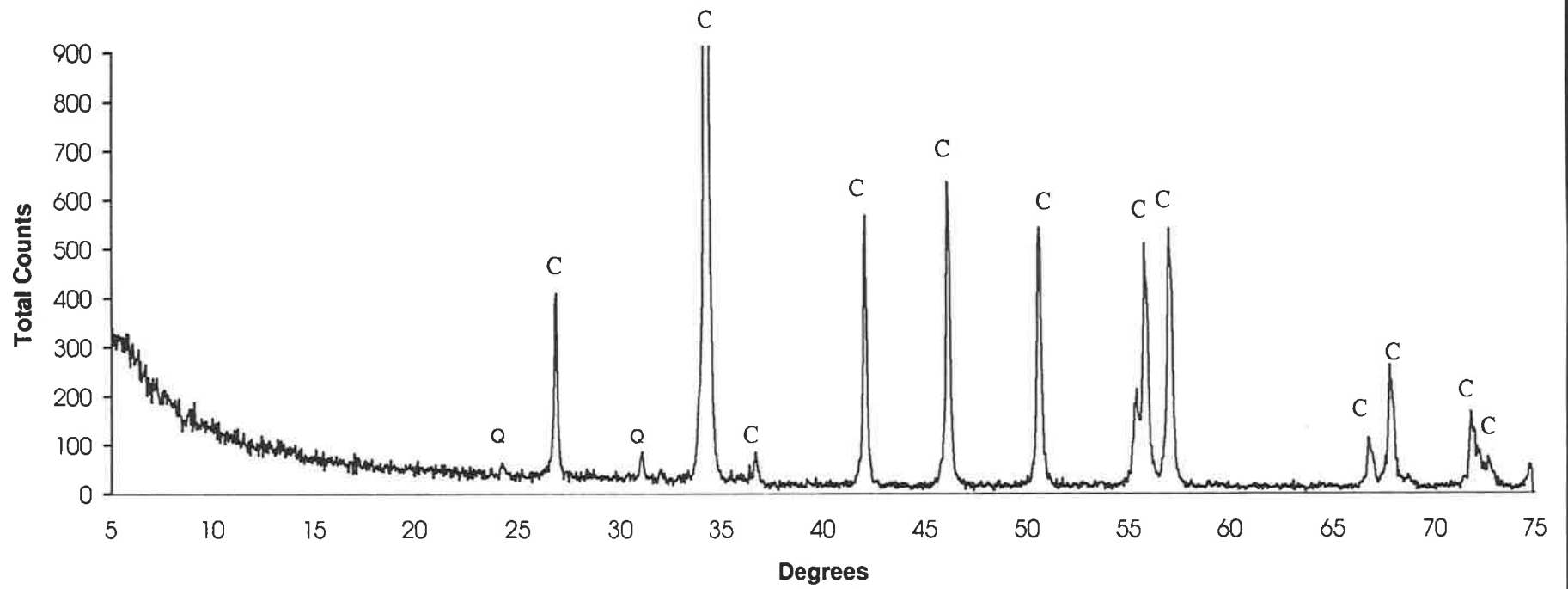
MANYA-6 (661.10 m)
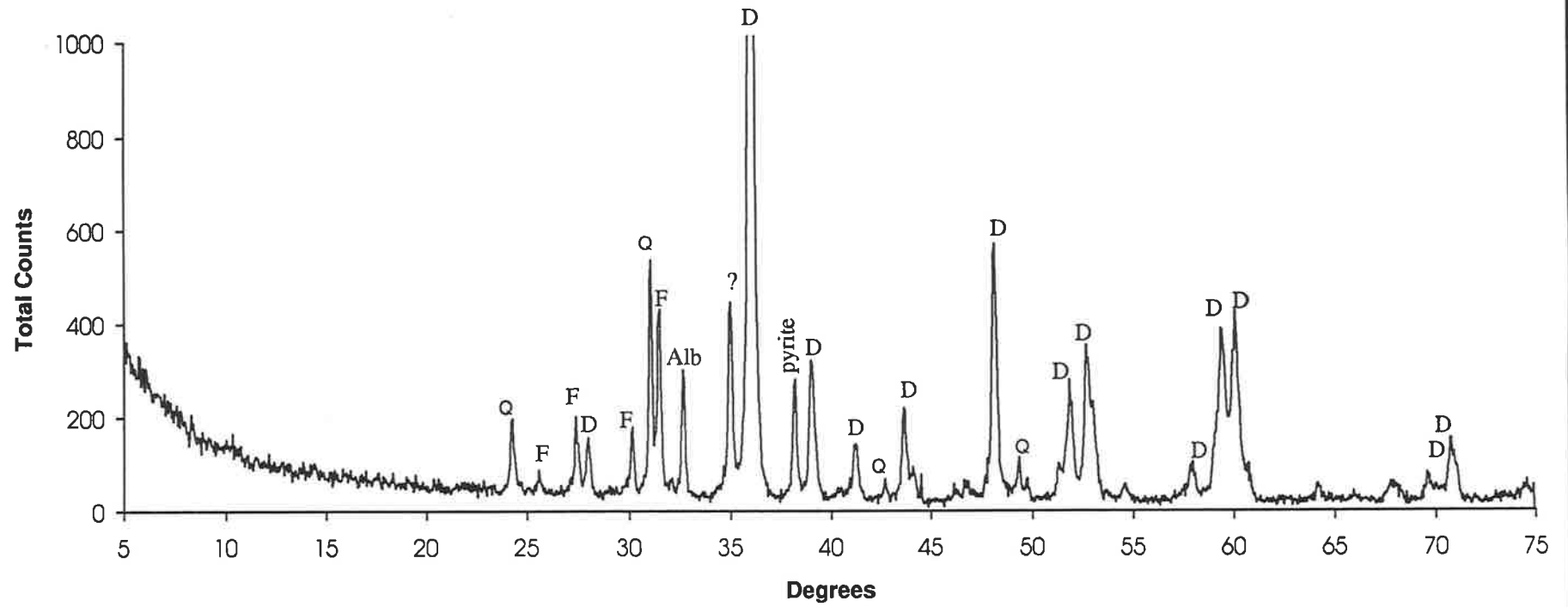
MANYA-6 (683.60 m)
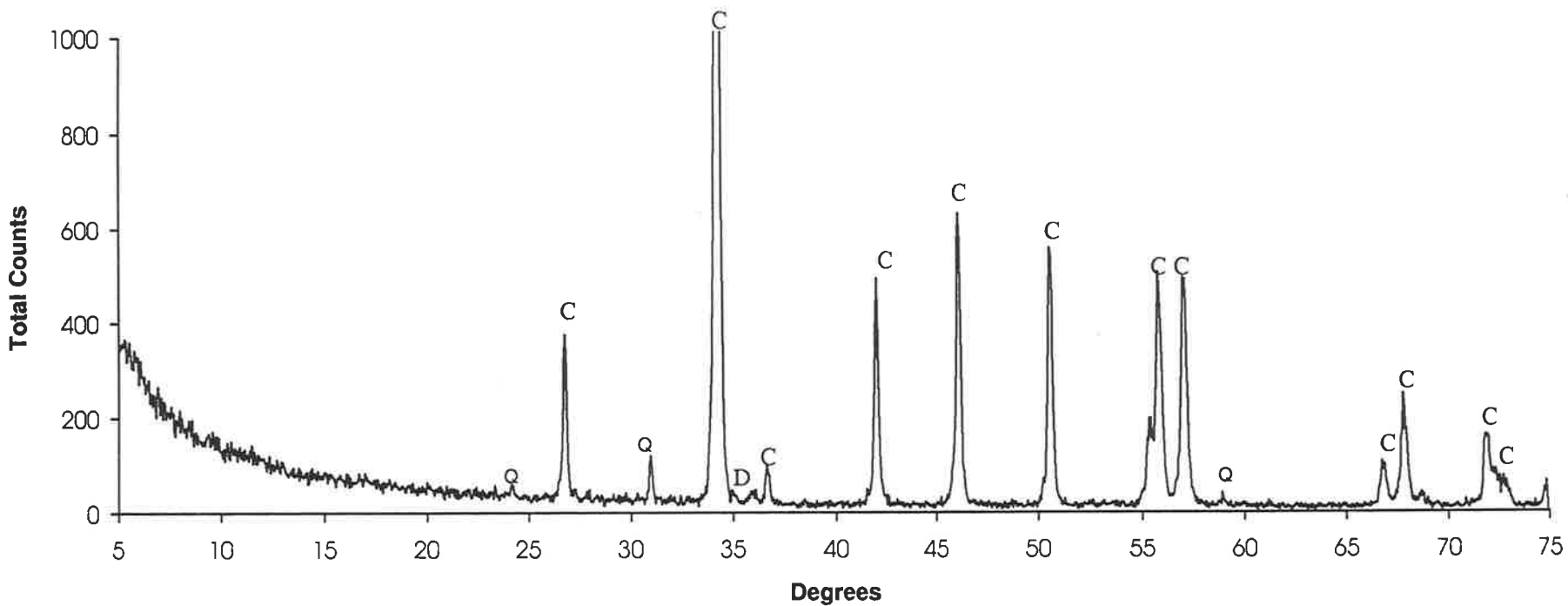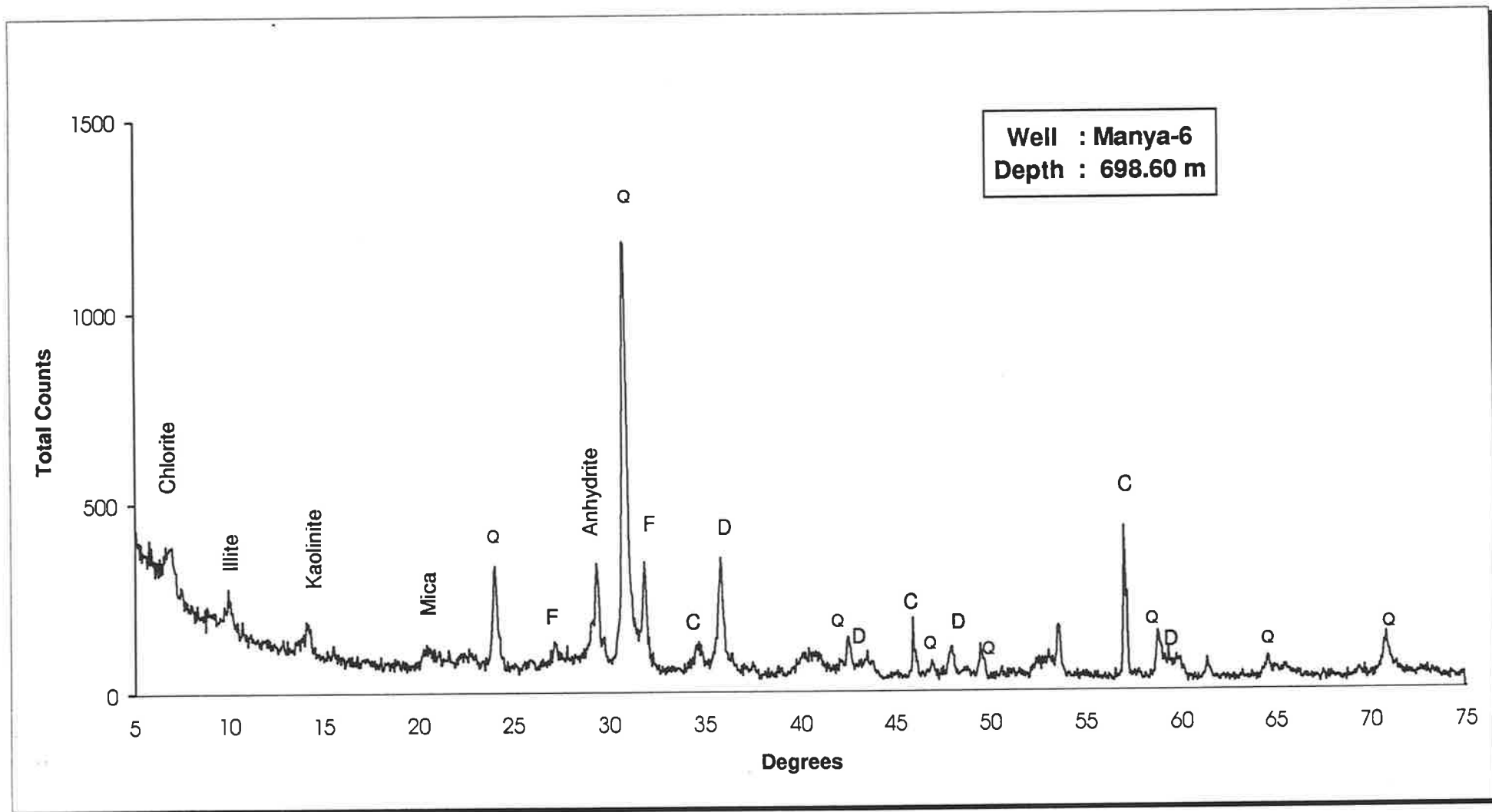
MANYA-6 (766.60 m)
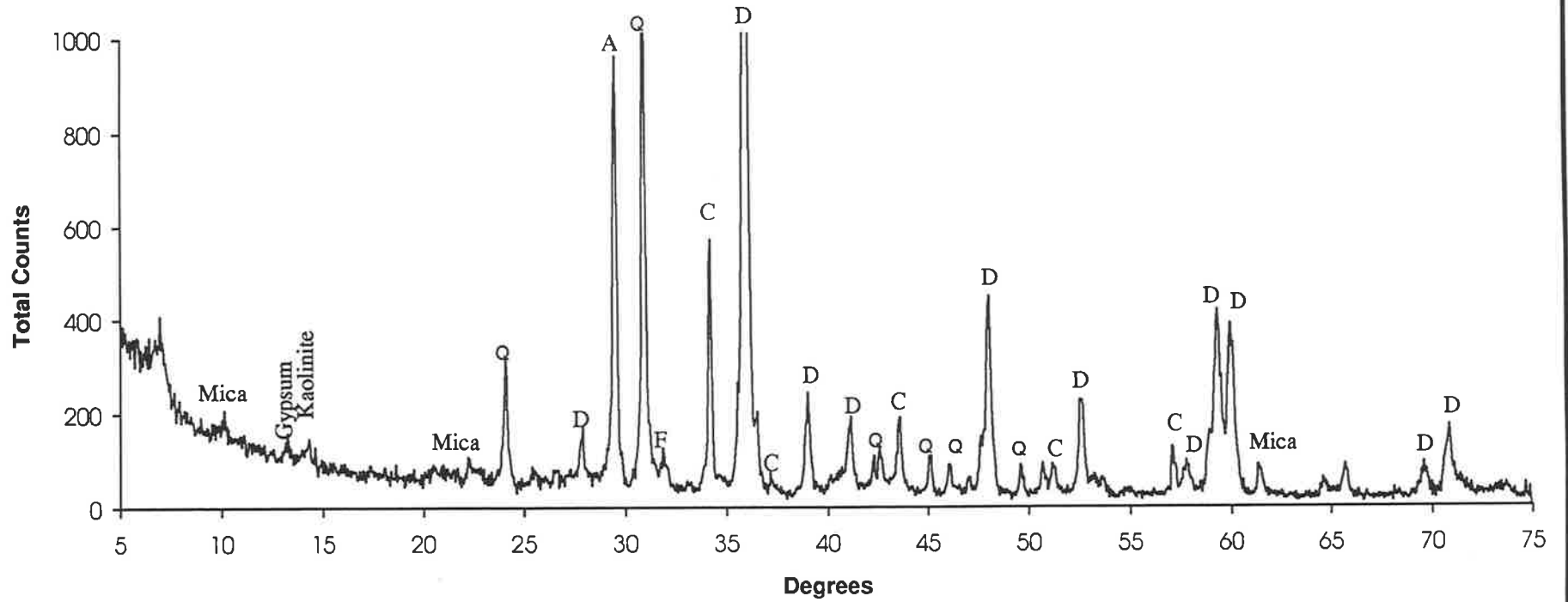
MANYA-6 (874.65 m)
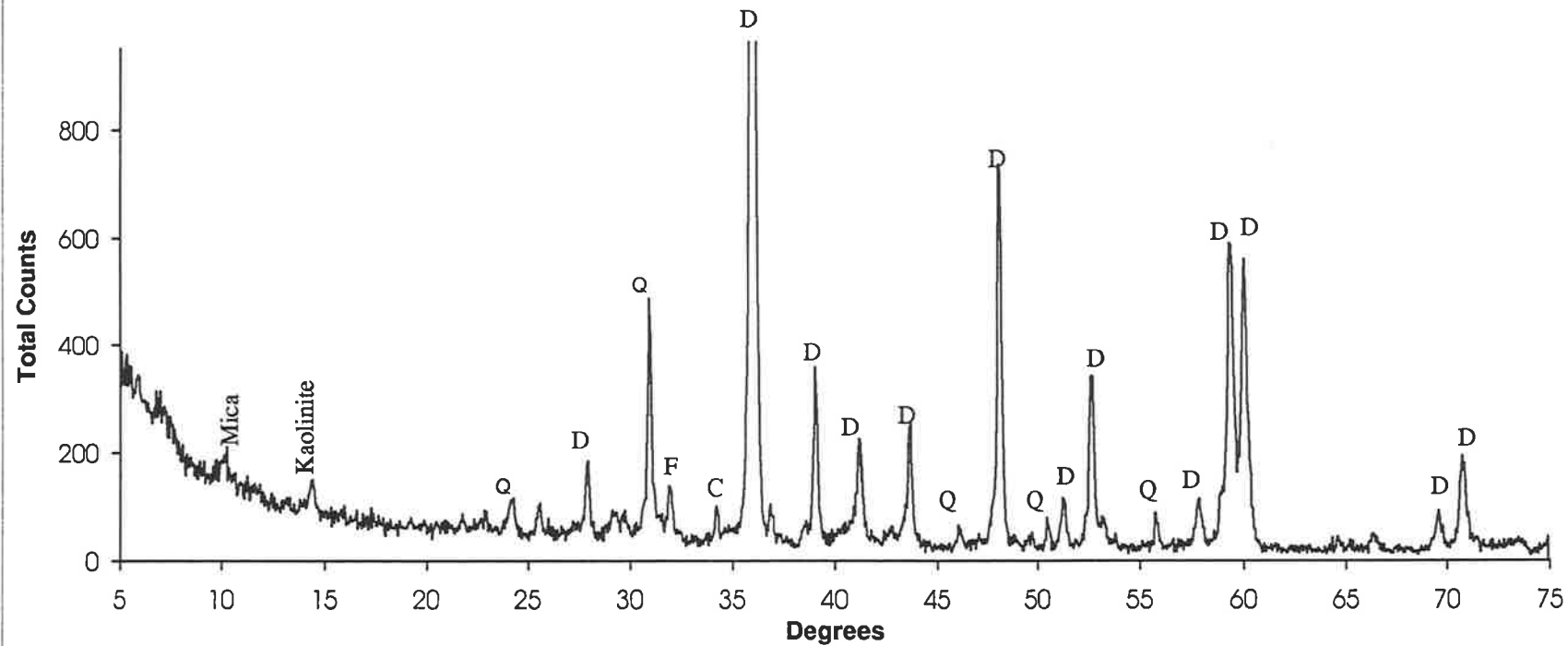
MANYA-6 (906.75 m)
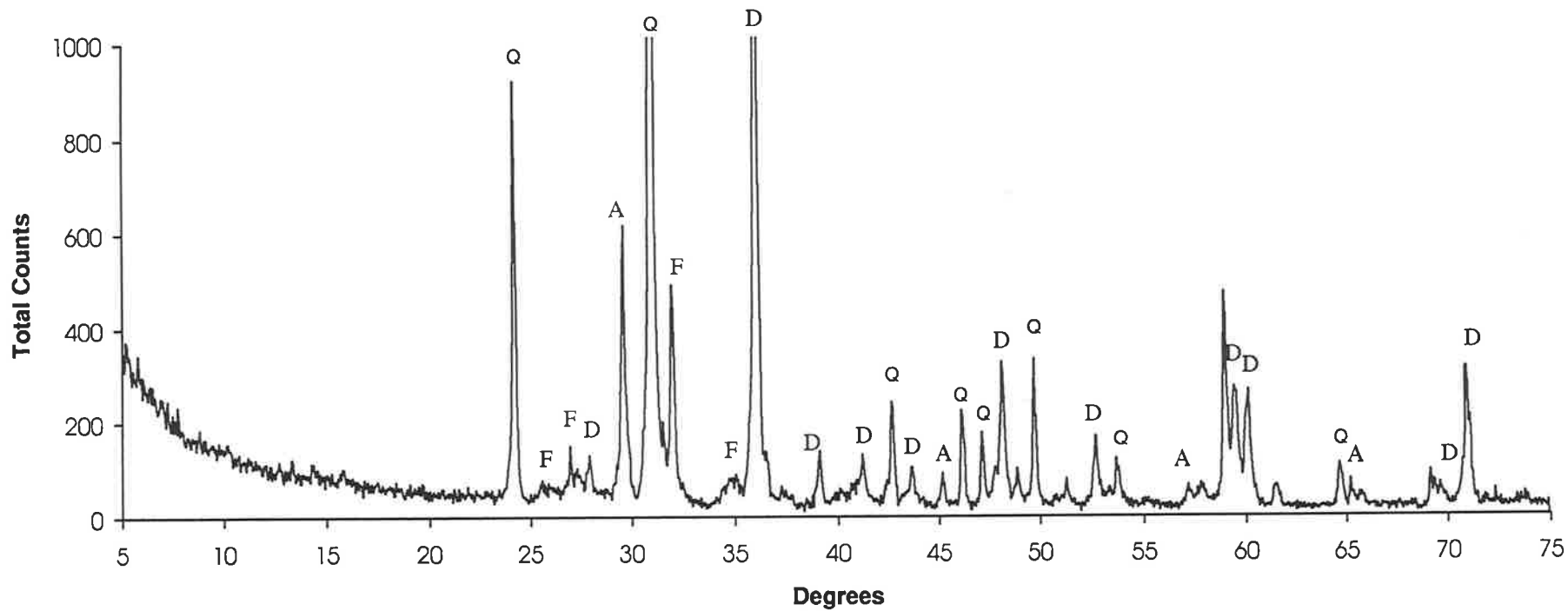
MANYA-6 (1009.50 m)
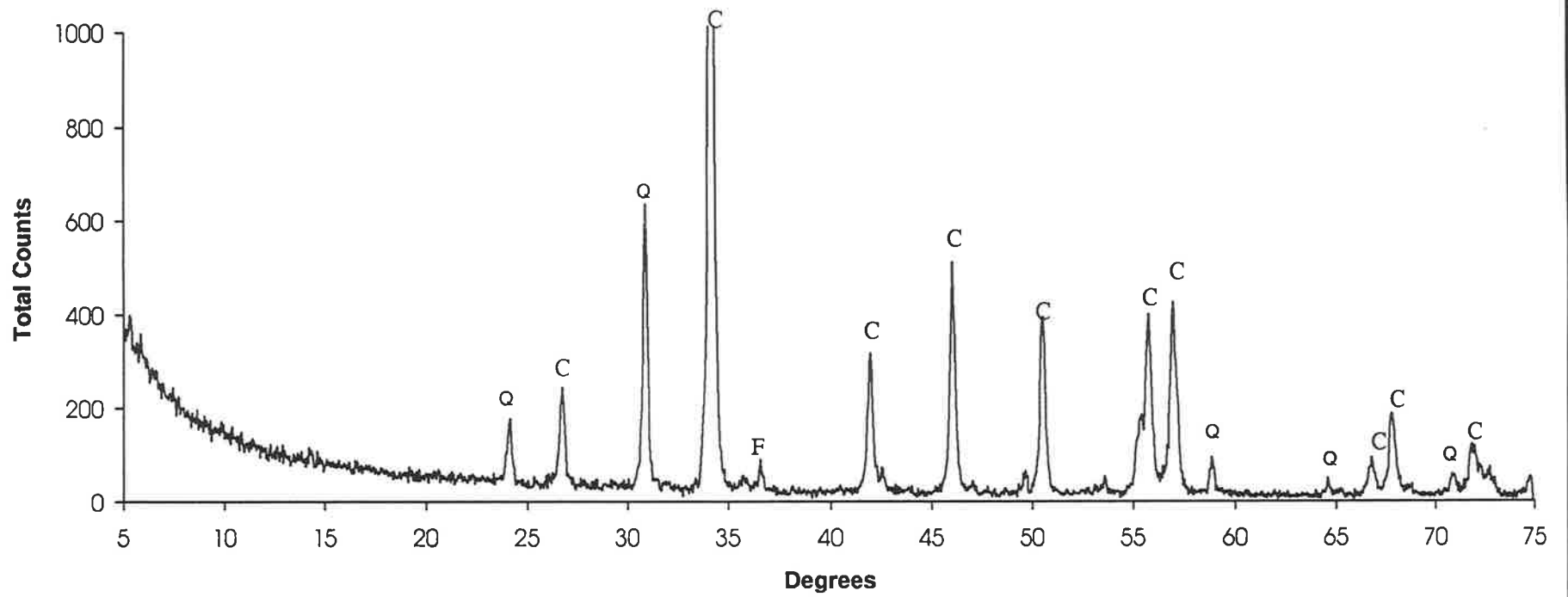
MANYA-6 (1020.05 m)
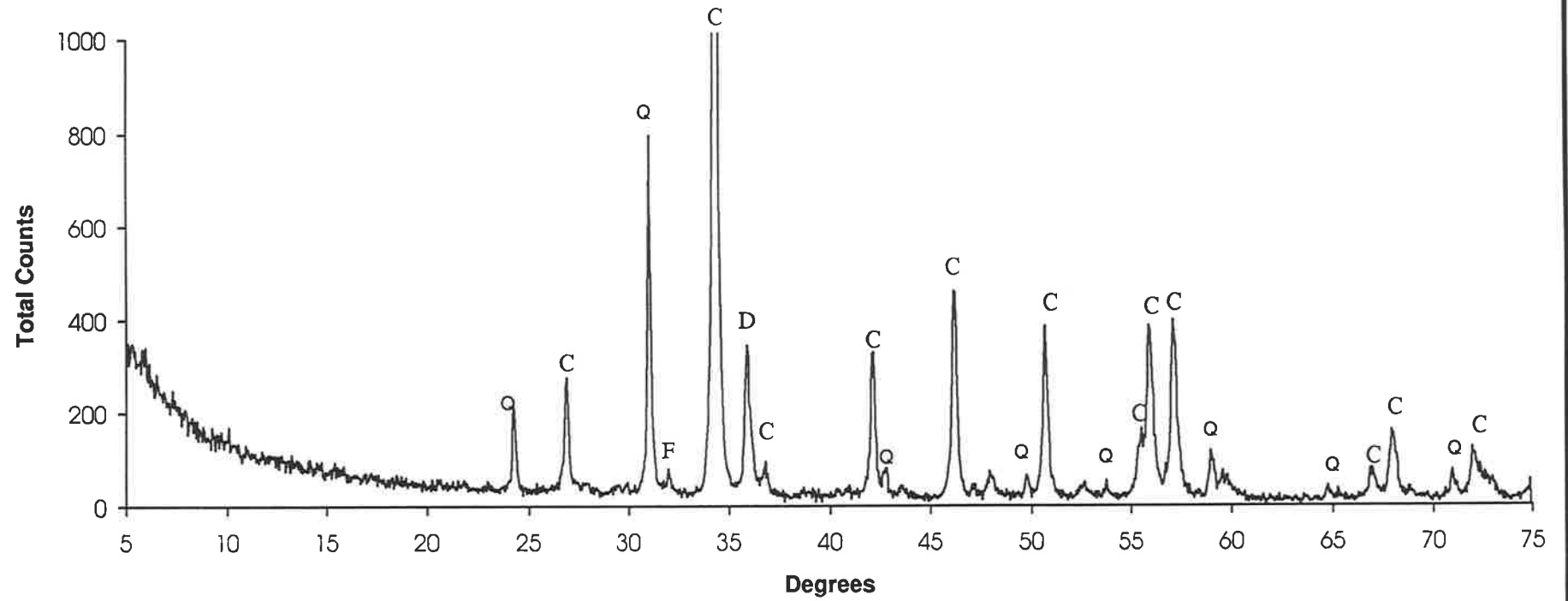
MANYA-6 (1039.90 m)
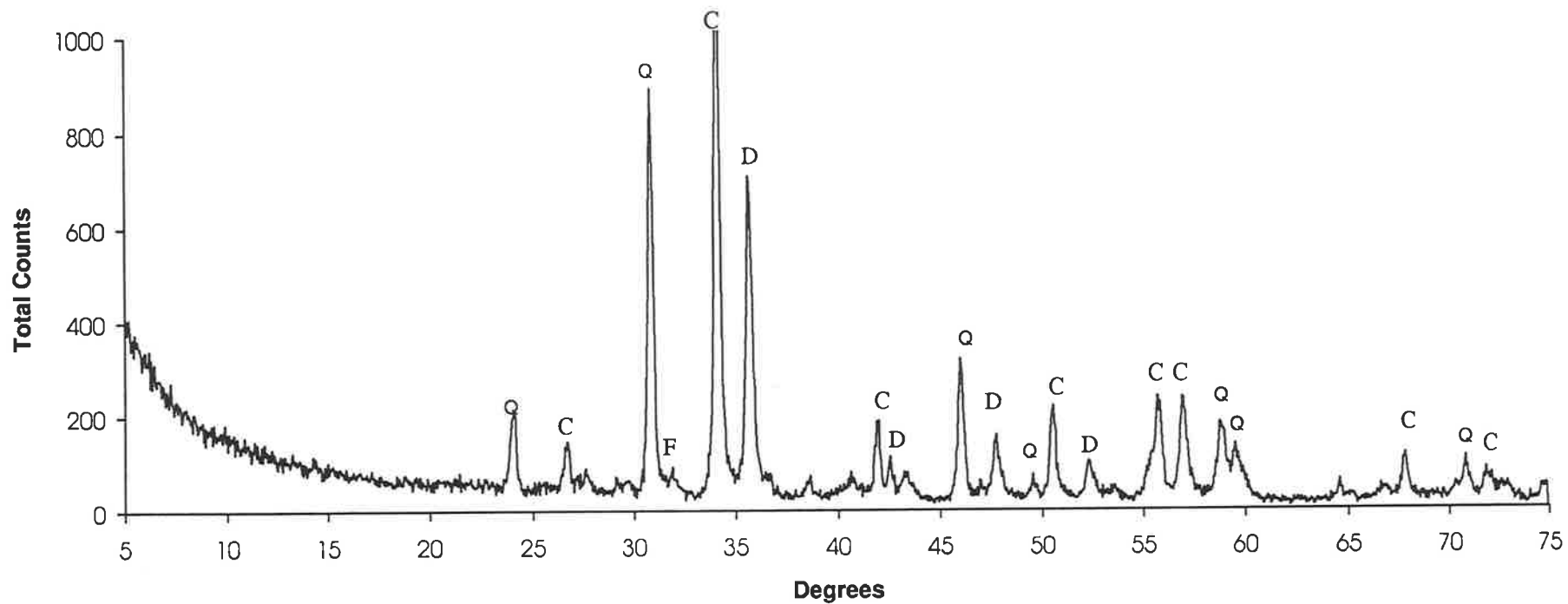
MANYA-6 (1072.10 m)

MANYA-6 (1145.70 m)
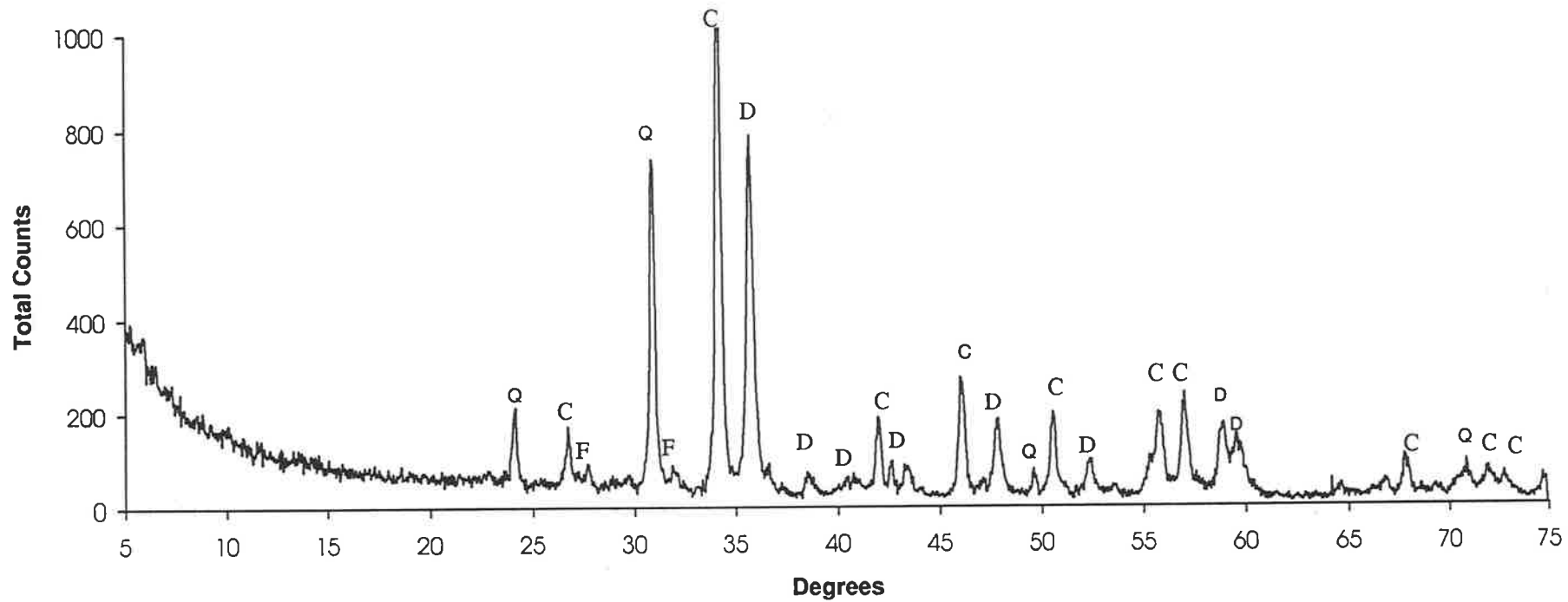
MANYA-6 (1165.85 m)
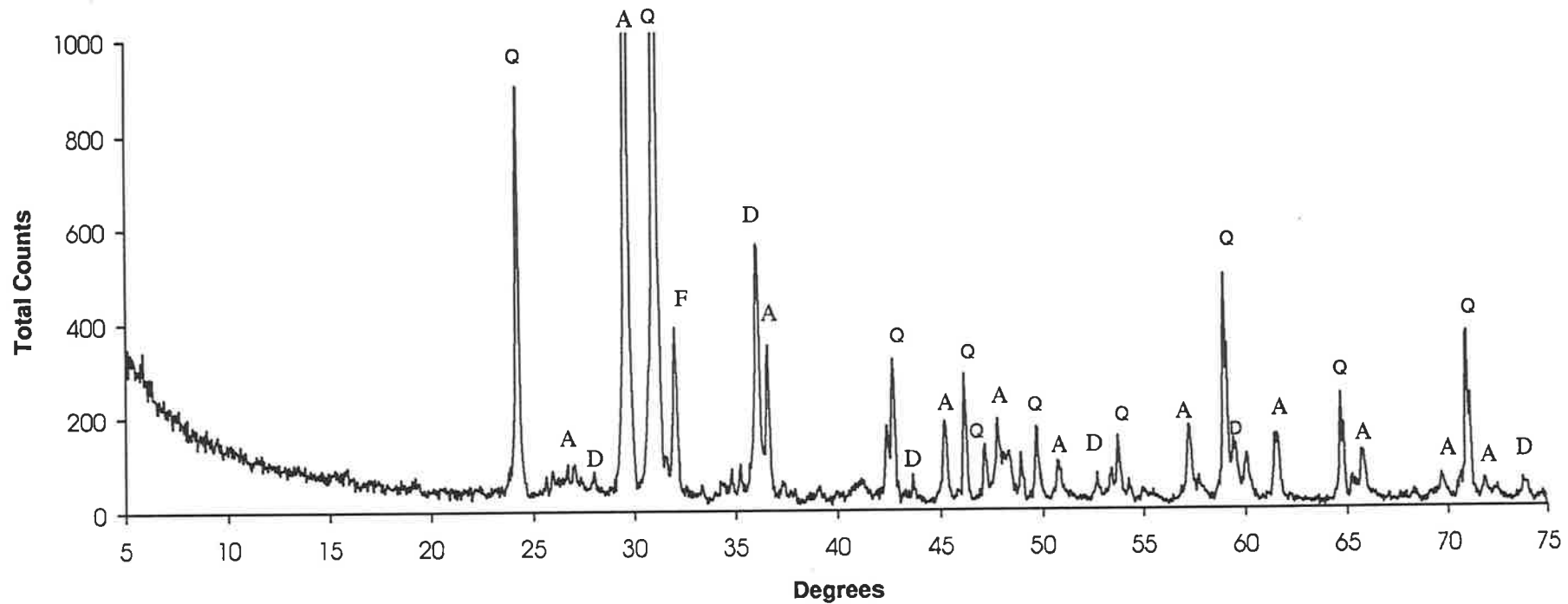
MANYA-6 (1178.75 m)
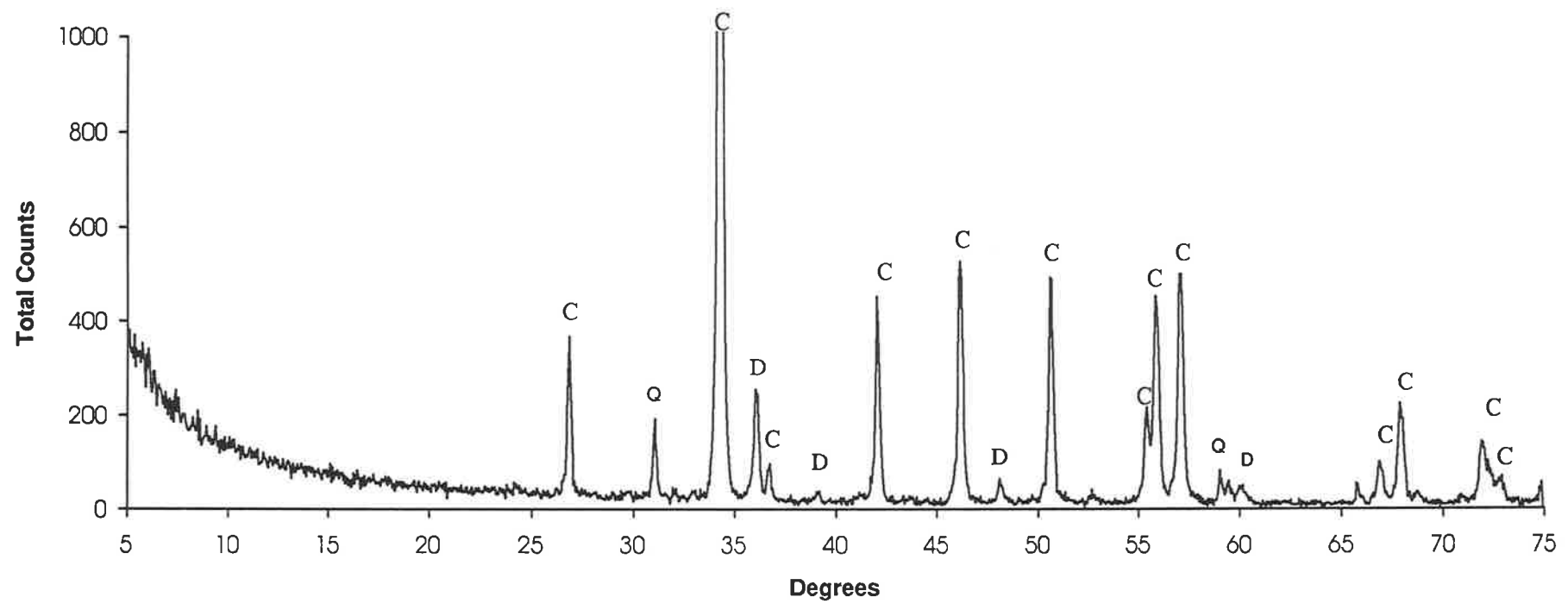
MANYA-6 (1180.90 m)
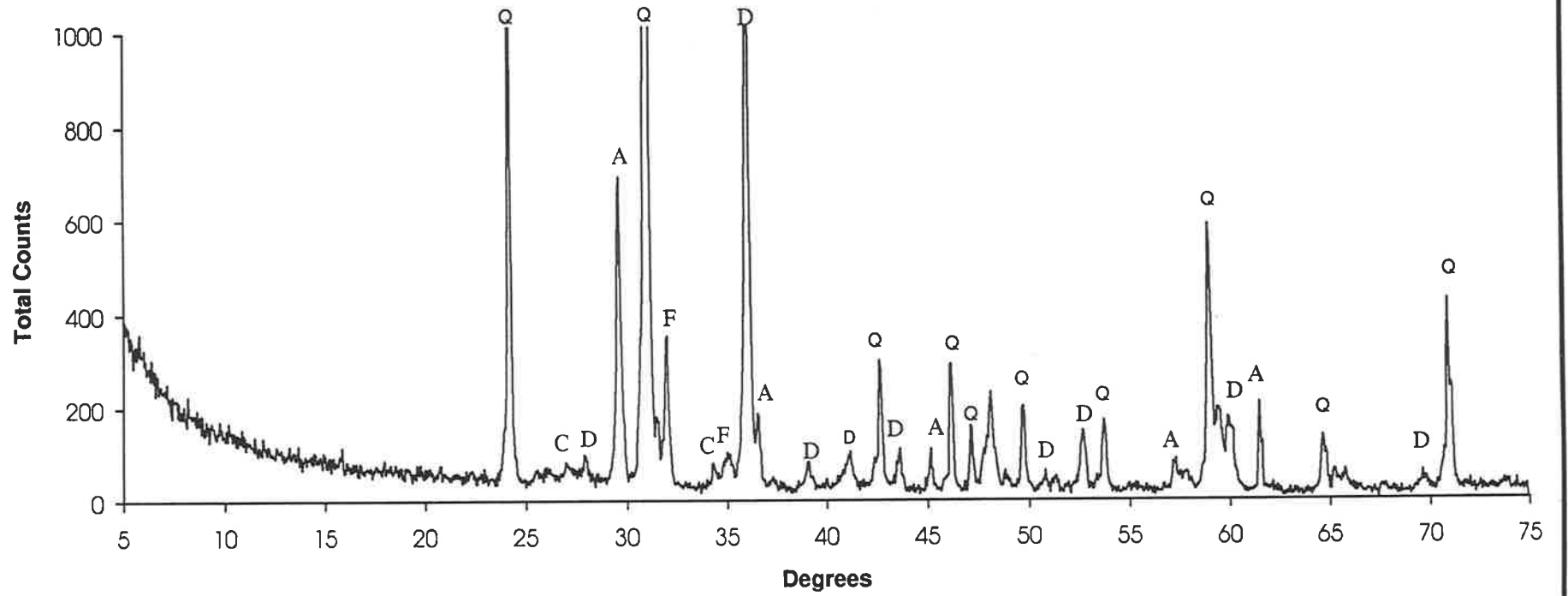
MANYA-6 (1230.60 m)
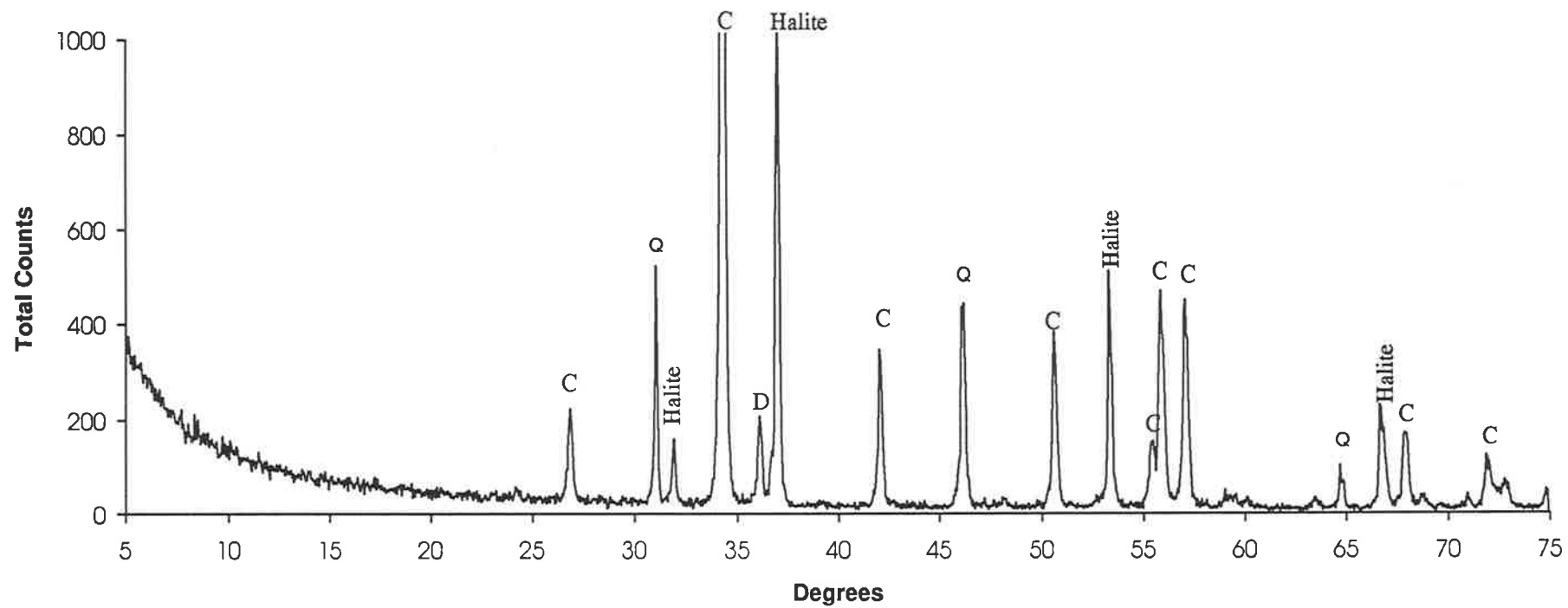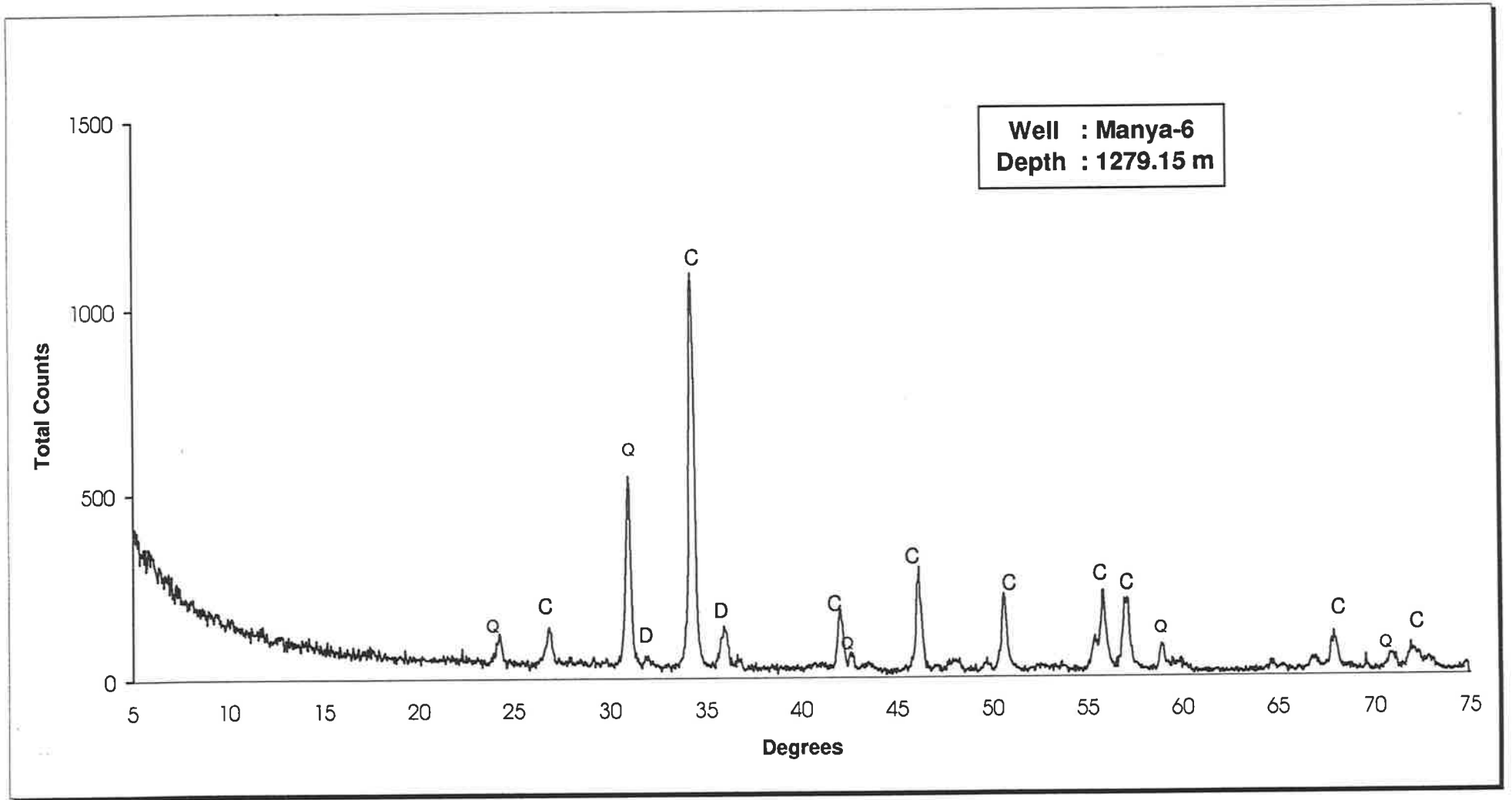
MARLA-3 (519.70 m)
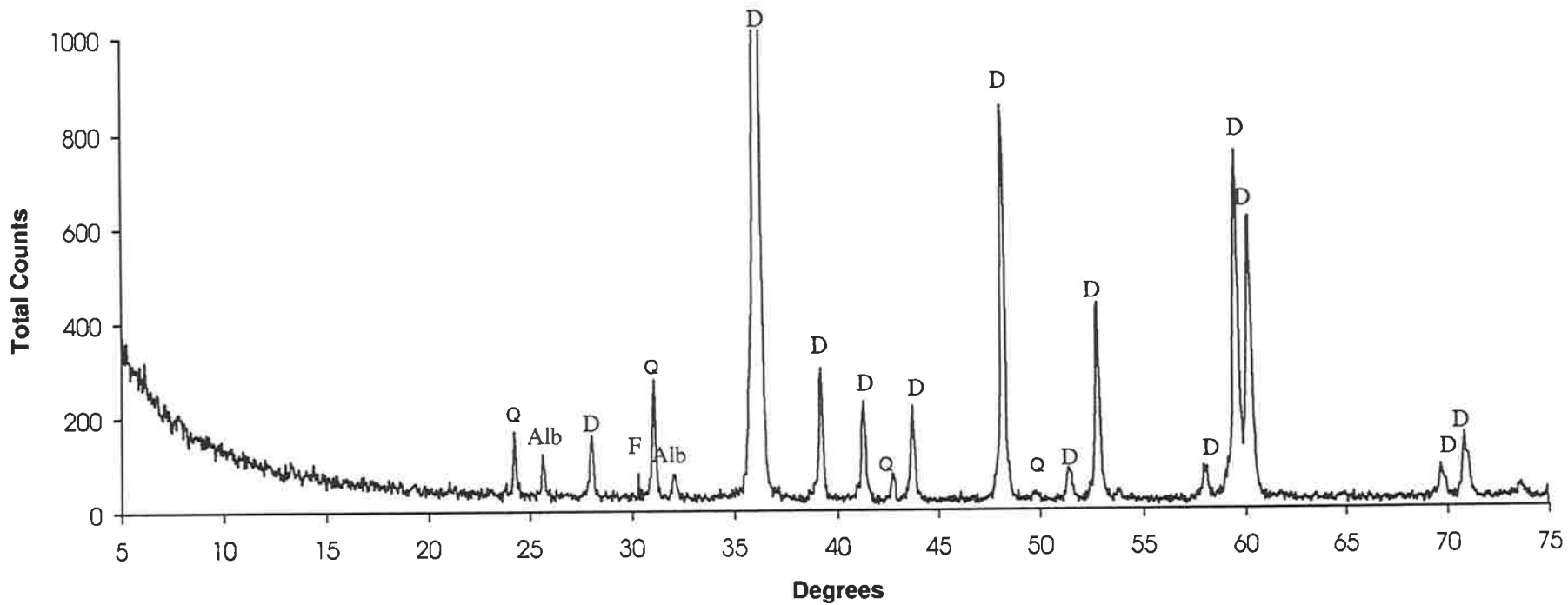
MARLA-3 (532.25 m)
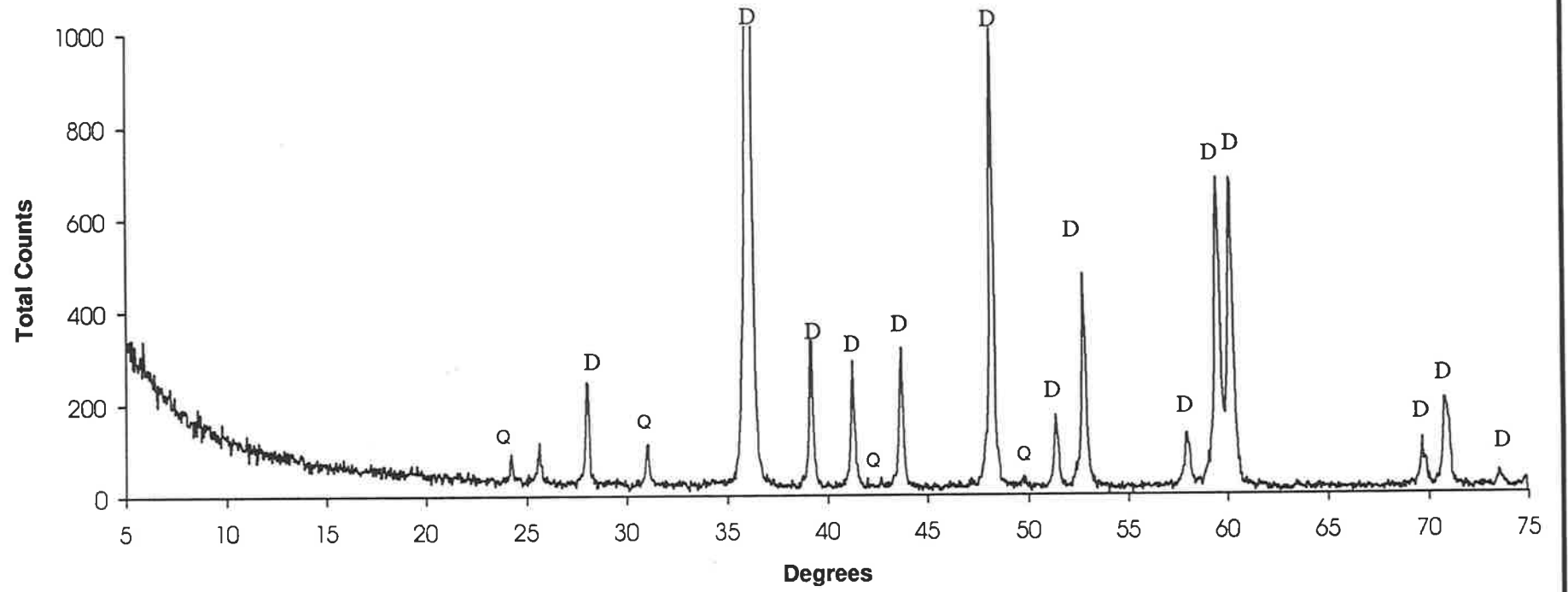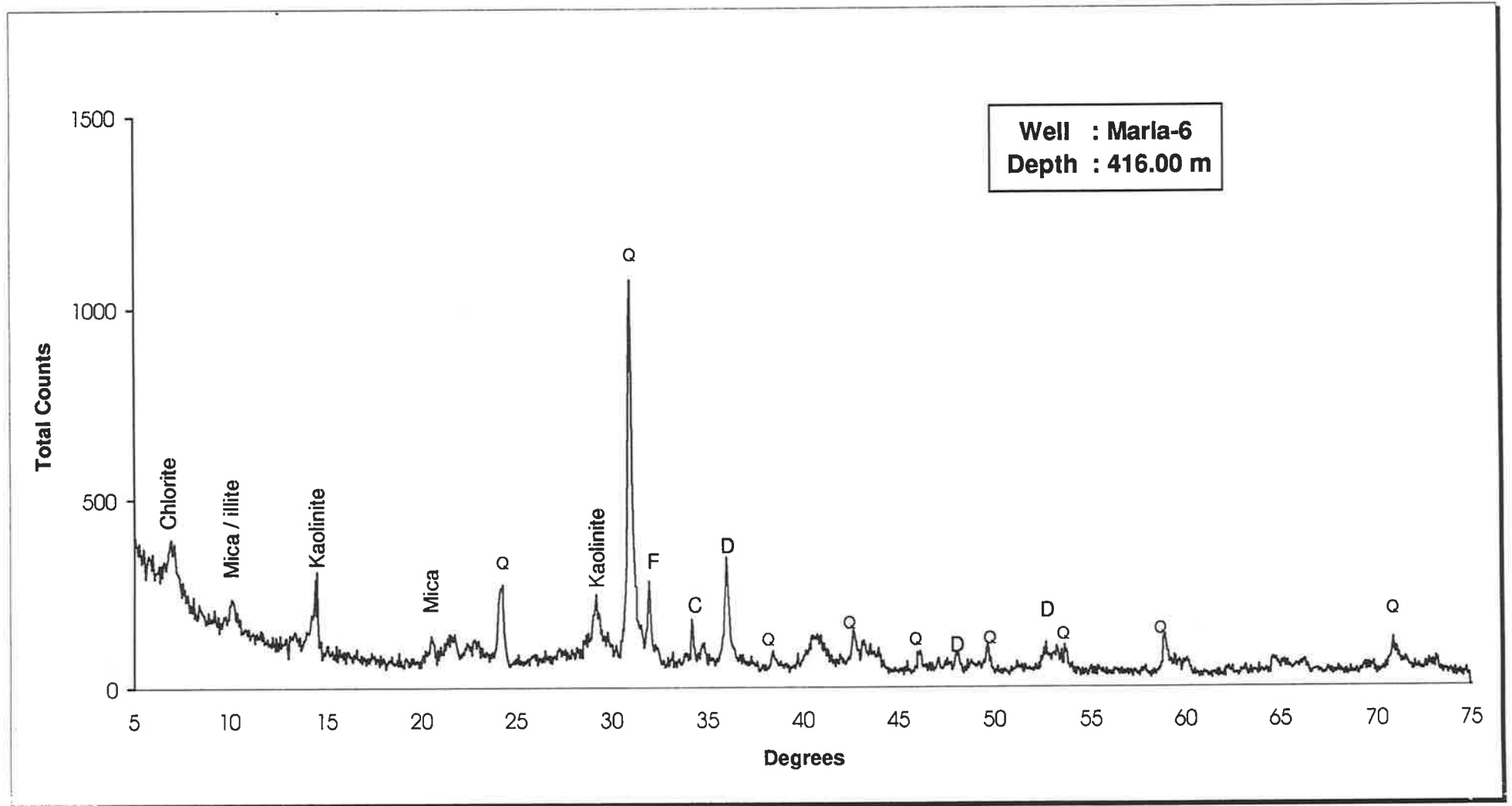
MARLA-6 (446.80 m)

MARLA-6 (602.80 m)
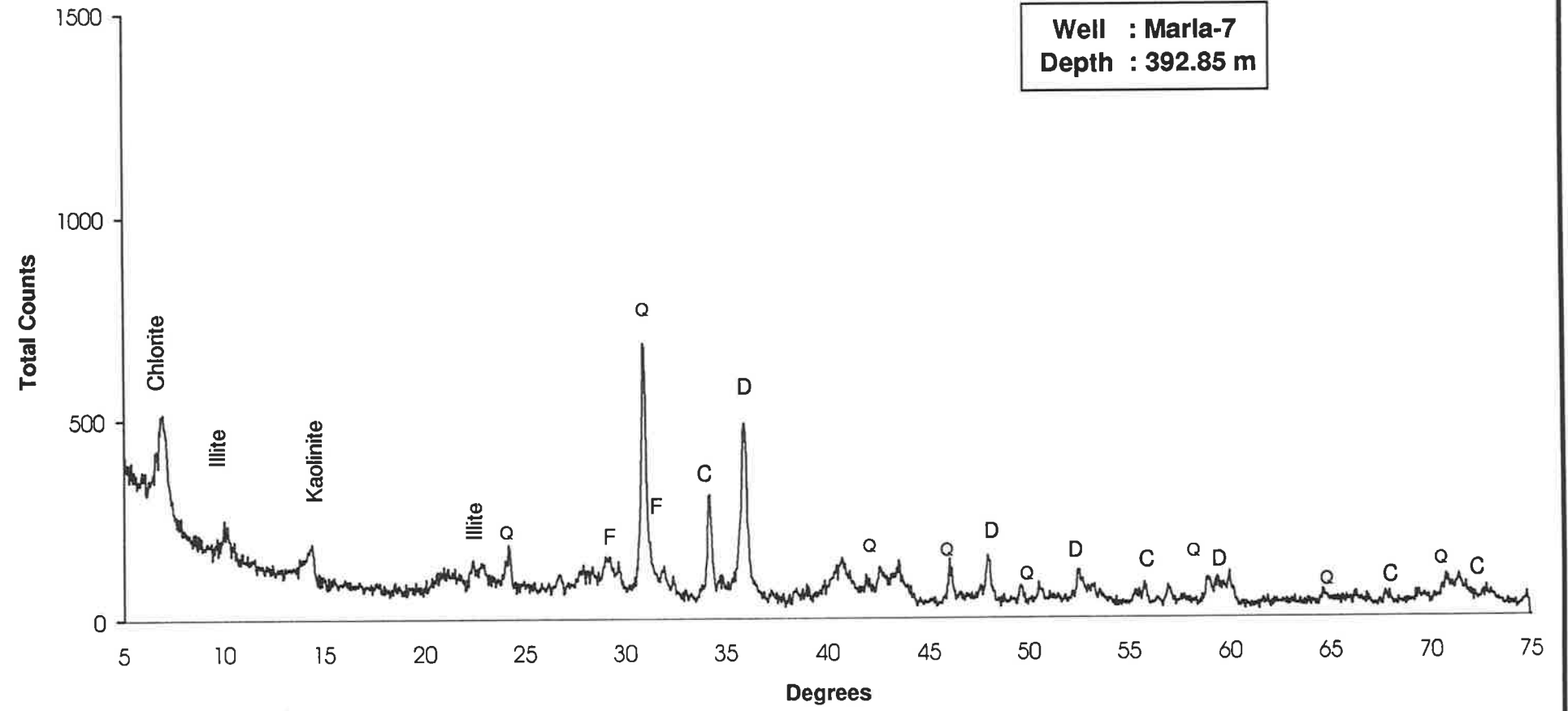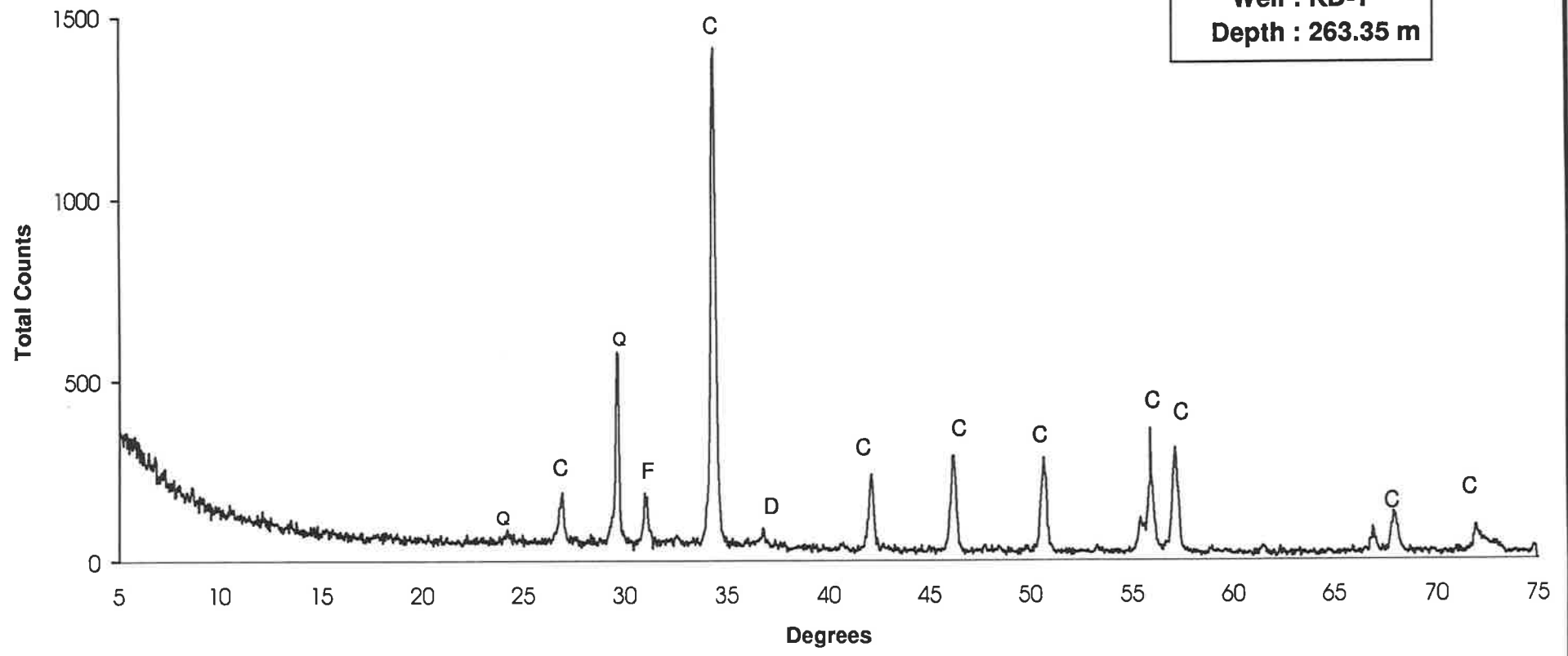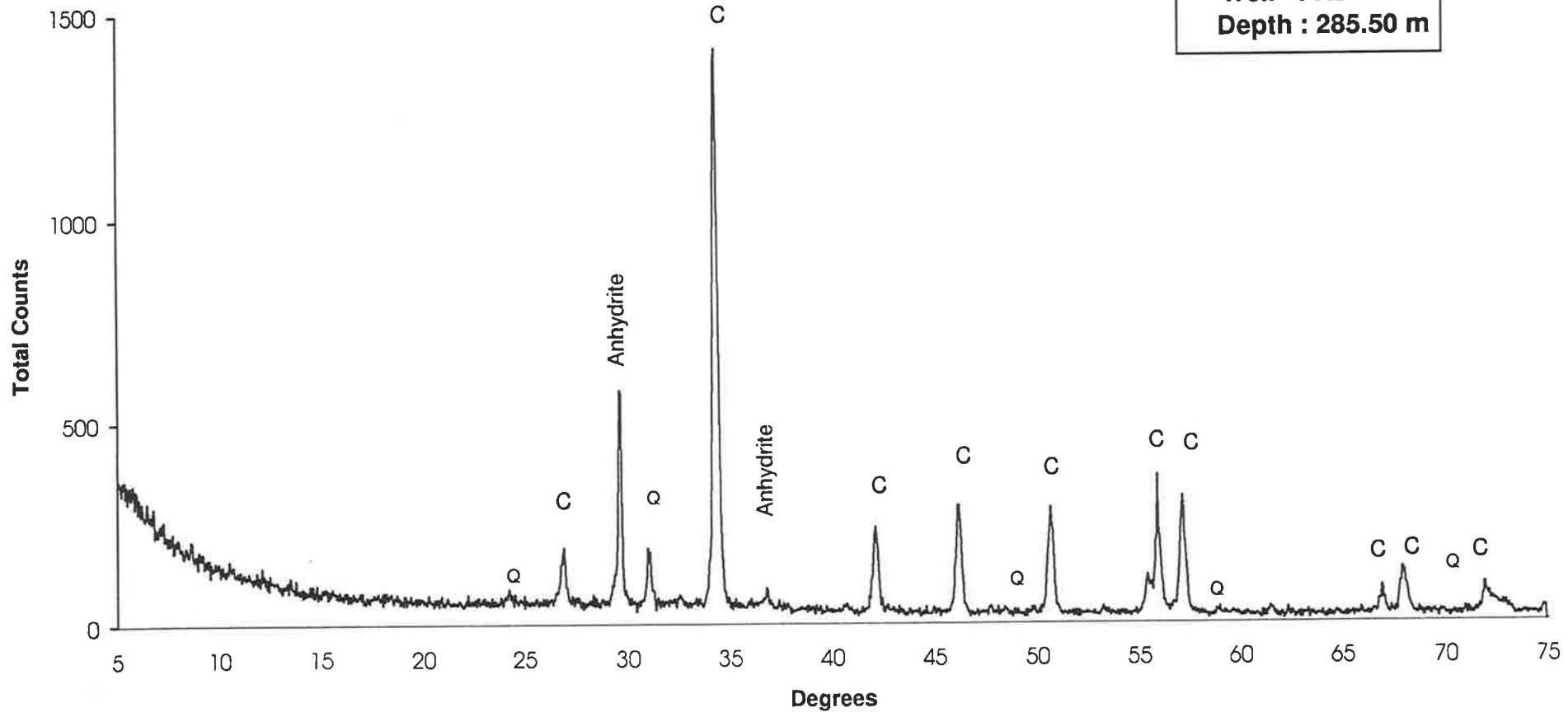
MARLA-6 (697.33 m)
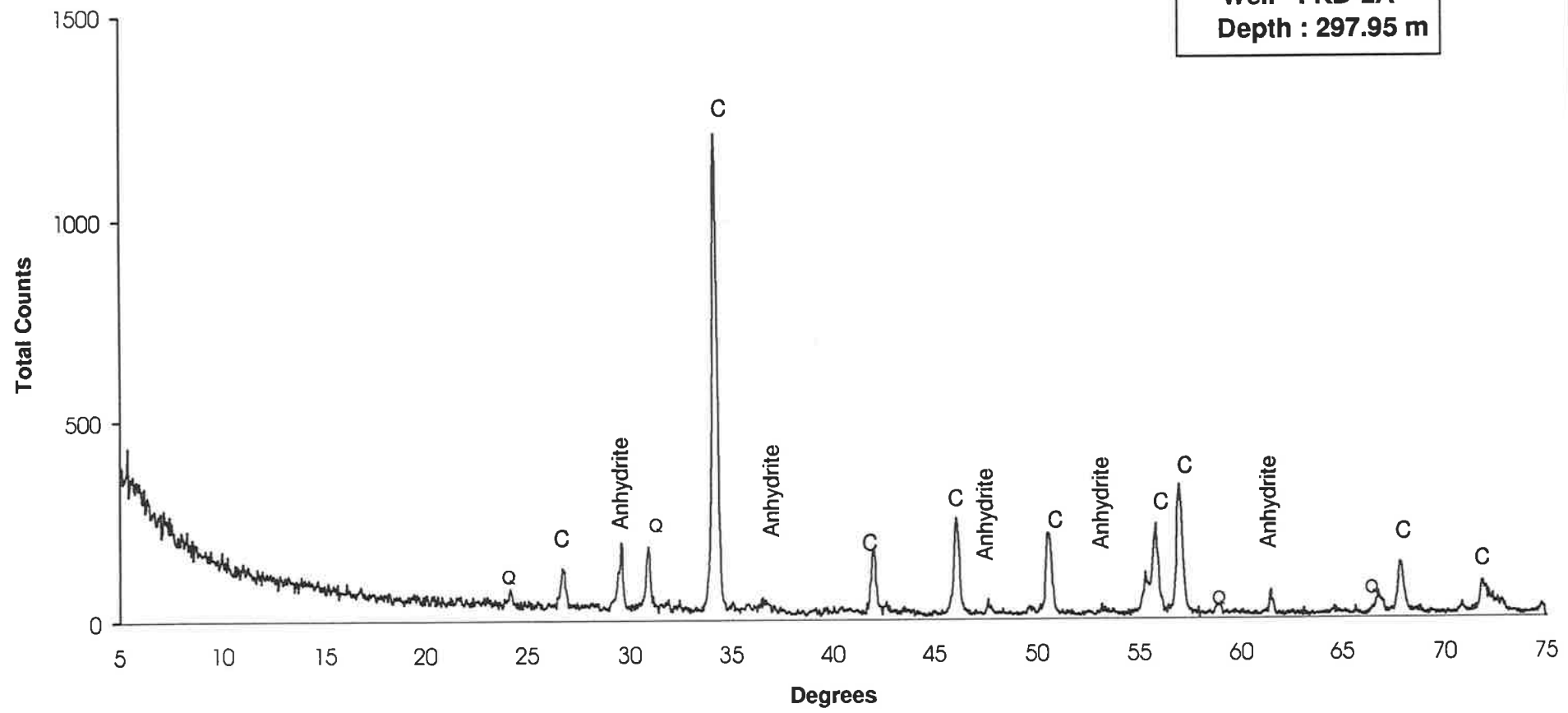
APPENDIX II

PETROGRAPHIC DESCRIPTIONS

OF RESERVOIR ROCKS

OULDBURRA FORMATION

OFFICER BASIN

CARBONATE PETROGRAPHIC DESCRIPTIONS

Well : Manya -3   Formation : Ouldburra
Depth : 192.70 m   Age   : Early Cambrian

Carbonate minerals	%	Skeletal components :
Calcite	5	
Dolomite	85	

Terrigenous minerals	%	Dolomitisation : Chiefly anhedral (0.2 mm)
Quartz		and subhedral (0.05 mm)
K feldspar		
Plagioclase		
Mica		
Others		

Other minerals	%	
Siderite		Compaction :
Anhydrite		
Gypsum		Porosity %
Halite		Primary (interparticle, shelter, intraparticle)
Chert		Secondary (vuggy, intercrystalline) ~10

Matrix	%	Rock name : Dolostone (mudstone)
Organic matter		

Comments : Vug-filling planar-e/euhedral dolomite exhibits zoning. The zoning character of this dolomite is attributable to at least three phases of dolomite generation from sea water with varying chemistry. Much of the porosity is related to original vugs however, there exists micro-intercrystalline porosity which is detected by using Scanning Electron Microscopy.

Well : Manya -3   Formation : Ouldburra
Depth : 213.60 m   Age   : Early Cambrian

Carbonate minerals	%	Skeletal components : Ghost ooid
Calcite	5	
Dolomite	90	

Terrigenous minerals	%	Dolomitisation : Chiefly anhedral (<0.2 mm)
Quartz		and euhedral (0.05 mm)
K feldspar		
Plagioclase		
Mica		
Others		

Other minerals	%	
Siderite		Compaction :

Anhydrite
Gypsum
Halite
Chert

Matrix   %
Organic matter

Porosity   %
Primary (interparticle, shelter, intraparticle)
Secondary (vuggy, intercrystalline)   3-5

Rock name : Dolostone (grainstone)

Well   : Manya -3
Depth   : 248.90 m

Formation : Ouldburra
Age   : Early Cambrian

Carbonate minerals	%
Calcite	10
Dolomite	82

Skeletal components : Ghost ooid

Terrigenous minerals	%
Quartz	3
K feldspar	2
Plagioclase	
Mica	
Others	

Dolomitisation   : Chiefly subhedral
and euhedral (<0.1 mm)

Roundness: Subrounded to rounded

Other minerals   %
Siderite
Anhydrite
Gypsum
Halite
Chert

Compaction :

Porosity   %
Primary (interparticle, shelter, intraparticle)
Secondary (intercrystalline, moldic)   <3

Matrix   %
Organic matter

Rock name : Dolostone (grainstone)

Comments : Relict limestone indicates partial replacement. Porosity has dramatically decreased by late vug-filling dolomite cement. The remaining moldic porosity seems to have no effective connectivity.

Well   : Manya -3
Depth   : 273.20 m

Formation : Ouldburra
Age   : Early Cambrian

Carbonate minerals	%
Calcite	4
Dolomite	>90

Skeletal components :

Terrigenous minerals	%
Quartz	1
K feldspar	
Plagioclase	

Dolomitisation   : Chiefly anhedral
(~0.2 mm)

Mica
Others

Other minerals	%		
Siderite		Compaction :	
Anhydrite			
Gypsum		Porosity	%
Halite		Primary (interparticle, shelter, intraparticle)	
Chert		Secondary (intercrystalline)	<3

Matrix	%	Rock name : Dolostone (mudstone)
Organic matter	trace	

Comments : Characteristic features include the presence of calcite veins running across the bedding and traces of bitumen residue associated with intercrystalline porosity.

Well   : Manya -3   Formation : Ouldburra
Depth : 685.90 m   Age   : Early Cambrian

Carbonate minerals	%	Skeletal components :
Calcite	5	
Dolomite	90	

Terrigenous minerals	%	Dolomitisation : Chiefly subhedral
(<0.062 mm)		
Quartz	1	
K feldspar		
Plagioclase		
Mica		
Others		

Other minerals	%		
Siderite		Compaction :	
Anhydrite			
Gypsum		Porosity	%
Halite		Primary (interparticle, shelter, intraparticle)	
Chert		Secondary (intercrystalline)	<3

Matrix	%	Rock name : Dolostone (mudstone)
Organic matter	~1	
Iron oxide	1	

Well   : Manya -3   Formation : Ouldburra
Depth : 795.80 m   Age   : Early Cambrian

Carbonate minerals	%	Skeletal components : Ooids
Calcite	6	

Dolomite	80	

Terrigenous minerals	%	Dolomitisation : Chiefly subhedral (<0.062 mm) and euhedral (0.08 mm)
Quartz	4	
K feldspar	3	
Plagioclase	1	
Mica		
Others		

Other minerals	%	
Siderite		Compaction : Solution seams
Anhydrite	1	
Gypsum	2	Porosity %
Halite		Primary (interparticle, shelter, intraparticle)
Chert		Secondary (intercrystalline, dissolution) <3

Matrix	%	Rock name: Dolostone (packstone to grainstone)
Organic matter		

Comments : Thin clastic bands occurring within dolomitic matrix contain evaporitic minerals (gypsum and anhydrite). Anhydrite is growing into silty mud and has partially replaced gypsum. Tepee and possible water escape structures are noticed. These indications may suggest that an evaporative mud flat environment existed during deposition.

Diagenesis: Early marine cements (dog-tooth spar) formed around ooid grains then silcification of the calcite cement was followed by ooid replacement by gypsum crystals which are arranged in a radial pattern extending from the edge of the ooid. This is analogous to fabrics found in carbonate ooids formed in hypersaline settings. Swallow tail-type gypsum is also recognised in interparticle spaces which is subsequently dissolved and replaced by anhydrite. Subsequently, pervasive dolomitisation of the limestone matrix together with calcite cement and partial gypsum dissolution resulted in secondary porosity (intercrystalline) generation. At later stages during burial, the rock suffered compaction which is reflected by microstylolite and/or solution seams parallel to bedding. These solution seams show evidence of hydrocarbon staining probably occurred when stylolites were active.

Well : Manya -6		Formation : Ouldburra
Depth : 652.30 m		Age : Early Cambrian

Carbonate minerals	%	Skeletal components : Few pellets and fossil fragments
Calcite	88	
Dolomite	<5	

Terrigenous minerals	%	Dolomitisation : Chiefly anhedral (<0.062 mm) and euhedral (0.03 mm)
Quartz	1	

K feldspar	<1		Compaction :High amplitude stylolite and
Plagioclase			solution seams
Mica	1		
Others			

Other minerals	%
Siderite	
Anhydrite	
Gypsum		Porosity	%
Halite		Primary (interparticle, shelter, intraparticle)
Chert		Secondary (dissolution)	<3

| Matrix | % | Rock name : Limestone (mudstone) |
| Organic matter | ~1 |

Comments : Fracture-fill calcite (~0.4 mm) coarsens towards the centre of cavity much in the same way as drusy calcite. These fractures are parallel and oblique to bedding and cross-cut solution seams and stylolites indicating that the calcite cement formed late diagenetically. Angular to subrounded quarts grains together with euhedral dolomite (~0.03 mm) occur within dissolution seams. Lithic limestone fragments are cemented by mosaic of calcite and rarely by dolomite cements. A few fossil fragments and peloids are scattered within the dolomitic matrix.

Well : Manya -6   Formation : Ouldburra
Depth : 661.10 m   Age   : Early Cambrian

Carbonate minerals	%	Skeletal components :
Calcite	2
Dolomite	92

Terrigenous minerals	%	Dolomitisation : Chiefly anhedral
Quartz	<2	subhedral (<0.02 mm) and euhedral (~0.03
mm)		
K feldspar		
Plagioclase		Grain size : 0.2 mm (mean)
		Roundness : Rounded to subrounded
Mica	<1	
Others		

Other minerals	%
Siderite		Compaction : Solution seams common
Anhydrite	
Gypsum		Porosity	%
Halite		Primary (interparticle, shelter, intraparticle)
Chert		Secondary (fracture, dissolution)	<3

| Matrix | % | Rock name : Dolostone (mudstone) |
| Organic matter | trace |

Comments: Rock exhibits stylolaminated structure. Clastic grains (quartz and potash feldspar) are commonly rounded to sub-rounded (~0.3 mm) and float in dolomite matrix. The fine grain quartz and euhedral dolomite are generally associated with solution seams. Porosity is low and presumably formed due to patrial dissolution of carbonate matrix and fracturing.

Well : Manya -6		Formation : Ouldburra
Depth : 683.60 m		Age : Early Cambrian

Carbonate minerals	%	Skeletal components :
Calcite	70	
Dolomite	2	

Terrigenous minerals	%	Dolomitisation : Chiefly subhedral
		(<0.062 mm) and euhedral (0.08 mm)
Quartz	10	
K feldspar	5	
Plagioclase	2	
Mica		
Others		

Other mineral %
Siderite
Anhydrite Compaction :
Gypsum Porosity %
Halite Primary (interparticle, shelter, intraparticle)
Chert Secondary (moldic, vuggy and dissolution) >10

Matrix % Rock name : Dolomitic sandy limestone
Organic matter (packstone)

Well : Manya -6		Formation : Ouldburra
Depth : 766.60 m		Age : Early Cambrian

Carbonate minerals	%	Skeletal components :
Calcite	8	
Dolomite	75	

Terrigenous minerals	%	Dolomitisation : Chiefly euhedral
		(<0.062 mm) and subhedral (<0.25 mm)
Quartz	4	
K feldspar	1	
Plagioclase	1	
Mica	2	
Others		

Other minerals %
Siderite Compaction : Stylolites

Anhydrite
Gypsum
Halite
Chert

Porosity		%
Primary (interparticle, shelter, intraparticle)		
Secondary (dissolution)		<8

Matrix	%
Organic matter	1

Rock name : Sandy dolomite (packstone)

Well : Manya -6
Depth : 874.65 m

Formation : Ouldburra
Age : Early Cambrian

Carbonate minerals	%
Calcite	2
Dolomite	85

Skeletal components : Ghost peloid

Terrigenous minerals	%

Dolomitisation : Chiefly anhedral, subhedral (<0.03 mm) and euhedral (~0.03 mm)

Quartz	2
K feldspar	
Plagioclase	
Mica	<1
Others	

Grain size : 0.03 mm (mean)

Other minerals	%
Siderite	
Anhydrite	
Gypsum	
Halite	
Chert	

Compaction : High amplitude stylolites (oil stained)

Porosity		%
Primary (interparticle, shelter, intraparticle)		
Secondary (dissolution)		>8

Matrix	%
Organic matter	1

Rock name : Dolostone (mudstone)

Well : Manya -6
Depth : 876.35 m

Formation : Ouldburra
Age : Early Cambrian

Carbonate minerals	%
Calcite	5
Dolomite	70

Skeletal components : Ghost peloid

Terrigenous minerals	%

Dolomitisation : Chiefly euhedral (<0.062 mm) and subhedral (<0.25 mm)

Quartz	3
K feldspar	1
Plagioclase	
Mica	
Others	

Other minerals	%	Compaction : Stylolites	
Siderite			
Anhydrite			
Gypsum		Porosity	%
Halite		Primary (interparticle, shelter, intraparticle)	
Chert		Secondary (dissolution)	>20

Matrix	%	Rock name : Dolostone (packstone to
Organic matter	1	grainstone)

Comments : Much of the secondary porosity has been generated through leaching of carbonate matrix by fluids (?meteoric) undersaturated with respect to $CaCO_3$ and $MgCO_3$. Hence, this dolomite unit is described to have excellent reservoir quality. The dark colour of the rock is attributable to the presence of organic matter (from kerogen maturation and dead oil).

Well : Manya -6	Formation : Ouldburra
Depth : 889.50 m	Age : Early Cambrian

Carbonate minerals	%	Skeletal components : Trilobite fragments
Calcite	85	
Dolomite	5	

Terrigenous minerals	%	Dolomitisation : Euhedral (<0.062
		mm) and subhedral (<0.25 mm)
Quartz	3	
K feldspar	1	
Plagioclase		
Mica		
Others		

Other minerals	%		
Siderite		Compaction : Stylolites are common	
Anhydrite			
Gypsum	1	Porosity	%
Halite		Primary (interparticle, shelter, intraparticle)	
Chert	1	Secondary (dissolution)	<3

Matrix	%	Rock name : Dolomitic sandy limestone
Organic matter	1	(packstone to grainstone)

Comments : Abundant trilobite fragments occur cemented within limestone matrix. Cavities are commonly rimmed by coarse crystalline and saddle dolomite exhibiting sweeping extinction under crossed nicols which is characteristic of cements formed at a high temperature. Associated with dolomite cement are megaquartz which coarsen to the centre of the cavity and also bitumen traces. Few gypsum crystals are found growing into small cavities. Rock has suffered chemical compaction resulting in the formation of stylolites that contain silt and possibly organic matter (kerogen).

Well : Manya -6
Depth : 896.46 m

Formation : Ouldburra
Age : Early Cambrian

Carbonate minerals	%
Calcite	85
Dolomite	8

Skeletal components :

Terrigenous minerals	%
Quartz	3
K feldspar	
Plagioclase	
Mica	
Others	

Dolomitisation : Subhedral (1-2 mm)

Other minerals	%
Siderite	1
Anhydrite	
Gypsum	
Halite	
Chert	

Compaction :

Porosity %
Primary (interparticle, shelter, intraparticle)
Secondary (dissolution) <3

Matrix	%
Organic matter	1

Rock name : Dolomitic limestone
(mudstone to packstone)

Comments : Saddle dolomite is very distinctive in this case and occurs as a cavity-filling cement which ranges in size from 1 to 2 mm and exhibits sweeping extinction under crossed nicols. This is overlaid by chalcedony lining margin of the cavity followed by large calcite crystals growing toward the centre of the cavity. At later stages of diagenesis due to prevailing dolomitisation calcite and chalcedony crystals are subjected to alteration. This is confirmed by using alizarin red S to discriminate between calcite and dolomite crystals. At the centre of cavity a rim of chalcedony crystals, fibrous in habit, indicates the second phase of diagenesis which postdates dolomitisation.

Well : Manya -6
Depth : 928.50 m

Formation : Ouldburra
Age : Early Cambrian

Carbonate minerals	%
Calcite	58
Dolomite	30

Skeletal components : Ghost ooid and fossil fragments

Terrigenous minerals	%
Quartz	3
K feldspar	1
Plagioclase	
Mica	
Others	

Dolomitisation : subhedral (~0.4 mm) and euhedral (~0.2 mm)

Compaction : High amplitude stylolites and solution seams are common

Other minerals	%
Siderite	

Anhydrite
Gypsum
Halite
Chert

		Porosity	%
		Primary (interparticle, shelter, intraparticle)	
		Secondary (dissolution)	5-8

Matrix	%
Organic matter	1

Rock name : Dolomitic sandy limestone (mudstone to packstone)

Well : Manya -6
Depth : 954.44 m

Formation : Ouldburra
Age : Early Cambrian

Carbonate minerals	%
Calcite	60
Dolomite	32

Skeletal components : Ghost ooid and fossil fragments

Terrigenous minerals	%
Quartz	2
K feldspar	
Plagioclase	
Mica	
Others	

Dolomitisation : Subhedral (<0.25 mm) and euhedral (<0.062 mm)

Other minerals	%
Siderite	
Anhydrite	

Compaction : Stylolites are common

Gypsum
Halite
Chert

		Porosity	%
		Primary (interparticle, shelter, intraparticle)	
		Secondary (dissolution)	~5

Matrix	%
Organic matter	1

Rock name : Dolomitic sandy limestone (mudstone to packstone)

Comments : Diagenetic path includes; partial replacement of limestone by dolomite followed by void-filling drusy calcite cement, hydrocarbon migration and stylolitisation during burial diagenesis. Relict limestone is red when stained with alizarin red S and the drusy calcite cement coarsens toward the cavity centre.

Well : Manya -6
Depth : 956.60 m

Formation : Ouldburra
Age : Early Cambrian

Carbonate minerals	%
Calcite	50
Dolomite	42

Skeletal components :

Terrigenous minerals	%
Quartz	
K feldspar	
Plagioclase	

Dolomitisation : Subhedral (>2 mm) and euhedral (<0. 2 mm)

Mica
Others

Other minerals	%	
Siderite		Compaction : Stylolites are common
Anhydrite		
Gypsum		Porosity %
Halite		Primary (interparticle, shelter, intraparticle)
Chert		Secondary (dissolution) 5-8

Matrix	%	Rock name : Dolomitic limestone
Organic matter	Trace	(wackstone to packstone)

Comments : Stromatactoid cavity-filling saddle dolomite is clean, white, ranges from 1 to 2 mm in size and exhibits sweeping extinction. Traces of hydrocarbon residue (dead oil) occur within intra-rhomb spaces probably suggesting formation of cement (saddle dolomite) from hydrocarbon migrating fluids.

Well   : Manya -6   Formation : Ouldburra
Depth : 1045.65 m   Age   : Early Cambrian

Carbonate minerals	%	Skeletal components : Sponge spicules,
pellets		
Calcite	82	
Dolomite	7	

Terrigenous minerals	%	Dolomitisation : Subhedral (<0.062 mm) and euhedral (<0.25 mm)
Quartz	4	
K feldspar	2	
Plagioclase		
Mica	1	
Others		

Other minerals	%	
Siderite		Compaction : Stylolites are common
Anhydrite		
Gypsum		Porosity %
Halite		Primary (interparticle, shelter, intraparticle)
Chert		Secondary (dissolution) <3

Matrix	%	Rock name : Dolomitic sandy limestone
Kaolinite	1	(mudstone)
Organic matter	Trace	

Comments : The presence of pellets together with sponge spicules within limestone matrix may suggest deeper water conditions and here is referred as maximum flooding surfaces in terms of sequence stratigraphy. Both monoaxon and triaxon spicules are identified which are commonly calcitic in nature. Sporadically distributed veins and voids are commonly

filled in with blocky calcite cement. Rock exhibits stylolaminated structure which reflects the degree to which the rock was compacted during burial.

Well : Manya -6   Formation : Ouldburra
Depth : 1056.23 m   Age   : Early Cambrian

Carbonate minerals	%
Calcite	80
Dolomite	7

Skeletal components : Trilobite fragments

Terrigenous minerals	%
Quartz	2
K feldspar	1
Plagioclase	
Mica	
Others	

Dolomitisation   : Subhedral (<0.25 mm)
and euhedral (<0.80 mm)

Other minerals	%
Siderite	
Anhydrite	
Gypsum	
Halite	
Chert	

Compaction :

Porosity	%
Primary (intraparticle)	1
Secondary (intercrystalline, vuggy)	5-8

Matrix	%
Kaolinite	1
Organic matter	Trace

Rock name : Dolomitic limestone (mudstone)

Comments : The presence of abundant trilobite fragments together with oncolites within limestone matrix may suggest shallow marine environment corresponding (subtidal) to transgressive systems tracts in terms of sequence stratigraphy. Oncoids and coated grains characterised by concentric rings and rarely with a core of quartz grain are common. Calcitisation (dedolomitisation) and geopetal infill noticed in this sample may suggest periodic exposure and oxidising conditions during diagenetic history.

Well : Manya -6   Formation : Ouldburra
Depth : 1178.75 m   Age   : Early Cambrian

Carbonate minerals	%
Calcite	33
Dolomite	29

Skeletal components :

Terrigenous minerals	%
Quartz	30
K feldspar	1
Plagioclase	2
Mica	1
Others	

Dolomitisation   : Subhedral (<1 mm)
and euhedral (<0.25 mm)

Grain size : 1.1 mm (mean)

Other minerals	%		Compaction : Stylolite parallel to bedding	
Siderite				
Anhydrite				
Gypsum			Porosity	%
Halite			Primary (intraparticle)	
Chert			Secondary (intercrystalline)	<3
Matrix	%		Rock name : Sandy dolomite (wackstone)	
Kaolinite	1			
Organic matter	>1			

Comments : Oil-stained stylolites appear to have acted as conduits for migrating hydrocarbon and contain euhedral dolomite cement plus detrital quartz. Occurrence of the euhedral dolomite and associated quartz seem to be strongly influenced by stylolites (pers. comm., John Warren, 1993). The Mg^{+2} required for the dolomitisation is thought to have either derived from the migrating hydrocarbon fluids or from basinal waters when stylolites were active. Diagenetically three types of dolomites are recognised. Type one dolomite (subhedral) formed early and shows planar fabric. Type two dolomite (euhedral) is concentrated in stylolites as mentioned before, whereas type three coarse crystalline-dolomite is clean and cross cuts stylolite suggesting a late diagenetic event. The early dolomite has partially and sporadically been calcitised (dedolomitised) indicating existence of oxidising conditions from time to time.

Well : Manya -6		Formation : Ouldburra	
Depth : 1234.95 m		Age : Early Cambrian	
Carbonate minerals	%	Skeletal components : Ghost ooids and lithic	
Calcite	78	fragments	
Dolomite	2		
Terrigenous minerals	%	Dolomitisation : Subhedral (~1 mm)	
Quartz	4		
K feldspar	2		
Plagioclase	<1	Grain size : 1.1 mm (mean)	
Mica	1		
Others			
Other minerals	%		
Siderite		Compaction : Stylolite parallel to bedding	
Anhydrite	trace		
Gypsum	<2	Porosity	%
Halite		Primary (intraparticle)	
Chert		Secondary (dissolution and moldic)	~10
Matrix	%	Rock name : Sandy limestone (wackstone)	
Kaolinite	1		
Organic matter			

Well : Manya -6   Formation : Ouldburra
Depth : 1298.15 m   Age   : Early Cambrian

Carbonate minerals	%
Calcite	5
Dolomite	>80

Skeletal components :

Terrigenous minerals	%
Quartz	3
K feldspar	1
Plagioclase	
Mica	
Others	

Dolomitisation   : subhedral (<0.1 mm)
and euhedral (<0.062 mm)

Grain size :

Other minerals	%
Siderite	
Anhydrite	
Gypsum	
Halite	
Chert	

Compaction : Stylolites are parallel
to bedding

Porosity	%
Primary (intraparticle)	
Secondary (intercrystalline)	>10

Matrix	%
Kaolinite	1
Organic matter	trace

Rock name : Dolostone (wackstone)

Comments: Thin bands of finely crystalline (<0.062 mm) sucrosic dolomite occur alternating with relatively coarse dolomite (<0.1 mm). Bitumen residue infill intra-rhomb spaces which is mainly associated with intercrystalline porosity.

Well : Manya -6   Formation : Ouldburra
Depth : 1359.16 m   Age   : Early Cambrian

Carbonate minerals	%
Calcite	5
Dolomite	75

Skeletal components :

Terrigenous minerals	%
Quartz	8
K feldspar	2
Plagioclase	
Mica	

Dolomitisation   : Subhedral to anhedral
(<0.062 to <0.1 mm)

Grain size : Silt size

Other minerals	%
Siderite	
Anhydrite	
Gypsum	
Halite	
Chert	

Compaction : Stylolites are parallel
to bedding

Porosity	%
Primary (intraparticle)	
Secondary (intercrystalline)	>10

Matrix	%	Rock name : Dolostone (wackstone)
Organic matter	trace	

Comments: Dolomite exhibits planar-s and non-planar fabric with straight extinction. In addition to intercrystalline porosity, partial dissolution of clastic components at grain contacts with dolomite crystals has led into further porosity enhancement.

Well : Manya -6
Depth : 1463.95 m

Formation : Ouldburra
Age : Early Cambrian

Carbonate minerals	%	Skeletal components :
Calcite	5	
Dolomite	75	

Terrigenous minerals	%	Dolomitisation : Subhedral to anhedral
Quartz	8	(<0.062 mm)
K feldspar	2	
Plagioclase		Grain size : Silt size
Mica		
Others		

Other minerals	%	Compaction :
Siderite		
Anhydrite		
Gypsum		Porosity	%
Halite		Primary (intraparticle)
Chert		Secondary (vuggy, intercrystalline)	8-
10		
Matrix	%	Rock name : Dolostone (wackstone)
Organic matter	trace	

Thin bands of finely crystalline (<0.062 mm) sucrosic dolomite occur alternating with relatively coarse dolomite (<0.1 mm). Bitumen residue infill intra-rhomb spaces which is mainly associated with vuggy and intercrystalline porosity.

Well : Manya -6
Depth : 1471.00 m

Formation : Ouldburra
Age : Early Cambrian

Carbonate minerals	%	Skeletal components :
Calcite	5	
Dolomite	70	

Terrigenous minerals	%	Dolomitisation : Subhedral to anhedral
Quartz	14	(<0.062 to 0.25 mm)
K feldspar	2	
Plagioclase		Grain size : Silt size
Mica		
Others		

Other minerals	%	Compaction :	
Siderite			
Anhydrite			
Gypsum		Porosity	%
Halite		Primary (intergranular)	4
Chert		Secondary (vuggy, intercrystalline)	~5

Matrix	%	Rock name : Sandy dolomite (wackstone)
Organic matter	trace	

Comments : Thin clastic layers with intergranular porosity occur within dolomitic matrix. Bitumen residue occurs both within quartz intergranular and dolomite intra-rhomb pore spaces.

Well : Marla -3		Formation : Ouldburra
Depth : 519.70 m		Age : Early Cambrian

Carbonate minerals	%	Skeletal components :
Calcite		
Dolomite	83	

Terrigenous minerals	%	Dolomitisation: Finely crystalline (<0.06 mm), anhedral is the dominant replacive dolomite and euhedral dolomite (0.06- <0.25 mm) occurs in subordinate amount.
Quartz	2	
K feldspar	1	
Plagioclase		
Mica		
Others		Compaction :

Other minerals	%		
Anhydrite	4		
Gypsum		Porosity	%
Halite		Primary (interparticle, shelter, intraparticle)	
Chert		Secondary (intercrystalline, vuggy)	10

Matrix	%	Rock name : Dolostone (mudstone to wackstone)

Comments : Dolomite is mainly replacive and has been formed due to intensive dolomitisation of precursor limestone resulting in intercrystalline and vuggy porosity. Medium size (<0.25 mm) dolomite shows zoning under cathodoluminescence.

Well : Marla -3		Formation : Ouldburra
Depth : 532.25 m		Age : Early Cambrian

Carbonate minerals	%	Skeletal components : Ooids and intraclasts

Calcite	3
Dolomite	85

Terrigenous minerals	%	Dolomitisation : Finely crystalline (<0.05 mm) mainly anhedral replacive dolomite with subordinate euhedral dolomite
Quartz		
K feldspar		
Plagioclase		
Mica		
Others		
		Compaction :
Other minerals	%	
Anhydrite	3	
Gypsum		Porosity %
Halite		Primary (interparticle, shelter, intraparticle)
Chert		Secondary (intercrystalline, vuggy) 8
Matrix	%	Rock name : Dolostone (grainstone)

Comments : Dolomite is replacive and exhibits mimic ooid reflecting ooid grainstone (limestone) origin. Porosity is mainly secondary formed largely by dolomitisation and, to lesser degree, by anhydrite dissolution.

Well : Marla -6		Formation : Ouldburra
Depth : 293.30 m		Age : Early Cambrian
Carbonate minerals	%	Skeletal components :
Calcite	10	
Dolomite	85	
Terrigenous minerals	%	Dolomitisation: Finely crystalline (<0.03 mm) Quartz mainly anhedral replacive dolomite with Subordinate euhedral dolomite(~0.03 mm)
Quartz		
K feldspar		
Plagioclase		
Mica		
Others		
		Compaction :
Other minerals	%	
Anhydrite		
Gypsum		Porosity %
Halite		Primary (interparticle, shelter, intraparticle)
Chert		Secondary (intercrystalline, vuggy) <5
Matrix	%	Rock name : Dolostone (mudstone)

Comments : Relict limestone occurs in minor amounts (stained with alizarin red S) indicating incomplete dolomitisation. Porosity is mainly intercrystalline.

Well : Marla -6
Depth : 308.30 m

Formation : Ouldburra
Age : Early Cambrian

Carbonate minerals	%
Calcite	10
Dolomite	82

Skeletal components :

Terrigenous minerals	%

Dolomitisation: Finely crystalline (<0.062mm) subhedral dolomite is dominant and euhedral dolomite (~0.8 mm) occurs in subordinate amounts

Quartz
K feldspar
Plagioclase
Mica
Others

Compaction :

Other minerals	%
Anhydrite	
Gypsum	
Halite	
Chert	

Porosity   %
Primary (interparticle, shelter, intraparticle)
Secondary (intercrystalline, vuggy)   <8

Matrix	%
Organic matter	trace

Rock name : Dolostone (mudstone)

Comments : Bitumen residue commonly fills in intra-rhomb spaces and small vug margins. Relict limestone patches were observed.

Well : Marla -6
Depth : 368.00 m

Formation : Ouldburra
Age : Early Cambrian

Carbonate minerals	%
Calcite	
Dolomite	78

Skeletal components :

Terrigenous minerals	%

Dolomitisation : Finely crystalline (<0.05 mm), mainly euhedral dolomite

Quartz	1
K feldspar	
Plagioclase	
Mica	
Others	

Compaction :

Other minerals	%		
Anhydrite			
Gypsum		Porosity	%
Halite		Primary (interparticle, shelter, intraparticle)	
Chert		Secondary (intercrystalline, vuggy)	>20

Matrix	%	Rock name : Sucrosic dolostone (mudstone)
Organic matter	1	

Comments : Dolomite crystals exhibit planar and euhedral fabric and have almost equal sizes. Such dolomite with intercrystalline porosity is also referred as sucrosic dolomite formed in supratidal (sabkha) type of environment which is also reflected by its carbon and oxygen isotope composition. Bitumen residue occurs in intra-rhomb spaces indicating hydrocarbon migration took place after dolomitisation.

Well : Marla -6   Formation : Ouldburra
Depth : 370.09 m   Age   : Early Cambrian

Carbonate minerals	%	Skeletal components :
Calcite	46	
Dolomite	45	

Terrigenous minerals	%	Dolomitisation : Finely crystalline
		(<0.025 mm), mainly euhedral dolomite
Quartz		
K feldspar		
Plagioclase		
Mica		
Others		
		Compaction :
Other minerals	%	
Anhydrite		
Gypsum		Porosity %
Halite		Primary (interparticle, shelter, intraparticle)
Chert		Secondary (intercrystalline, vuggy) 5-8

Matrix	%	Rock name : Dolomitic limestone (mudstone)
Organic matter	1	

Comments : Dolomite and limestone occur almost in equal amounts suggesting partial dolomitisation. Intercrystalline porosity is mainly associated with dolomitic part.

Well : Marla -6   Formation : Ouldburra
Depth : 376.00 m   Age   : Early Cambrian

Carbonate minerals	%	Skeletal components :
Calcite	4	
Dolomite	85	

Terrigenous minerals	%	Dolomitisation : Finely crystalline (<0.025 mm), mainly subhedral and euhedral dolomite

Quartz
K feldspar
Plagioclase
Mica
Others

Compaction :

Other minerals	%	
Anhydrite		
Gypsum		Porosity %
Halite		Primary (interparticle, shelter, intraparticle)
Chert		Secondary (intercrystalline, vuggy) ~10

Matrix	%	Rock name : Dolostone (mudstone)
Organic matter	1	

Comments : Relict limestone forms almost less than 5% of the total rock which is left due to incomplete dolomitisation. Bitumen residue occurs in intra-rhomb spaces associated with intercrystalline porosity

Well : Marla -6   Formation : Ouldburra
Depth : 377.38 m   Age   : Early Cambrian

Carbonate minerals	%	Skeletal components : Ooids
Calcite	3	
Dolomite	90	

Terrigenous minerals	%	Dolomitisation : Finely crystalline (<0.025 mm) xenotopic dolomite

Quartz	<1	
K feldspar		
Plagioclase		
Mica		
Others		

Compaction :

Other minerals	%	
Anhydrite		
Gypsum		Porosity %
Halite		Primary (interparticle, shelter, intraparticle)
Chert		Secondary (moldic, vuggy) ~5

Matrix	%	Rock name : Dolostone (grainstone)
Organic matter	1	

Comments : Characteristic features of this thin section include, mimic ooids, incomplete dolomitisation with vuggy and moldic porosity.

Well	: Marla -6		Formation : Ouldburra
Depth	: 437.35 m		Age : Early Cambrian

Carbonate minerals	%	Skeletal components :
Calcite	4	
Dolomite	90	

Terrigenous minerals	%	Dolomitisation : Finely crystalline (<0.025 mm), with euhedral to subhedral fabric

Quartz   <1
K feldspar
Plagioclase
Mica
Others

Compaction :

Other minerals	%
Anhydrite	
Gypsum	
Halite	
Chert	

Porosity   %
Primary (interparticle, shelter, intraparticle)
Secondary (micro-intercrystalline)   <3

Matrix	%
Organic matter	1

Rock name : Dolostone (mudstone)

Well	: Marla -6		Formation : Ouldburra
Depth	: 444.40 m		Age : Early Cambrian

Carbonate minerals	%	Skeletal components :
Calcite	2	
Dolomite	88	

Terrigenous minerals	%	Dolomitisation : Finely crystalline (<0.05 mm), with planar crystal boundaries

Quartz
K feldspar
Plagioclase
Mica
Others

Compaction :

Other minerals	%
Anhydrite	
Gypsum	
Halite	
Chert	

Porosity   %
Primary (interparticle, shelter, intraparticle)
Secondary (vuggy, intercrystalline)   >10

Matrix	%
Organic matter	<1

Rock name : Dolostone (mudstone)

Comments : Incomplete replacement is evident from relict limestone patches. Gypsum pseudomorph appears to have formed during early diagenesis suggesting supratidal environment at the time of deposition which is completely altered to calcite. Bitumen residue fills in intra-rhomb spaces indicating hydrocarbon migration occurred after dolomitisation.

Well : Marla -6   Formation : Ouldburra
Depth : 446.80 m   Age   : Early Cambrian

Carbonate minerals	%	Skeletal components :Ooids and intraclasts
Calcite	2	
Dolomite	86	

Terrigenous minerals	%
		Dolomitisation : Mainly anhedral (<0.25 mm) dolomite with subordinate subhedral (0.07 mm)
Quartz	2
K feldspar	
Plagioclase	
Mica	
Others	

Compaction :

Other minerals	%
Anhydrite	
Gypsum	
Halite	
Chert	

Porosity   %
Primary (interparticle, shelter, intraparticle)
Secondary (intercrystalline)   >10

Matrix	%	Rock name : Dolostone (packstone to grainstone)
Organic matter	<1	

Comments : Some quartz grains are etched at contact with dolomite crystals which could be either affected by highly alkaline fluids or gradual replacement by dolomite cement formed during burial diagenesis. Bitumen residue sparsely occupies intra-rhomb spaces.

Well : Marla -6   Formation : Ouldburra
Depth : 457.60 m   Age   : Early Cambrian

Carbonate minerals	%	Skeletal components :
Calcite	1	
Dolomite	79	

Terrigenous minerals	%
		Dolomitisation : Mainly subhedral (<0.062 mm) dolomite with subordinate euhedral (0.07 mm)
Quartz	
K feldspar	
Plagioclase	

Mica
Others

Compaction :

Other minerals   %
Anhydrite
Gypsum   Porosity   %
Halite   Primary (interparticle, shelter, intraparticle)
Chert   Secondary (intercrystalline)   >20

Matrix   %   Rock name : Dolostone (mudstone)
Organic matter   <1

Comments : Hydrocarbon staining is evident and is associated with abundant
intercrystalline porosity.

Well   : Marla -6   Formation : Ouldburra
Depth : 469.10 m   Age   : Early Cambrian

Carbonate minerals   %   Skeletal components :Ooids and intraclasts
Calcite   4
Dolomite   78

Terrigenous minerals   %   Dolomitisation   : Mainly subhedral
                                  (<0.062 mm) dolomite with subordinate
                                  euhedral (0.07 mm)

Quartz   8
K feldspar   5
Plagioclase
Mica
Others
                                  Compaction :

Other minerals   %
Anhydrite   <1
Gypsum   Porosity   %
Halite   Primary (interparticle, shelter, intraparticle)
Chert   Secondary (intercrystalline)   <3

Matrix   %   Rock name : Dolostone (packstone to grainstone)
Organic matter   <1

Comments : Characteristic features include the presence of burrow filled by silt and
anhydrite laths. The former clastic grains are thought to brought about by moving
organisms whereas the latter mineral is a diagenetic product. Mimic ooids and relict
limestone suggest oolitic limestone precursor.

Well   : Marla -6   Formation : Ouldburra
Depth : 496.12 m   Age   : Early Cambrian

Carbonate minerals	%	Skeletal components : Few ooids and
		intraclasts
Calcite	3	
Dolomite	94	

Terrigenous minerals	%	Dolomitisation : Mainly subhedral
		(0.2-0.5 mm) and anhedral (<0.2 mm)
		dolomite
Quartz		
K feldspar		
Plagioclase		
Mica		
Others		
		Compaction : Micro-stylolite

Other minerals	%	
Anhydrite		
Gypsum		Porosity %
Halite		Primary (interparticle, shelter, intraparticle)
Chert		Secondary (intercrystalline, vuggy) <3

Matrix	%	Rock name : Dolostone (wackstone to packstone)
Organic matter	<1	

Comments : Dolomite with subhedral to euhedral fabric exhibits zoning under cathodoluminescence. Alternating orange (calcium-rich and dark (iron-rich) zones may indicate changes in sea-water chemistry. Thin dark bands (micro-stylolite) with serrated margins, oriented parallel to bedding contain organic matter (?kerogen) concentrated through pressure solution phenomenon.

Well   : Marla -6   Formation : Ouldburra
Depth : 499.10 m   Age   : Early Cambrian

Carbonate minerals	%	Skeletal components : Ooid and intraclasts
Calcite	3	
Dolomite	87	

Terrigenous minerals	%	Dolomitisation: Mainly anhedral
		(<0.062 mm) and euhedral subhedral
Quartz		(<0.08 mm) and saddle dolomite (~1 mm)
K feldspar		
Plagioclase		
Mica		
Others		
		Compaction :

Other minerals	%	
Anhydrite		
Gypsum		Porosity %
Halite		Primary (interparticle, shelter, intraparticle)

Chert		Secondary (vuggy, intercrystalline)	>10

Matrix	%	Rock name : Dolostone (grainstone)
Organic matter	<1	

Comments : Petrographically this rock is characterised by dominant sugary-replacive dolomite, relict limestone, ghost ooid and the presence of coarse crystalline together with saddle dolomite occurring within vugs.

Well : Marla -6   Formation : Ouldburra
Depth : 510.14 m   Age   : Early Cambrian

Carbonate minerals	%	Skeletal components : Ooid and intraclasts
Calcite	3	
Dolomite	90	

Terrigenous minerals   %   Dolomitisation   : Euhedral to anhedral
Quartz   (0.2-0.5 mm) and coarse crystalline (<2 mm)
K feldspar
Plagioclase
Mica
Others
                                                    Compaction :

Other minerals   %
Anhydrite
Gypsum   Porosity   %
Halite   Primary (interparticle, shelter, intraparticle)
Chert   Secondary (intercrystalline, vuggy)   5-8

Matrix	%	Rock name : Dolostone (grainstone)
Organic matter	<1	

Well : Marla -6   Formation : Ouldburra
Depth : 519.10 m   Age   : Early Cambrian

Carbonate minerals	%	Skeletal components :
Calcite	3	
Dolomite	87	

Terrigenous minerals   %   Dolomitisation   : Chiefly anhedral
                                                    (<0.2 mm) with subordinate subhedral crystals
Quartz
K feldspar
Plagioclase   Compaction :

Mica
Others

Other minerals	%			
Anhydrite				
Gypsum		Porosity		%
Halite		Primary (interparticle, shelter, intraparticle)		
Chert		Secondary (vuggy, intercrystalline)		8-10
Matrix	%	Rock name : Dolostone (mudstone)		
Organic matter	<1			

Comments : Vuggy porosity is the dominant type and is often associated with bitumen residue. Solution seams, aligned parallel and anastomosing to bedding, also appear to contain bitumen residue left after hydrocarbon migration.

Well   : Marla -6   Formation : Ouldburra
Depth : 551.15 m   Age   : Early Cambrian

Carbonate minerals	%	Skeletal components : Ooids
Calcite	3	
Dolomite	76	

Terrigenous minerals	%	Dolomitisation : Chiefly anhedral (<0.042 mm) with subordinate void-filling subhedral (<1 mm) dolomite
Quartz	8	
K feldspar	2	
Plagioclase	2	
Mica		
Others		

Other minerals	%			
Siderite	3	Compaction : Solution seams		
Anhydrite				
Gypsum		Porosity		%
Halite		Primary (interparticle, shelter, intraparticle)		
Chert		Secondary (intercrystalline, dissolution		<6
Matrix	%	Rock name : Sandy dolomite (packstone to grainstone)		
Organic matter	<1			

Comments : Incomplete dolomitisation of early limestone is reflected by the presence of relict limestone and ghost ooids. Other features include void-filling coarse crystalline saddle dolomite with sweeping extinction and the presence of micro-stylolite and/or solution seams with associated dead oil. The clastic components include mainly immature quartz and microcline etched at grain contact with dolomite cement. Some clastic grains are surrounded by a thin rim which closely mimics quartz and feldspar overgrowths. However, in this case, the abundant inclusions in the outer rim allow recognition of volcanic source of these clastic grains from that of quartz overgrowths. Quartz overgrowth cements are normally inclusion free.

Well   : Marla -6   Formation : Ouldburra
Depth : 551.90 m   Age   : Early Cambrian

Carbonate minerals   %   Skeletal components : Minor ooids
Calcite   3
Dolomite   90

Terrigenous minerals   %   Dolomitisation   : Chiefly anhedral
                                       (<0.08 mm) with subordinate subhedral (<1
                                       mm)dolomite

Quartz   3
K feldspar   1
Plagioclase
Mica
Others
Other minerals   %
Siderite   Compaction : High amplitude stylolites
Anhydrite
Gypsum   Porosity   %
Halite   Primary (interparticle, shelter, intraparticle)
Chert   Secondary (intercrystalline)   <3

Matrix   %   Rock name : Sandy dolomite (packstone to
                                       grainstone)
Organic matter   <1

Comments : Some dolomite crystals (coarse crystalline) are calcitised (dedolomitised)
evident from alizarin red S staining. Another striking feature is the presence of high
amplitude stylolites which act as barrier to migrating fluids.

Well   : Marla -6   Formation : Ouldburra
Depth : 567.40 m   Age   : Early Cambrian

Carbonate minerals   %   Skeletal components : Minor ooids
Calcite   2
Dolomite   88

Terrigenous minerals   %   Dolomitisation   : Chiefly anhedral
                                       (<0.1 mm) with subordinate subhedral (<0.2
                                       mm)

Quartz
K feldspar
Plagioclase
Mica
Others

Other minerals   %
Siderite   Compaction : Micro-stylolites

Anhydrite
Gypsum
Halite
Chert

Porosity   %
Primary (interparticle, shelter, intraparticle)
Secondary (vuggy, intercrystalline)   >10

Matrix   %
Organic matter   <1

Rock name : Dolomite (mudstone to wackstone)

Comments : Oil residue is commonly associated with intercrystalline porosity and solution seams as well.   Calcitisation (dedolomitisation) seems to decrease remarkably with increasing depth, this may suggest that the fluids precipitated calcite, were not basinal but probably meteoric in origin otherwise this underlying unit would have been more affected by Calcitisation (dedolomitisation) with compare to the upper dolomite bed.

Well   : Marla -6

Formation : Ouldburra

Depth : 602.80 m

Age   : Early Cambrian

Carbonate minerals   %
Calcite   4
Dolomite   83

Skeletal components :

Terrigenous minerals   %

Dolomitisation   : Polymodal, chiefly anhedral (<0.2 mm) with subordinate subhedral (<0.3 mm) and euhedral (~0.2 mm) dolomite

Quartz   2
K feldspar   1
Plagioclase
Mica
Others

Other minerals   %
Siderite
Anhydrite
Gypsum
Halite
Chert

Compaction : Micro-stylolites

Porosity   %
Primary (interparticle, shelter, intraparticle)
Secondary (intercrystalline, vuggy)   ~10

Matrix   %
Organic matter   <1

Rock name : Dolomite (mudstone to wackstone)

Comments : The clastic components include mainly immature quartz and potash feldspar sporadically etched by dolomite cement at grains contact. The euhedral dolomite cement exhibits zoning under cathodoluminescence.   Bitumen residue concentrated in micro-stylolite is often associated with clastic grains.

Well : Marla -6		Formation : Ouldburra
Depth : 614.00 m		Age : Early Cambrian

Carbonate minerals	%	Skeletal components :
Calcite	4	
Dolomite	85	

Terrigenous minerals   %   Dolomitisation   : Polymodal, chiefly anhedral (<0.2 mm) with subordinate subhedral (<0.3 mm) and euhedral (~0.2 mm) dolomite

Quartz	2
K feldspar	1
Plagioclase	
Mica	
Others	

Other minerals	%	
Siderite		Compaction : Stylolites (low & high
amplitude)		
Anhydrite		
Gypsum		Porosity %
Halite		Primary (interparticle, shelter, intraparticle)
Chert		Secondary (vuggy) 5-8

Matrix	%	Rock name : Dolomite (mudstone to wackstone)
Organic matter	<1	

Well : Marla -6		Formation : Ouldburra
Depth : 648.10 m		Age : Early Cambrian

Carbonate minerals	%	Skeletal components : Ooids and intraclasts
Calcite		
Dolomite	88	

Terrigenous minerals   %   Dolomitisation   : Bimodal, chiefly anhedral (~0.2 mm) with cavity-filling subhedral (<1 mm) dolomite

Quartz	2
K feldspar	
Plagioclase	
Mica	
Others	

Other minerals	%	
Siderite		Compaction : Micro-stylolites
Anhydrite		
Gypsum		Porosity %
Halite		Primary (interparticle, shelter, intraparticle)

Chert		Secondary (vuggy, intercrystalline)	~10

Matrix	%	Rock name : Dolomite (grainstone)
Organic matter	<1	

Comments : Characteristic features of this unit include ghost ooids, absence of relict limestone indicating complete limestone (oolitic grainstone) replacement, and the presence of bitumen residue associated with vuggy and intercrystalline porosity. Reservoir quality tends to increase by generation of secondary porosity with depth at this interval. Micro-stylolites occur parallel to bedding. Some vug-filling euhedral dolomite exhibits zoning under cathodoluminescence.

Well : Marla -6 Formation : Ouldburra
Depth : 666.40 m Age : Early Cambrian

Carbonate minerals	%	Skeletal components :
Calcite		
Dolomite	78	

Terrigenous minerals	%	Dolomitisation: Chiefly subhedral and euhedral (0.4 mm) and anhedral (0.8 mm) dolomite
Quartz	2	
K feldspar		
Plagioclase		
Mica		
Others		

Other minerals	%	
Siderite		Compaction : Micro-stylolites
Anhydrite		
Gypsum		Porosity %
Halite		Primary (interparticle, shelter, intraparticle)
Chert		Secondary (vuggy, intercrystalline) ~20

Matrix	%	Rock name : Dolomite (mudstone)
Organic matter	<1	

Comments : Complete limestone replacement (early dolomitisation) and subsequent recrystallisation possibly during burial diagenesis resulted in further porosity enhancement. Hence, this unit exhibits excellent reservoir quality. Other striking features include the presence of common micro-stylolites, zoned vug-filling dolomite, calcitised (dedolomitised) traces and bitumen residue associated with intercrystalline porosity.

Well : Marla -7 Formation : Ouldburra
Depth : 330.15 m Age : Early Cambrian

Carbonate minerals	%	Skeletal components :

Calcite	3		
Dolomite	78		

Terrigenous minerals	%	Dolomitisation : Chiefly subhedral
		(<0.05 mm)
Quartz	3	
K feldspar	1	
Plagioclase		Roundness: Angular
Mica		Sorting: Well sorted

Others

Other minerals	%	
Siderite		Compaction : Micro-stylolites
Anhydrite		
Gypsum		Porosity %
Halite		Primary (interparticle, shelter, intraparticle)
Chert		Secondary (intercrystalline) ~15

Matrix	%	Rock name : Dolomite (mudstone)
Organic matter	<1	

Comments : Incomplete dolomitisation is evident from red limestone traces detected by using alizarin red S. Porosity is generally confined to thin interlaminated layers which is also stained by migrated hydrocarbons.

Well : Marla -7
Formation : Ouldburra
Depth : 342.30 m
Age : Early Cambrian

Carbonate minerals	%	Skeletal components : Ghost ooids and fossil
Calcite		fragments
Dolomite	78	

Terrigenous minerals	%	Dolomitisation : Chiefly subhedral
		(<0.05 mm)
Quartz	3	
K feldspar	1	
Plagioclase	1	
Mica		
Others		

Other minerals	%	
Siderite		Compaction : Micro-stylolites
Anhydrite		
Gypsum	1	Porosity %
Halite		Primary (interparticle, shelter, intraparticle)
Chert		Secondary (intercrystalline) ~15

Matrix	%	Rock name : Dolomite (grainstone)

Organic matter   <1

Comments : This dolostone unit is described by complete limestone replacement, mimic ooids and fossil fragments and recrystallisation of previously formed dolomite. A few gypsum crystals are found growing into cavities.

Well   : Marla -7   Formation : Ouldburra
Depth : 358.00 m   Age   : Early Cambrian

Carbonate minerals	%	Skeletal components :
Calcite	48	
Dolomite	42	

Terrigenous minerals	%	Dolomitisation : Chiefly euhedral (<0.05 mm) and subhedral (<0.025 mm)
Quartz		
K feldspar		
Plagioclase		
Mica		
Others		

Other minerals	%	
Siderite		Compaction :
Anhydrite		
Gypsum		Porosity %
Halite		Primary (interparticle, shelter, intraparticle)
Chert		Secondary (intercrystalline) ~10

Matrix	%	Rock name : Dolomitic limestone (mudstone)
Organic matter		

Comments : Dolomite is sugary in nature and has partially replaced precursor limestone.

Well   : Marla -7   Formation : Ouldburra
Depth : 437.80 m   Age   : Early Cambrian

Carbonate minerals	%	Skeletal components :
Calcite	10	
Dolomite	80	

Terrigenous minerals	%	Dolomitisation : Chiefly euhedral (~0.01 mm) and subhedral (<0.025 mm)
Quartz		
K feldspar		
Plagioclase		
Mica		
Others		

Other minerals	%

Siderite	Compaction :
Anhydrite	
Gypsum	Porosity %
Halite	Primary (interparticle, shelter, intraparticle)
Chert	Secondary (intercrystalline) ~10
Matrix %	Rock name : Dolostone (mudstone)
Organic matter	

Well   : Marla -7
Depth : 454.72 m

Formation : Ouldburra
Age   : Early Cambrian

Carbonate minerals	%	Skeletal components :
Calcite	4	
Dolomite	68	
Terrigenous minerals	%	Dolomitisation : Chiefly euhedral
		(<0.01 mm)
Quartz	2	
K feldspar	1	
Plagioclase		
Mica		
Others		
Other minerals	%	
Siderite		Compaction :
Anhydrite	5	
Gypsum	2	Porosity %
Halite	15	Primary (interparticle, shelter, intraparticle)
Chert		Secondary (intercrystalline) <3
Matrix	%	Rock name : Dolostone (mudstone)
Organic matter		

Comments : Dolomite has replaced a dense mudstone. Open horizontal spaces possibly formed due to fracturing are filled in by halite hoppers together with gypsum and anhydrite. The anhydrite is scattered in halite and often replaces early gypsum. This unit seems to have good seal potential.

Well   : Marla -7
Depth : 477.50 m

Formation : Ouldburra
Age   : Early Cambrian

Carbonate minerals	%	Skeletal components :
Calcite	4	
Dolomite	90	
Terrigenous minerals	%	Dolomitisation : Chiefly euhedral and
Quartz	2	subhedral (0.02-0.04 mm)

K feldspar	l
Plagioclase	
Mica	
Others	

Other minerals	%		Compaction :
Siderite			
Anhydrite			
Gypsum			Porosity	%
Halite			Primary (interparticle, shelter, intraparticle)	
Chert			Secondary (intercrystalline)	<3

| Matrix | % | | Rock name : Dolostone (mudstone) |
| Organic matter | | | |

Well : Marla -7 Formation : Ouldburra
Depth : 479.80 m Age : Early Cambrian

Carbonate minerals	%	Skeletal components :
Calcite	5	
Dolomite	91	

Terrigenous minerals	%		Dolomitisation : Chiefly euhedral
			(<0.05 mm) and subhedral (~0.01 mm)
Quartz	2		
K feldspar	l		
Plagioclase			
Mica	l		
Others			

Other minerals	%		
Siderite			
Anhydrite			Compaction :
Gypsum			Porosity	%
Halite			Primary (interparticle, shelter, intraparticle)	
Chert			Secondary (intercrystalline)	<3

Others	%		
Matrix	%		Rock name : Dolostone (mudstone)
Organic matter			

Comments : Biotite flakes aligned parallel to bedding are commonly concentrated in thin clastic layer interbedded with carbonate matrix. Traces of precursor limestone suggest incomplete dolomitisation.

Well : Marla -7 Formation : Ouldburra
Depth : 481.50 m Age : Early Cambrian

| Carbonate minerals | % | Skeletal components : |

Calcite	4
Dolomite	87

Terrigenous minerals	%	Dolomitisation : Chiefly euhedral (<0.25 mm) and subhedral (<0.05 mm)
Quartz	2	
K feldspar	1	
Plagioclase		
Mica	1	
Others		

Other minerals	%	
Siderite		Compaction : Solution seams
Anhydrite		
Gypsum		Porosity %
Halite		Primary (interparticle, shelter, intraparticle)
Chert		Secondary (vuggy, intercrystalline) 3-5

Matrix	%	Rock name : Dolostone (mudstone)
Organic matter		

Comments : Biotite flakes aligned parallel to bedding are commonly concentrated in thin clastic layer interbedded with carbonate matrix. Traces of precursor limestone within dolomite suggest incomplete dolomitisation.

Well : Marla -7 Formation : Ouldburra
Depth : 488.50 m Age : Early Cambrian

Carbonate minerals	%	Skeletal components :
Calcite	2	
Dolomite	88	

Terrigenous minerals	%	Dolomitisation : Chiefly subhedral (<0.062 mm)
Quartz	4	
K feldspar	2	
Plagioclase		
Mica		
Others		

Other minerals	%	
Siderite		Compaction : Stylolite are common
Anhydrite		
Gypsum		Porosity %
Halite		Primary (interparticle, shelter, intraparticle)
Chert		Secondary (intercrystalline) <3

Matrix	%	Rock name : Sandy dolostone (mudstone to
Organic matter	1	wackstone)

Comments : Thin clastic bands occur interbedding with carbonate matrix and contain organic matter (?bitumen residue) together with iron oxide.

SANDSTONE AND MIXED SILICICLASTIC/CARBONATE PETROGRAPHIC DESCRIPTIONS

Well : Manya-3   Formation : Ouldburra
Depth : 294.10   Age : Early Cambrian
Grain Size : 1.5 mm Max   Roundness : Subangular to rounded
           0.2 mm Min   Sorting : Moderately sorted

Composition :

Framework

Quartz	monocrystalline	45 %
	polycrystalline	5 %
Feldspar	plagioclase	1 %
	orthoclase, microcline	2 %
Micas		%
Rock fragments		%
Heavy minerals		%

Matrix

Clay	kaolinite	1 %
	illite	%
Silt		%
Micrite		%
Organic matter		%

Cement

Quartz	overgrowth	%
Feldspar	overgrowth	%
Calcite		6 %
Dolomite		28 %
Siderite		%
Anhydrite		%

Porosity :

Primary (intergranular, intragranular)		% 2	
Secondary	dissolution	% 8	
	fracture	%	Rock Type : Litharenite
	intercrystalline	% 2	

Comments: Clastic grains are cemented in mainly dolomite and to lesser degree in poikilotopic calcite cement. These grains show largely straight and point contacts however, concavo-convex contacts are rarely seen. Some quartz and feldspar grains acted as nuclei for ooids. In some areas, the feldspar grains show corroded edges in contact with dolomite suggesting dissolution by dolomitising fluids. Porosity is mainly secondary and appears to have generated by leaching of carbonate matrix, dolomitisation and feldspar dissolution.

Well	: Manya -6	Formation	: Ouldburra
Depth	: 842.20 m	Age	: Early Cambrian
Grain Size	: 1.5 mm Max	Roundness	: Subangular to rounded
	0.2 mm Min	Sorting	: Moderate

Composition :

Framework

Quartz	monocrystalline	44 %
	polycrystalline	4 %
Feldspar	plagioclase	2 %
	orthoclase, microcline	4 %
Micas		%
Rock fragments		%
Heavy minerals		%

Matrix

Clay	kaolinite	%
	illite	%
Silt		%
Micrite		%
Organic matter		%

Cement

Quartz	overgrowth	2 %
Feldspar	overgrowth	1 %
Calcite		10 %
Dolomite		3 %
Siderite		25 %
Anhydrite		%

Porosity :

Primary (intergranular, intragranular)		%	
Secondary	dissolution	<3 %	
	fracture	%	Rock Type : Litharenite
	intercrystalline		

Comments: Some quartz and feldspar grains are etched at grain edges by prevailing anhydrite cement. Rock cemented before compaction and replacing dolomite has a cross-cut relationship with other components indicating it to be a late cement. Minor porosity formed due to feldspar grain dissolution.

Well	: Manya-6	Formation	: Ouldburra
Depth	: 906.75 m	Age	: Early Cambrian
Grain Size	: 1.2 mm Max	Roundness	: Subangular to rounded
	0.1 mm Min	Sorting	: Moderately to well sorted

Composition :

Framework

Quartz	monocrystalline	60 %
	polycrystalline	2 %
Feldspar	plagioclase	1 %
	orthoclase, microcline	3 %
Micas		%

| Rock fragments | | | % |
| Heavy minerals | | | % |

Matrix

Clay	kaolinite		2 %
	illite		%
Silt			%
Micrite			%
Organic matter			%

Cement

Quartz	overgrowth		%
Feldspar	overgrowth		%
Calcite			%
Dolomite			9 %
Siderite			9 %
Anhydrite			2 %
Barite			1 %

Porosity :

Primary (intergranular, intragranular)		3 %	
Secondary	dissolution	7 %	
	fracture	%	Rock Type : Litharenite
	intercrystalline	%	

Comments: Majority of clastic grains are cemented by carbonate and anhydrite with few grains displaying point contacts. This may suggest that early cement formation prior to compaction. Anhydrite laths occur replacing calcite and dolomite which have already replaced quartz. Barite crystals characterised by square cleavage pattern are associated with anhydrite. Porosity is secondary and generated significantly by dissolution of carbonate and to a lesser degree by feldspar although, little intergranular porosity exists in quartz pore spaces.

N.B. Samples from depth intervals 912.50 m, 1035.05 m, 1165.85 m, 1180.90 m, 1187.75 m and 1248.86 m exhibit similar diagenetic history otherwise they have relatively lower porosity (4-8 %) and slightly variable quartz content.

Well	: Manya-6	Formation	: Ouldburra
Depth	: 1373.00 m	Age	: Early Cambrian
Grain Size	: 1.0 mm Max	Roundness	: Angular to subangular
	0.02 mm Min	Sorting	: Poorly to moderately sorted

Composition :

Framework

Quartz	monocrystalline		54 %
	polycrystalline		2 %
Feldspar	plagioclase		4 %
	orthoclase, microcline		2 %
Micas			4 %
Rock fragments			1 %
Heavy minerals			%
Pyrite			1 %

<u>Matrix</u>

Clay	kaolinite		2 %
	illite		%
Silt			%
Micrite			%
Organic matter			%

<u>Cement</u>

Quartz	overgrowth		%
Feldspar	overgrowth		%
Calcite			12 %
Dolomite			4 %
Siderite			%
Anhydrite			10 %
Gypsum			2 %

<u>Porosity</u> :

Primary (intergranular, intragranular)		1 %	
Secondary	dissolution	2 %	
	fracture	%	Rock Type : Litharenite
	intercrystalline	%	

Comments: Anhydrite, calcite and dolomite constitute the main cementing material. Anhydrite grows displacively into mud and rarely replaces quartz. Gypsum forms coated grains sometimes referred as oolitic growths which is characterised by a nucleus surrounded by numerous concentric and slightly eccentric rings of gypsum marked by brown bands of inclusions. These grains are presumably formed in agitated shallow marine water and transported distant. Most quartz grains are cemented prior to compaction and rarely exhibit straight or concavo-convex contacts.

An ephemeral mud flat environment may be inferred from alternating carbonate (mudstone) and clastic (silty sandstone) thin bands.

N.B. Sample from 1471.00 m depth is very similar to the one previously discussed.

Well : Manya-6		Formation	: Ouldburra
Depth : 1646.25 m		Age	: Early Cambrian
Grain Size : 0.8 mm Max		Roundness	: Subangular to rounded
0.1 mm Min		Sorting	: Moderately sorted

Composition :

<u>Framework</u>

Quartz	monocrystalline		63 %
	polycrystalline		2 %
Feldspar	plagioclase		4 %
	orthoclase, microcline		8 %
Micas			2 %
Rock fragments			%
Heavy minerals			1 %
Pyrite			1 %

<u>Matrix</u>

Clay	kaolinite		%
	illite		%

Silt			%
Micrite			%
Organic matter			%

Cement

Quartz	overgrowth		3 %
Feldspar	overgrowth		2 %
Calcite			Trace %
Dolomite			%
Siderite			%
Anhydrite			2 %
Gypsum			%

Porosity :

Primary (intergranular, intragranular)		4 %		
Secondary	dissolution	8 %		
	fracture	%	Rock Type : Sublitharenite	
	intercrystalline	%		

Comments: Sandstone and siltstone thin bands occur stacked one above the other. These bands are carbonate free and silty bands contain more mica flaks than sandy ones. Apparently, much of the present porosity is secondary and generated due to dissolution of carbonate cement and anhydrite by acidic fluids. Few quartz and feldspar grains are partially dissolved at grain contacts probably by more likely highly alkaline fluids associated with carbonate cement. Cementing materials include predominantly quartz and feldspar overgrowths plus minor amounts of pyrite and anhydrite and traces of calcite. Rock has undergone compaction which is reflected by straight and concavo-convex contacts observed in some quartz grains.

Well : Manya-6		Formation : Ouldburra	
Depth : 1676.75 m		Age : Early Cambrian	
Grain Size : 1.0 mm Max		Roundness : Subangular to rounded	
0.1 mm Min		Sorting : Moderately sorted	

Composition :

Framework

Quartz	monocrystalline		65 %
	polycrystalline		2 %
Feldspar	plagioclase		5 %
	orthoclase, microcline		6 %
Micas			1 %
Rock fragments			1 %
Heavy minerals			1 %
Pyrite			%

Matrix

Clay	kaolinite		%
	illite		%
Silt			%
Micrite			%
Organic matter			%

Cement

Quartz	overgrowth		2 %
Feldspar	overgrowth		<1 %
Calcite			Trace %
Dolomite			%
Siderite			%
Anhydrite			3 %
Gypsum			%

Porosity :

Primary (intergranular, intragranular)		4 %	
Secondary	dissolution	6 %	
	fracture	%	Rock Type : Sublitharenite
	intercrystalline	%	

Comments: Rock has been slightly affected by compaction because of early cementation which is also evident from straight and concavo-covex contacts shown by only a few quartz and feldspar grains. Secondary porosity has mainly developed due to dissolution of calcite cement and partial dissolution of quartz and feldspar. This is documented by the presence of traces of calcite in intergranular spaces and etching of clastics at grain margins.

Anhydrite seems to be diagenetic and grows into clastic grains replacing some feldspar and rarely quartz grains. In some instances, the anhydrite occupies pore spaces therefore, acting as a porosity-reducing agent. Traces of bitumen residue are found in intergranular pore spaces.

Well : Marla -3   Formation : Ouldburra
Depth : 557.60 m   Age   : Early Cambrian

Clastic grain size : 0.5 mm (mean)   Roundness : Angular to subangular

Carbonate minerals	%	Sorting : poorly to moderately sorted
Calcite	19	Skeletal components : Ooids and intraclasts
Dolomite	5	
Siderite	2	

Dolomitisation : Finely crystalline (<0.06 mm anhedral is the dominant replacive dolomite

Terrigenous minerals	%
and	
Quartz	48
K feldspar	4
Plagioclase	6
Mica	
Others	

euhedral dolomite (0.06- <0.25 mm) occurs in subordinate amount.

Cement :   %
Quartz overgrowths   2
Calcite overgrowths   2

Other minerals	%
Anhydrite	1
Gypsum	5
Halite	
Chert	
Zircon	trace

Porosity   %
Primary (interparticle, shelter, intraparticle)   2
Secondary (intercrystalline, vuggy)   2

Matrix
Clay (kaolinite)　　　　trace

Rock name : Mixed siliciclastic/carbonate
　　　　　　　　　(sublitharenite)

Organic matter　　　<1
Iron oxide　　　　　2

Comments : Alternating clastic and carbonate thin layers occur are separated by dark bands containing OM and iron oxide. Few quartz and plagioclase grains are fractured and filled with calcite , iron oxide and by traces of ?clay. Some quartz and feldspar grains show pitted margins indicating selective corrosion caused probably by more highly alkaline fluids. Elongated gypsum plates seem to be replaced by calcite. Clastic-replacing siderite appears to predate calcite and dolomite cements. Poikilotopic calcite cement, mimic ooids, cavity-filling spherulitic chalcedony (much in the same way as drusy calcite) and the presence of organic matter concentrated in solution seams are other conspicuous features of this mixed siliciclastic/carbonate unit. Intense silicification of precursor oolitic limestone may also suggest invasion of hot hydrothermal fluids operated during burial diagenesis.

Well　　: Marla-6
Depth　　: 486.36 m
Grain Size : 2.00　mm Max
　　　　　　0.05　mm Min

Formation　: Ouldburra
Age　　　　: Early Cambrian
Roundness　: Subangular to rounded
Sorting　　　: Poorly to moderately sorted

Composition :

Framework

Quartz	monocrystalline	65	%
	polycrystalline	2	%
Feldspar	plagioclase	5	%
	orthoclase, microcline	6	%
Micas			%
Rock fragments		1	%
Heavy minerals			%
Chert		1	%

Matrix

Clay	kaolinite		%
	illite		%
Silt		11	%
Micrite			%
Organic matter		1	%

Cement

Quartz	overgrowth		%
Feldspar	overgrowth		%
Calcite		4	%
Dolomite		2	%
Siderite			%
Anhydrite			%
Gypsum			%

Porosity :
Primary (intergranular, intragranular)　　　<1 %

Secondary	dissolution	1 %	
	fracture	%	Rock Type : Feldspathic litharenite
	intercrystalline		

Comments: Thin multiple layers of mixed siliciclastic/carbonate show coarsening upward character. Large pebble-sized quartz grains are cemented before compaction which is marked by the presence of pendant calcite cement formed in vadose zone. Porosity is low and presumably formed by carbonate cement dissolution.

Well : Marla-6   Formation : Ouldburra
Depth : 512.66 m   Age   : Early Cambrian
Grain Size : 0.2   mm Max   Roundness : Subangular to rounded
            0.05   mm Min   Sorting   : Poorly to moderately sorted

Composition :

Framework

Quartz	monocrystalline	77 %
	polycrystalline	3 %
Feldspar	plagioclase	5 %
	orthoclase, microcline	%
Micas		%
Rock fragments		%
Heavy minerals		%
Chert		11 %

Matrix

Clay	kaolinite	%
	illite	%
Silt		%
Micrite		%
Organic matter		%

Cement

Quartz	overgrowth	%
Feldspar	overgrowth	%
Calcite		3 %
Dolomite		1 %
Siderite		%
Anhydrite		%
Gypsum		%

Porosity :

Primary (intergranular, intragranular)		%	
Secondary	dissolution	%	
	fracture	%	Rock Type : Silicified ooid
	grainstone		(sublitharenite)
	intercrystalline		

Comments: This is an typical example of silica (chert) replacement of an oolitic limestone. Brownish colour is a result of numerous very small inclusions of water and air-filled

vacuoles within the chert structure and is typical of most chert. There is no visible porosity because of intensive silicification.

Diagenetic history of this sample is very similar to the sample from 697.33 m which will follow next in more detail.

Well : Marla-6   Formation : Ouldburra

Depth : 521.08 m   Age : Early Cambrian

Grain Size : 1.00 mm Max   Roundness : Subangular to subrounded

           0.02 mm Min   Sorting : Poorly sorted

Composition :

Framework

Quartz	monocrystalline	46 %
	polycrystalline	2 %
Feldspar	plagioclase	4 %
	orthoclase, microcline	3 %
Micas		2 %
Rock fragments		5 %
Heavy minerals		2 %
Chert		%

Matrix

Clay	kaolinite	%
	illite	%
Silt		17 %
Micrite		%
Organic matter		<1 %

Cement

Quartz	overgrowth	%
Feldspar	overgrowth	%
Calcite		8 %
Dolomite		5 %
Siderite		%
Anhydrite		%
Gypsum		%

Porosity :

Primary (intergranular, intragranular)		<1 %	
Secondary	dissolution	1 %	
	fracture	%	Rock Type : Litharenite
	intercrystalline		

Comments: Rock is thinly bedded with bands of silty and coarse-grained sandstone which occur one above the other suggesting periodic changes in sea level or in source supply. Fractured large quartz and feldspar grains are subsequently filled by calcite cement. Few dolomite rhombs are calcitised (dedolomitised) which is a late event. This may suggest that rock has been affected by oxidising fluids at some stage during burial.

N.B. Sample from 566.74 m depth is mineralogically almost similar to the previous discussed before. The only difference is the presence of solution seams stained by migrated hydrocarbons.

Well   : Marla-6
Depth   : 697.33 m
Grain Size : >2 mm Max
           0. 2 mm Min

Formation : Ouldburra
Age : Early Cambrian
Roundness : Subangular to rounded
Sorting : Poorly sorted

Composition :

Framework

Quartz	monocrystalline	41 %
	polycrystalline	2 %
Feldspar	plagioclase	5 %
	orthoclase, microcline	3 %
Micas		%
Rock fragments		12 %
Heavy minerals		%
Chert		%

Matrix

Clay	kaolinite	%
	illite	%
Silt		%
Micrite		%
Organic matter		1 %

Cement

Quartz	overgrowth	%
Feldspar	overgrowth	%
Calcite		12 %
Dolomite		17 %
Sphalerite		6 %
Anhydrite		1 %
Gypsum		%

Porosity :

Primary (intergranular, intragranular)		%
Secondary	dissolution	%
	fracture	%
	grainstone	
	intercrystalline	

Rock Type : Silicified ooid
(litharenite)

Comments : This sample provids significant information regarding digenetic history of the Ouldburra Formation carbonates. Diagenetic processes are schematically represented in Chapter Fig. 3.6.

Diagenesis commenced with marine calcite cement (pendant and/or meniscus) followed by leaching of some calcitic intraclasts giving rise to moldic porosity. This stage was followed by successive growth of isopachous, botryoidal and mammiliform calcite cements around the ooids. Subsequent chert replacement resulted in silicification of the ooids and the previously formed cements. At this stage the chert continued to grow on the early formed cements and into the cavity centre much in the same way as drusy calcite. Finally, sphalerite mineralisation possibly originated from hydrothermal sources postdates cross-cutting dolomite cement and partial grain dissolution. The presence of sphalerite was also confirmed by XRD analysis. Dark colour of sphalerite is commonly attributed to its higher iron content and formation at higher temperature (Deer et al., 1978). This view is in

accordance with higher levels of maturity measured from an organic-rich sample at the upper section from 671.5 m depth (VRcalc=1.68%).

Well : Marla-7	Formation	: Ouldburra
Depth : 422.33 m	Age	: Early Cambrian
Grain Size : 2.0 mm Max	Roundness	: Subangular to rounded
0.2 mm Min	Sorting	: Moderately sorted

Composition :

Framework

Quartz	monocrystalline	59 %
	polycrystalline	1 %
Feldspar	plagioclase	6 %
	orthoclase, microcline	3 %
Micas		%
Rock fragments		1 %
Heavy minerals		1 %
Chert		%

Matrix

Clay	kaolinite	%
	illite	%
Silt		2 %
Micrite		6 %
Organic matter		1 %

Cement

Quartz	overgrowth	1 %
Feldspar	overgrowth	%
Calcite		%
Dolomite		4 %
Anhydrite		5 %
Halite		10 %

Porosity :

Primary (intergranular, intragranular)		%	
Secondary	dissolution	%	
	fracture	%	Rock Type : Litharenite
	intercrystalline		

Comments: Sandstone is interbedded by thin about 1 mm thick silty layers. Clastic grains are floating in halite which is often cubic in habit and remains dark under crossed nicols. Gypsum appears as radiating elongate crystals replaced by displacively growing anhydrite. Dolomite is rarely replaced by anhydrite. Bitumen residue is also noticed within solution seams. No visible porosity was detected.

Samples from 463.16 m, 468.11 m and 470.13 m depth intervals have petrographic characteristics very similar to the previous sample.

Well   : Marla-7
Depth   : 474.34 m
Grain Size : 2.0   mm Max
           0. 2   mm Min

Formation   : Ouldburra
Age   : Early Cambrian
Roundness   : Subangular to rounded
Sorting   : Moderately sorted

Composition :
Framework

Quartz	monocrystalline	48 %
	polycrystalline	2 %
Feldspar	plagioclase	3 %
	orthoclase, microcline	2 %
Micas		%
Rock fragments		5 %
Heavy minerals		%
Chert		%

Matrix

Clay	kaolinite	%
	illite	%
Silt		1 %
Micrite		2 %
Organic matter		1 %

Cement

Quartz	overgrowth	2 %
Feldspar	overgrowth	%
Calcite		5 %
Dolomite		4 %
Anhydrite		10 %
Halite		%

Porosity :

Primary (intergranular, intragranular)		10 %	
Secondary	dissolution	5 %	
	fracture	%	Rock Type : Litharenite
	intercrystalline		

Comments: Rock cemented before compaction but, some grains are little affected by compaction during burial which is reflected by straight contacts and rare feldspar fracturing. It appears that considerable amount of intergranular porosity has been retained because of labile nature of the quartz grains. In addition to primary porosity, subsequent dissolution of carbonate cement and feldspar has led to further porosity enhancement. This is evident from pitted and honey-comb appearance of plagioclase and microcline grains.

Well   : Marla-7
Depth   : 488.50 m
Grain Size : 1.0   mm Max
           0. 1   mm Min

Formation   : Ouldburra
Age   : Early Cambrian
Roundness   : Subangular to rounded
Sorting   : Moderately sorted

Composition :
Framework

Quartz	monocrystalline	66 %
	polycrystalline	2 %
Feldspar	plagioclase	7 %
	orthoclase, microcline	2 %
Micas		1 %
Rock fragments		%
Heavy minerals		4 %
Chert		%

Matrix

Clay	kaolinite	1 %
	illite	%
Silt		4 %
Micrite		%
Organic matter		<1 %

Cement

Quartz	overgrowth	1 %
Feldspar	overgrowth	%
Calcite		4 %
Dolomite		4 %
Anhydrite		3 %
Halite		%

Porosity :

Primary (intergranular, intragranular)		%
Secondary	dissolution	4 %
	fracture	%	Rock Type : Feldspathic litharenite
	intercrystalline	

Comments: Rock exhibits banded structure and is characterised by alternate bands of clastic and micritic carbonate stacked one above the other. Muscovite flakes aligned within the clastic bands are parallel to bedding. Clastic components appear to have cemented before compaction because they do not exhibit any remarkable evidence of strain or stress at grain boundaries. However, rock has been subjected to compaction during burial which is reflected by hydrocarbon-stained solution seams. Some feldspar grains show evidence of dissolution and alteration to clay (kaolinite). In addition, dissolution of minor amounts of carbonate matrix and anhydrite resulted in secondary porosity generation to some extent.

N.B. Samples from 492.60 m and 496.78 m depth have slightly higher percent of porosity (5-8%) otherwise their petrographic characters are similar to the previous sample.

APPENDIX III

COLOUR AND BLACK & WHITE PLATES

OF THIN SECTIONS AND

SEM MICROGRAPHS

OULDBURRA FORMATION

OFFICER BASIN

a

0.25 mm

b

1 mm

c

0.3 mm

d

0.5 mm

e

0.5 mm

f

0.25 mm
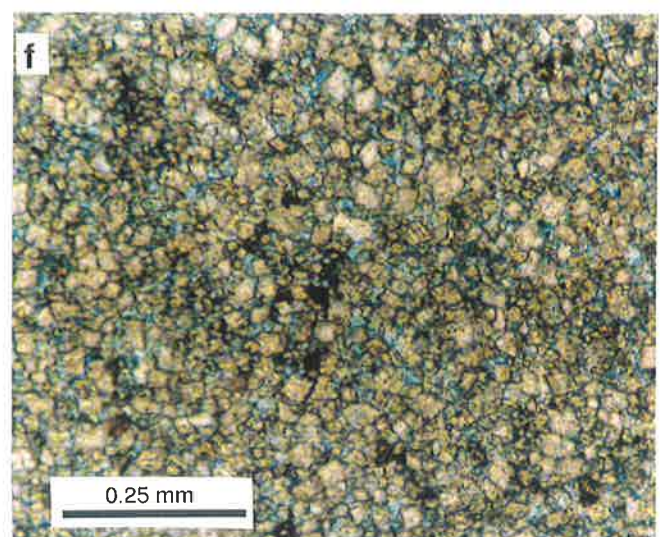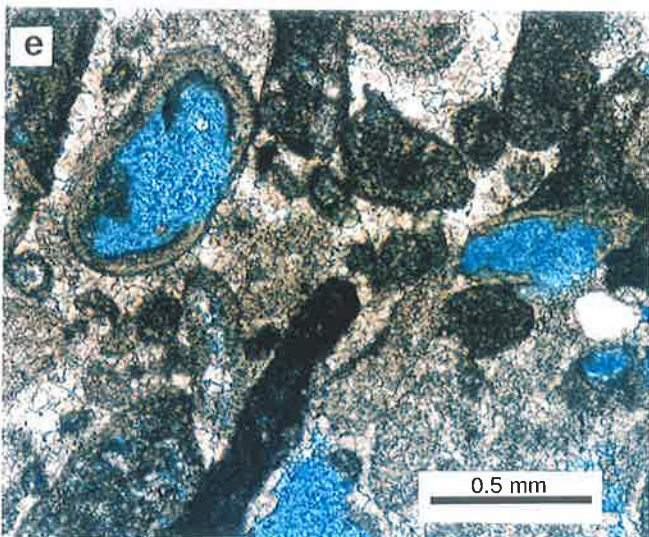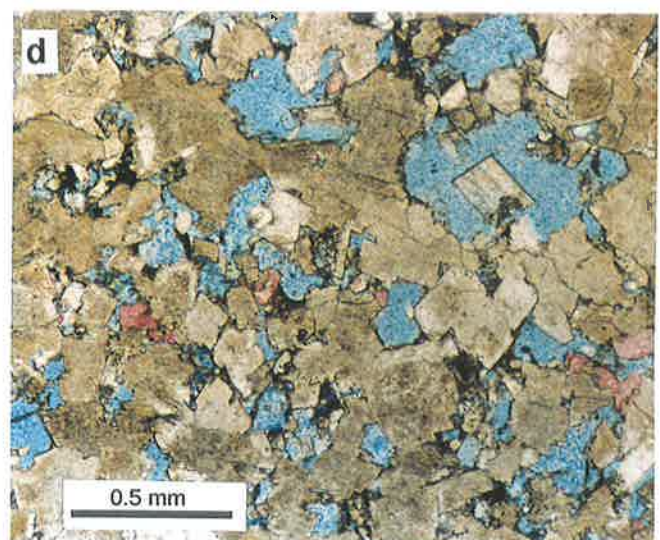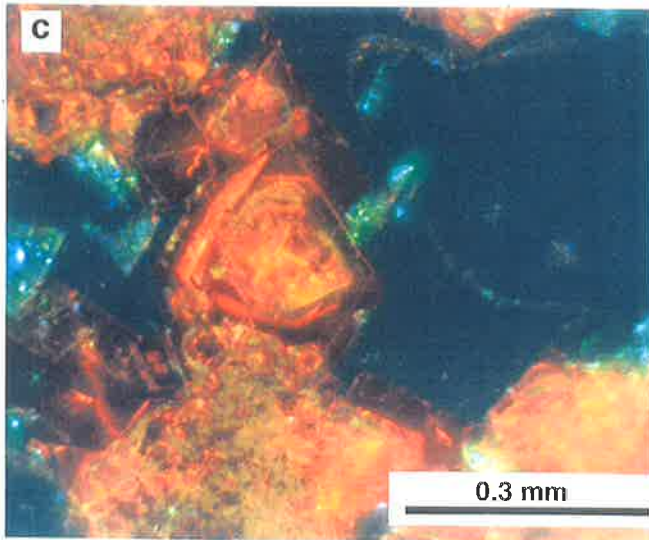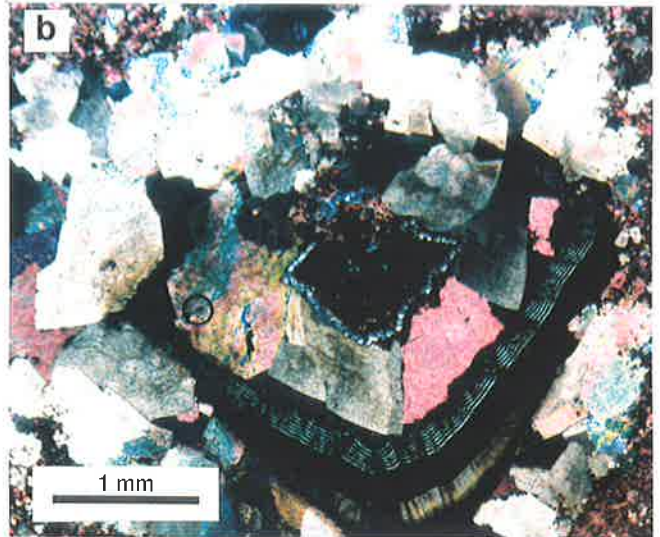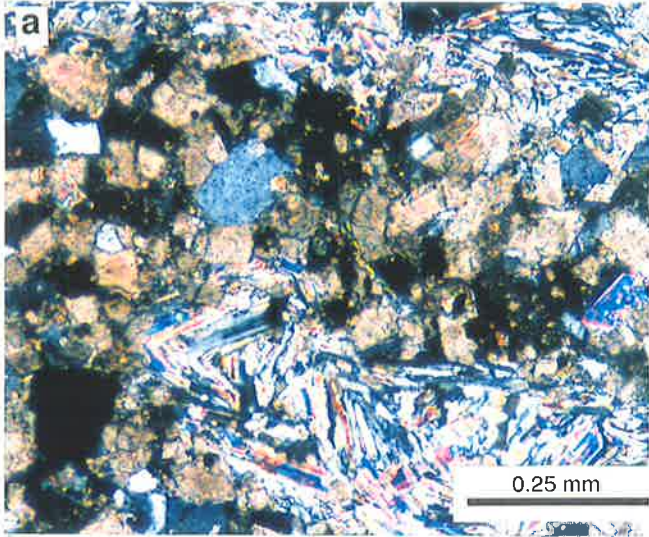
Plate 3.2

a) rank-II dolomite reservoir with a mixture of nonplanar polymodal and planar-s dolomite crystals.

b) rank-III dolomite reservoir showing moldic and intercrystalline porosity. Note the hydrocarbon residue coating the void.

c) rank IV anhedral xenotopic dolomite, no visible porosity.

d) hydrocarbon residue with solution seams associated with euhedral late cement dolomite.
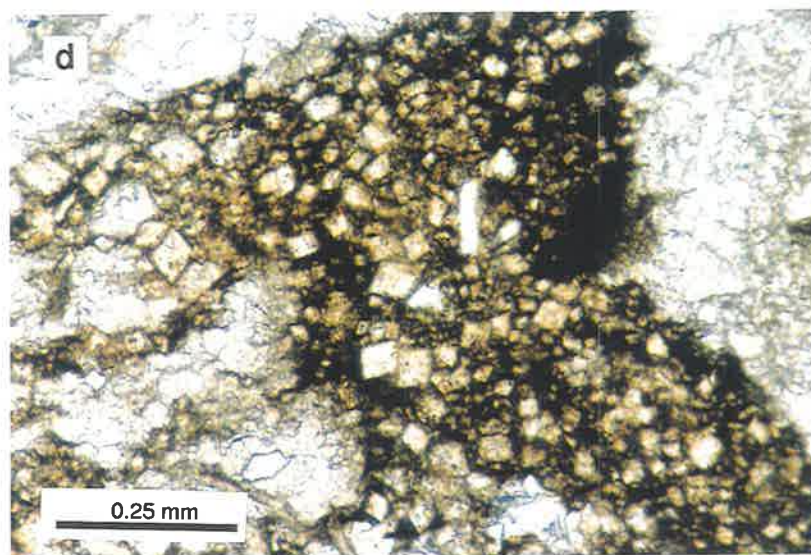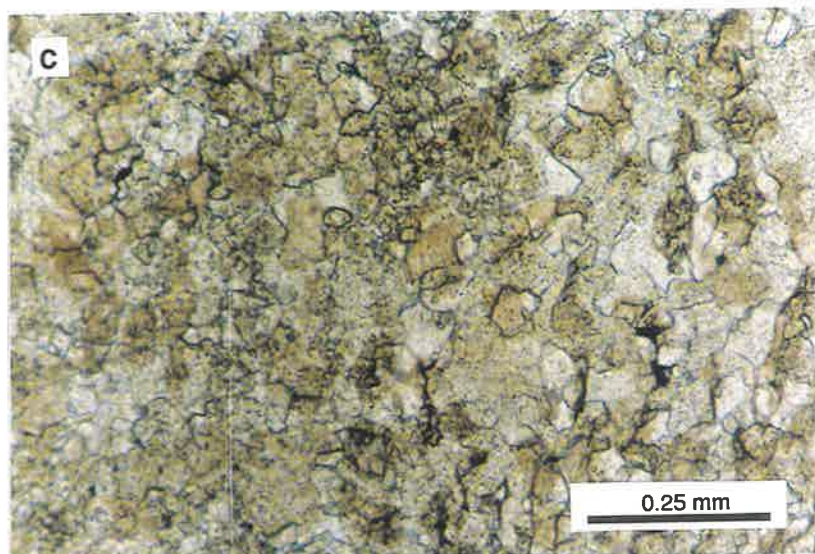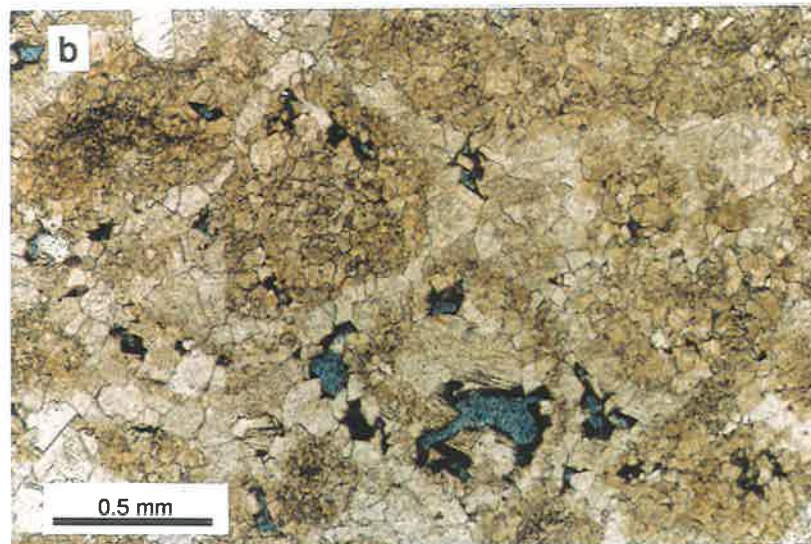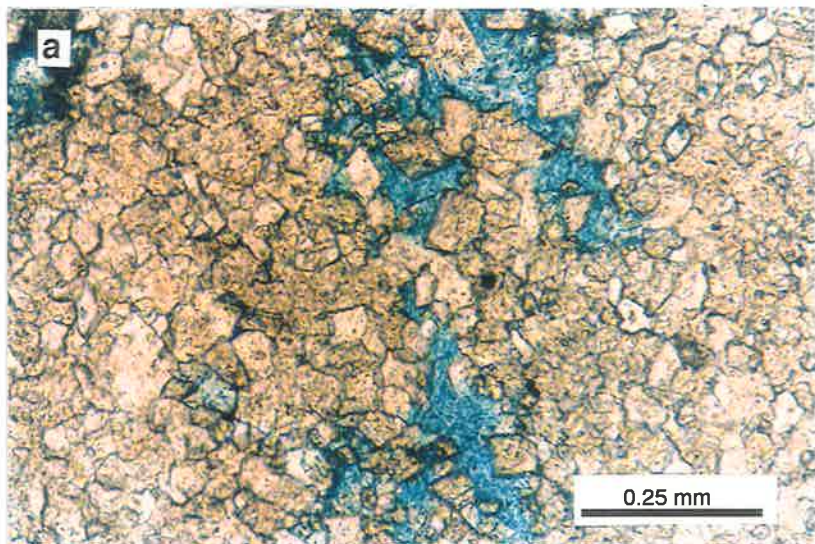
Plate 3.3

a) Dolostone, leached intraclastic peloid packstone classified as rank-I (excellent) dolomite reservoir.

b) Sucrosic dolomite with excellent reservoir characteristics.

c) Dolomitic limestone with abundant sutured-stylolites, relatively low amplitude, aligned parallel to bedding. Minor local fractures postdate stylolites.

d) Leached dolomite zone showing vuggy porosity and high amplitude stylolites with fractures.

5 cm

0

MANYA-6
880.00 m

a

5 cm

0

MARLA-6
368.30 m

b

MARLA-7
295.00 m

0 cm 5

c

MARLA-7
498.90 m

0 cm 5

d

Plate 3.4

a) Mixed siliciclastic / carbonate unit showing common anhydrite and potash feldspar cements. Large lath-shaped anhydrite grows into mud displacively suggesting deposition in evaporative mud flat environment (Manya-6, 1180.90 m).

b) Potash feldspar shown at centre, is the most common mineral associated with anhydrite and gypsum. Microporosity (secondary) formed due to partial anhydrite dissolution (Manya-6, 1180.90 m).

c) Dolomitic thin layers within mixed siliciclastic / carbonate unit, have significant intercrystalline porosity (Manya-6, 906.75 m).

d) The lath-shaped anhydrite cement, shown at bottom left, occurs within fine crystalline dolomite. Secondary porosity is generated by dolomitisation and partial anhydrite dissolution (Manya-6, 906.75 m).

e) Dolomite (mudstone to packstone) with intercrystalline and vuggy porosity (Marla-3, 519.70 m).

f) Coarse calcite crystal shown at centre, occurs as a late burial cement which shows etching at the edge caused by corrosive basinal fluids (Marla-3, 519.70 m).

g) The dolomitised ooid grains (ooid grainstone) have relatively higher porosity at grain contact (Marla-3, 519.70 m).

h) Same as g but zoomed. Substantial microporosity exists in intra-rhomb spaces.

a

b
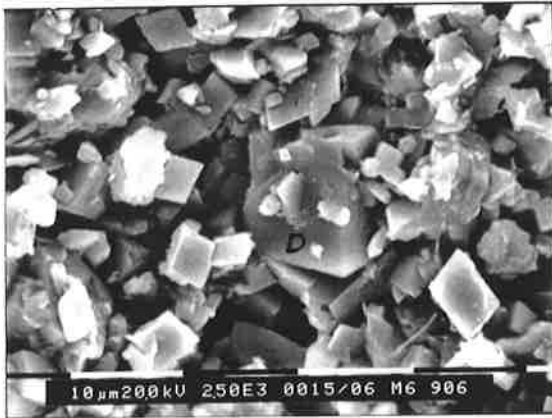
c

d
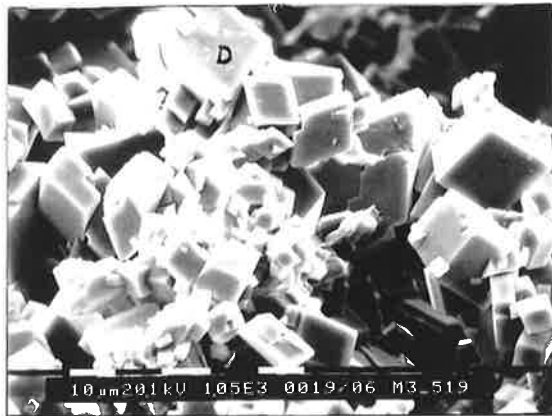
e

f
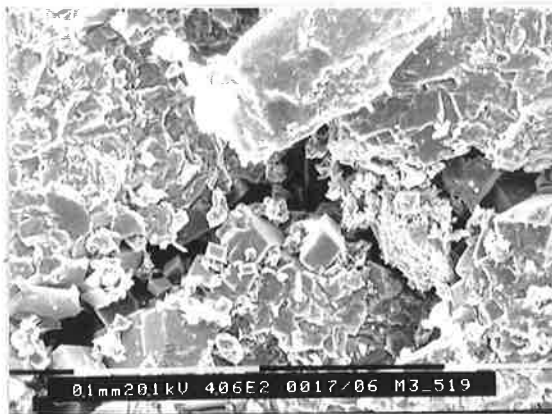
g
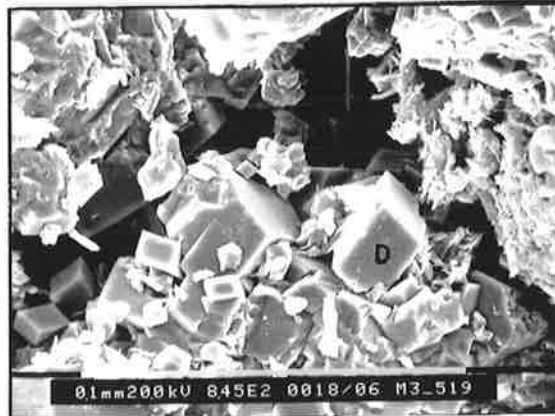
h

Plate 6.1

a) Sandstone with common anhydrite and minor dolomite cements. Anhydrite crystals are squeezed in between clastic grains which exhibit tangential contacts due to compaction. Subsequent partial anhydrite dissolution gave rise to minor amount of microporosity, plane polarised light, Manya-6 (1165.85 m).

b) Same as (a) under crossed nicols.

c) Sandstone exhibiting concavo-convex contacts and a thin rim of quartz overgrowth shown by arrows. Only minor amounts of porosity formed due to anhydrite and dolomite dissolution. Spherical grain with high relief is zircon, plane polarised light, Manya-6 (1180.90 m).

d) Same as (c) under crossed nicols.

e) A mixed siliciclastic/carbonate bed with porosity >15 % (stained blue), consists of quartz, feldspar and dolomite. Secondary porosity generated mainly by carbonate matrix dissolution, plane polarised light, Manya-6 (1471.00 m).

f) Same as (e) under crossed nicols.

g) Sandstone (sublitharenite) with bitumen residue infilling inter- and intragranular pore spaces. No other types of cement except minor quartz overgrowth and traces of calcite. Minor amounts of porosity generated by feldspar dissolution (shown by arrows), Manya-6 (1676.75 m).

h) Same as (g) under crossed nicols.
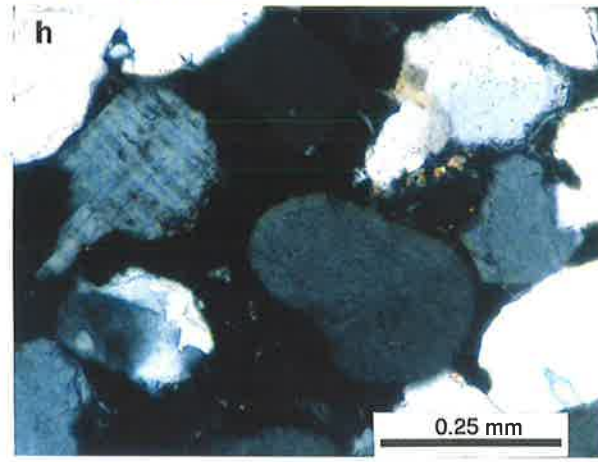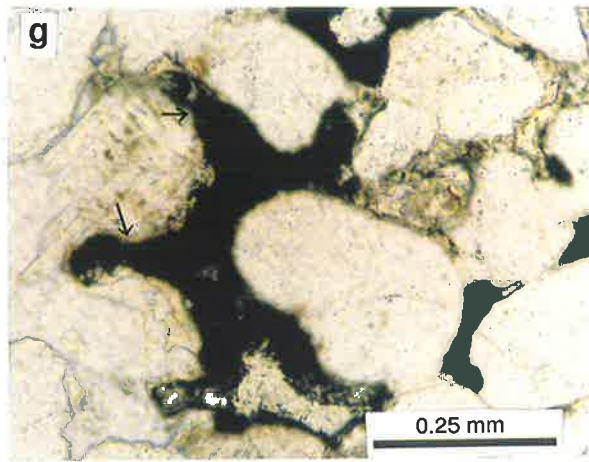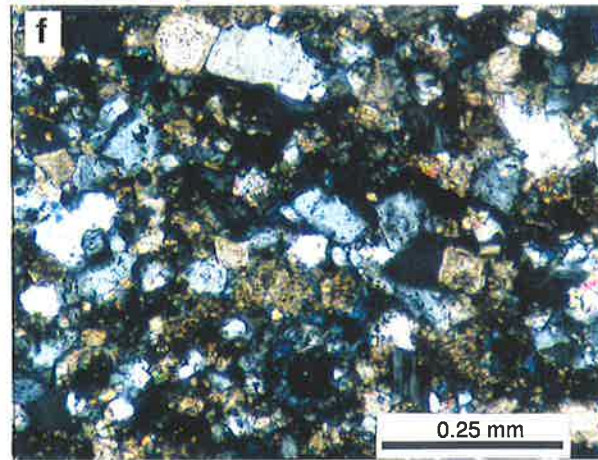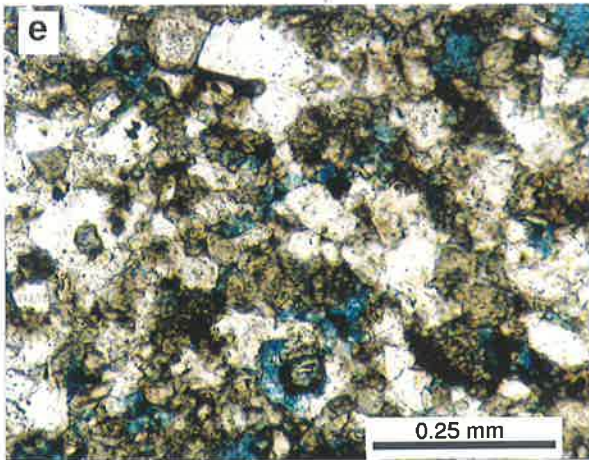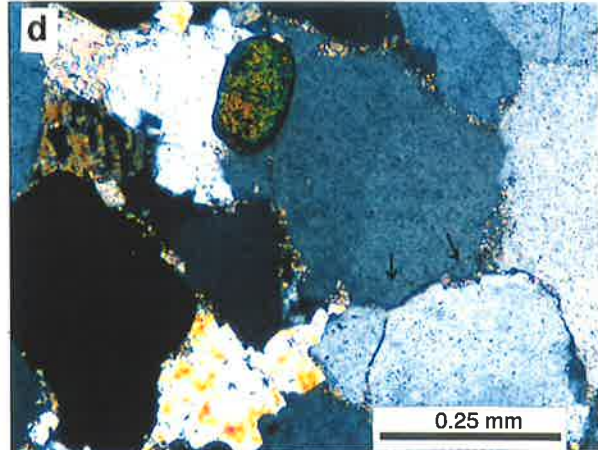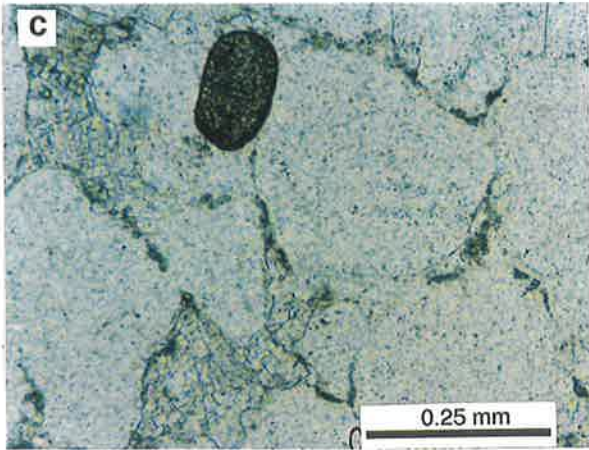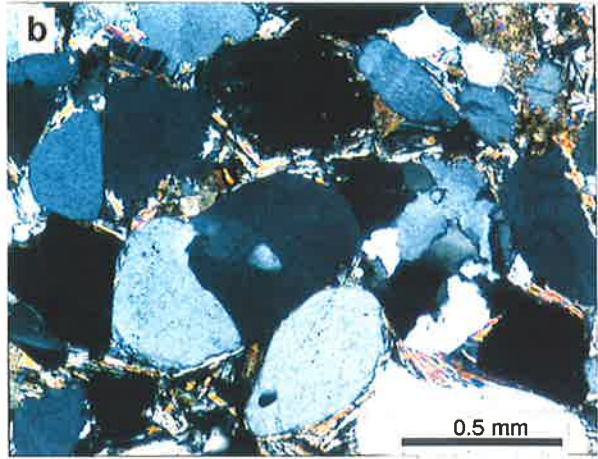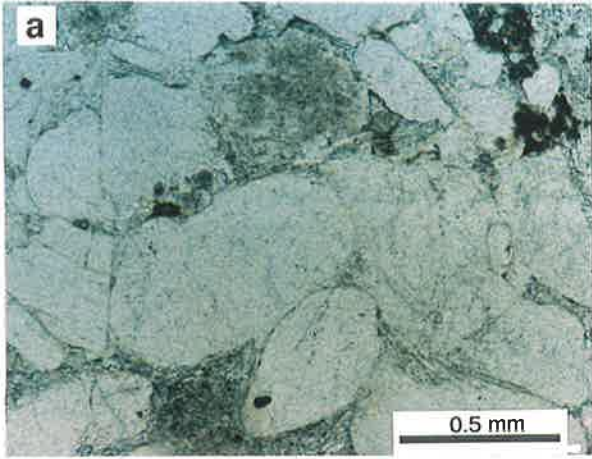
APPENDIX IV

POROSITY AND PERMEABILITY DATA

OULDBURRA FORMATION

OFFICER BASIN

Well	Depth (m)	Core Porosity	Log Porosity (ρb)	Permeability (md)	Sequences	Lithology (%)	Thickness (m)	Depth Interval
Manya-3	414.2	23.2	15	0.764	C1.3	lst (100)	3.5	411-414.5
Manya-3	468	21	20	596	C1.2	dol/sst (20:80)	4.5	476.5-472
Manya-3	468.85	23	24	372	C1.2	dol/sst (20:80)		476.5-472
Manya-3	484	27	28	215	C1.2	dol (100)	8	483-491
Manya-3	521.4	5.8	9	0.005	C1.2	lst (100)	7.5	515-522.5
Manya-3	556.05	5.7	4	0.112	C1.2	lst (100)	3	556-559
Manya-6	876.35	23	23	1490	C1.1	dol (100)	14	872-886
Manya-6	876.75	22.6	21	1640	C1.1	dol (100)		872-886
Manya-6	906.6	10.2	15	8.8	C1.1	sst/dol (80:20)	2	904.6-906.6
Manya-6	1471	6.1	13	0.08	C1.1	dol/sst (65:35)	6	1471-1477
Marla-3	519.8	9.3	11	305	ND	dol (100)	3	518-521
Marla-3	532.2	21	21	23.1	ND	dol/sst (90:10)	3	532-535
Marla-6	602.8	6.2	15	338	C1.1	dol/sst (65:35)	2	601-603

N.B., lst = Limestone, sst = Sandstone, dol = Dolomite, ND = Not determined.

Table 1   Porosity correlation using core porosity vs log porosity (density) for carbonate and mixed carbonate siliciclastics, Ouldburra Formation, Officer Basin.

Well	Sample Depth (m)	Log Porosity (density)	Visual Porosity (%)	Lithology (%)	Thickness (m)	Depth Interval
Manya-3	294.1	20	12	dol/sst (35:65)	9	289-298
Manya-6	683	15	12	lst (100)	1.5	683-684.5
Manya-6	906.6	15	12	sst/dol (65:35)	2	904.6-906.6
Manya-6	928.5	5	7	lst/dol (90:10)	1	928-929
Manya-6	954.44	4	5	lst/dol (90:10)	5	950-955
Manya-6	1045.65	4	2	lst/dol (90:10)	1	1045-1046
Manya-6	1056.23	8	8	lst/dol (50:50)	1.5	1056-1057
Manya-6	1186.3	5	7	lst (100)	3	1184-1187
Manya-6	1234.95	17	15	dol/sst (90:10)	3	1232-1235
Manya-6	1298.15	16	14	dol (100)	1.5	1297-1298.5
Manya-6	1359.16	15	13	dol (100)	1.5	1359-1360.5
Manya-6	1463.95	16	10	dol (100)	4	1463-1467
Manya-6	1471	17	16	dol/sst (90:10)	6	1471-1477
Manya-6	1471.6	14	12	dol/sst (80:20)	"	1471-1477
Marla-3	519.8	15	12	dol (100)	3	518-521
Marla-3	532.25	16	8	dol (100)	3	532-535
Marla-3	602.8	16	10	dol/sst (90:10)	1.5	602-603.5
Marla-6	368	30	28	dol (100)	4	364-368
Marla-6	370.04	11	7	dol/lst (50:50)	1	370-371
Marla-6	376	18	10	dol (100)	1.5	376-377.5
Marla-6	377.38	2	4	dol (100)	"	376-377.5
Marla-6	437.6	12	7	dol (100)	2	437-439
Marla-6	457.6	20	25	dol (100)	1.5	456.5-458
Marla-6	519.1	12	10	dol (100)	3	517-520
Marla-6	567.4	19	12	dol (100)	1	567-568
Marla-6	648.1	18	10	dol (100)	3	645.5-648.5
Marla-6	658.5	18	20	dol/sst (50:50)	3	657-660
Marla-6	666.4	21	22	dol/sst (90:10)	3	663-666
Marla-7	330.15	14	15	dol/lst (60:40)	2.5	328.5-331
Marla-7	342.3	12	10	lst/dol (60:40)	2	341-343
Marla-7	358	10	10	dol (100)	3	355-358
Marla-7	437.8	16	12	dol (100)	1	437-439
Marla-7	479.8	7	3	dol/sst (80:20)	2	478-480
Marla-7	481.5	6	5	lst/dol (60:40)	1.5	481.5-483

N.B., dolo = Dolomite, sst = Sandstone, lst = Limestone,

Table 2 Porosity from visual observation (thin section) and log porosiy (density)
; Ouldburra Formation, Office Basin.

APPENDIX V

LOG PROFILES

OF SELECTED POROUS INTERVALS

OULDBURRA FORMATION

OFFICER BASIN

MANYA-3

Total thickness of dolomite and mixed dolomite-sandstone beds with porosity about 20% is approximately 16 m.

MARLA-3

Legend:
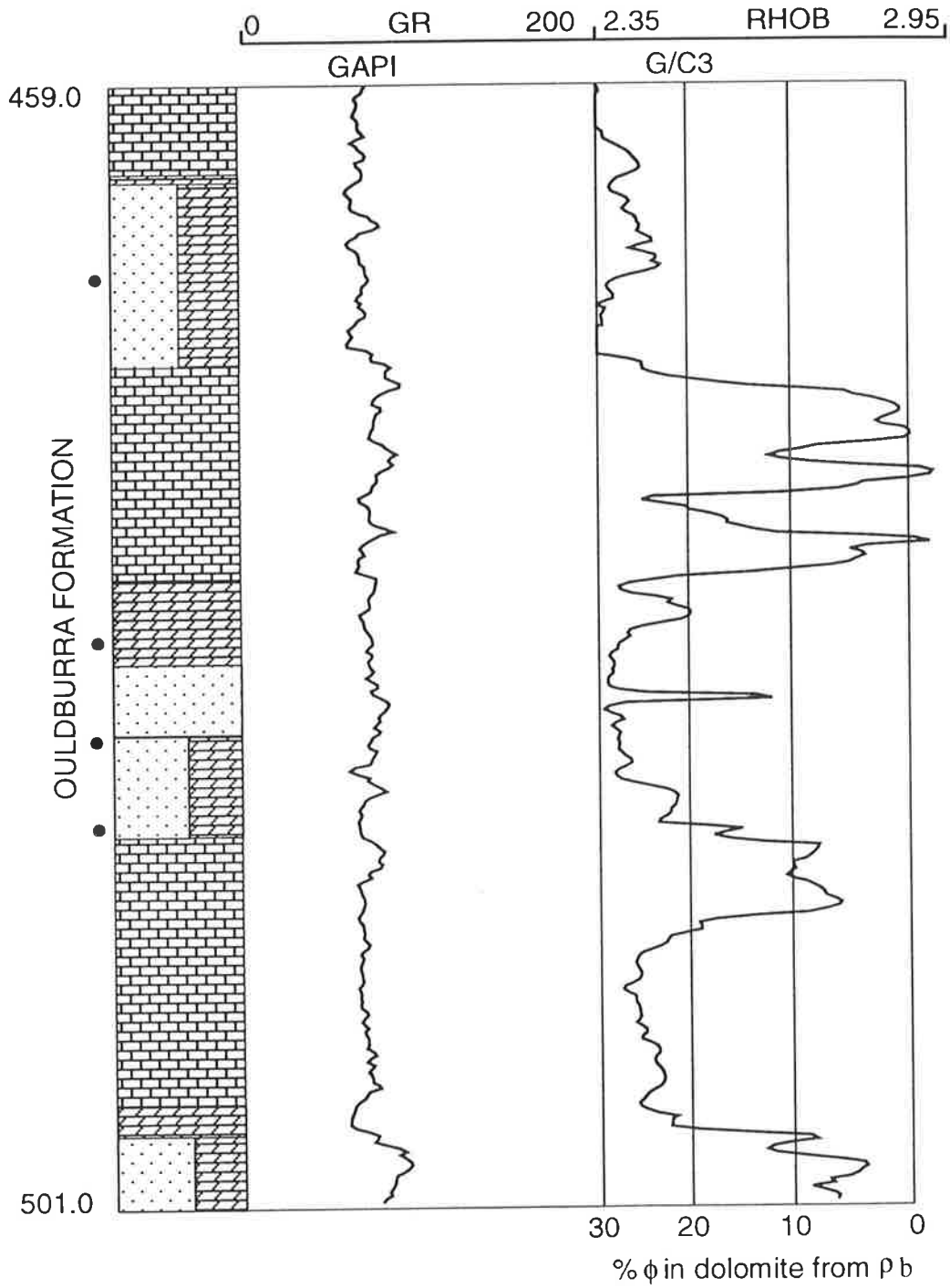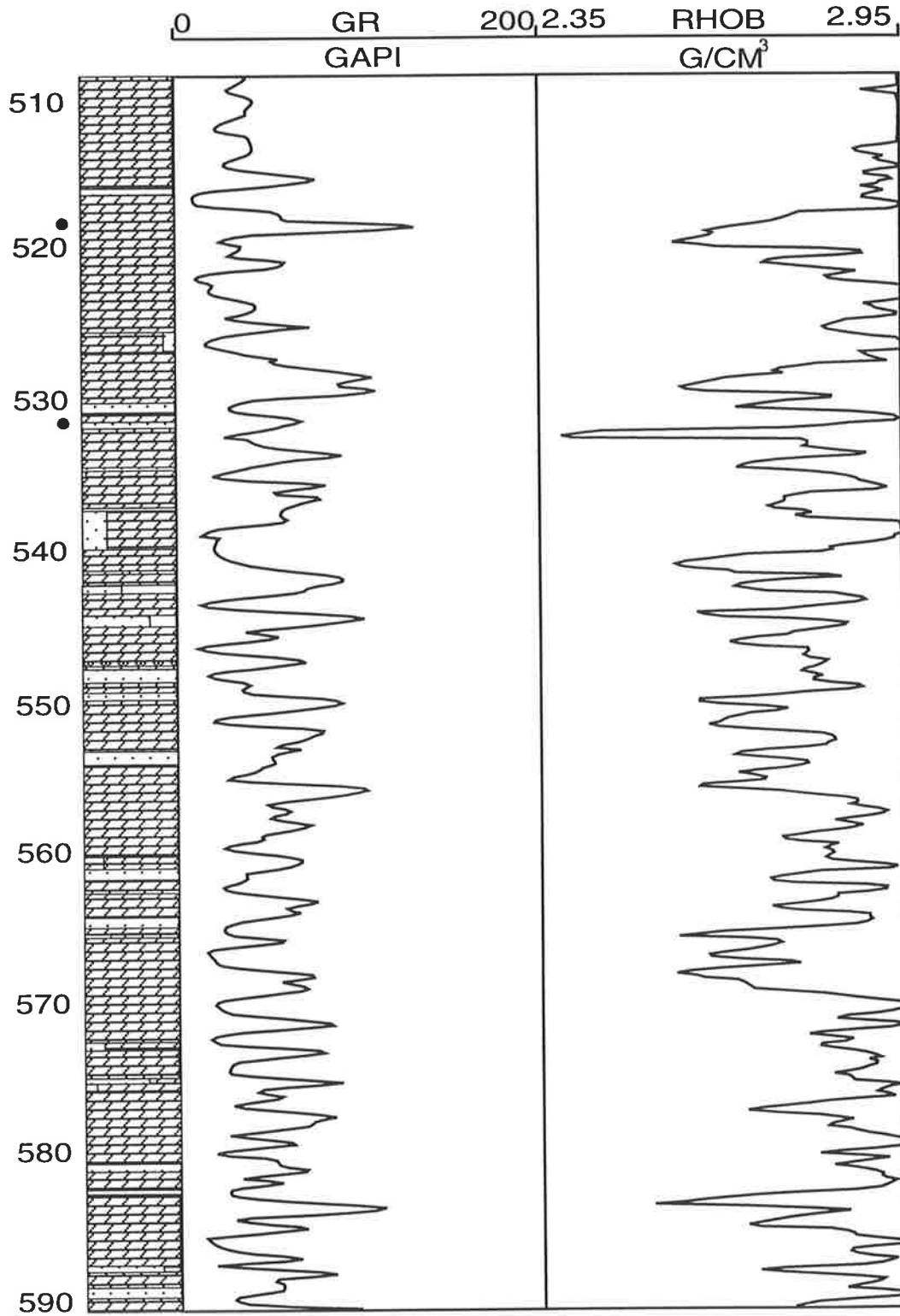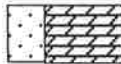
- ▨ DOLOMITE
- ▦ LIMESTONE
- ▧ SANDSTONE
- ⬚ DOLOMITIC SANDSTONE
- ▨ SANDY DOLOMITE
- ● SAMPLE LOCATIONS

Total thickness of beds with porosity >15% is approximately 12 m

MARLA-6
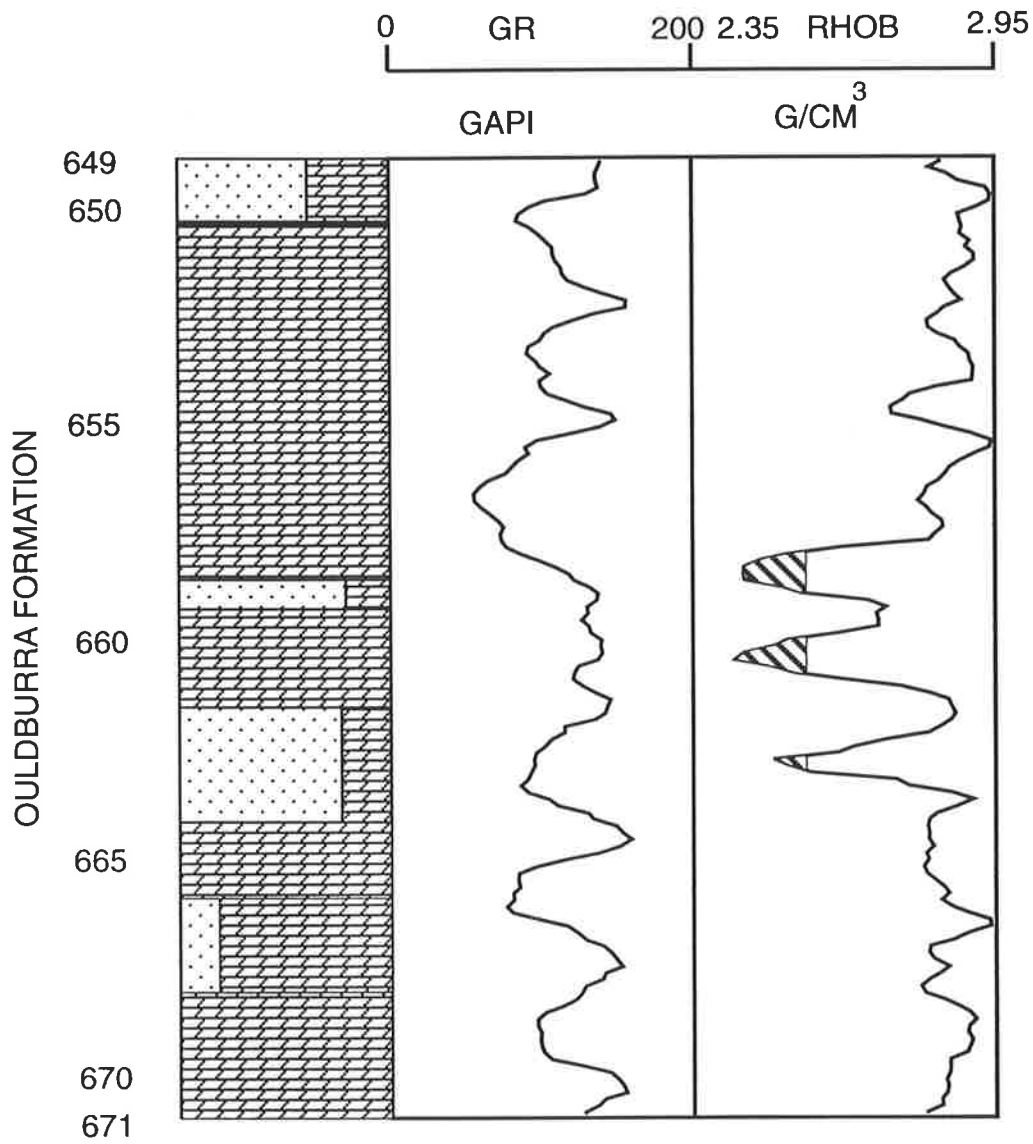
Total thickness of beds with porosity > 20% is approximately 3m and are shown by hatched area on density log.

APPENDIX VI

ROCK-EVAL PYROLYSIS DATA

OULDBURRA FORMATION

OFFICER BASIN

WELL : MARLA -3											
DEPTH m	TOC %	Tmax	S1	S2	S3	S1+S2	PI	S2/S3	PC	HI	OI
508.30	0.02										
509.45	0.03										
513.05	0.01										
546.45	0.05										
568.45	0.09										
576.90	0.18										
586.20	0.14										
601.25	0.13										
619.60	0.79	438	0.2	0.63	0.22	0.83	0.24	0.26	0.06	79	27
624.85	0.08										
626.25	0.66	392	0.03	0.02	0.41	0.05	0.75	0.04	0	3	62
WELL : MARLA -6											
416.00	1.34	422	0.22	1.22	0.41	1.44	0.15	2.97	0.12	91	30
573.10	0.19										
585.00	0.05										
637.05	0.27										
655.50	0.09										
671.25	1.13	341	0.14	0.13	0.18	0.27	0.54	0.72	0.02	11	15
684.70	0.28										
700.25	0.47	237	0.08	0	0.41	0.08	1	0	0	0	87
WELL : MARLA -7											
333.75	0.09										
347.30	0.05										
378.50	0.13										
383.05	0.10										
392.85	0.53	403	0.11	0.32	0.25	0.45	0.26	1.28	0.03	60	47
443.15	0.12										
445.00	0.10										
448.45	0.21										
517.76	0.21										
WELL : MANYA -3											
246.70	0.37	419	0.01	0.01	0.28	0.02	0.5	0.04	0	2	75
266.10	0.22										
367.20	0.18										
411.30	0.11										
411.65	0.20										
418.00	0.37	221	0.01	0.01	0.24	0.02	0.5	0.04	0	2	64
470.50	0.17										
470.90	0.2										
475.00	0.17										
515.80	0.43										
598.60	0.11										
631.70	0.27										
639.90	0.21										
681.30	0.14										
760.20	0.17										

DEPTH/m	TOC %	T$_{max}$	S1	S2	S3	S1+S2	PI	S2/S3	PC	HI	OI
WELL : MANYA-6											
578.62	0.10										
601.04	0.10										
622.92	0.08										
629.18	0.04										
635.28	0.26										
648.73	0.11										
652.30	0.07										
657.92	0.36	294	0.03	0	0.5	0.03	1.0	0	0	0	139
660.17	0.10										
679.20	0.22										
690.70	0.12										
691.15	0.19										
691.75	0.97	307	0.35	0.4	0.67	0.75	0.47	0.59	0.06	41	69
691.95	0.13										
695.25	0.12										
696.16	0.17										
698.00	0.68	436	0.31	0.26	0.38	0.57	0.54	0.68	0.05	38	56
698.60	0.82	476	0.31	0.5	0.43	0.81	0.38	1.16	0.07	61	52
698.90	0.06										
703.65	0.07										
704.50	0.09										
704.95	0.04										
718.48	0.41										
723.54	0.05										
732.72	0.93	359	0.05	0.08	0.38	0.13	0.42	0.21	0.01	9	41
746.39	0.09										
746.67	0.13										
767.00	0.09										
769.05	0.12										
771.15	0.19										
771.30	0.19										
771.90	0.09										
773.84	0.34	279	0.04	0	0.43	0.04	1.0	0	0	0	126
777.10	0.06										
777.95	0.10										
779.60	0.26										
780.03	0.48	333	0.07	0.03	0.23	0.1	0.7	0.13	0	6	48
780.90	0.14										
784.00	0.13										
785.10	0.15										
785.77	0.34	279	0.04	0	0.39	0.04	1.0	0	0	0	115
785.85	0.17										
798.67	0.14										
807.94	0.63	317	0.07	0.03	0.07	0.1	0.7	0.42	0	5	11
810.50	0.43	279	0.03	0.01	0.21	0.04	0.75	0.04	0	2	49
826.24	0.69	317	0.05	0.04	0.39	0.09	0.62	0.1	0	6	57

839.79	0.09									
856.05	0.13									
879.96	0.12									
896.95	0.19									
899.80	0.91	279	0.04	0.03	0.1	0.07	0.67	0.3	0	3	11
930.47	0.17									
939.18	0.14									
966.27	0.08									
999.44	0.34	279	0.01	0	0. 1	0.01	0.01	0	0	0	27
1009.50	0.09									
1020.05	0.11									
1038.10	0.13									
1057.03	0.31	279	0	0	0.12	0	0	0	0	0	39
1067.22	0.15									
1072.10	0.15									
1125.48	0.22									
1126.95	0.63	279	0.01	0	0.15	0.01	0.01	0	0	0	24
1145.70	0.26									
1170.55	0.19									
1183.02	0.14									
1193.50	0.19									
1229.70	0.64	241	0.02	0.01	0.19	0.03	1.0	0.05	0	2	30
1231.16	0.57									
1231.94	0.22	266	0.01	0	0.28	0.01	0.01	0	0	0	49
1247.92	0.32	241	0	0	0.14	0	0	0	0	0	44
1267.52	0.43	266	0	0	0.37	0	0	0	0	0	86
1275.00	0.15									
1277.15	0.42	466	0.06	0.15	0.9	0.21	0.29	0.17	0.02	36	214
1277.30	0.31									
1277.85	0.19									
1278.25	0.35									
1279.15	0.52	304	0.09	0.06	0.69	0.15	0.6	0.09	0.01	12	133
1279.76	0.64	241	0.01	0	0.59	0.01	0.01	0	0	0	92
1291.60	0.32									
1292.60	0.16									
1294.75	0.32									
1302.12	0.38	205	0	0	0.46	0	0	0	0	0	121
1312.70	0.61									
1332.28	0.33	281	0.03	0	1.03	0.03	1.0	0	0	0	312
1339.02	0.21									
1364.01	0.28									
1381.75	0.18									
1386.63	0.37	241	0.03	0.01	0.32	0.04	0.75	0.03	0	3	86
1392.40	0.31	232	0.01	0	0.48	0.01	0.01	0	0	0	155
1419.34	0.36	241	0.06	0.11	0.31	0.17	0.37	0.35	0.01	31	86
1459.23	0.32	241	0.02	0.06	0.28	0.08	0.25	0.21	0	19	88
1490.80	0.04									

WELL : KD-1											
DEPTH m	TOC %	T_{max}	S1	S2	S3	S1+S2	PI	S2/S3	PC	HI	OI
263.35	1.18	427	0.59	4.59	5.37	5.18	0.11	0.85	0.43	388	455
275.43	0.20	435	0.25	1.02	0.30	1.27	0.20	3.40	0.11	510	10
WELL : KD-2A											
211.80	0.34	430	0.15	0.97	0.31	1.12	0.13	0.09	0.34	285	91
285.50	0.73	427	0.49	3.20	4.76	3.69	0.13	0.67	0.30	438	652
297.95	0.59	425	0.70	2.20	3.35	2.90	0.24	0.66	0.24	372	567

Rock-Eval pyrolysis data used in this study, Ouldburra Formation Officer Basin.

APPENDIX VII

ORGANIC PETROGRAPHIC DESCRIPTIONS

OF POLISHED SECTIONS OF

OULDBURRA FORMATION

OFFICER BASIN

Description of polished section

Sample   : Manya-6 (691.75 m)   Lithology: Stylolitic limestone

Formation   : Ouldburra

Age   : Early Cambrian

Percent OM	Maceral Group	Maceral Subgroup	Maceral
5	Liptinite	-	Alginite (lamalginite)
95	Liptinite	-	Bituminite

Classification of OM after AS2856-1986

OM constitutes almost 3 % of the total rock and most of it appears as a stack of thin lamellae (bituminite) concentrated within microstylolites concordant to bedding. Clay (?kaolinite) intimately associated with the OM occurs along stylolitic planes. Thin layers (2 mm) of clastic grains ranging in size from 0.02 to 0.06 mm occur within laminated micritic limestone probably indicating periodic changes in environment or source material. The bituminite is dark brown under reflected white light and does not fluoresce under blue light excitation. However, associated discontinuous filaments (lamalginite), occurring in minor quantity, fluoresce reddish brown.

Description of polished section

Sample   : Manya-6 (1279.15 m)   Lithology: Laminated micritic limestone

Formation   : Ouldburra

Age   : Early Cambrian

Percent OM	Maceral Group	Macearl Subgroup	Maceral
60	Liptinite	-	Alginite (lamalginite)
40	Liptinite	-	Bituminite

OM occurs predominantly as lamalginite. Thin lamellae 4 to 7 μm thick are concordant with bedding. The lamalginite is dark grey under white reflected light and fluoresces brown (weakly) under ultra-violet excitation. Thinly laminated organic-rich layers contain

scattered cubic pyrite crystals which are bright yellow under reflected white light. The close ssociation of pyrite and OM suggests sulphate reduction during early diagenesis.

Round and/or oval bodies (2 to 3 µm) occur at contact between micritic limestone layers. These bodies appear red in fluorescence mode suggesting migrated oil, which is also confirmed by gas chromatography of saturated hydrocarbons.

This source rock was deposited in an anoxic to suboxic environment.

Description of polished section

Sample   : Marla-3 (626.25 m)   Lithology: Laminated silty dolostone

Formation   : Ouldburra

Age   : Early Cambrian

Percent OM	Maceral Group	Maceral Subgroup	Maceral
4	Liptinite	-	Alginite (lamalginite)
96	Liptinite	-	Bituminite

Bituminite is the major maceral. It occurs as laminae which contain disseminated pyrite crystals and micrinite granules (size range 1 to 3 µm). The bituminite seems to be concentrated in dissolution seams which occur vertically stacked 2 to 6 mm apart. A few dissolution seams contain siliciclastic grains such as quartz, feldspar and mica flaks. Almost all the lamalginite (except a few scattered stringers) has been oxidised. Small and round bodies of OM with intense orange fluorescence fill in intra-pore spaces and are probably migrated hydrocarbons.

Burrows, commonly filled by silt, occur within the micritic carbonate matrix. The presence of such burrows reflects the activity of bioturbating organisms during early diagenesis. This petrographic evidence indicates that suboxic conditions existed during the deposition of carbonate rock.

Description of polished section

Sample   : Marla-6 (416.00 m)   Lithology: Thinly bedded micritic dolostone

Formation   : Ouldburra

Age   : Early Cambrian

Percent OM	Maceral Group	Maceral Subgroup	Maceral
40	Liptinite	-	Alginite (lamalginite)
60	Liptinite	-	Bituminite

OM forms about 2 to 3 % of the sample and appears to be micritinised bituminite and lamalginite. The bituminite occurs as thin laminae or stylolitic films and is dark brown under white reflected light. The micrinite granules within the bituminite are oval and their size ranges from 2 to 5 µm. Under white reflected light these granules, together with scattered pyrite crystals, are bright white. In ultra-violet excitation the bituminite does not fluroesce. Such bituminite was probably derived from lamalginite through intense bacterial degradation at or near the sediment-water interface (Plate 7.2b). Lamalginite occurs as discontinuous and anastomosing films 30 to 60 µm in length and aligned parallel to bedding. The lamalginite is dark grey under white reflected light and displays dark orange in fluorescence mode. Small oval and spherical blebs of OM of varying size (1.5 - 11 µm), scattered in a fine micritic matrix, are yellow to orange under blue light excitation. Given the high maturity of this sample (VRcalc = 1.26 %), these oil blebs were almost certainly generated *in situ*. This source was deposited under suboxic to anoxic conditions and has probably been deeply buried since early diagenesis.

Description of polished section

Sample   : Marla-7 (392.85 m)   Lithology: Laminated dolostone

Formation   : Ouldburra

Age   : Early Cambrian

Percent OM	Maceral Group	Maceral Subgroup	Maceral
10	Liptinite	-	Alginite (lamalginite)
90	Liptinite	-	Bituminite

OM forms about 2 to 3 % of the sample and is dominantly bituminite occurring as thick bands generally parallel to bedding. This material is dull brown in white reflected light and

shows no fluorescence in blue light excitation (Plate 7.2a). Scattered pyrite crystals occur within the bituminite bands, reflecting bacterial sulphate reduction during early diagenesis. Given the thinly bedded dolostone (mudstone) lithology of the sample and the presence of only liptinite maceral, an anoxic to suboxic environment may be inferred.

Description of polished section

Sample   : KD -1 (263.35 m)   Lithology: Laminated limestone

Formation   : Ouldburra

Age   : Early Cambrian

Percent OM	Maceral Group	Maceral Subgroup	Maceral
90	Liptinite	-	Alginite (lamalginite)
5	Liptinite	-	Telalginite (*G. prisca*)
5	Thucholite and organic debris		

OM comprises about 4 to 5 % of the rock with lamalginite as the dominant maceral. The lamalginite occurs as discontinuous filaments that locally form fine mat-like masses (Plate 7.2d). Grouped lamellae are 60 to 120 μm long and 1.5 to 16 μm thick. Under white reflected light they appear grey and red brown, but fluoresce yellow to orange in blue light excitation.

Spherical or oval-shaped algal bodies (telalginite), probably primitive *Gloeocapsomorpha prisca* (Plate 7.3e and f), occur in close proximity to the lamalginite. These telalginite macerals are 18 to 30 μm long and 8 to 12 μm thick, and commonly exhibit no recognisable internal structure. The telalginite is yellow in fluorescence mode, suggesting an early mature to mature source rock. The lamalginite and telalginite are more commonly associated with shaley bands rather than with the carbonate matrix.

Framboidal pyrite is also associated with the OM. Lenses of gypsum are likewise common in the vicinity of organic-rich bands, suggesting that preservation of OM was favoured by hypersalinity. Large rounded or spherical bodies of bitumen balls (10 - 30 μm in diameter) with a core of zircon occur in close proximity to lamalginite. These bitumen balls are generally referred to as "thucholite" which are grey under white reflected light but fluoresce orange at their rims under ultra-violet light. Non-fluorescent cores surrounded by

slightly fluorescing haloes are features that differentiates these bodies from reservoir-type bitumens.

Depending upon their size, the thucholites have variable reflectances which range from 0.3 % to 0.73 % in small to medium thucholites and up to 1.01 % in large thucholites.

Description of polished section

Sample   : KD -1 (275.43 m)   Lithology: Laminated micritic limestone

Formation   : Ouldburra

Age   : Early Cambrian

Percent OM	Maceral Group	Maceral Subgroup	Maceral
85	Liptinite	-	Alginite (lamalginite)
10	Liptinite	-	Bituminite
5	Liptinite	-	Alginite (telalginite)

OM occurs predominantly as discontinuous grouped lamellae 40 to 200 μm long and 5 to 8 μm thick. Under reflected white light they appear grey and red brown but fluoresce yellow to orange in fluorescence mode. Bituminite is grey in reflected white light, occurring as thick masses of 20 to 30 μm and is commonly associated with silty material. It fluoresces dull brown with an orange tint in ultra-violet excitation, indicating an early mature source rock.

Discrete oval or disc-shaped bodies (telalginite) that constitute up to 5 % of the total OM, occur in close proximity to lamalginite and appear yellow in fluorescence mode. The presence of well-preserved, abundant lamalginite and telalginite suggests preservation of autochthonous OM under anoxic conditions.

Description of polished section

Sample   : KD -2A (211.80 m)   Lithology: Micritic limestone

Formation   : Ouldburra

Age   : Early Cambrian

Percent OM	Maceral Group	Maceral Subgroup	Maceral
20	Liptinite	-	Alginite (lamalginite)
80	Liptinite	-	Bituminite

OM is predominantly micrinitised bituminite which occurs as thick massive lamellae and is closely associated. These bituminites are commonly concentrated in thin dark shaley bands aligned parallel to bedding. OM constitutes up to 2 % of the whole rock and generally includes common bituminite, lamalginite and disseminated organic debris. Thin, elongate and discontinuous filaments (lamalginite) commonly occur in close relationship with bituminite masses. This minor component appears yellow to light orange in fluorescence mode. Such a relationship suggests that the massive laminated bituminite was probably derived from lamalginite through intense bacterial degradation at or near the sediment-water interface.

Description of polished section

Sample : KD -2A (285.50 m)   Lithology: Micritic limestone

Formation : Ouldburra

Age : Early Cambrian

Percent OM	Maceral Group	Maceral Subgroup	Maceral
95	Liptinite	-	Alginite (lamalginite)
5	Liptinite	-	Alginite (telalginite including ?G. prisca)

OM constitutes up to 4 % of the total rock and includes abundant lamalginite with minor amounts of telalginite and thucholite.

Primitive ?G. prisca appear as spherical to subspherical algal bodies with cellular internal structure (Plate 7.4a–c). This telalginite is brown in reflected white light but fluoresces yellow to light orange in blue light excitation.

Thucholites of varying sizes (10-30 μm in diameter) are closely associated with lamalginite. These thucholites have variable reflectances: 0.34 - 0.53 % in small to medium thucholites and 0.92 % in large thucholites.

Stringers live oil fill fissures and veins. They appear dark brown under reflected white light and fluoresce orange in ultra-violet excitation. Because the live oil is commonly concentrated in close vicinity to abundant lamalginite (Plate 7.4e and f), an *in situ* origin of the oil is likely.

Description of polished section

Sample   : KD -2A (297.95 m)   Lithology: Micritic limestone

Formation   : Ouldburra

Age   : Early Cambrian

Percent OM	Maceral Group	Maceral Subgroup	Maceral
50	Liptinite	-	Alginite (lamalginite)
50	Liptinite	-	Bituminite

The dispersed OM comprises bituminite and lamalginite in almost equal quantities. Together they constitute about 3 % of the whole rock. The bituminite occurs as pod-like masses aligned almost parallel to bedding. These bituminite masses are dull brown in reflected white light and fluoresces dark orange weakly under blue light excitation.

Thucholites of varying sizes (10-50 μm in diameter) occur closely associated with lamalginite. These thucholites have reflectances which range from 0.66 - 0.70 % in medium-sized thucholites to 1.71 % in large thucholite.

Scattered framboidal pyrite is associated with both lamalginite and bituminite. There is also structureless organic debris, disseminated in the carbonate matrix, that fluoresces orange in ultra-violet light.

Live oil appears to fill small veins and fissures in vicinity of the lamalginite masses. This organic-rich limestone is early mature nature of the rock and so an indigenous origin for the live oil is likely.

APPENDIX VIII

COLOUR AND BLACK & WHITE

PLATES OF MICROFOSSILS IN

ORGANIC-RICH CARBONATES

OULDBURRA FORMATION

OFFICER BASIN

Plate 7.1

a) Microlaminated to thinly bedded dolomitic mudstone. Relict algal lamination appears dark under polarised light (Manya-6, 1312.70 m).

b) Micritic limestone with abundant sponge spicules (monoaxon and triaxon) and peloids, stained with Alizarin Red-S (Manya-6, 1073.30 m).

c) Dolomitic limestone (wackstone to grainstone) with abundant trilobite and tabular fossil fragments, stained with Alizarin Red-S (Manya-6, 1056.23 m).

d) Silty carbonate mudstone, microlaminated to laminated with possible planar algal lamination (Manya-6, 1038.10 m).

e) The same sample with dissolution seams and stylolites parallel to bedding (Manya-6, 1038.10 m).

f) Dolomitic limestone with calcite pseudomorphs of sulphate evaporite (gypsum) in upper right corner and abundant bioclastic debris, stained with Alizarin Red-S (Manya-6, 889.50 m).
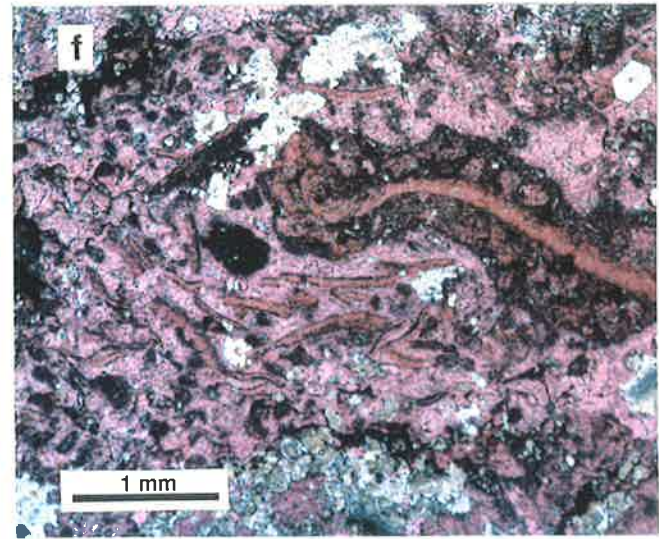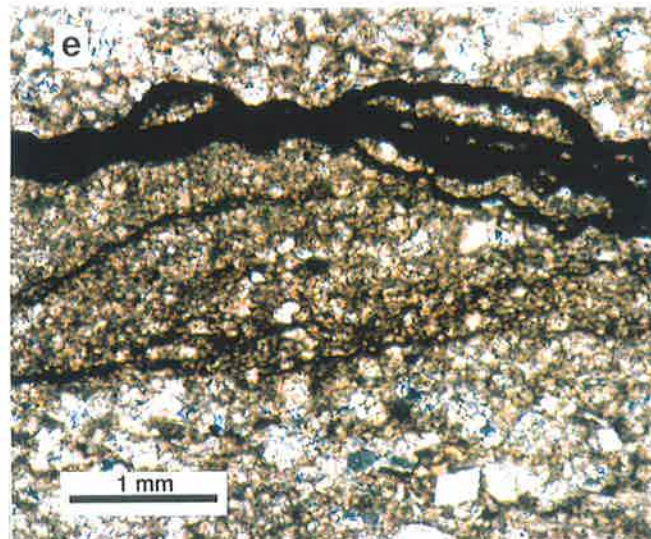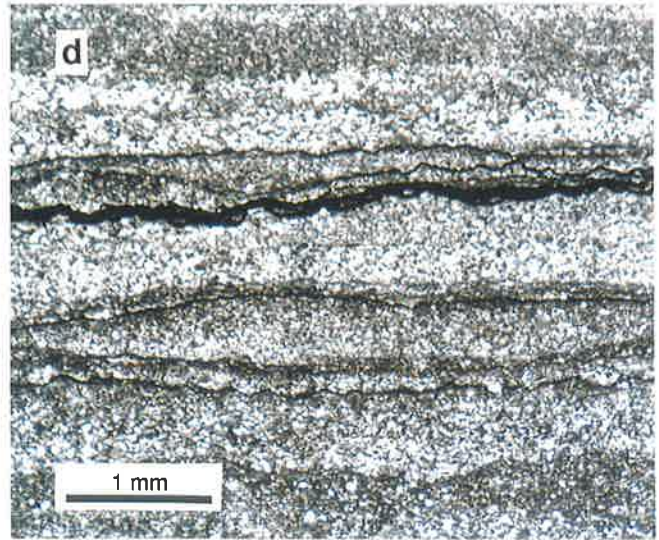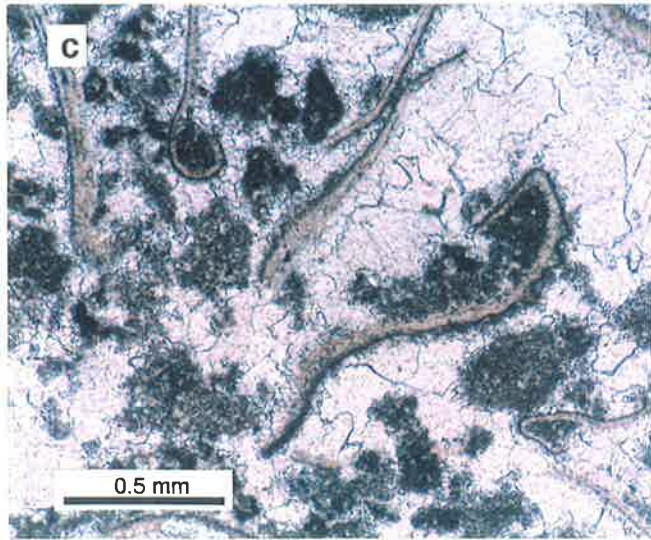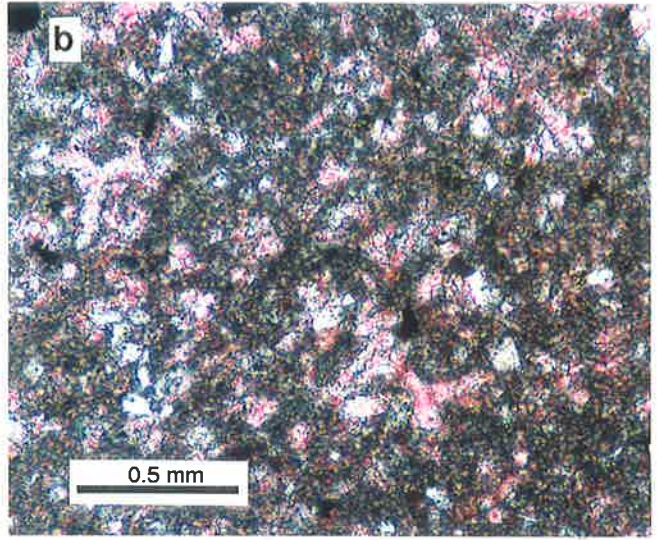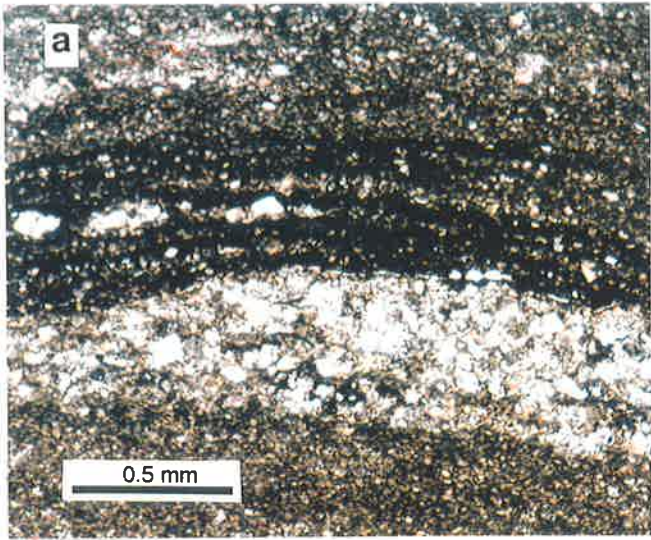
Plate 7.2

Dispersed organic matter in Ouldburra Formation from the Manya Trough and Tallaringa Trough

a) Marla-7, 392.85 m depth; reflected white light mode; typical bituminite with micrinitic (white) and pyrite (bright yellow).

b) Marla-6, 416.00 m depth; fluorescence-mode; disseminated organic matter (algal origin) and insitu oil?

c) KD-1, 263.35 m depth; reflected white light mode; bright patches are pyrite; perpendicular to bedding.

d) Same as (c) in fluorescence-mode; common lamalginite of varying sizes.

e) KD-1, 263.35 m depth; thucholite with a core of zircon; reflected white light-mode.

f) Same as (e) in fluorescence mode; decreasing reflectance, and increasing fluorescence, from centre to the margin suggests continuos process of hydrocarbon polymerisation and accretion.
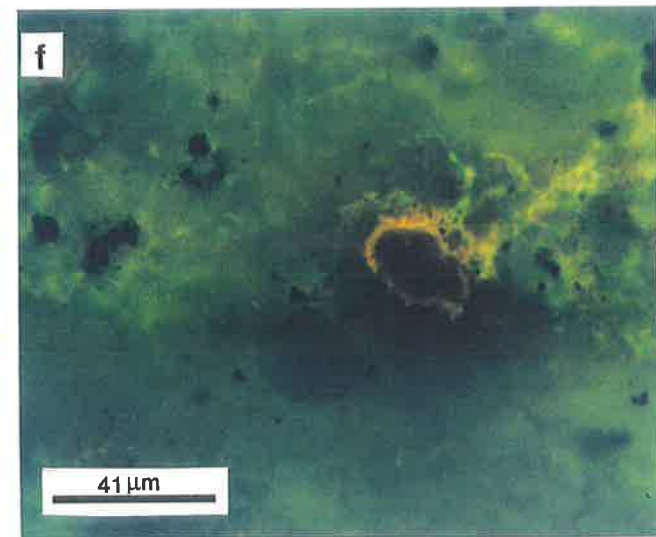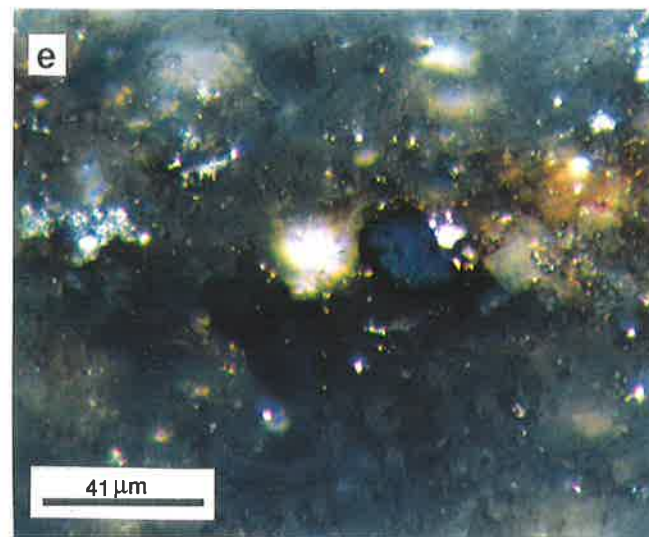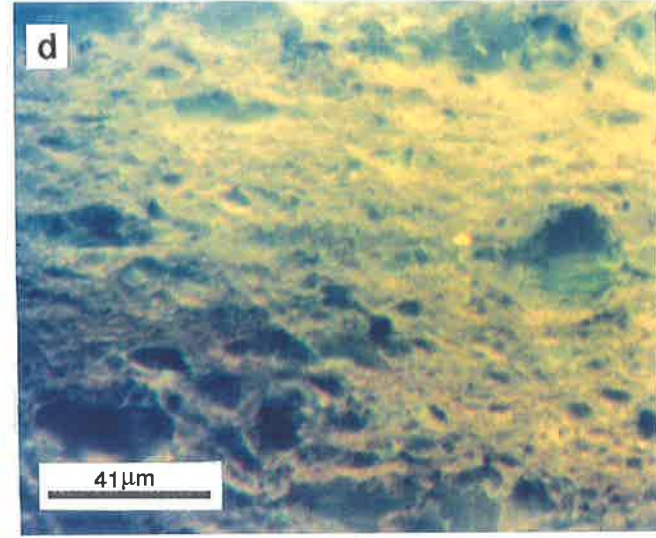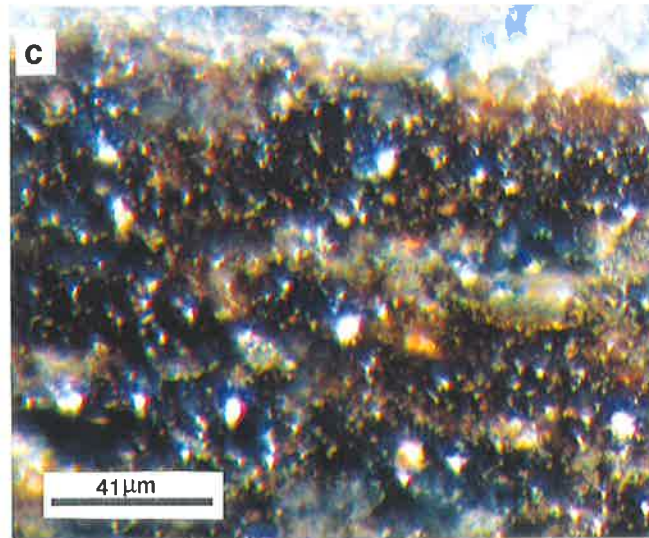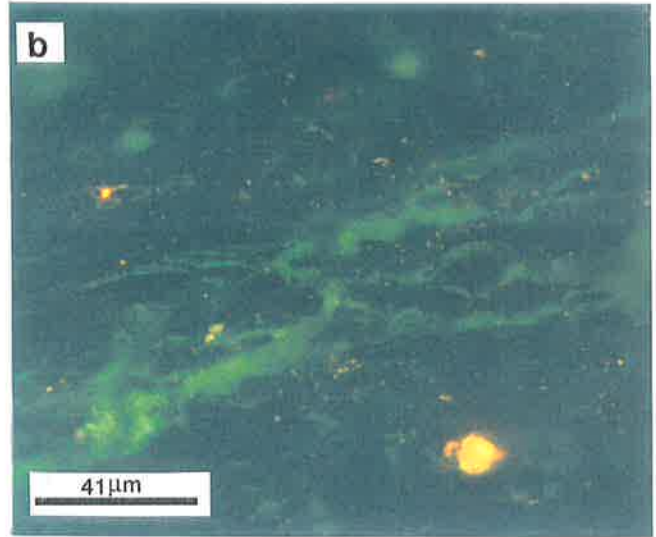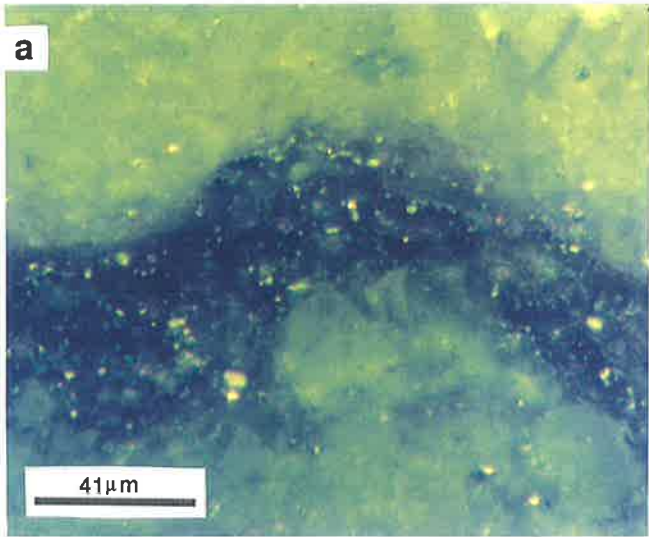
Plate 7.3

Dispersed organic matter in Ouldburra Formation from the Manya Trough and Tallaringa Trough

a) KD-2A, 285.50 m depth; very large thucholite at centre and smaller at top right corner; perpendicular to bedding; reflected white light mode.

b) Same as (a) in fluorescence-mode with golden fluorescing haloes; strands of lamellar alginite sometimes merge into rounded bodies (thucholite).

c) KD-1, 263.35 m depth; telalginite (*G. prisca*) at the centre and lamalginite with insitu oil that fills small veins and intergranular spaces; fluorescence mode; perpendicular to bedding.

d) KD-1, 263.35 m depth; telalginite (*G. prisca*) at the centre and discontinuous lamalginite; black patches are pyrite; fluorescence mode; perpendicular to bedding.

e) KD-1, 263.35 m depth; telalginite (*G. prisca*) at the bottom and discontinuous lamalginite appears brown under reflected white light; bright patches are pyrite.

f) Same as (e) in fluorescence-mode; *G. prisca* shows golden yellow to light brown fluorescence; lamalginite appears as matlike masses and fluoresces yellow.

a | 41 μm
b | 41 μm
c | 18 μm
d | 18 μm
e | 18 μm
f | 18 μm
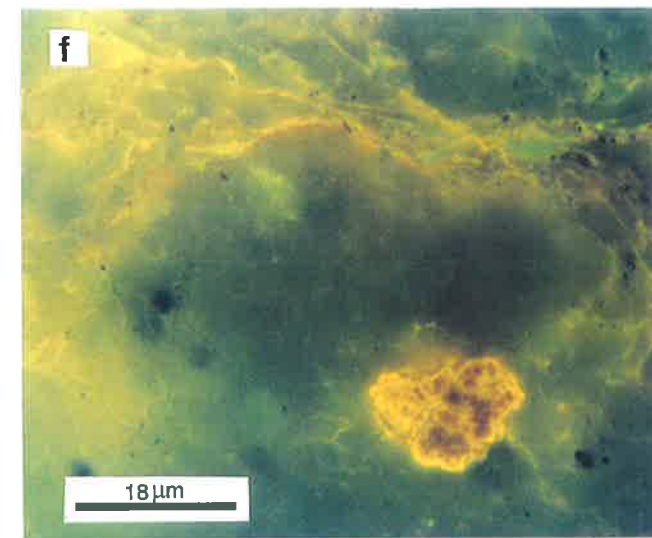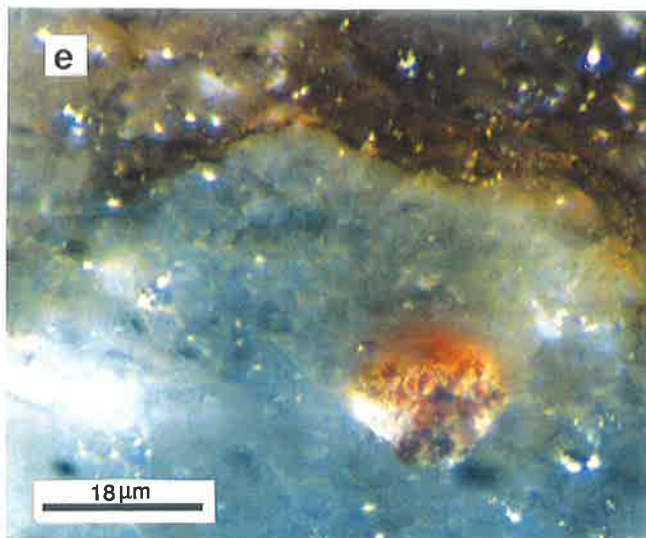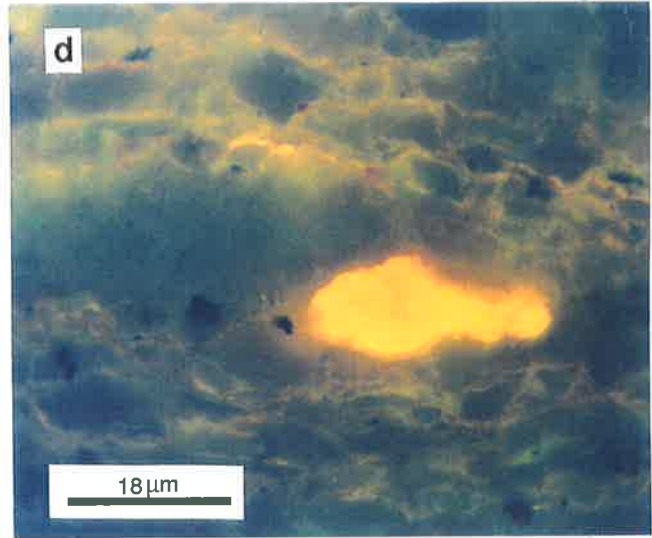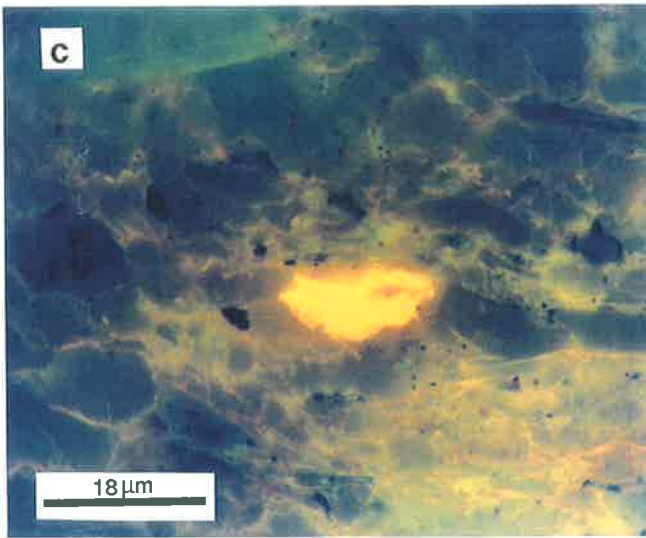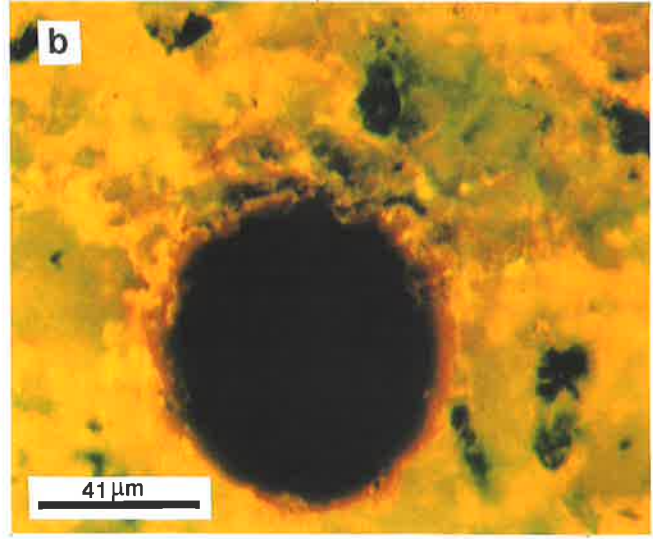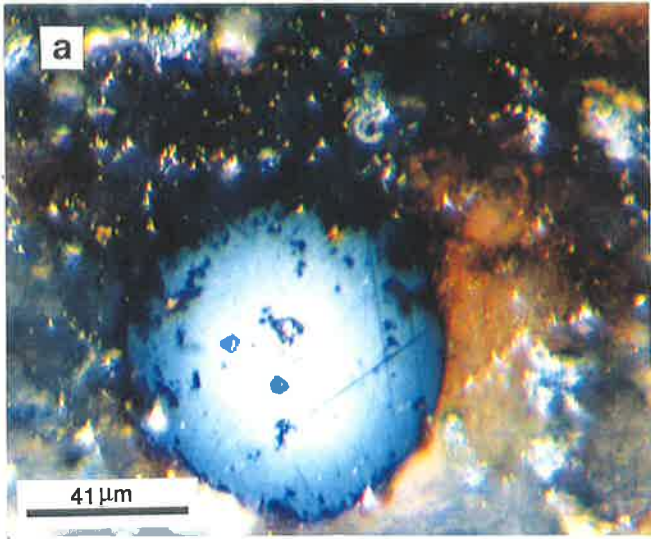
Plate 7.4

Dispersed organic matter in Ouldburra Formation from the Manya Trough and Tallaringa Trough

a) KD-2A, 285.50 m depth; telalginite (*G. prisca*) at the centre surrounded by discontinuous lamalginite (brown strands); reflected white light mode; perpendicular to bedding.

b) Same as (a) in fluorescence-mode; *G. prisca* shows cellular structure.

c) KD-2A, 285.50 m depth; *G. Prisca* surrounded by common lamalginite; reflected white light-mode; perpendicular to bedding.

d) Same as (c) in fluorescence mode; *G. prisca* shows yellow to light brown fluorescence and is surrounded by common lamalginite.

e) KD-2A, 285.50 m depth; indigenous oil (live oil) fills veins and intergranular spaces; reflected white light mode; perpendicular to bedding.

f) Same as (e) in fluorescence-mode; live oil fluoresces orange.

a

18 μm

b

18 μm

c

41 μm

d

41 μm

e

18 μm

f

18 μm
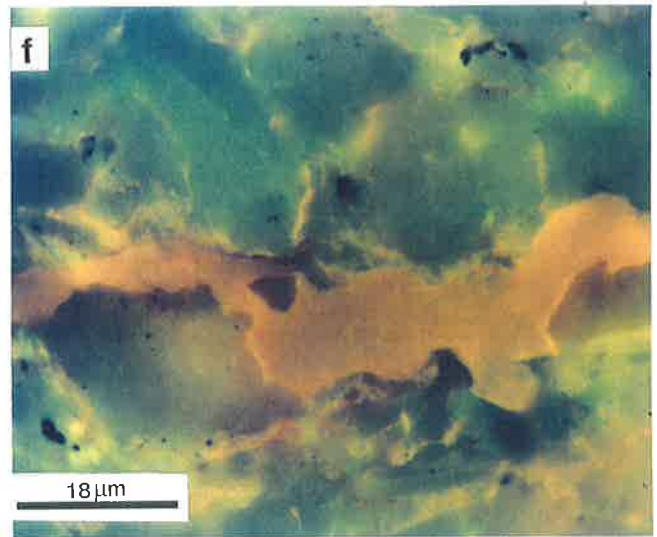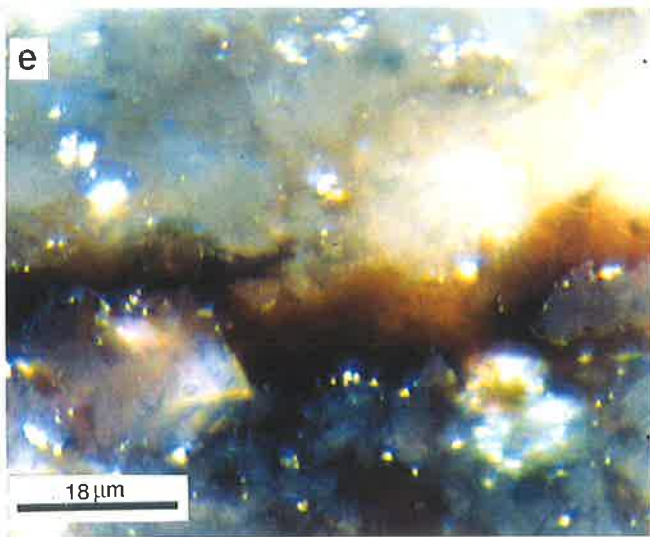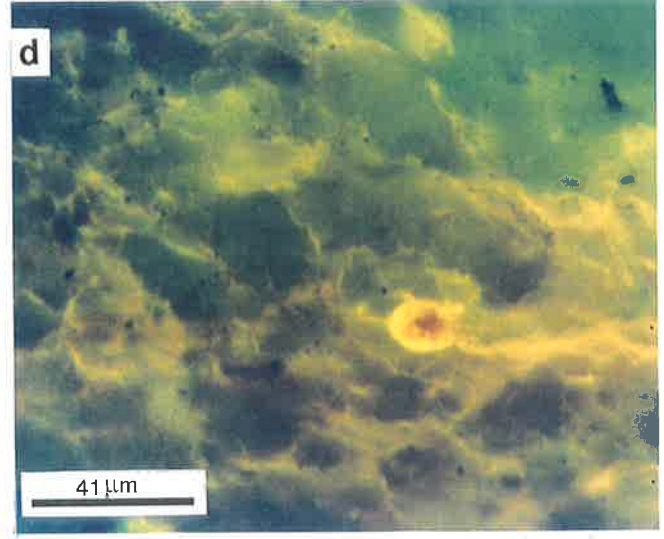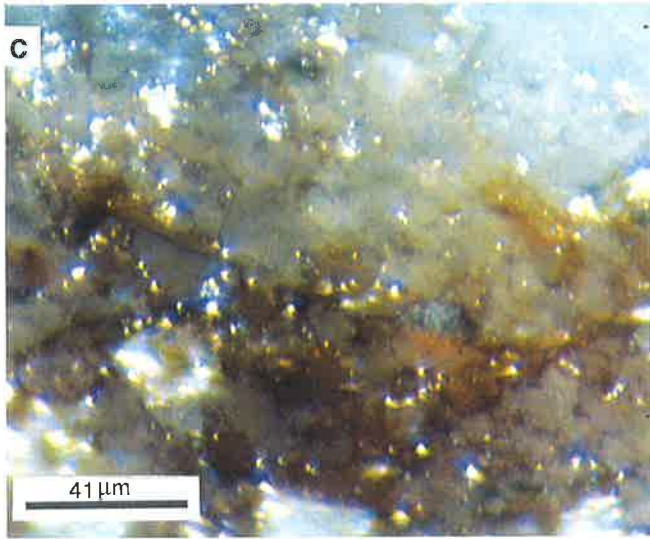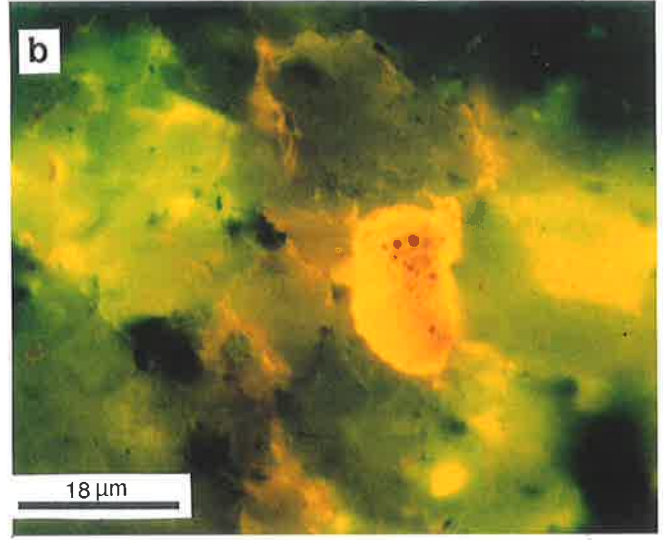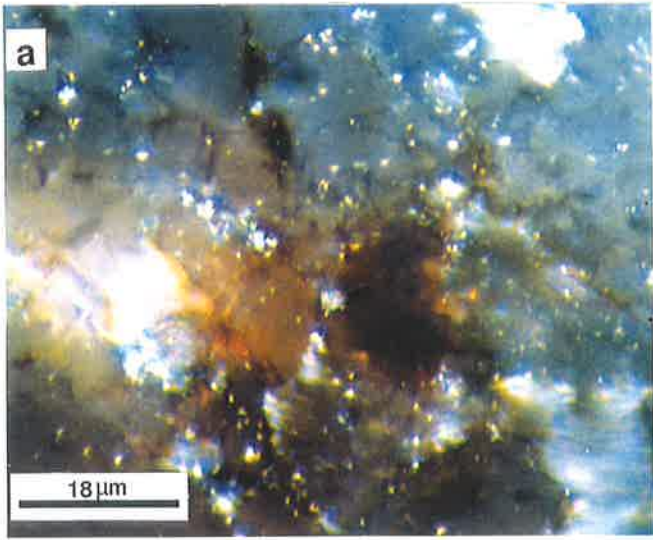
Plate 7.5

a) Sphaeromorph acritarch (FOV = 75 μm). A possible source organism for dinosterane in these rocks.

b) Benthic filamentous cyanobacteria, a dominant form of organic matter (FOV = 75 μm).

c) Membrane-like cyanobacterial mat and cyanobacterial coccoids indicated by arrows (FOV = 75 μm).
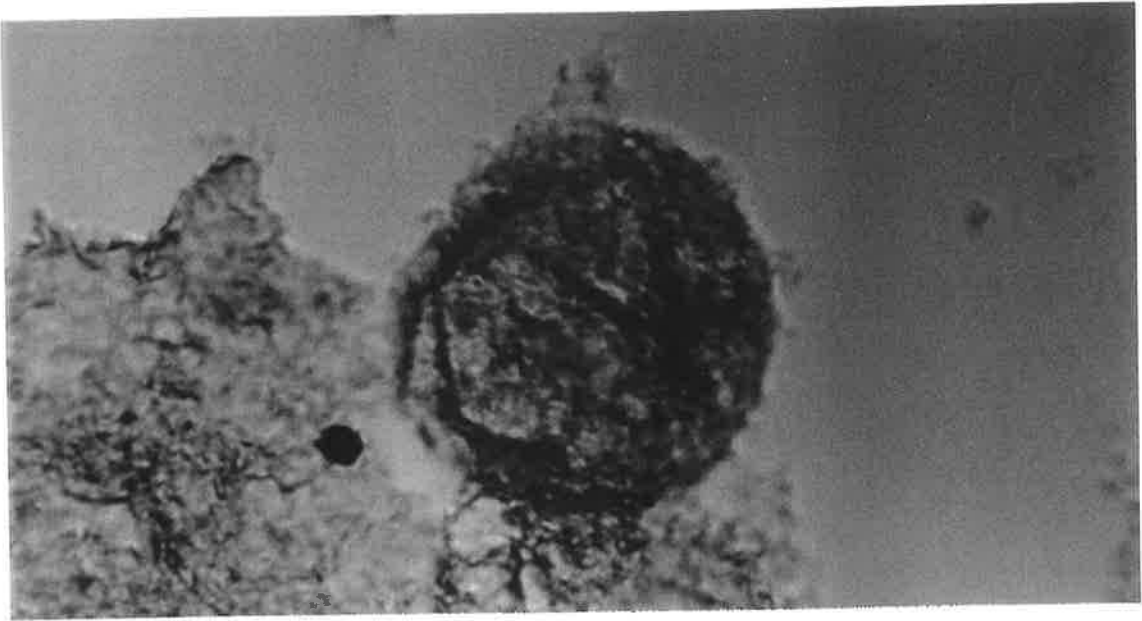
a
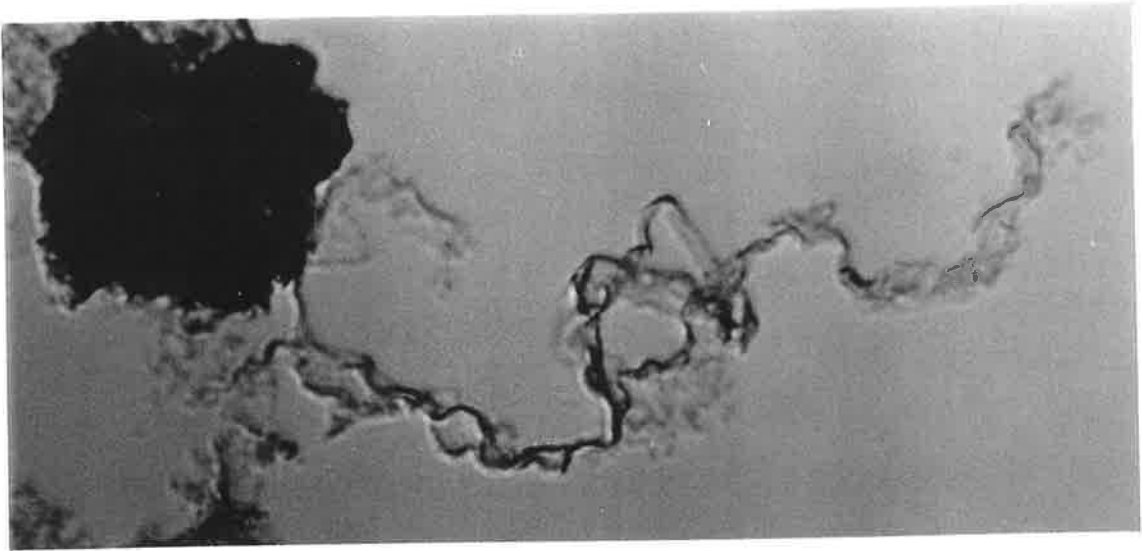
b
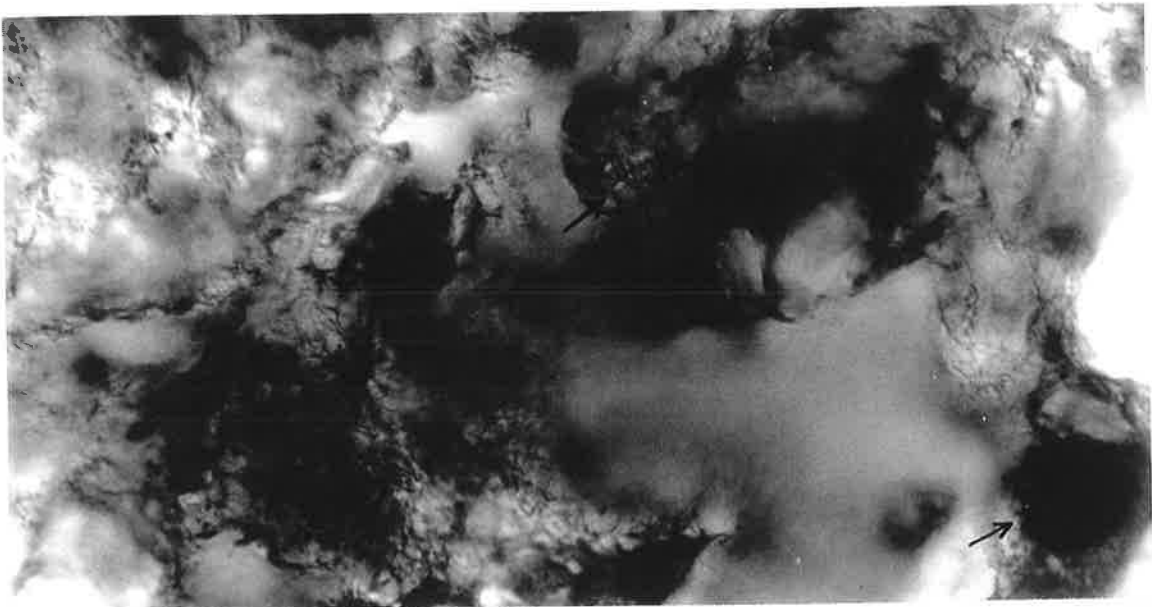
c

APPENDIX IX

GAS CHROMATOGRAMS OF

SATURATED HYDROCARBONS

OULDBURRA FORMATION

OFFICER BASIN

KEY

- Peak assignements refer to the carbon atom number of normal alkanes

- Pr = Pristanr

- Ph = Phtane
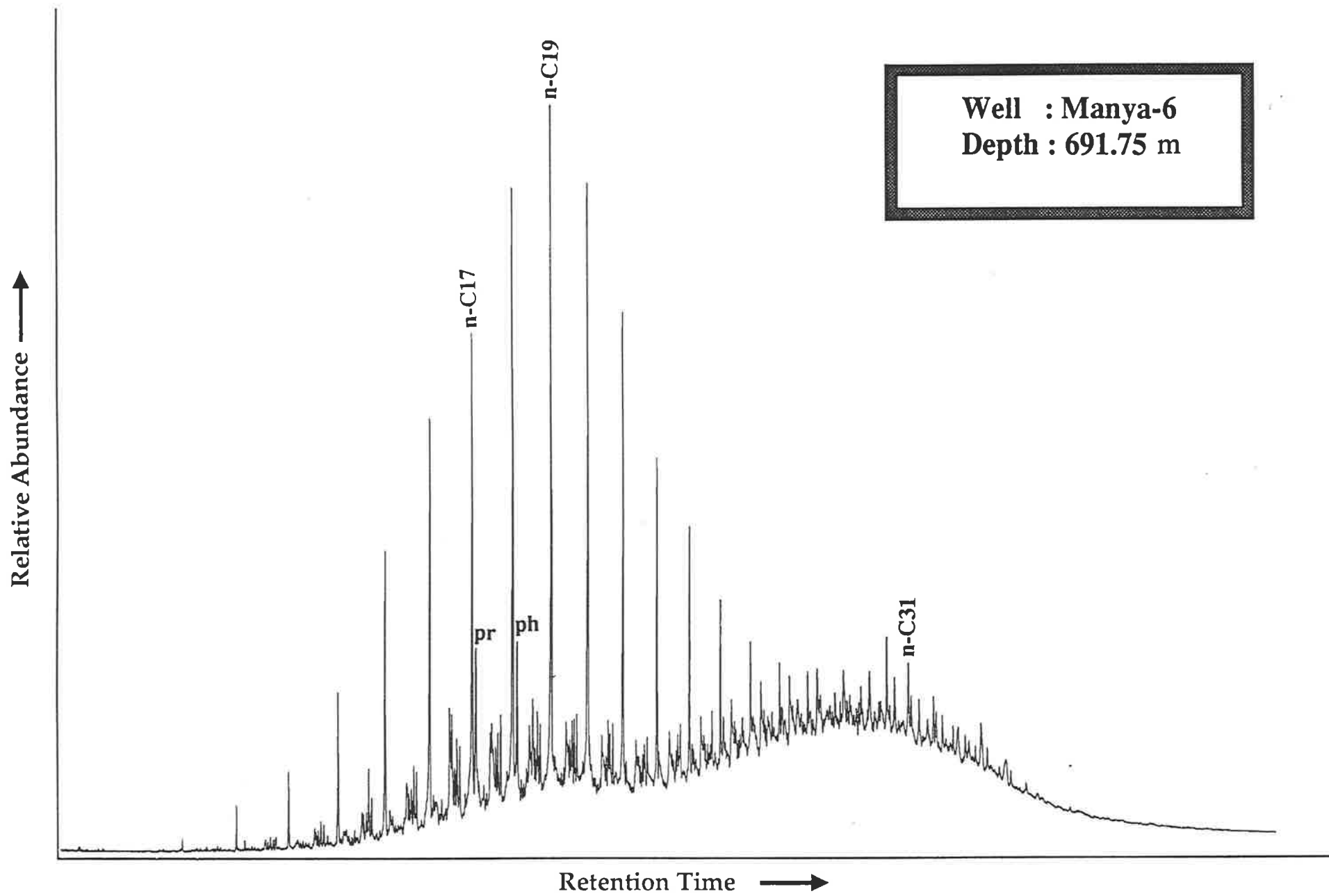
Well : Manya-6
Depth : 698.60 m
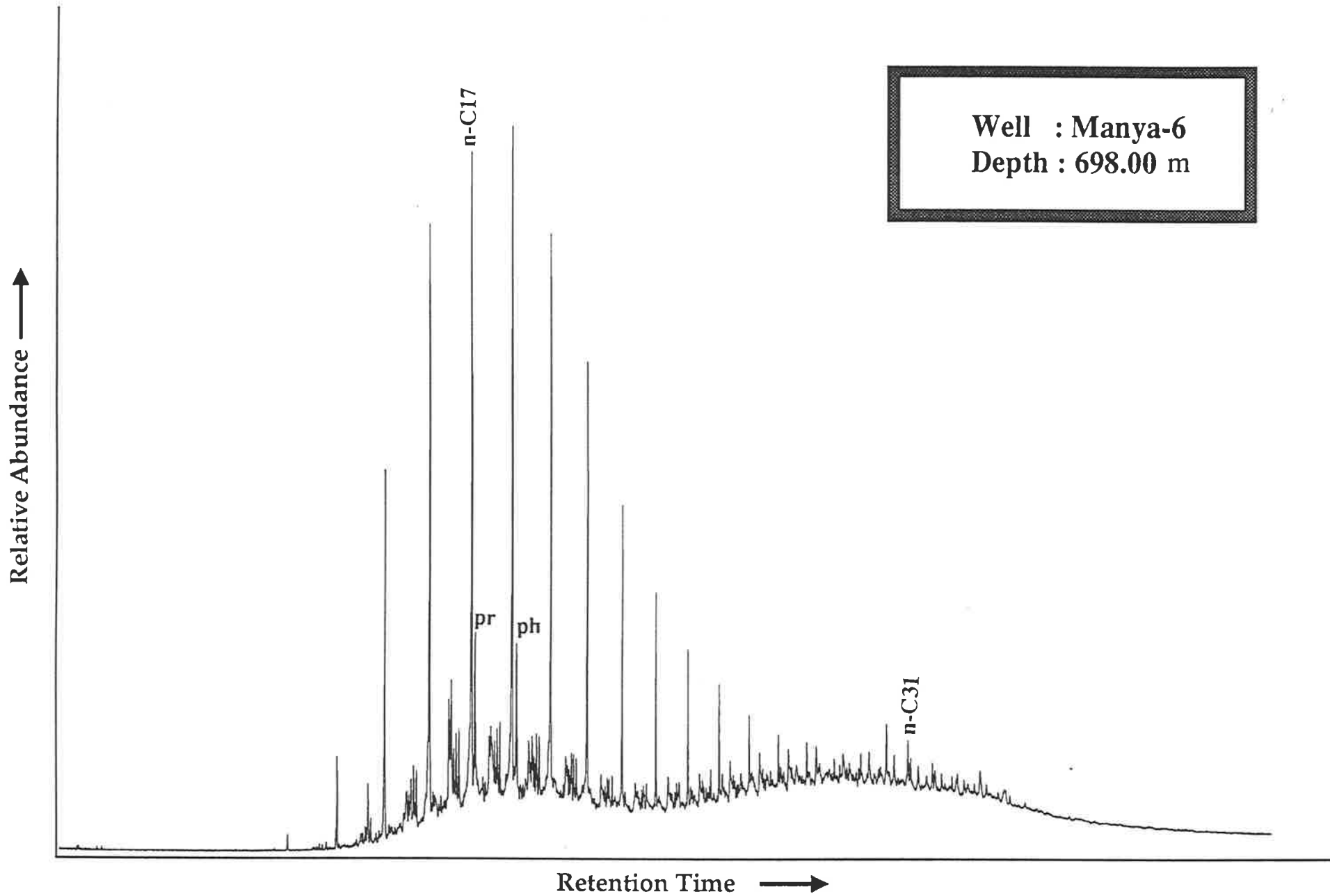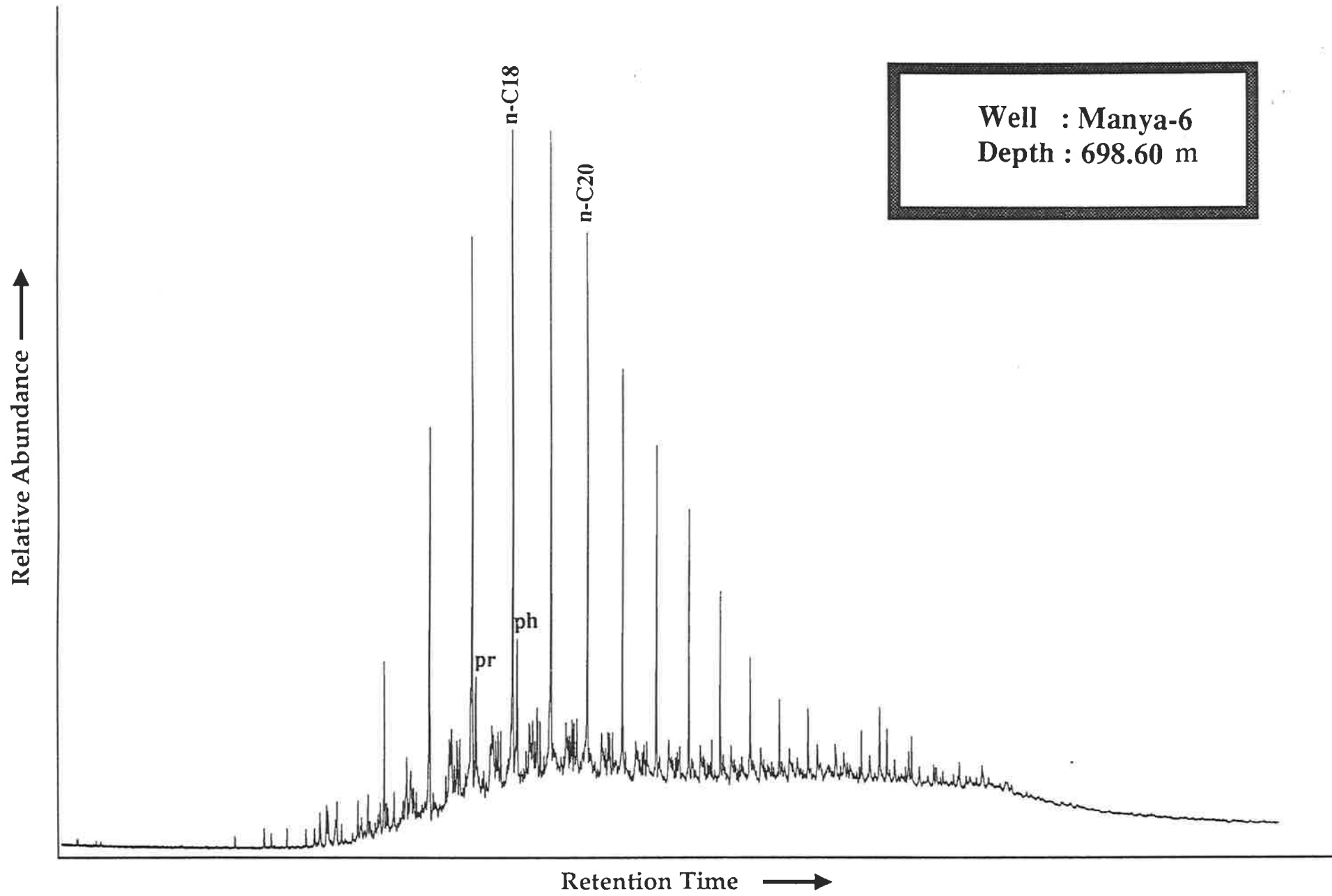
Well : Manya-6
Depth : 1279.15 m
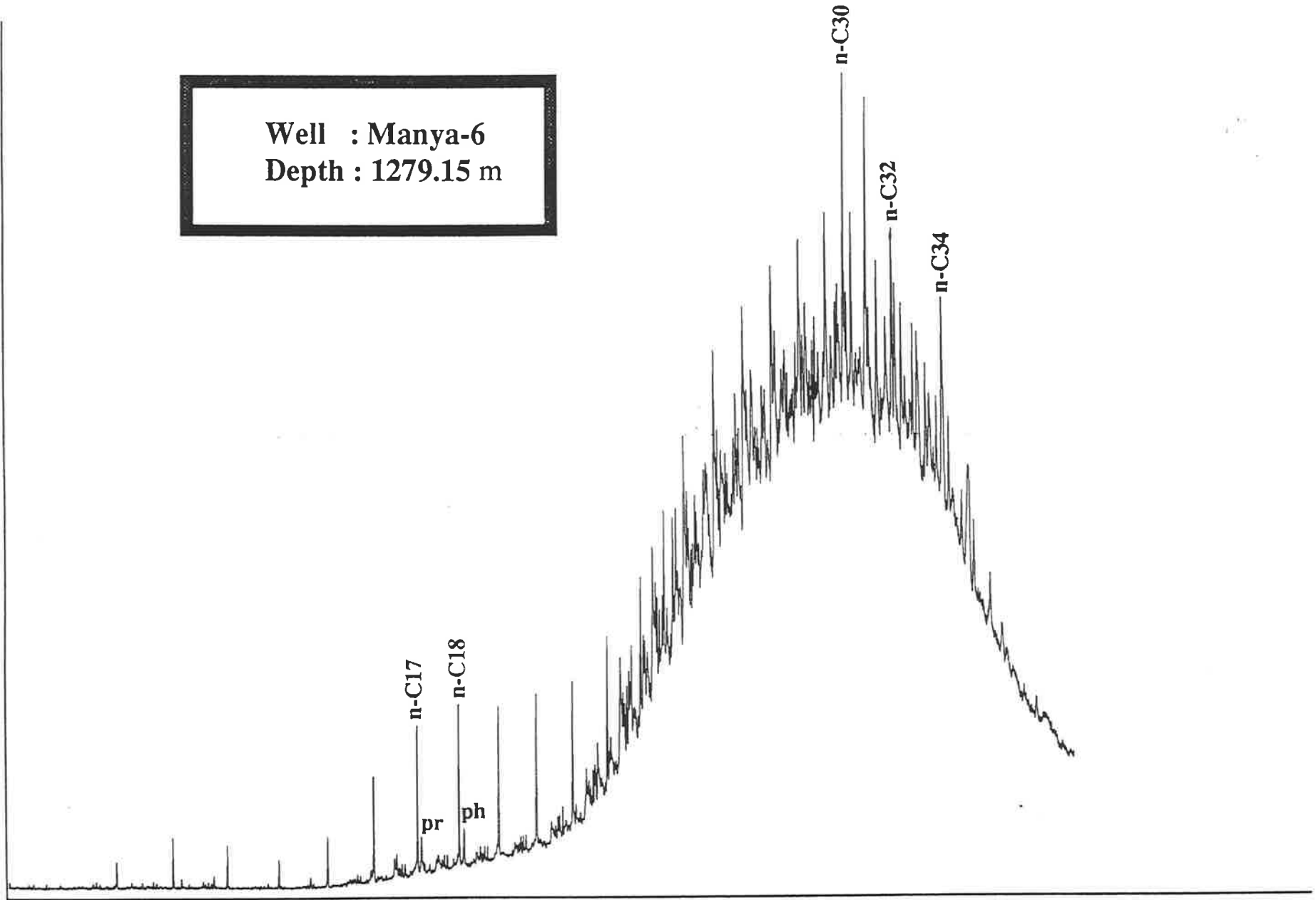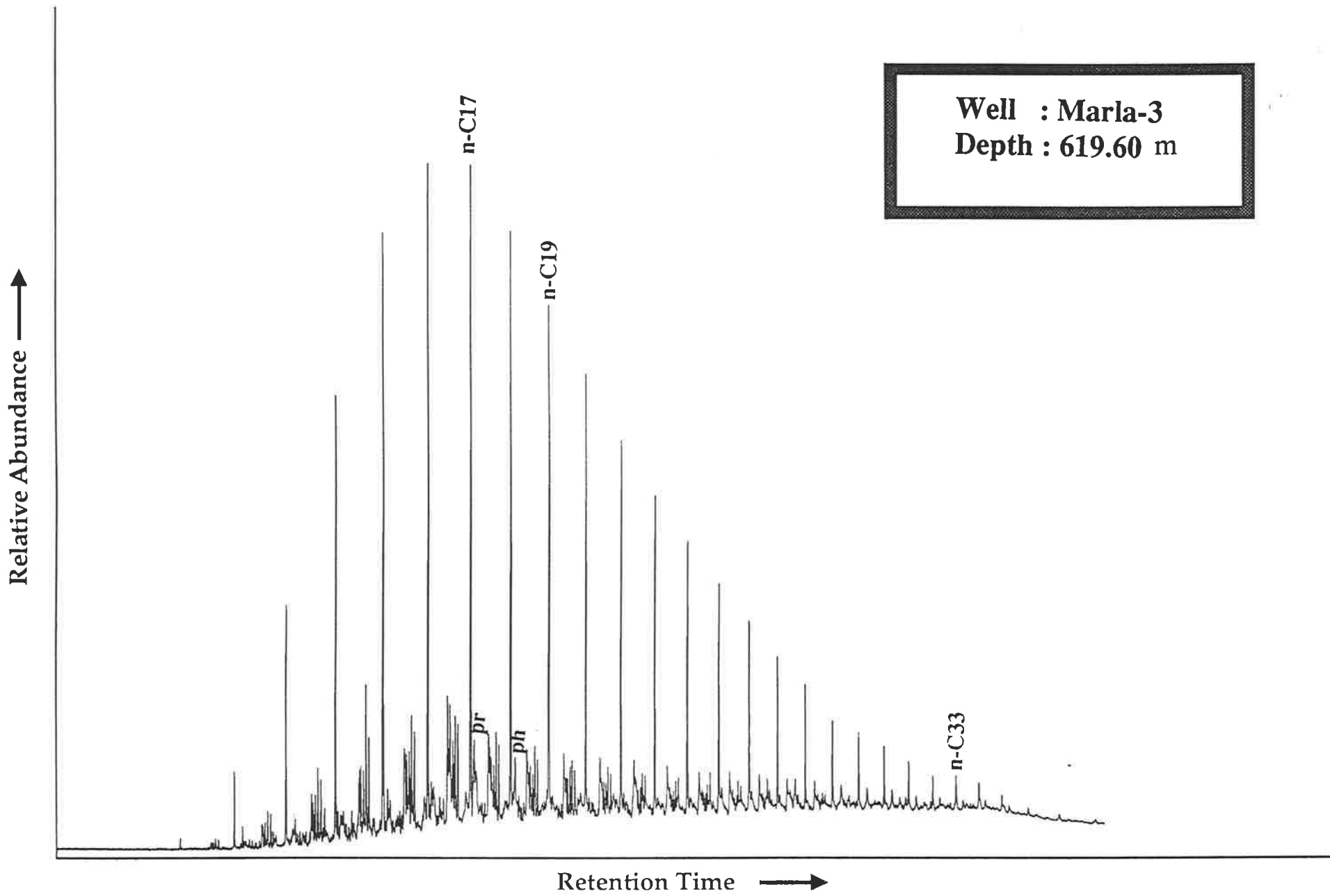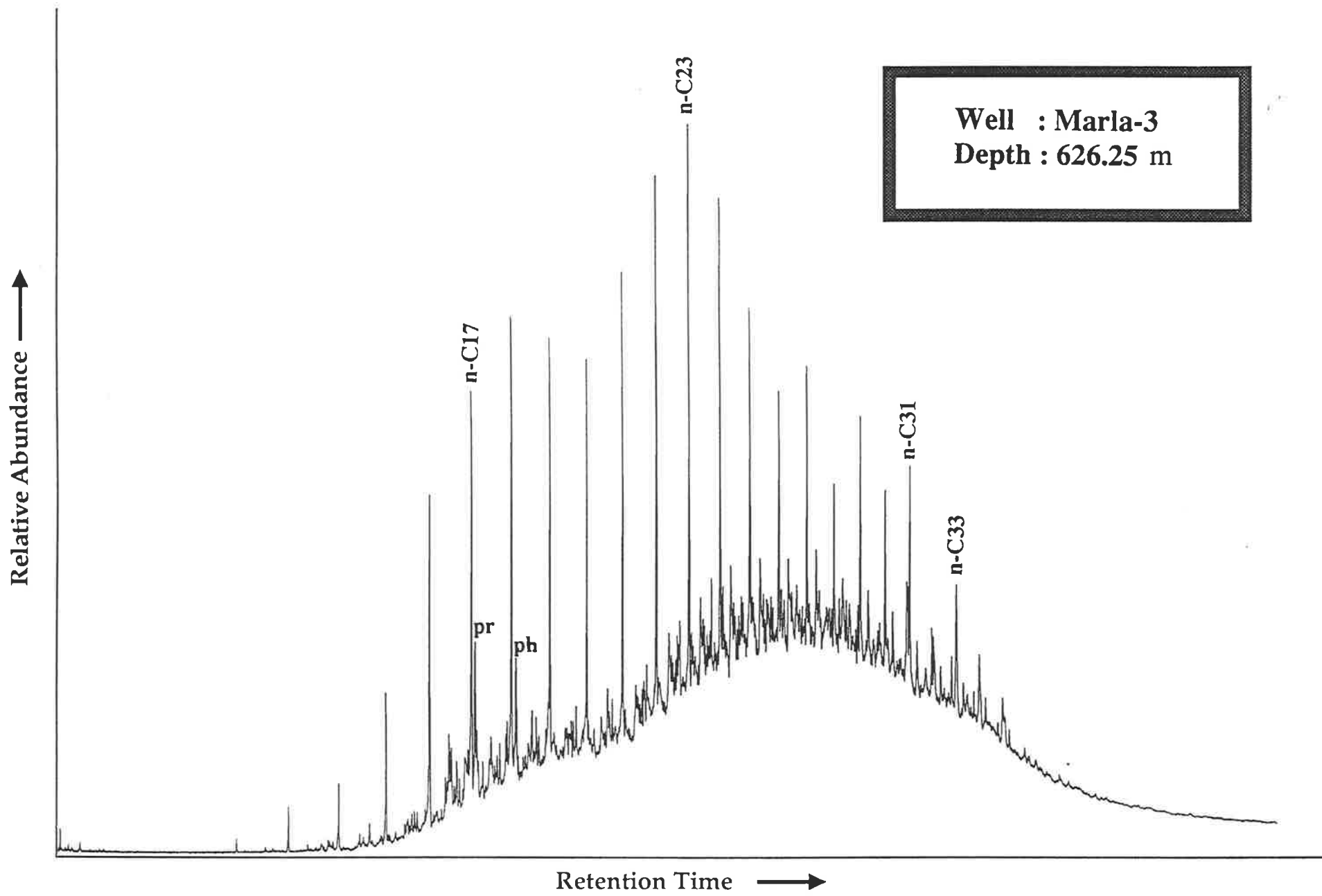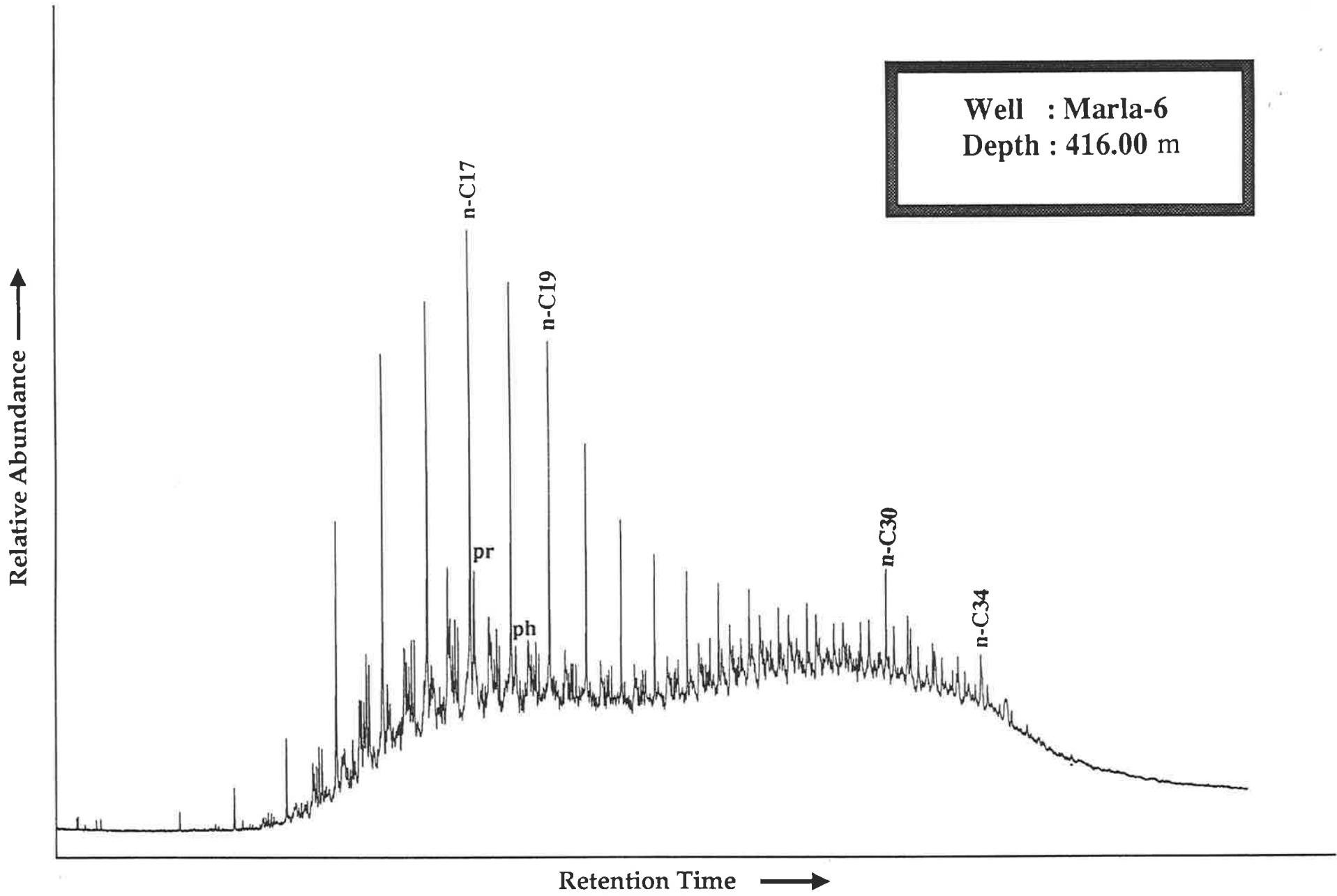
Well : Marla-3
Depth : 619.60 m

Well : Marla-6
Depth : 671.25 m
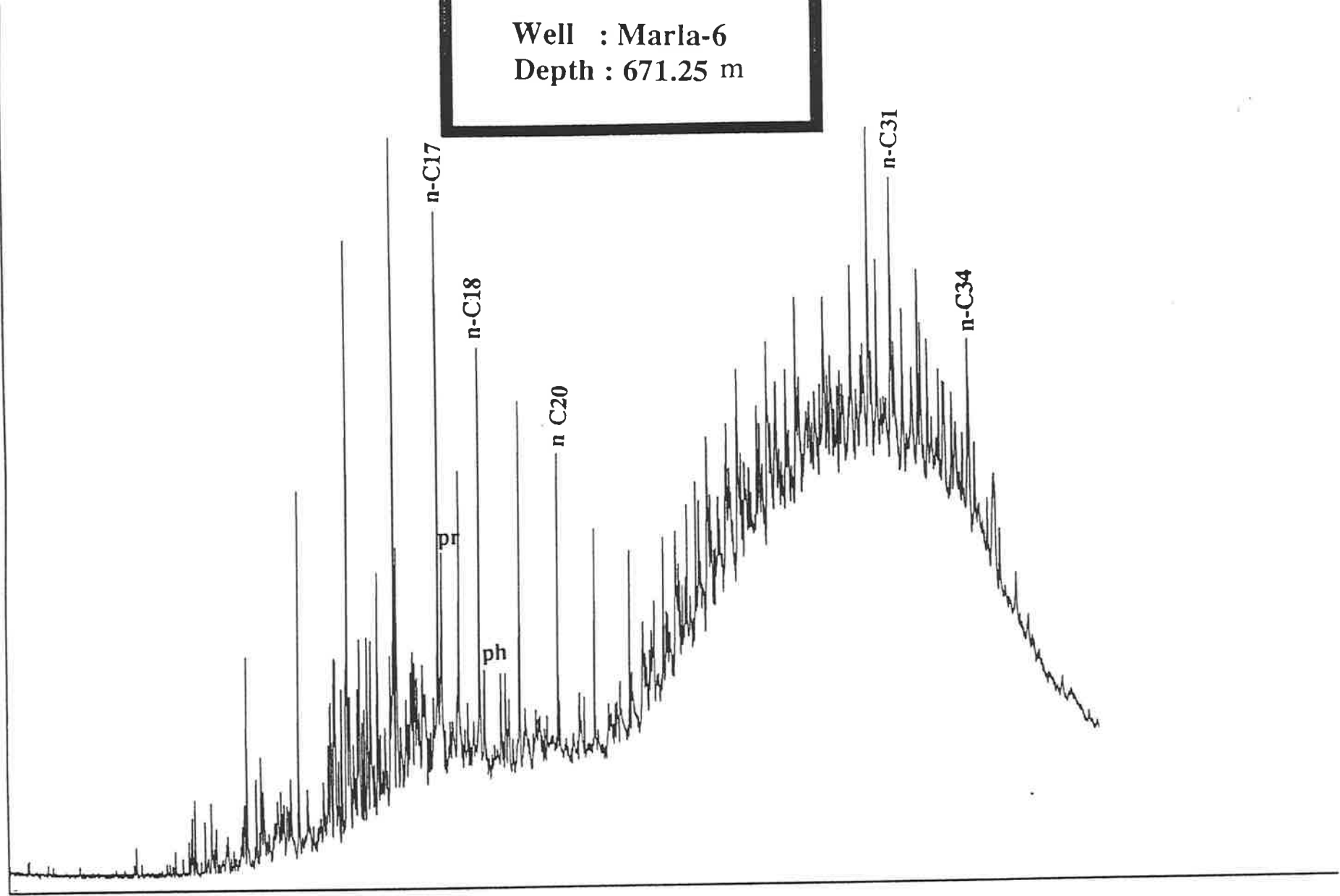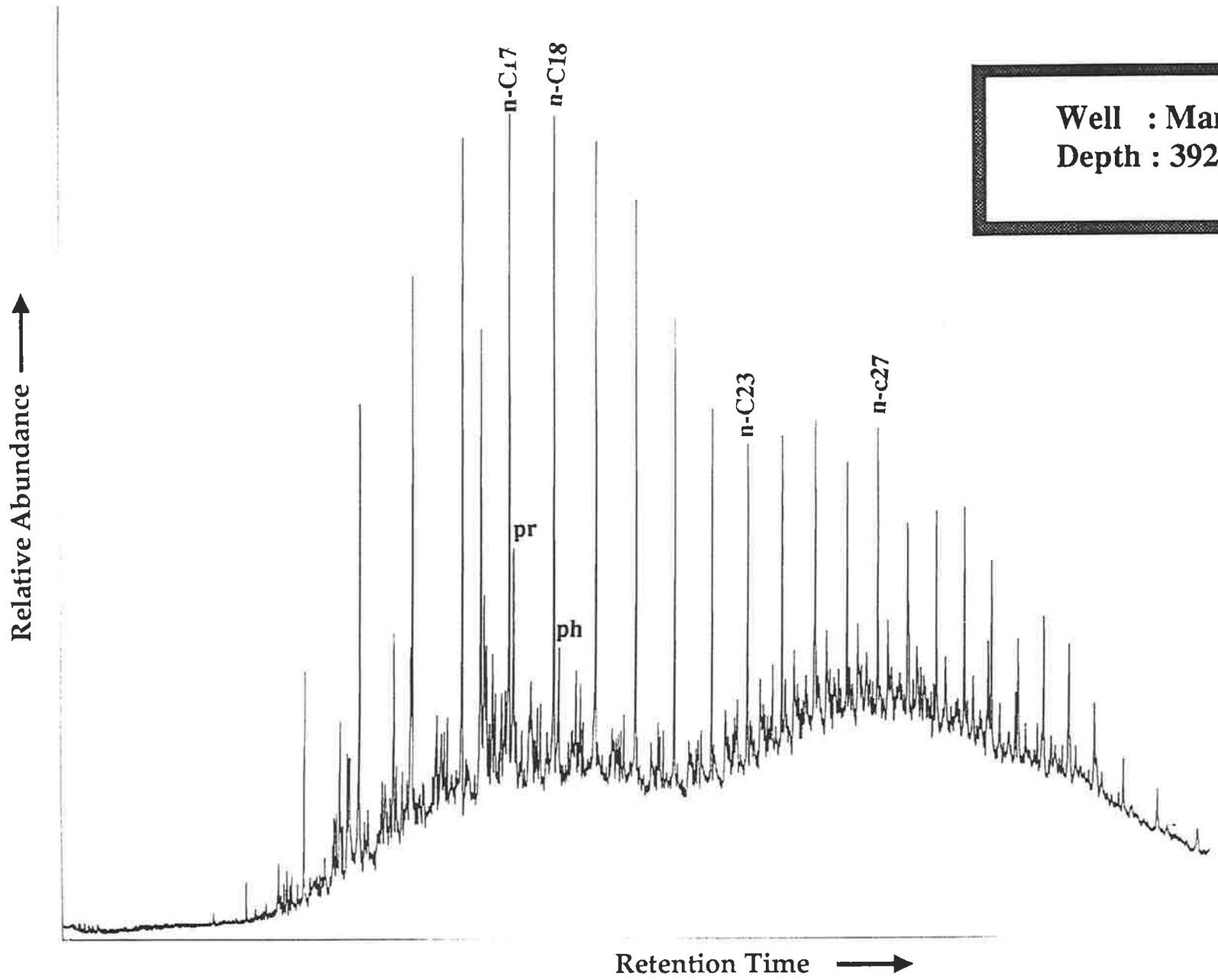
Well : Marla-7
Depth : 392.85 m

Well : KD-2A
Depth : 285.50 m
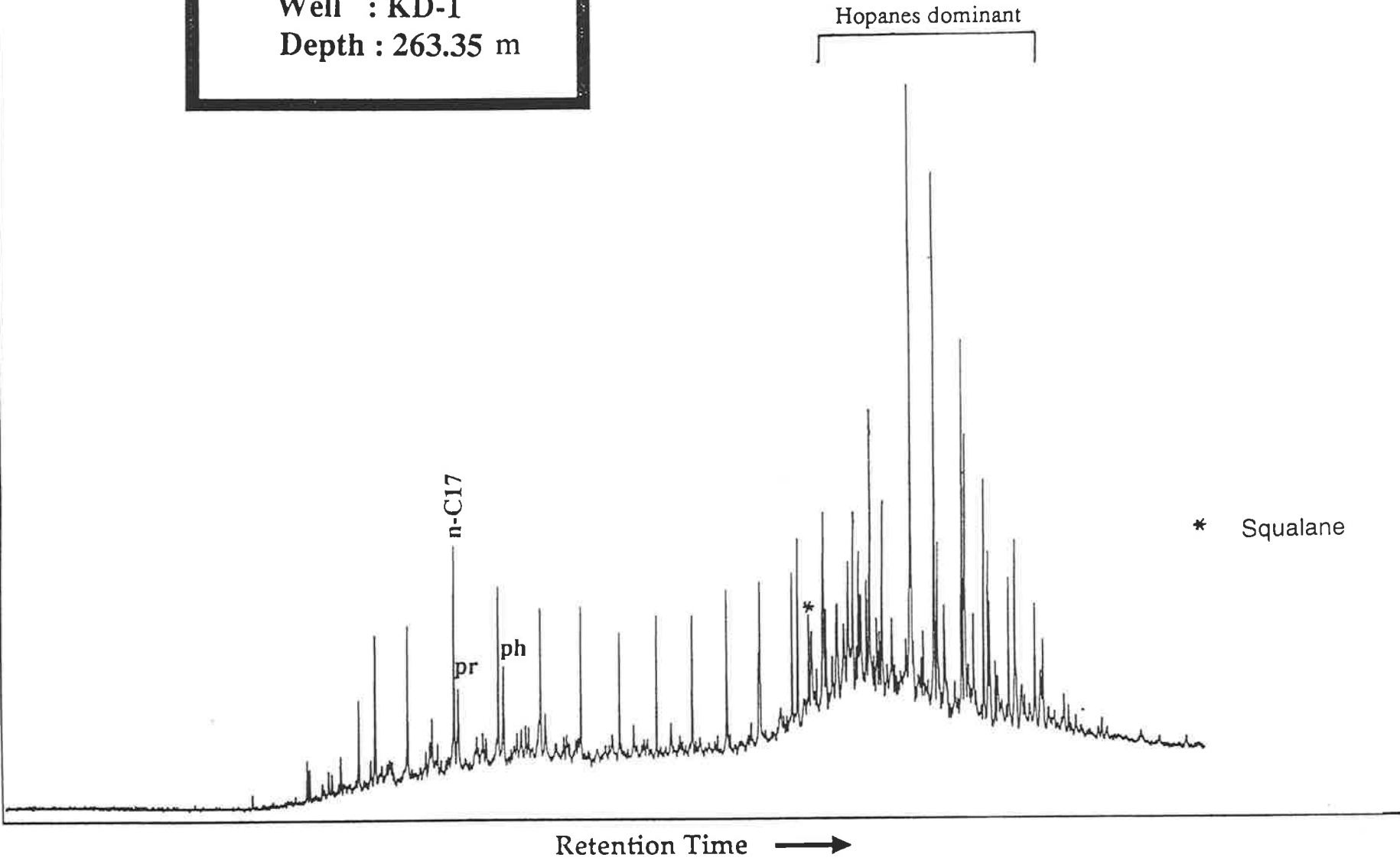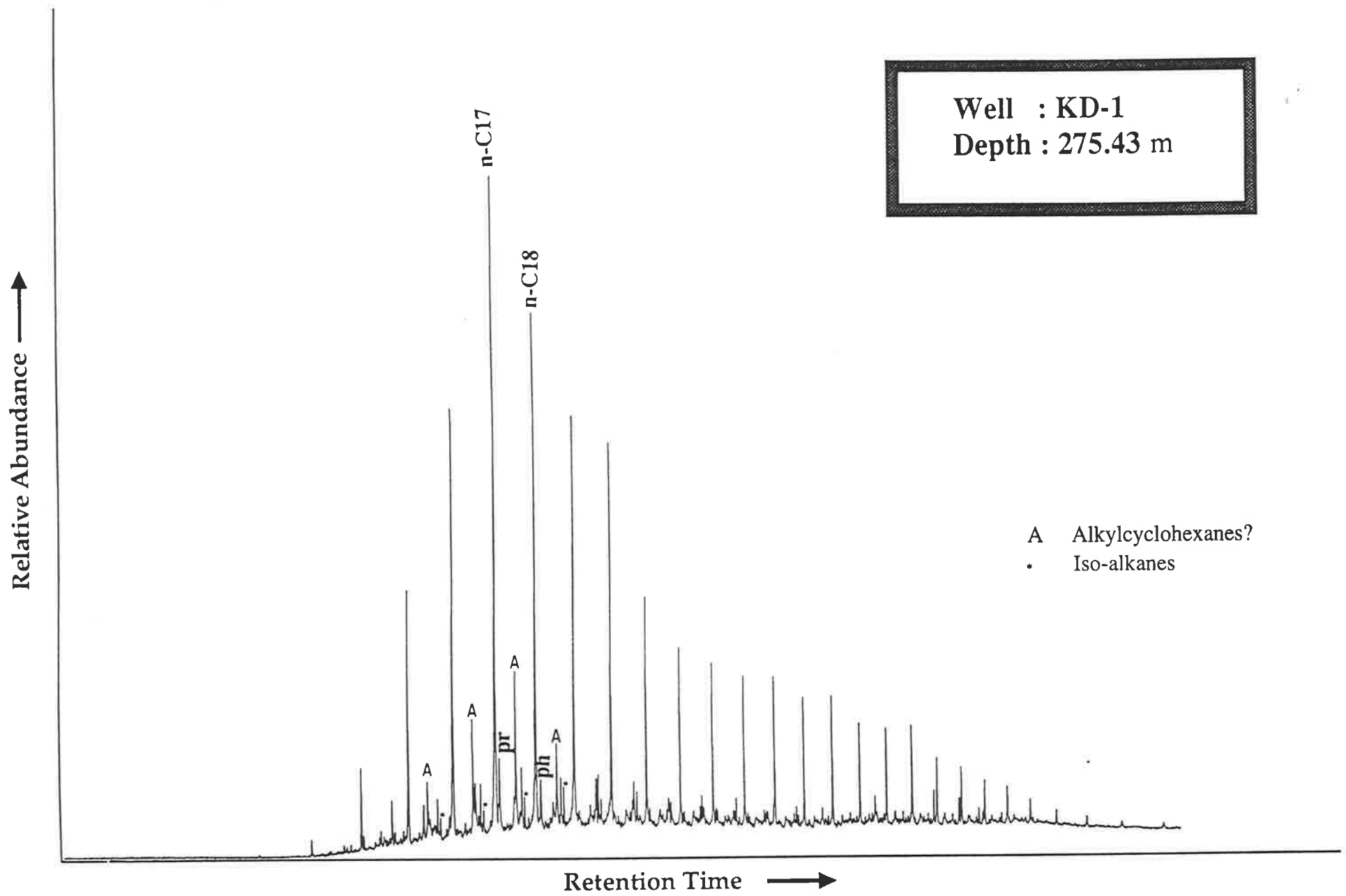
Hopanes dominant

Relative Abundance →

n-C17

pr

ph

*
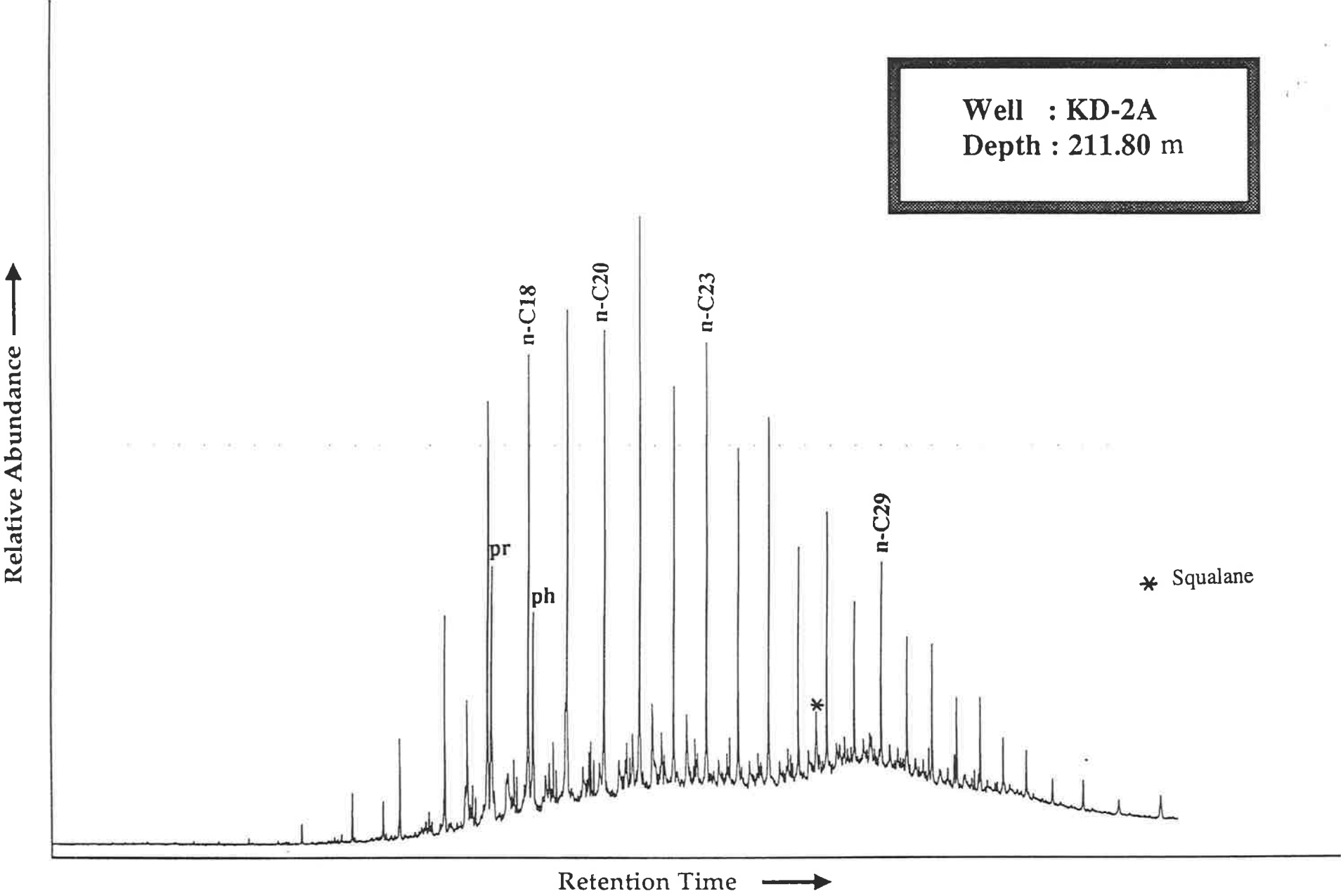
* squalane
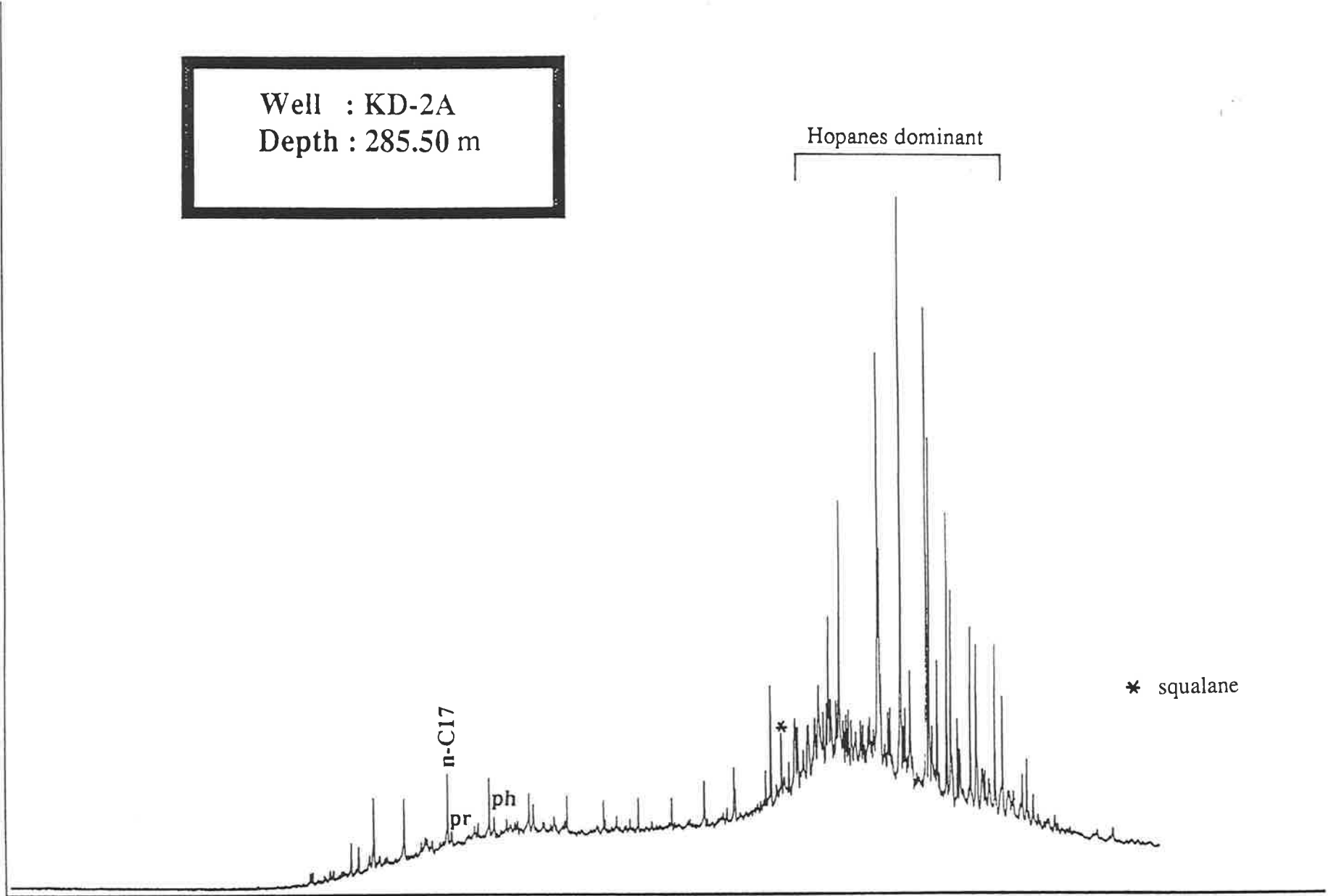
Retention Time →
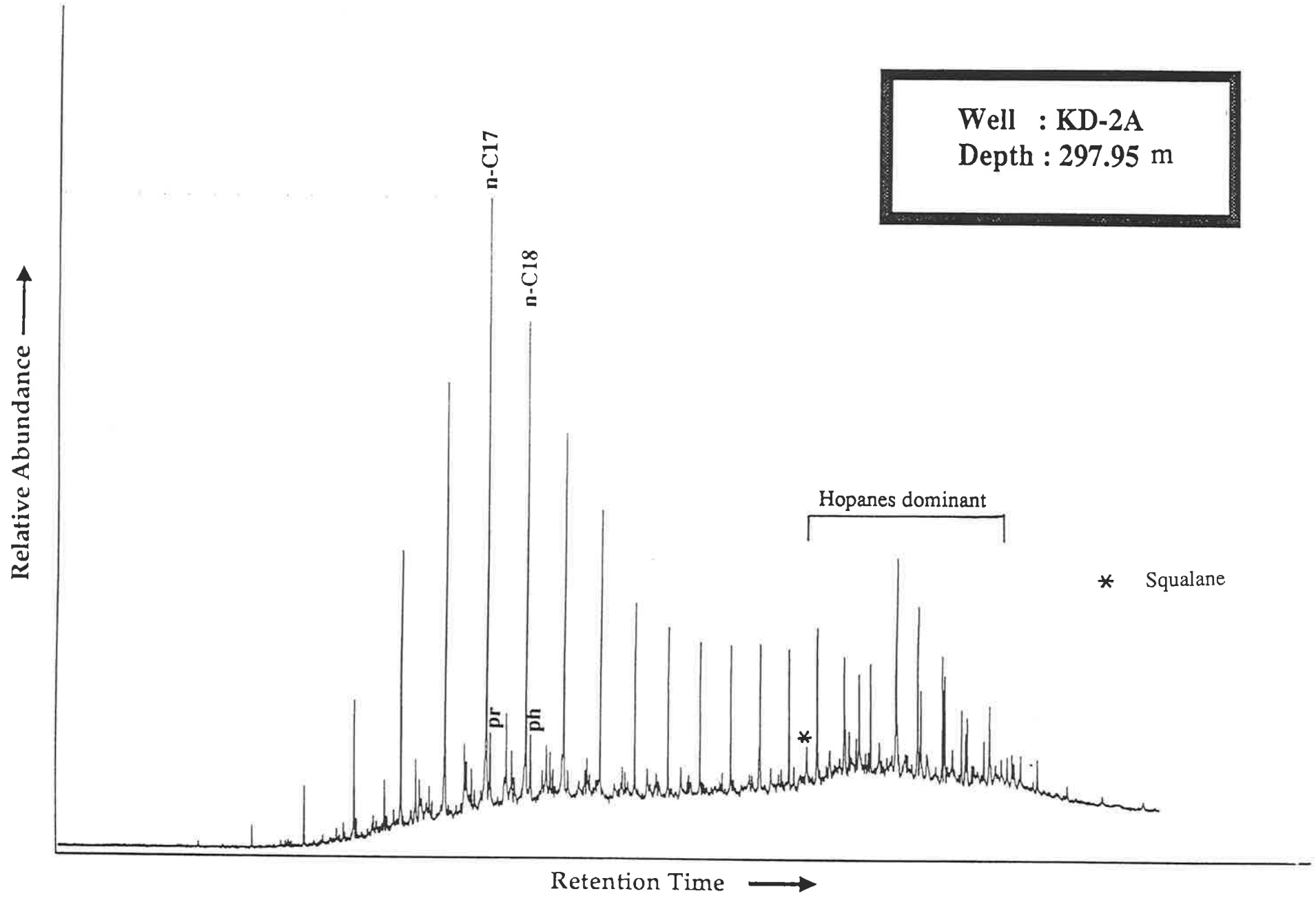
APPENDIX X

PYROLYSIS GAS CHROMATOGRAMS

OF KEROGEN

OULDBURRA FORMATION

OFFICER BASIN

KEY

-Numbered peaks denote chain length of *n*-alk-1-ene and *n*-alkane doublets

-Bz = Benzene

- Tol = Toluene.

- X = Xylenes

- S = Internal Standard.

Manya-6 698.6 m
Pyrolysis-GC
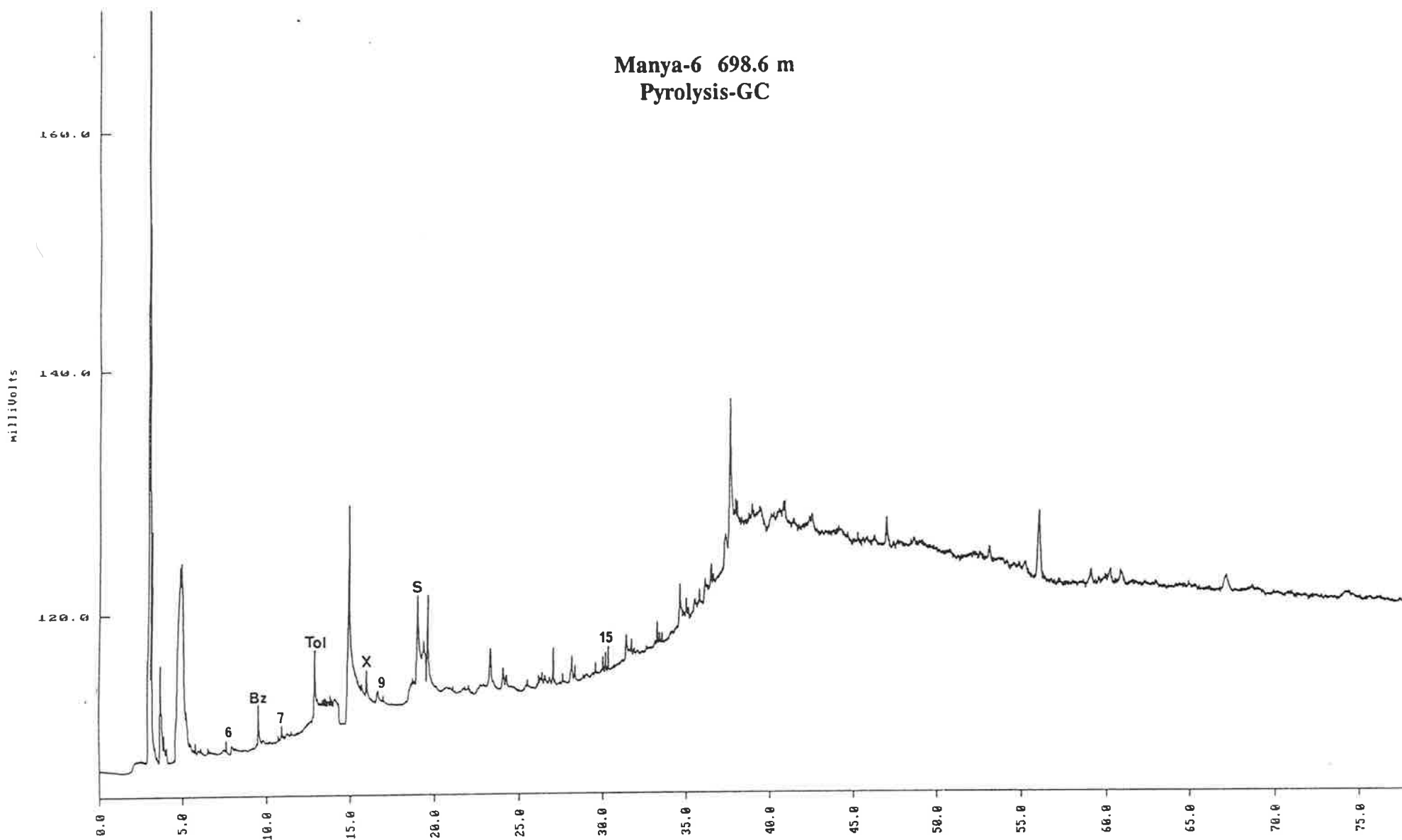
Marla-6 416 m
Pyrolysis-GC
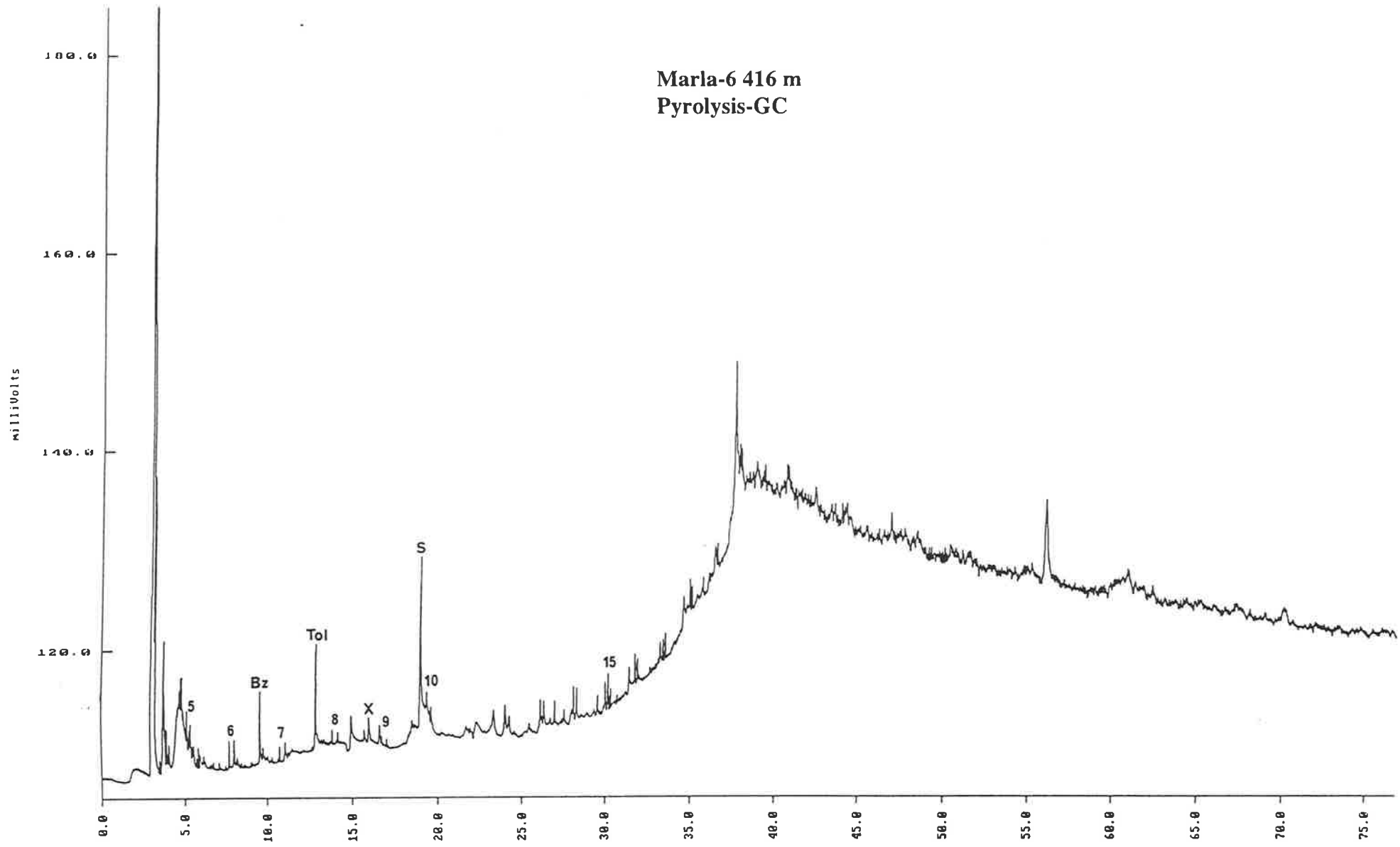
Marla-7 392.8 m
Pyrolysis-GC

KD-1 263.35 m
Pyrolysis-GC
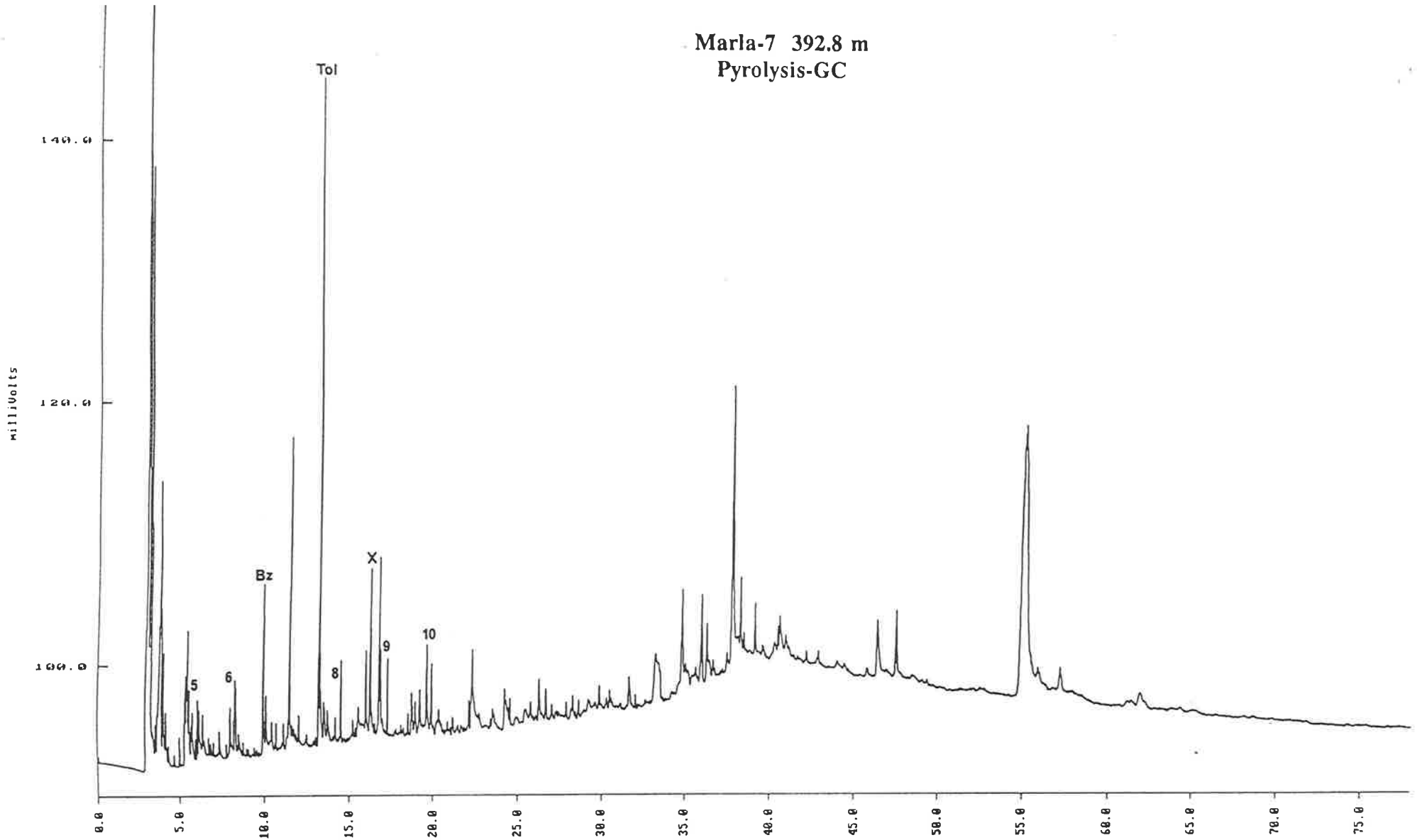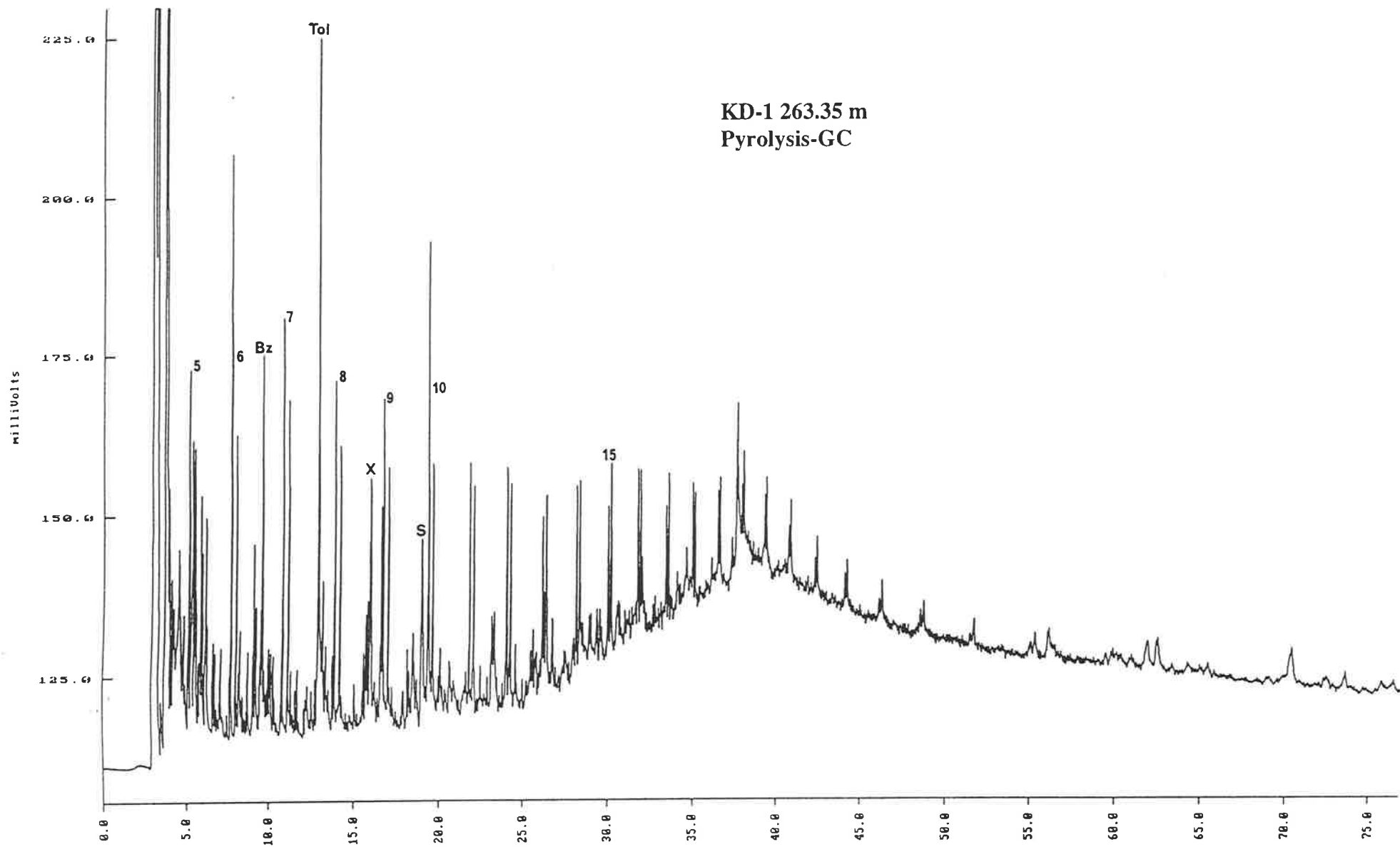
KD-2A 285 m
Pyrolysis-GC
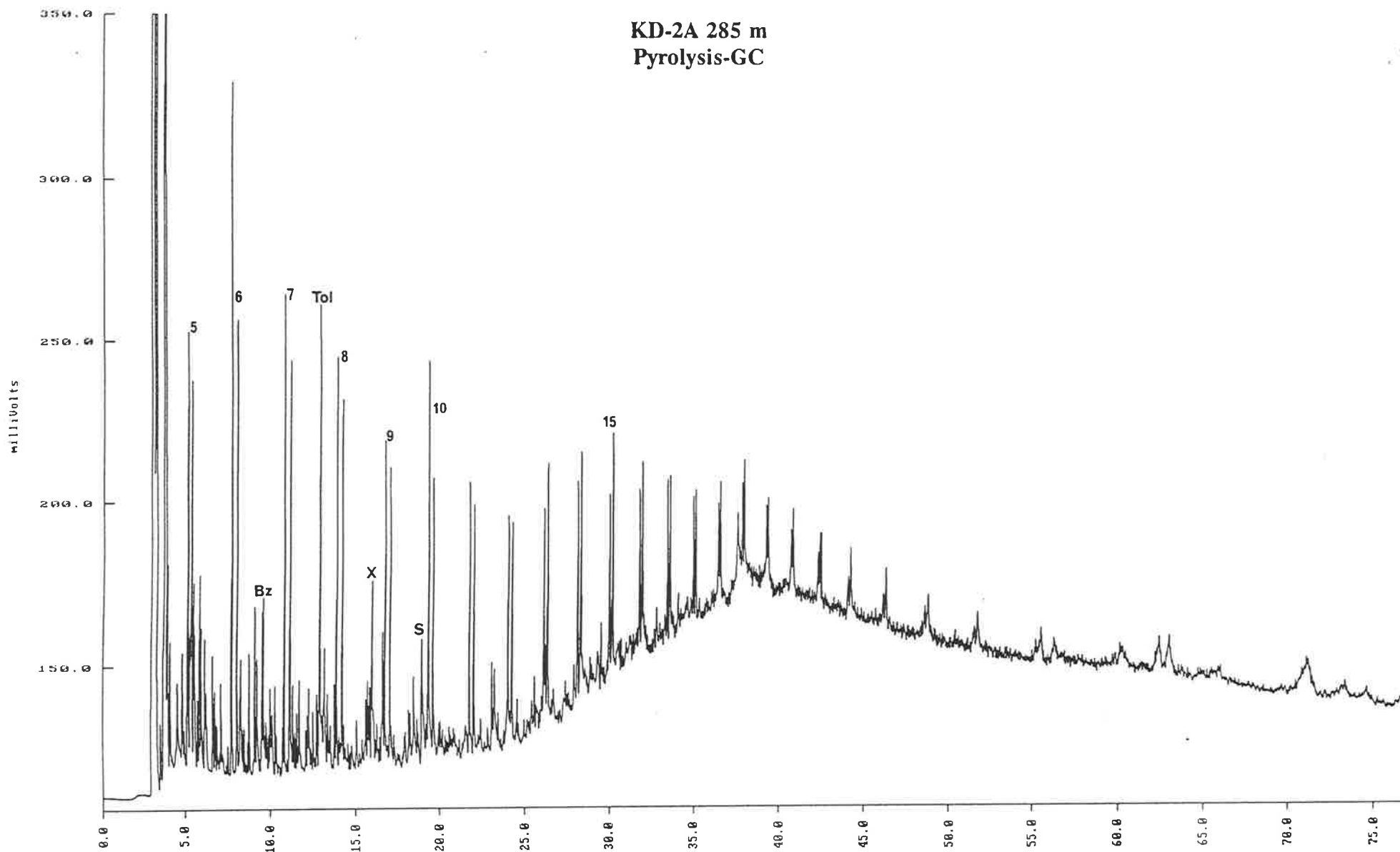
APPENDIX XI

MASS CHROMATOGRAMS OF

TRIAROMATIC HYDROCARBONS

OULDBURRA FORMATION

OFFICER BASIN

CHRO: BMRARO2 ver 1 on UIC 3 1   11-AUG-94 Elapse: 00:03:03.5   1
Samp: MARLA-6 416.00m   Start : 06:45:20   3219
Comm: DB-5 30m,10psi on-col,ICL=BMAROM,200uA 1100V,S=150 M=60
Mode: EI +Q3MS LMR UP LR
Oper: MICHAELSEN   Inlet :
Peak: 1000.00 mmu   Label wndw: 1910 > 2495   Masses: 128 > 253
Area: 0, 4.00   Baseline : 0, 3   Label : 0, 40.00
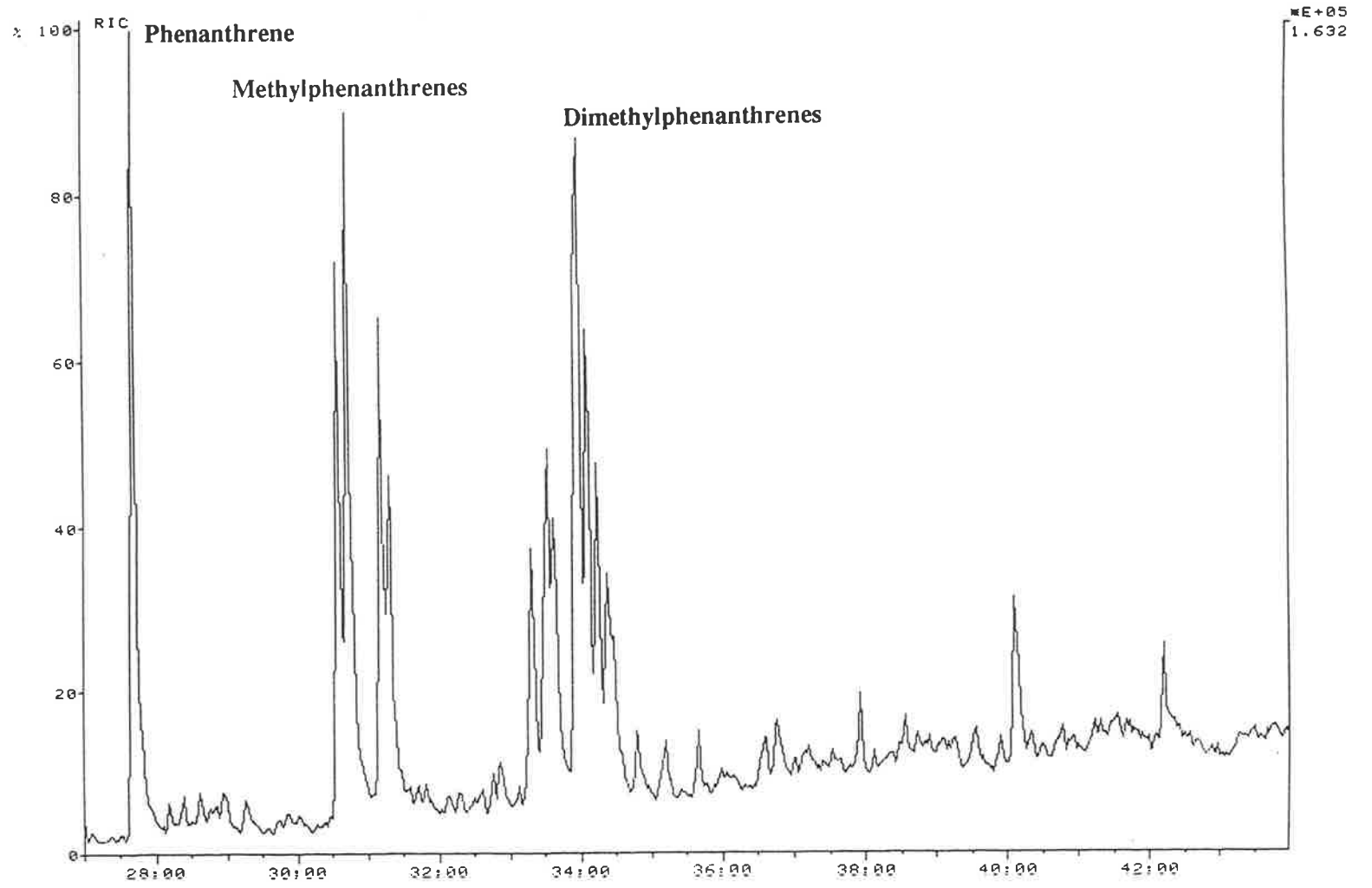
CHRO: BMRARO5 ver 1 on UIC 3 1   11-AUG-94 Elapse: 00:03:05.4   1
Samp: MARLA-7 392.85m   Start : 08:16:24 3217
Comm: DB-5 30m,10psi on-col,ICL=BMAROM,200uA 1100V,S=150 M=60
Mode: EI +Q3MS LMR UP LR
Oper: MICHAELSEN   Inlet :
Peak: 1000.00 mmu   Label wndw: 1907 > 2493   Masses: 128 > 253
Area: 0, 4.00   Baseline : 0, 3   Label : 0, 40.00
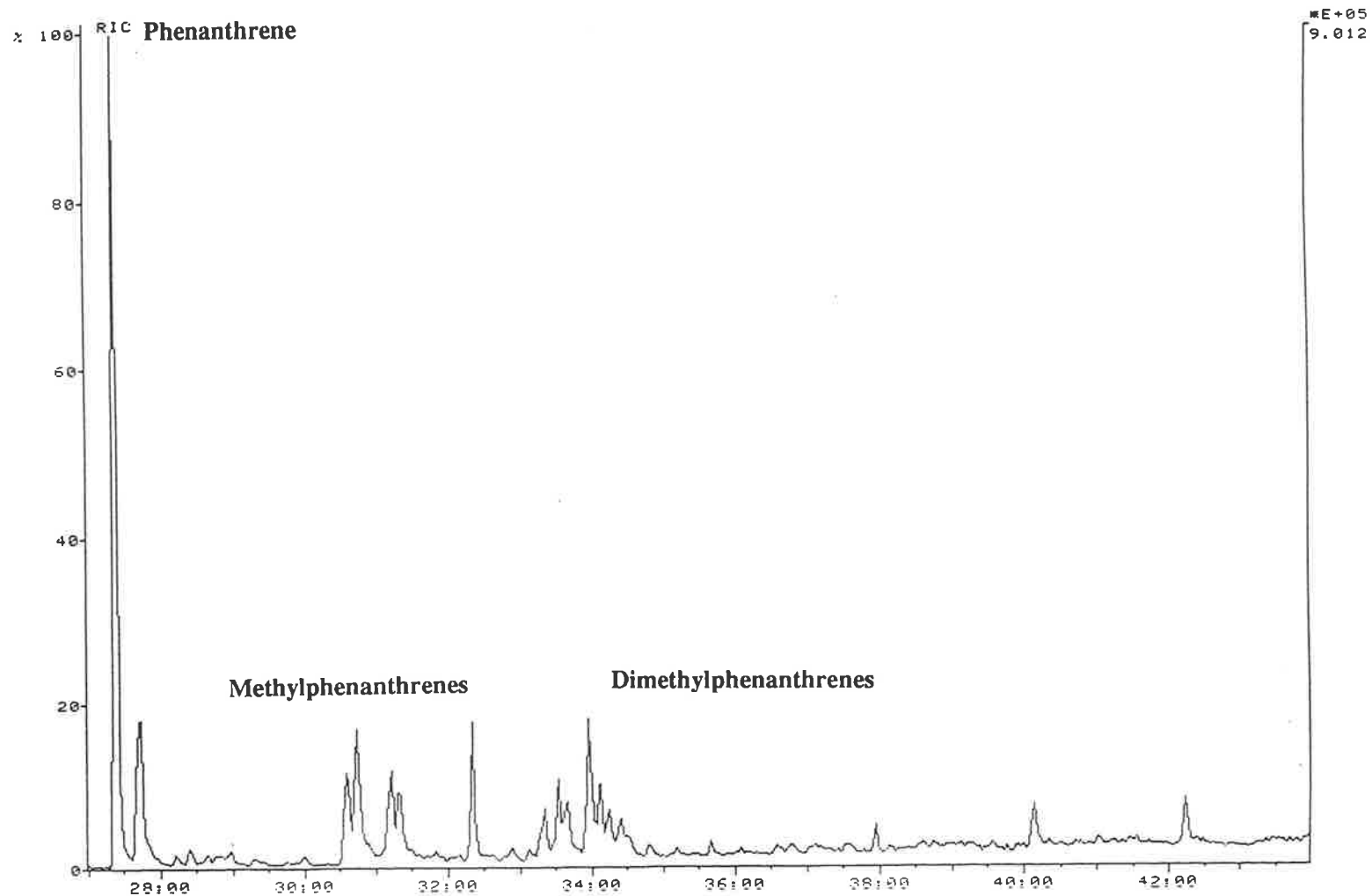
CHRO: BMRARO1 ver 1 on UIC 3 1   11-AUG-94 Elapse: 00:03:05.3   1
Samp: KD-1   263.35m   Start : 03:26:30   3217
Comm: DB-5 30m,10psi on-col,ICL=BMAROM,200uA 1100V,S=150 M=60
Mode: EI +Q3MS LMR UP LR
Oper: MICHAELSEN   Inlet :
Peak: 1000.00 mmu   Label wndw: 1908 > 2493   Masses: 128 > 253
Area: 0, 4.00   Baseline : 0, 3   Label : 0, 40.00
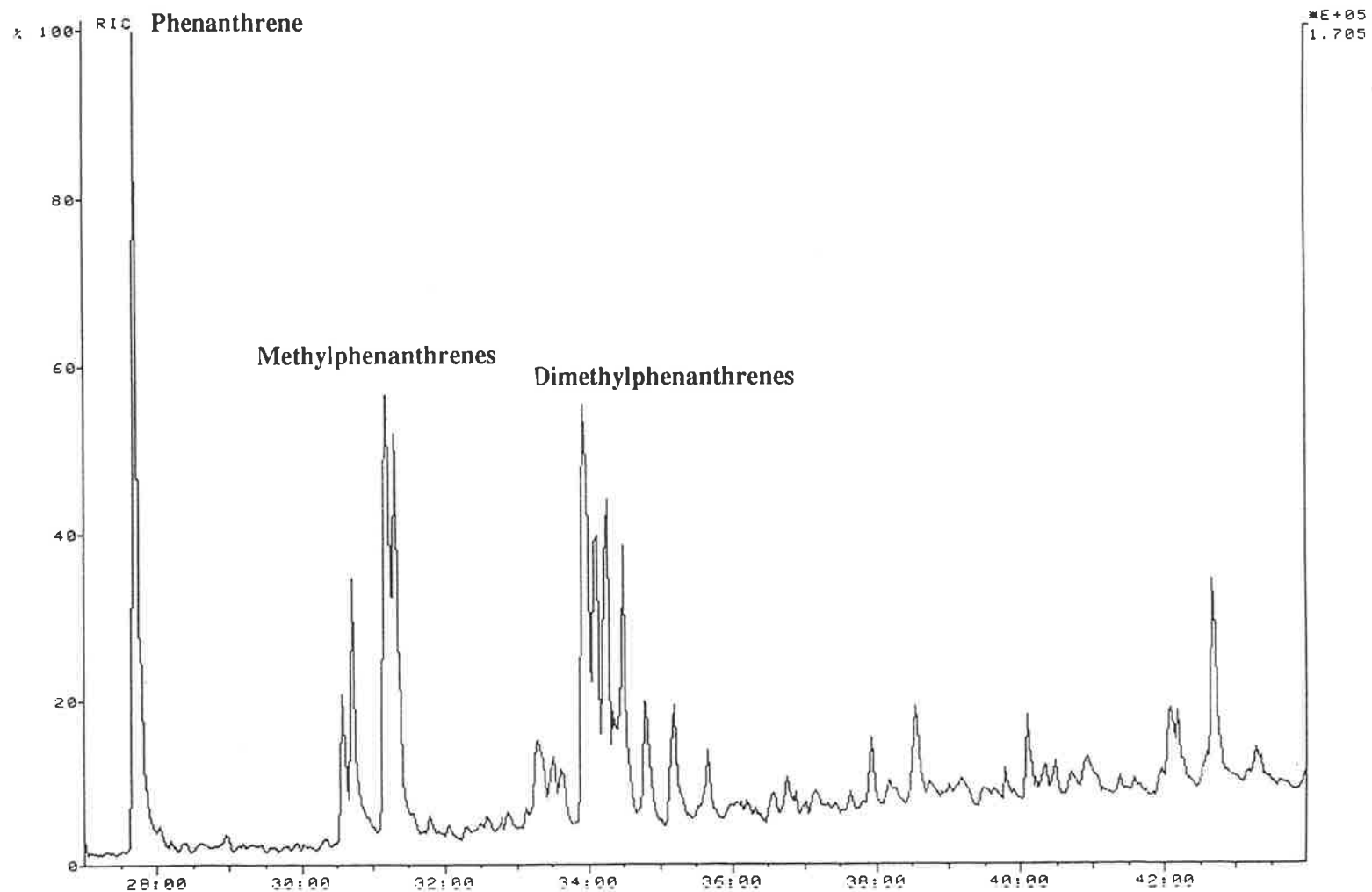
CHRO: BMRARO3 ver 1 on UIC 3 1   11-AUG-94 Elapse: 00:03:05.4   1
Samp: KD-2A 285.5m   Start : 01:55:02   2686
Comm: DB-5 30m,10psi on-col,ICL=BMAROM,200uA 1100V,S=150 M=60
Mode: EI +Q3MS LMR UP LR
Oper: MICHAELSEN   Inlet :
Peak: 1000.00 mmu   Label undw: 1908 > 2493   Masses: 205 > 253
Area: 0, 4.00   Baseline : 0, 3   Label : 0, 40.00
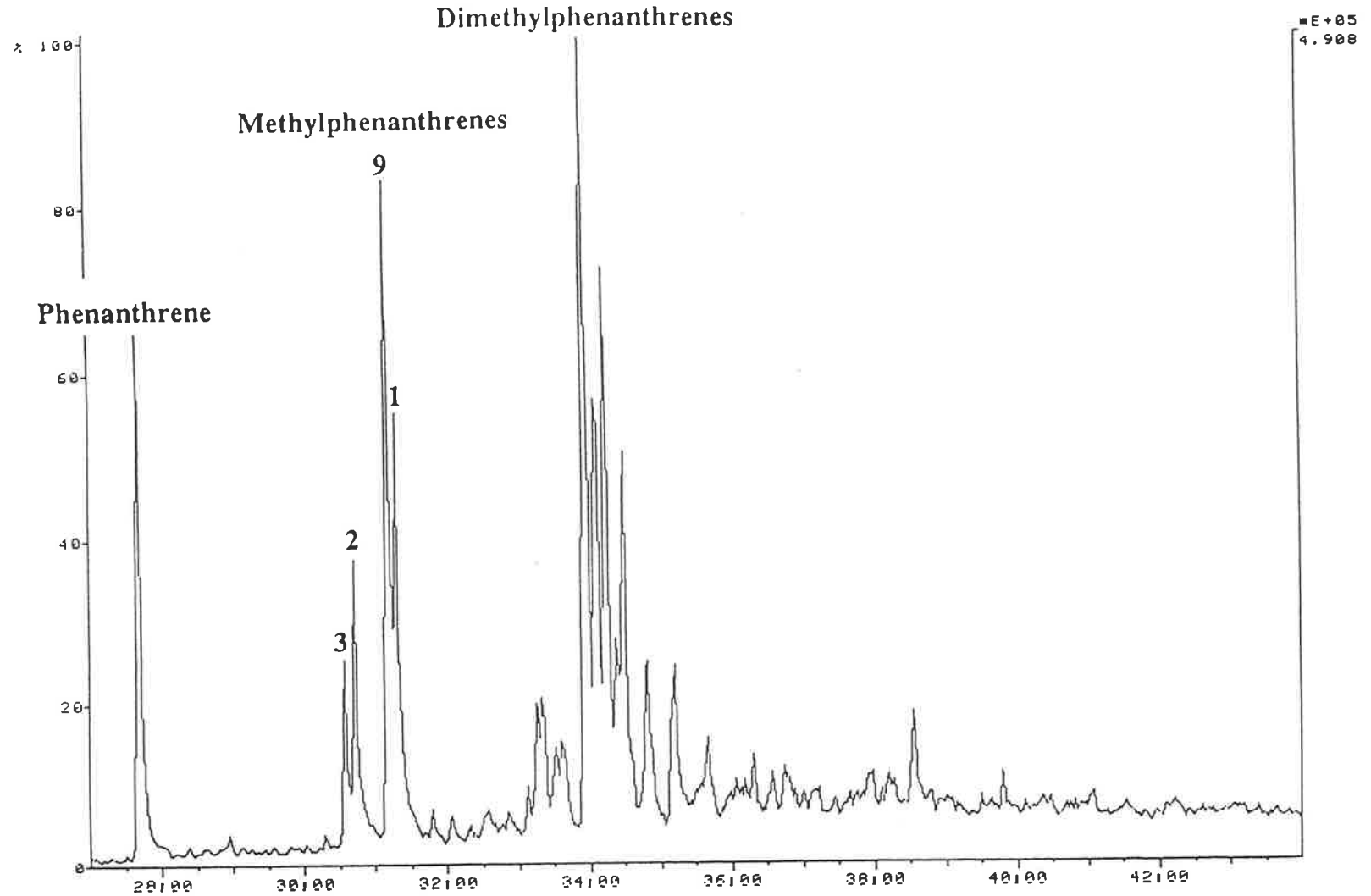
CHRO: BMRARO4 ver 2 on UIC 3 1   11-AUG-94 Elapse: 00:03:04.6   1
Samp: KD-2A 297.95m   Start : 05:06:06 3218
Comm: DB-5 30m,10psi on-col,ICL=BMAROM,200uA 1100V,S=150 M=60
Mode: EI +Q3MS LMR UP LR
Oper: MICHAELSEN   Inlet :
Peak: 1000.00 mmu   Label wndw: 1909 > 2494   Masses: 128 > 253
Area: 0, 4.00   Baseline : 0, 3   Label : 0, 40.00
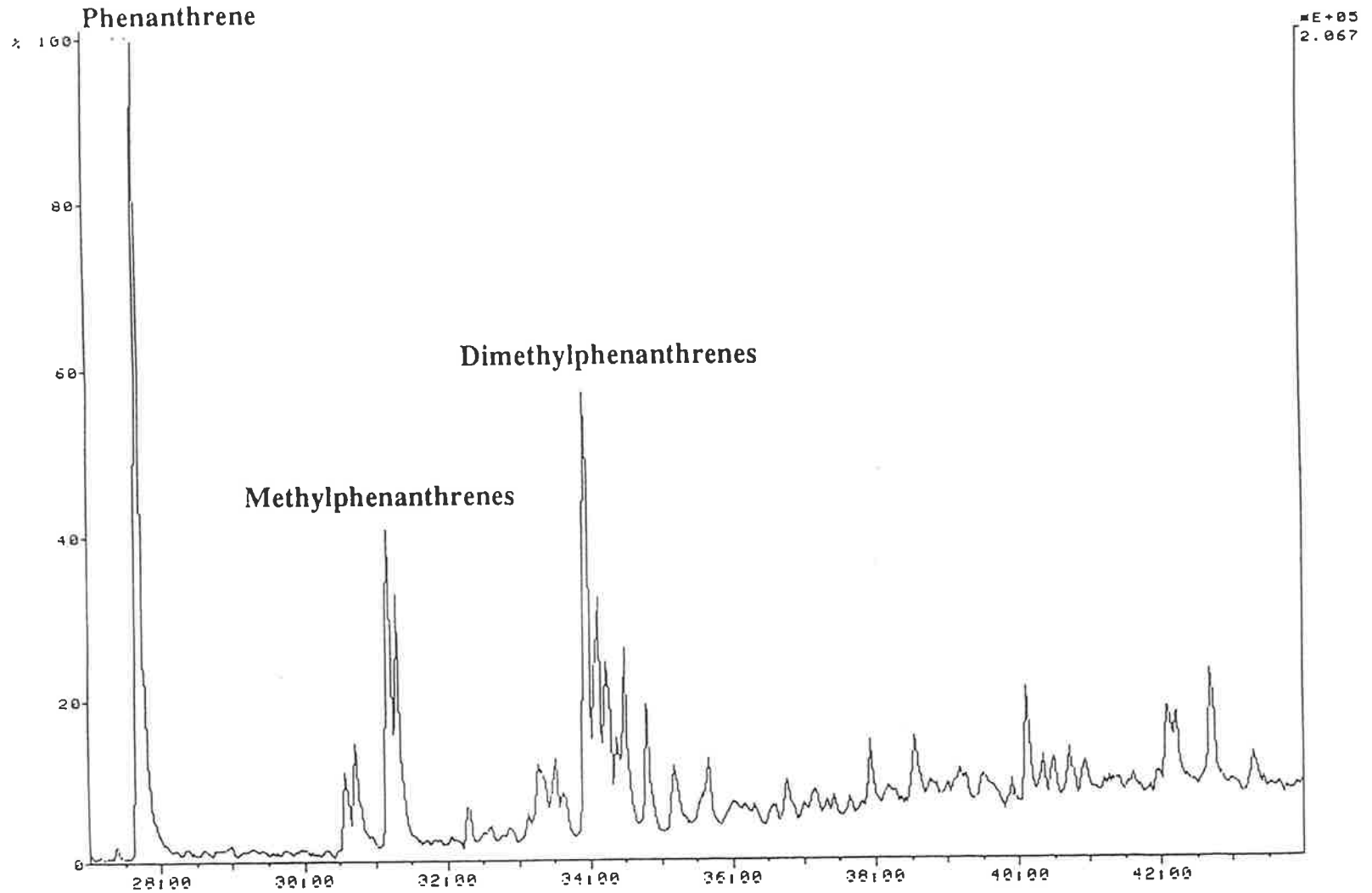
Phenanthrene

Dimethylphenanthrenes

Methylphenanthrenes

APPENDIX XII

PEAK IDENTITIES

AND

MASS CHROMATOGRAMS (GC-MS, GC-MS-MS)

OF SATURATED HYDROCARBONS

OULDBURRA FORMATION

OFFICER BASIN

KEY TO MASS FRAGMENTOGRAMS

m/z 82 (n-alkylcyclohexanes)

16–32 numbers indicate number of carbon atoms in compound

m/z 183 (acyclic isoprenoid alkanes)

Numbers indicate number of carbon atoms in compound

Identities of common terpanes (hopanes and moretanes) in the *m/z* 191 mass chromatograms (GC-MS data).

Peak No.	Identification	Carbon No.
1	18α-22,29,30-trisnorneohopane (Ts)	27
2	17α-22,29,30-trisnorhopane (Tm)	27
3	17α-29,30-bisnorhopane	28
4	17α-28,30-bisnorhopane	28
5	17α-norhopane	29
6	18α-30-norneohopane (C29Ts)	29
7	17β-normoretane	29
8	17α-hopane	30
9	18α-neohopane (C30Ts)*	30
10	17β-moretane	30
11&12	17α-homohopane (22S + 22R)	31
13 & 14	17β-homohopane (22S + 22R)	31
15 & 16	17α-homohopane (22S + 22R)	32

* Courtesy of B. Michaelsen, The University of Adelaide.

Identities of common terpanes in the *m/z* 205 mass chromatograms (GC-MS data).

Peak No.	Identification	Carbon No.
1	2α(Me)-22,29,30-trisnorneohopane [2α(Me)-Ts]	28
2	2α(Me)-22,29,30-trisnorhopane [2α(Me)-Tm]	28
3	2α(Me)-29,30-bisnorhopane	29
4	2αMe)-28,30-bisnorhopane*	30
5	3β(Me)-22,29,30-trisnorhopane 3β([Me)-Tm]	30
6	2α(Me)-30-norhopane	30
7	?2α(Me)-30-norneohopane [2α(Me)-C29Ts]	31
8	2α(Me)-30-hopane	30
9	3β(Me)-30-norhopane	31
10	3β(Me)-hopane	31

* Courtesy of B. Michaelsen, The University of Adelaide.

Identities of common steranes and diasteranes in the m/z 217 mass chromatograms (GC-MS data).

Peak No.	Identification	Ring stereochemistry	Carbon No.
Regular steranes			
3	5α(H) 14α(H) 17α(H) 20S	αα	27
4	5α(H) 14β(H) 17β(H) 20R + 20S	ββ	27
5	5α(H) 14α(H) 17α(H) 20R	αα	27
6	5α(H) 14α(H) 17α(H) 20S	αα	28
7	5α(H) 14β(H) 17β(H) 20R	ββ	28
8	5α(H) 14β(H) 17β(H) 20S	ββ	28
9	5α(H) 14α(H) 17α(H) 20R	αα	28
10	5α(H) 14α(H) 17α(H) 20S	αα	29
11	5α(H) 14β(H) 17β(H) 20R	ββ	29
12	5α(H) 14β(H) 17β(H) 20S	ββ	29
13	5α(H) 14α(H) 17α(H) 20R	αα	29
Diasteranes			
1	20S diasteranes	βα	27
2	20R diasteranes	βα	27
14	20S diasteranes	βα	29
15	20R diasteranes	βα	29

Identities of steranes in the m/z 372→217, 386→217, 400→217, 386→231, 400→231, 414→231 and 414→98, transitions and m/z 231 and 98 mass chromatograms (GC-MSMS data).

Peak No.	Identification
Steranes	
2α-Methyl-steranes	
1	2α(Me)-cholestane (20S +20R)
2	2α(Me)-24-methylcholestane (20S +20R;24S+24R)
3	2α(Me)-24-ethylcholestane (20S +20R;24S+24R)
3β- Methyl-steranes	
4	3β(Me)-24-cholestane (20S +20R)
5	3β(Me)-24-methylcholestane (20S+20R)
6	3β(Me)-24-ethylcholestane (20S+20R; 24S+24R)
4α-Methyl-steranes	
7'	4α(Me)-24-ethylcholestane (20S+20R; 24S+24R)
8	4α-23,24-trimethylcholestane (20S+20R; 23S+23R; 24S+24R) [dinosterane]
Diasteranes	
9	diacholestane (20S+20R)
10	24-methyldiacholestane (20S+20R; 24S+24R)
11	24-ethyldiacholestane (20S+20R; 24S+24R)
12	24-n-propyldiacholestene (20S+20R; 24S+24R)
13	24-iso- propyldiacholestene (20S+20R)
14	24-nordiacholestene (20S+20R)
15	27-nordiacholestene (20S+20R)

C₃₁ homohopane

$m/z = 191$

C₃₀ hopane

18α-30-norneohopane (C₂₉ Ts)

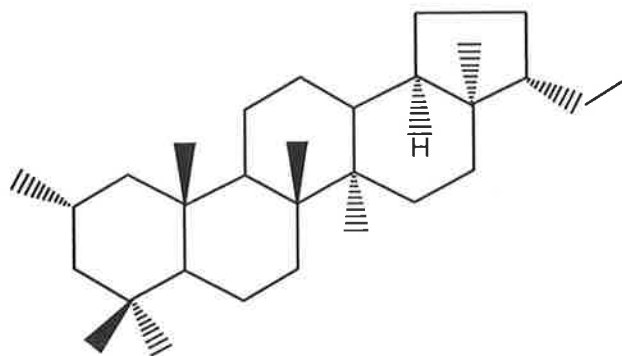**18α-neohopane (C₃₀ Ts)**

C₃₁ (20R) moretane

Tm

Ts
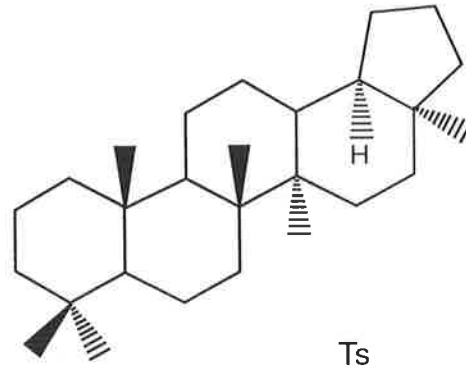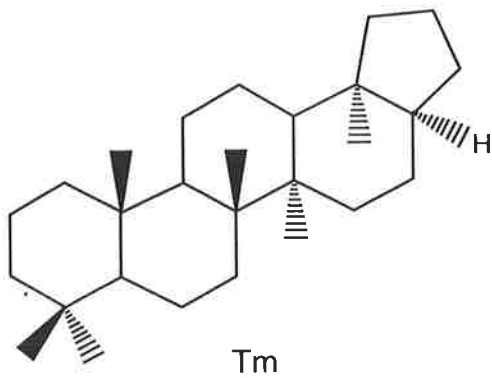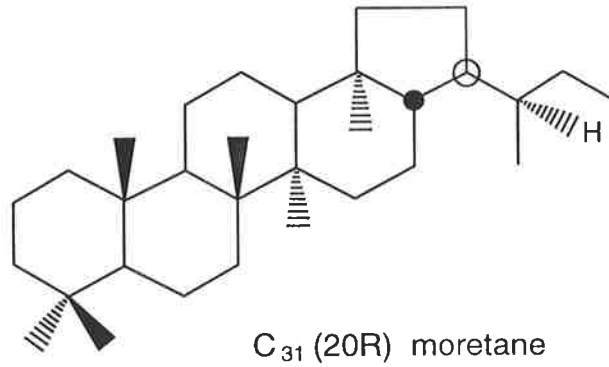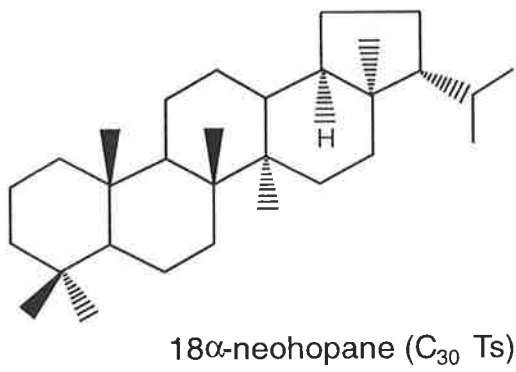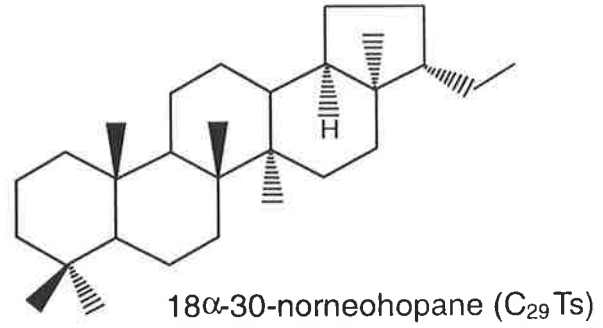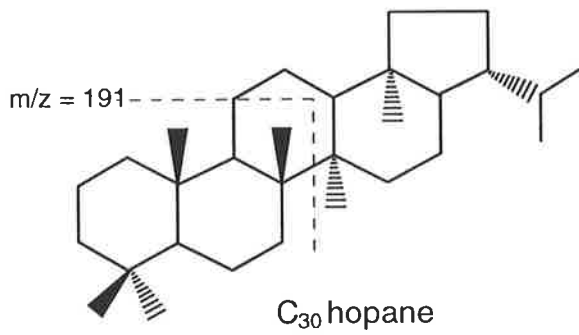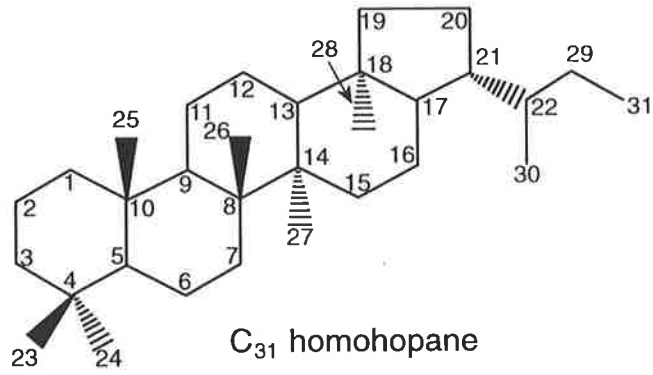
Structure and nomenclature of some important molecular fossils (triterpanes) from the Ouldburra Formation, Officer Basin.
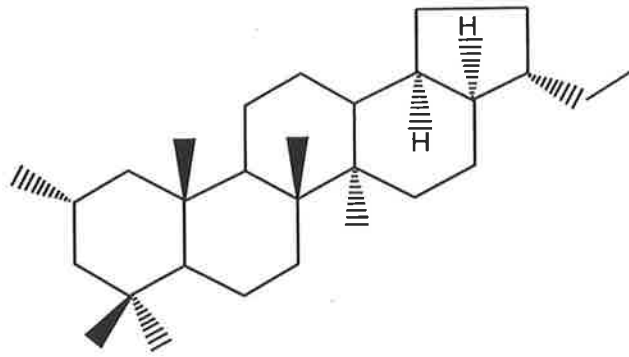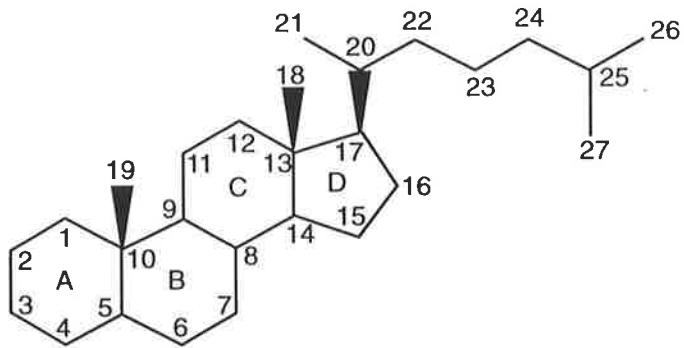
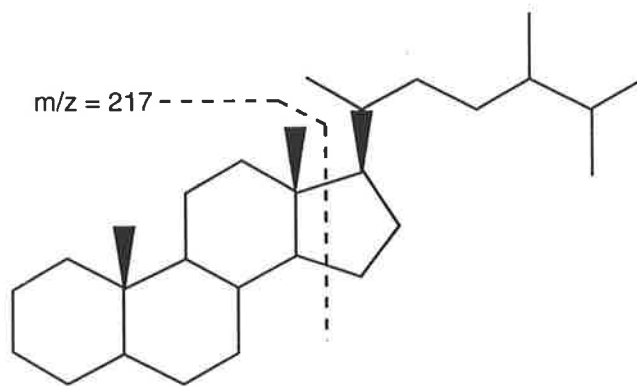2α(Me)-28,30-bisnorhopane
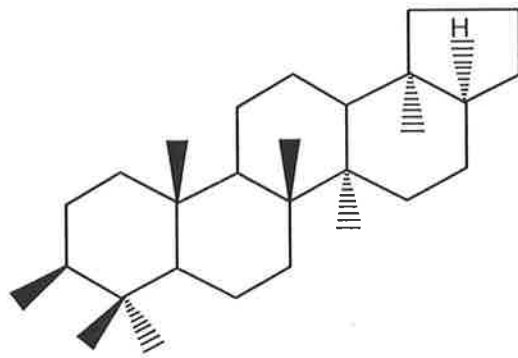
3β(Me)-22,29,30-trisnorhopane
[3β(Me)-Tm]

2α(Me)-30-norneohopane
[2α(Me)-C$_{29}$Ts]
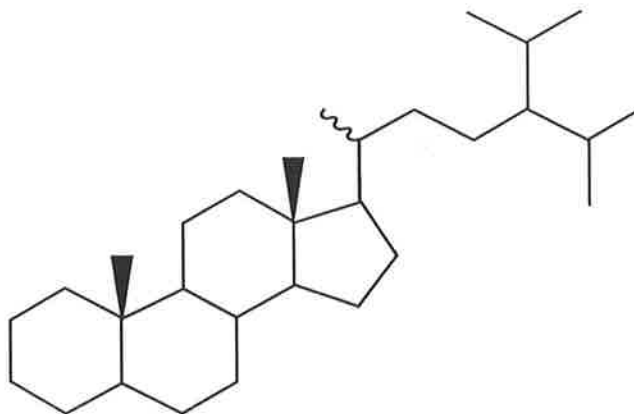
Structure of some important molecular fossils (2α and 3β-methylhopanes) from the Ouldburra Formation, Officer Basin.

C_{27} sterane (cholestane)

$m/z = 217$

C_{28} sterane (24-methylcholestane)

24-isopropylcholestane (sponge marker)

Structure and nomenclature of some important molecular fossils (steranes) from the Ouldburra Formation, Officer Basin.
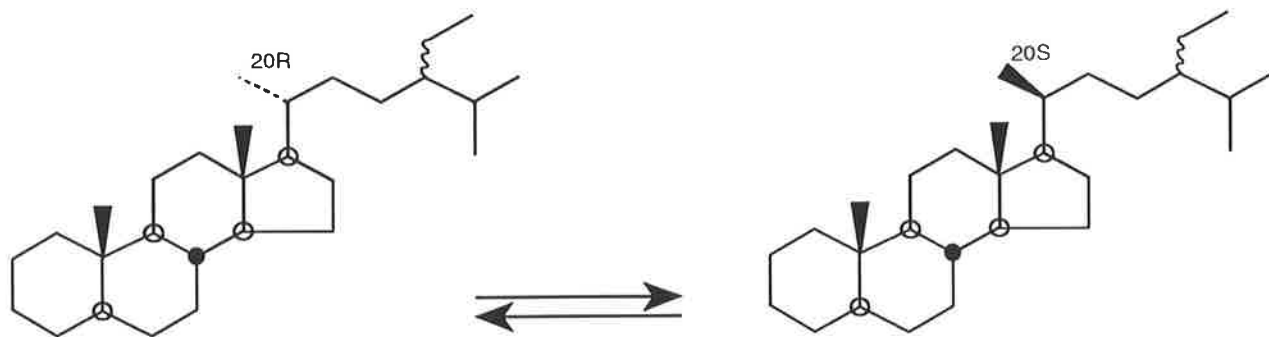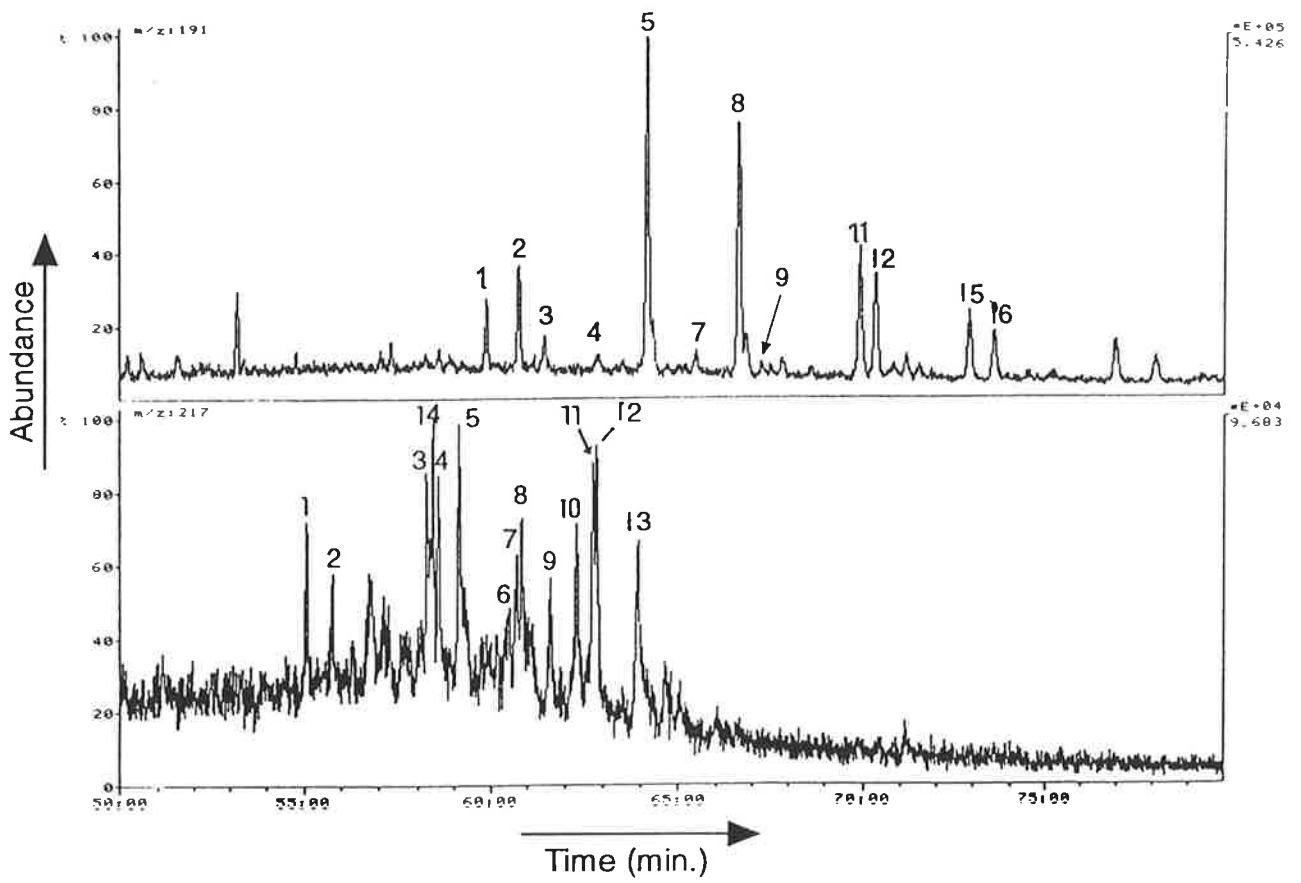
C$_{29}$ 5α(H),14α(H),17α(H)-steranes
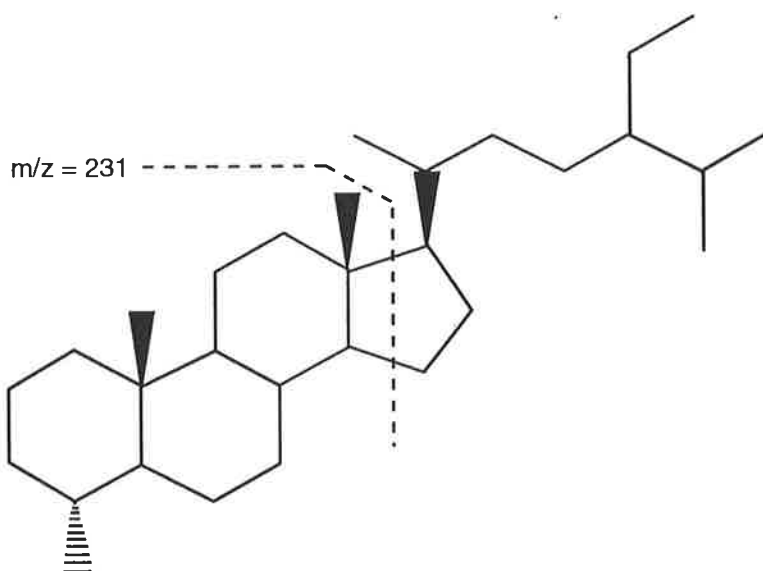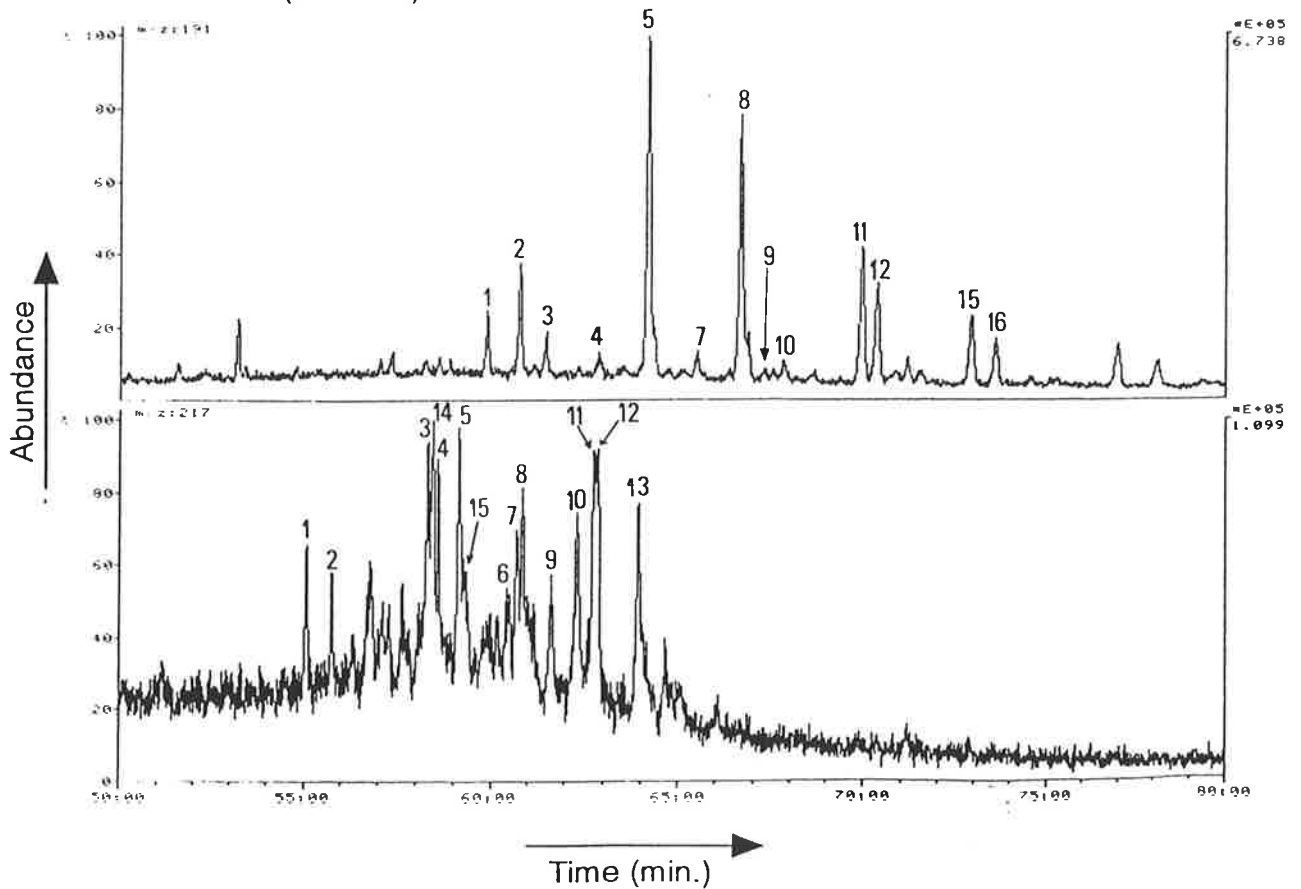

C$_{30}$ 4-methyl-24-ethylcholestane
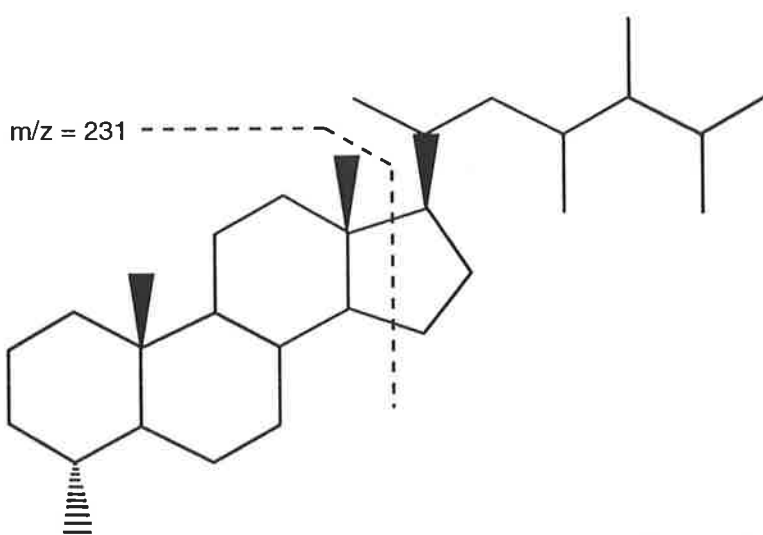
C$_{30}$ 4,23,24-trimethylcholestane (dinosterane)

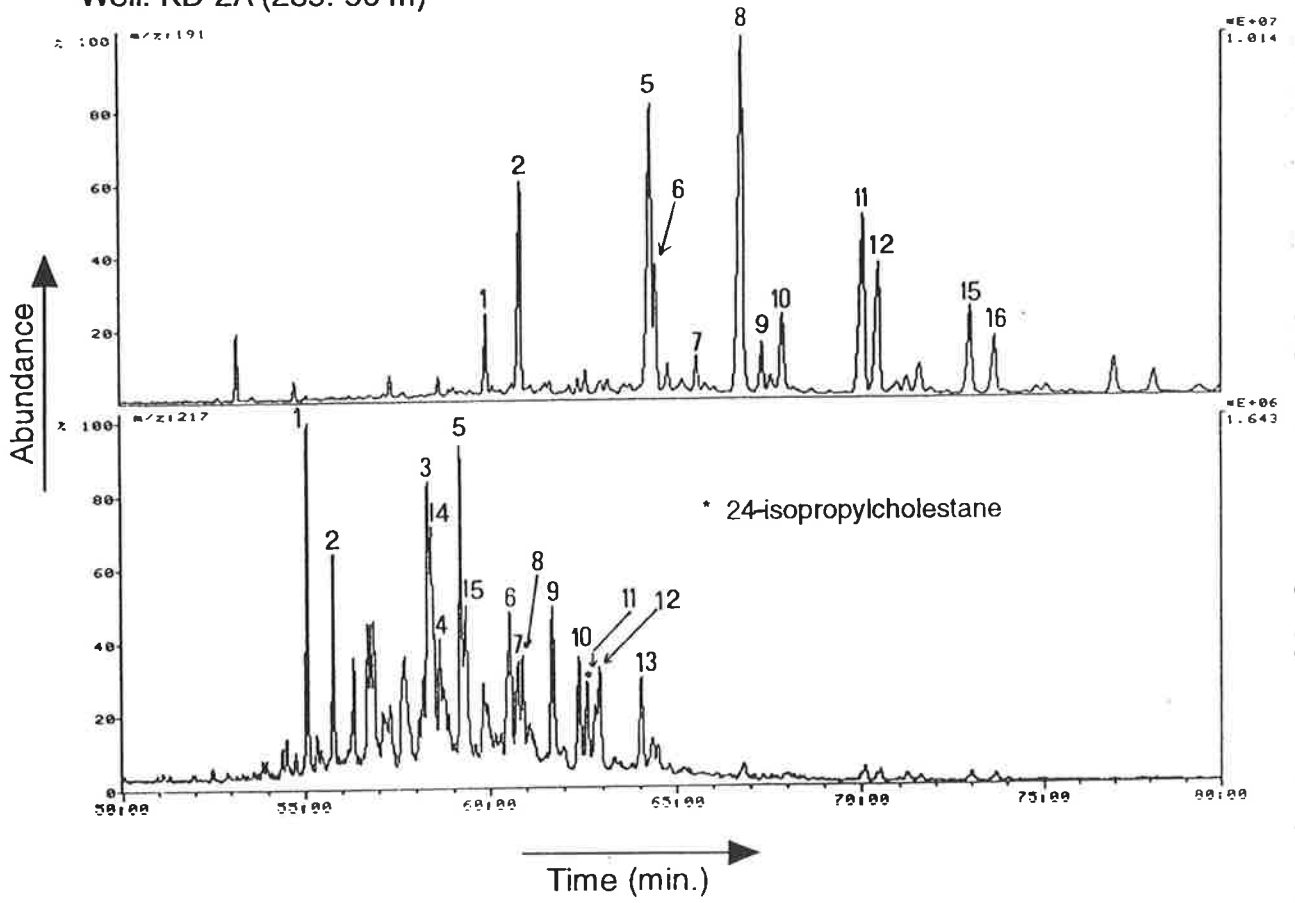Well: Manya-6 (698. 60 m)

Well: Manya-6 (1279.15 m)

Well: Marla-3 (619. 60 m)

Well: Marla-6 (416.0 m)

Well: KD-2A (285. 50 m)

Abundance

Time (min.)

* 24-isopropylcholestane

Well: KD-2A (297.95 m)

Abundance

Time (min.)

* 24-isopropylcholestane

KD-1 263.35 m

* 24-isopropylcholestane

KD-1, 263.35 m

Alkylcyclohexanes

KD-1, 263.35 m

← Squalane

Acyclic isoprenoids

Abundance

Scanning time